UNIVERSIDADE FEDERAL DO RIO GRANDE DO SUL

INSTITUTO DE GEOCIÊNCIAS

PROGRAMA DE PÓS-GRADUAÇÃO EM GEOCIÊNCIAS

ASSOCIAÇÃO DE FÁCIES, PADRÕES DE VESICULAÇÃO E PETROLOGIA DOS DERRAMES BÁSICOS DA FORMAÇÃO SERRA GERAL NA OMBREIRA SUL DA CALHA DE TORRES (RS)

CARLA JOANA SANTOS BARRETO

ORIENTADOR – Prof. Dr. Evandro Fernandes de Lima

Porto Alegre – 2016

UNIVERSIDADE FEDERAL DO RIO GRANDE DO SUL

INSTITUTO DE GEOCIÊNCIAS

PROGRAMA DE PÓS-GRADUAÇÃO EM GEOCIÊNCIAS

ASSOCIAÇÃO DE FÁCIES, PADRÕES DE VESICULAÇÃO E PETROLOGIA DOS DERRAMES BÁSICOS DA FORMAÇÃO SERRA GERAL NA OMBREIRA SUL DA CALHA DE TORRES (RS)

CARLA JOANA SANTOS BARRETO

ORIENTADOR – Prof. Dr. Evandro Fernandes de Lima

BANCA EXAMINADORA

Dra. Isabela de Oliveira Carmo – Petróleo Brasileiro, Cenpes PDEXP/GEOTEC

Prof. Dr. Valdecir Janasi – Instituto de Geociências, Universidade de São Paulo

Prof. Dr. Breno Leitão Waichel – Departamento de Geociências, Universidade Federal de Santa Catarina

Tese de doutorado apresentada como requisito parcial para a obtenção do Título de Doutor em Ciências

Porto Alegre - 2016

Barreto, Carla Joana

Associação de fácies, padrões de vesiculação e petrologia dos derrames básicos da Formação Serra Geral na ombreira sul da calha de Torres (RS) . / Carla Joana Barreto. - Porto Alegre: IGEO/UFRGS, 2016.

[192 f.] il.

Tese (Doutorado).- Universidade Federal do Rio Grande do Sul. Programa de Pós-Graduação em Geocências. Instituto de Geociências. Porto Alegre, RS - BR, 2016.

Orientador(es):Evandro Fernandes de Lima

1. Província Paraná-Etendeka 2. Formação Serra Geral 3. Reservatório vulcânico 4. Isótopos de Sr, Nd e Pb I. Título.

CDU 55

Catalogação na Publicação
Biblioteca Instituto de Geociências - UFRGS
Sibila F. Tengaten Binotto CRB 10/1743

Universidade Federal do Rio Grande do Sul - Campus do Vale Av. Bento Gonçalves, 9500 - Porto Alegre - RS - Brasil
CEP: 91501-970 / Caixa Postal: 15001.
Fone: +55 51 3308-6329 Fax: +55 51 3308-6337
E-mail: bibgeo@ufrgs.br

" Talvez não tenha conseguido fazer o melhor, mas lutei para que o melhor fosse feito. Não sou o que deveria ser, mas Graças a Deus, não sou o que era antes"
(Marthin Luther King).

Agradecimentos

A **Deus** pelo dom da vida, por ter possibilitado que eu chegasse até o final deste trabalho com saúde;

Agradeço a minha família, em especial aos meus pais e a minha madrinha que me incentivam desde sempre. Ao meu amado irmão que é meu exemplo de determinação e foco;

À Universidade Federal do Rio Grande do Sul (UFRGS), em especial, ao Programa de Pós-graduação em Geociências (PPGGEO), pela infraestrutura disponibilizada;

Ao Programa de Recursos Humanos da Petrobrás (PRH PB-215) pela concessão da bolsa de estudos e pelo apoio financeiro durante as etapas de campos, análises isotópicas e cursos internacionais de vulcanologia;

Ao Dr. Jair Weschenfelder, coordenador do PRH PB-215 e a Dra. Luana Portz, Pesquisadora Visitante da UFGRS/Petrobrás, que sempre se mostraram disponíveis a atender as demandas solicitadas durante o doutorado;

A CAPES FCT (projeto 133913-2) pela concessão da bolsa doutorado sanduiche em Coimbra, Portugal;

Agradeço ao querido amigo e orientador Dr. Evandro Lima pelos ensinamentos e pela grande oportunidade de aprender sobre esse mundo apaixonante das vulcânicas. Obrigada por ter confiado no meu trabalho e na minha capacidade de chegar até o fim deste doutorado;

Ao Prof. Jean-Michel Lafon pela amizade e parceria de anos de convívio, sempre disposto a me ajudar nas incansáveis discussões isotópicas e por todo apoio no laboratório de geocronologia da Universidade Federal do Pará;

Ao prof. Carlos Sommer pelas incontáveis discussões e apoio tanto pessoal quanto logístico durante todo o meu doutorado;

Aos pesquisadores portugueses Fernando Lopes, Tereza Barata e João Fernandes pelo maravilhoso acolhimento com que me receberam em Coimbra;

Agradeço aos amigos queridos que tive a felicidade de conhecer em Portugal: Vivi, Luiz, Silvano, André, Salma, Igor... Vocês tornaram minha estadia em Coimbra inesquecível. Nossos cafés, jantares, vinhos, karaokê naquele segundo andar... São realmente lembranças que levarei pra vida toda;

Aos colegas do grupo de Estratigrafia e Petrologia de Sequências Vulcânicas: Lucas, Natália, Milena e Fernando pela ajuda nas etapas de campo e na preparação das amostras.

Aos técnicos do Laboratório Pará-Iso (UFPA): Etiana Oliveira, Jeferson Barbosa, Izanete Melo e Elma Oliveira;

Agradeço imensamente aos amigos que fiz em Porto Alegre: Awilsa, Mari, Rossana, Carla, Karine, Camila, Fabi, Nina, Gustavo, Isis. Não é fácil estar longe de casa! Vocês, com certeza tornaram tudo mais fácil...

A minha querida amiga Kamilla, que tem exercitado sua paciência infinita para me aconselhar nos momentos que eu enlouquecia achando que estava tudo errado. Obrigada por acreditar mais na minha capacidade do que eu mesma; pelas críticas construtivas e sugestões em alguns artigos, e não podemos esquecer as incontáveis conversas reconfortantes sobre o futuro.

UFRGS
UNIVERSIDADE FEDERAL DO RIO GRANDE DO SUL

Instituto de Geociências

Programa de Pós-Graduação em Geociências

RESUMO

A investigação foi realizada no extremo sul do Brasil, nos derrames básicos da Formação Serra Geral, entre os municípios de Santa Cruz do Sul-Herveiras e Lajeado. Na área estão expostas sucessões de derrames baixo Ti com morfologias *pahoehoe* e *rubbly*, pertencentes a Província Ígnea Paraná-Etendeka. Na sequência de derrames em Santa Cruz do Sul-Herveiras foram identificadas 16 litofácies e três associações de litofácies 1- *pahoehoe* composta inicial, 2- *pahoehoe* simples inicial e 3- *rubbly* simples tardia. Nos derrames *pahoehoe* compostos (< 1m espessura), o rápido resfriamento permitiu a geração de *pipe* vesículas e vesículas V1. Nos derrames *pahoehoe* simples (2-6 m de espessura), uma grande quantidade de estruturas de segregação foi gerada: proto-cilindros e cilindros; *pods*; camadas de vesículas S1 e S2 e camadas de cilindros; *pipes*, vesículas V1 e gigantes. Nos derrames *rubbly* (> 30m espessura), apenas vesículas tipo V1 e gigantes são preservadas. Estudos petrográficos indicaram que os processos de dissolução de cristais e liberação de gás originaram porosidades primárias, enquanto processos de alteração e fraturamento geraram uma grande quantidade de porosidades secundárias. No entanto, a precipitação de minerais secundários nos poros tende a reduzir o espaço disponível para armazenamento de fluidos, demonstrando que apenas a existência de poros é insuficiente para a existência de um reservatório vulcânico. Geoquimicamente, todos os derrames estudados podem ser classificados como do tipo Gramado. As composições variam de basaltos a andesito basálticos de afinidade toleítica nos perfis Santa Cruz e Lajeado, enquanto na área do Morro da Cruz, os derrames do tipo *ponded pahoehoe* exibem composições de andesitos. A assimilação crustal sugerida para estas sequências vulcânicas permite explicar as altas razões isotópicas iniciais de Sr (0,707798–0,715751), e os valores baixos de ε_{Nd} (-8,36 a -5,41), com associadas variações isotópicas de Pb (18,42 $<^{206}Pb/^{204}Pb<$ 18,86; 15,65 $<^{207}Pb/^{204}Pb<$ 15,71; 38,62 $<^{208}Pb/^{204}Pb<$ 39,37). A evolução magmática dos derrames básicos de Santa Cruz do Sul-Herveiras e Lajeado iniciou com o armazenamento de líquidos máficos durante um curto período em câmaras magmáticas rasas, associados a um processo de contaminação crustal significativo, o qual permitiu a ascensão de magmas com composição de olivina basaltos, os quais exibem morfologia *pahoehoe* composta em superfície. A contínua cristalização

fracionada dentro da câmara magmática concomitante com assimilação em graus variáveis de distintos contaminantes com idades Paleoproterozoica e Neoproterozoica, somada a uma contribuição significativa de recarga de magma permitiu a ascensão de magma com composição andesito basáltica, o qual exibe morfologia *pahoehoe* simples em superfície. A contínua recarga de magma na câmara magmática concomitante a graus mais elevados de assimilação levaram a formação de lavas andesito basálticas com assinaturas isotópicas mais contaminadas e que exibem na superfície morfologia *rubbly pahoehoe*. Processos de diferenciação dos líquidos concomitantes as maiores taxas de assimilação de distintos contaminantes durante um período prolongado em um câmara magmática rasa, a qual é distinta daquela onde os magmas de Santa Cruz do Sul-Herveiras e Lajeado estavam armazenados, favoreceu a formação dos andesitos do Morro da Cruz, que exibem as assinaturas mais contaminadas da ombreira sul da Sinclinal de Torres.

ABSTRACT

This study was performed in the southern Brazil, in the basic lava flows of the Serra Geral Formation, between the localities of Santa Cruz do Sul-Herveiras and Lajeado. Low Ti lava flow successions with pahoehoe and rubbly morphologies occur in the study area, which belong to Paraná-Etendeka Igneous Province. In the volcanic sequence of the Santa Cruz do Sul-Herveiras, the basaltic lava flows were divided into 16 lithofacies and grouped into three lithofacies associations: 1- early compound pahoehoe, 2- early simple pahoehoe, and 3- late simple rubbly. In the compound pahoehoe lava flows (< 1m thickness), the fast cooling allowed the generation of pipe vesicles and V1-type vesicles. In the simple pahoehoe lava flows (2-6 m thickness), a large amount of segregation structures were generated: proto-cylinder, cylinder, pods, S1 and S2-type vesicle sheets, pipe vesicles, V1-type and giant vesicles. In the rubbly pahoehoe lava flows (> 30 m thickness), just V1-type and giant vesicles are preserved. Petrographic studies indicate that the dissolution of deuteric crystals and gas releasing processes formed the primary porosities, while processes such as alteration and fracturing generated the secondary porosities. However, the precipitation of secondary minerals in vesicles and cavities decreases the available space for fluid storage, which suggest that the existence of pores alone is insufficient for creating volcanic reservoirs. Geochemically, all the studied lava flows could be classified in the Gramado type. The geochemical compositions in the Santa Cruz do Sul-Herveiras and Lajeado profiles range from basalt to basaltic andesites with tholeiitic affinity, while in the Morro da Cruz area, the ponded pahoehoe lava flows exhibit andesite compositions. The process of crustal assimilation suggested for these volcanic sequences allow explains the high and widespread initial Sr isotopic ratios at 0.707798–0.715751 and the low ε_{Nd} at −8.36 to −5.41, with associated Pb isotopic variations (18.42 < $^{206}Pb/^{204}Pb$ < 18.86; 15.65 < $^{207}Pb/^{204}Pb$ <15.71; 38.62 < $^{208}Pb/^{204}Pb$ < 39.37). The magmatic evolution of the SCSH and LJ basic lava flows begins with the storage of mafic liquids during a short period at shallow-level magma chamber, associated to significant crustal contamination that allowed the magma ascent with composition of olivine basalts that exhibit

compound pahoehoe morphology at surface. The continuous fractional crystallization within the magma chamber coupled with variable assimilation degrees of distinct contaminants with Paleoproterozoic and Neoproterozoic ages, in addition to significant contribution of magma recharge led to magma ascent with basaltic andesite composition that display at surface the simple pahoehoe morphology. The continuous magma recharge in the magma chamber coupled with higher assimilation degree allowed the formation of basaltic andesite lavas with more contaminated isotopic signatures that exhibit rubbly morphology at the surface. Differentiation process of liquids coupled with the highest assimilation degrees of distinct contaminants during longer time in a shallow-level magma chamber, which is distinct from that where SCSH and LJ magmas have been stored, led to formation of andesites of the Morro da Cruz that exhibit the most contaminated isotopic signatures of south hinge of the Torres Syncline.

LISTA DE TABELAS

LISTA DE FIGURAS

SUMÁRIO

Estrutura e organização da tese

No capítulo 1 é apresentada a introdução com os principais temas que motivaram este estudo, bem como os objetivos propostos para esta tese. Em seguida, é apresentada a área de estudo e os materiais utilizados. Uma descrição detalhada dos métodos utilizados durante o desenvolvimento da tese também é apresentada nesse capítulo.

No capítulo 2 consta uma breve discussão sobre as Grandes Províncias Ígneas, Províncias Basálticas Continentais e a Província Paraná-Etendeka.

O capítulo 3 trata sobre o estado atual da arte de conceitos fundamentais para melhor compreensão da tese que consistem em: 1) morfologias de derrames basálticos e seus estilos de *emplacement*; 2) aplicação da análise de fácies em rochas vulcânicas básicas; 3) padrões de vesiculação e as estruturas de segregação em derrames basálticos.

No capítulo 4 são apresentados os aspectos gerais do arcabouço geológico regional da Bacia do Paraná, com ênfase para as principais características estratigráficas e evolutivas da "Sinclinal" ou calha de Torres, cuja área de estudo está inserida. Ainda nesse capítulo, é apresentado o Grupo São Bento, o qual é subdividido nas formações Botucatu e Serra Geral. Um subtópico destacando os processos envolvidos na gênese dos magmas alto e baixo Ti e as correlações quimioestratigráficas do magmatismo Serra Geral foi inserido nesse capítulo.

No capítulo 5 são apresentados os três artigos científicos submetidos a periódicos internacionais, atendendo as normas estabelecidas pelo Programa de Pós-Graduação em Geociências da Universidade Federal do Rio Grande do Sul. Dessa forma, cada capítulo pode ser lido de forma relativamente independente dos demais sem prejuízo da compreensão.

O primeiro artigo intitulado "*Lithofacies analysis of basic lava flows of the Paraná igneous province in the south hinge of Torres Syncline, Southern Brazil*" foi aceito e publicado no periódico: *Journal of Volcanology and Geothermal Research* (Barreto *et al.,* 2014b). O segundo artigo intitulado "Vesicle-rich *segregation structures and recognition of primary and secondary porosities in pahoehoe and rubbly lava flows of the Paraná igneous province, Southern Brazil*" foi submetido, revisado e enviado para avaliação final dos revisores da revista *Bulletin of*

Volcanology. O terceiro artigo intitulado "*Geochemical and Sr-Nd-Pb isotopic insights of the low-Ti basalts from southern Paraná Igneous Province, Brazil: the role of crustal contamination*" foi aceito para publicação no periódico International Geology Review.

No capitulo 6 são reunidas as considerações finais da tese com a síntese integradora das principais conclusões obtidas com os artigos científicos para a evolução geológica da ombreira sul da "Sinclinal" ou calha de Torres. Para finalizar, as referências bibliográficas citadas nos capítulos que antecedem os artigos são listadas no capítulo 7, permanecendo as referências dos artigos listados nos mesmos.

Nos anexos consta toda a produção cientifica gerada durante o doutorado, com o objetivo de mostrar o avanço no conhecimento sobre o tema. O anexo A refere-se à carta de resubmissão do segundo artigo "*Vesicle-rich segregation structures and recognition of primary and secondary porosities in pahoehoe and rubbly lava flows of the Paraná igneous province, Southern Brazil"*. O anexo B refere-se à carta de aceite do terceiro artigo "*Geochemical and Sr-Nd-Pb isotopic insights of the Low-Ti basalts from southern Paraná Igneous Province, Brazil: the role of crustal contamination"*.

O anexo C é constituído pela separata do artigo "*Stratigraphical framework of basaltic lavas in Torres Syncline main valley, southern Paraná-Etendeka Volcanic Province*" em que a autora da tese é coautora do artigo.

Os anexos D e E são resumos apresentados no II worskhop interno do PRH PB-15 e Reunião Anual de Avaliação dos PRH'S, respectivamente. O anexo F refere-se a um resumo apresentado no VIII Simpósio Sul-Brasileiro de Geologia – SSBG (Porto Alegre), e os anexos G, H, I são resumos apresentados no 47º Congresso Brasileiro de Geologia (Salvador). O anexo J é referente a um resumo apresentado no IX Simpósio Sul-Brasileiro de Geologia (Florianópolis). Anexos K e L são referentes aos resumos apresentados no VI Simpósio de Vulcanismo e Ambientes Associados (São Paulo) e 1º Semana Acadêmica dos Pós-graduandos do Insituto de Geociências da UFRGS-Integrando as Geociências (Porto Alegre). Os anexos M e N referem-se aos resumos apresentados no American Geophysical Union Fall Meeting (San Francisco-EUA).

CAPÍTULO 1

Introdução

As grandes províncias ígneas (Large Igneous Provinces - *LIPs*; Coffin & Eldholm, 1994) ocorrem em contextos tanto continentais ou oceânicos ou mesmo na transição entre ambos, e se caracterizam pela colocação de grandes volumes de lavas (≈10^6 km^3) em intervalos de tempo relativamente curtos (<5 Ma) e em grandes extensões territoriais (> 0,1Mkm^2). *LIPs* têm sido objeto de estudo ao longo de décadas devido a sua associação com mudanças ambientais globais que incluem eventos de extinção em massa, mudanças topográficas regionais e quebra de continentes. Além disso, as *LIPs* estão associadas com uma grande quantidade de depósitos de minérios e possuem grande importância para a indústria de óleo/gas e sistemas aquíferos (Ernst, 2014).

Uma parcela considerável das pesquisas desenvolvidas em *LIPs* foca em províncias basálticas continentais e platôs de bacias oceânicas, os quais caracterizam eventos importantes do Mesozoico-Cenozoico. O registro geológico nesses ambientes continentais e oceânicos é geralmente bem preservado e tem sido fundamental para o desenvolvimento de conceitos chave para as *LIPs*, tais como a grande extensão e volumes, e a curta duração do magmatismo (Ernst, 2014).

Os estudos em províncias basálticas continentais têm se concentrado, sobretudo, em aspectos geoquímicos (Hawkesworth *et al*., 1988; Ewart *et al.,* 1998) e geocronológicos (Renne *et al.,* 1996; Hamilton *et al.,* 1998), com ênfase para discussões sobre plumas mantélicas (White & McKenzie, 1989) e correlações regionais quimioestratigráficas (Milner *et al.,* 1992, 1995; Peate *et al.,* 1992; Peate, 1997). Essa forma de abordagem advém da concepção inicial de que os grandes derrames de lava eram simples sucessões de pacotes tabulares espessos, os quais possuiam uma estratigrafia simples denominada *layer cake* (Jerram, 2002).

Recentemente, uma nova abordagem na pesquisa de províncias continentais considera que as sucessões vulcânicas são formadas por arquiteturas externas e internas complexas, as quais possibilitaram a investigação da arquitetura de fácies e vulcanologia física de uma forma mais sistemática, fornecendo informações sobre taxas de efusão, mecanismos de *emplacement* e paleotopografia (Self *et al.,* 1997;

Jerram *et al.,* 1999; Jerram, 2002; Single & Jerram, 2004; Farrell, 2010; Lima *et al.,* 2012a, 2012b; Waichel *et al.,* 2012). Para melhor compreender a arquitetura externa e a variação interna nos derrames, a utilização do método de litofácies e associação de litofácies é importante, pois fornece informações sobre os padrões de empilhamento e heterogeneidades internas das sucessões vulcânicas.

Os padrões de vesiculação dos derrames básicos das províncias basálticas continentais são gerados a partir de bolhas de gases aprisionadas durante o resfriamento das lavas (Wilmoth & Walker, 1993). Estes gases podem ser gerados pela supersaturação em voláteis durante a ascensão e colocação das lavas (primeiro ponto de ebulição) ou pela diferenciação e cristalização de fases anidras que enriquecem relativamente em fluidos o líquido residual (segundo ponto de ebulição). Aproximadamente 20 a 60% de vesículas esféricas são tipicamente descritas na base e topo das lavas *pahoehoe*. Em contrapartida, vesículas irregulares e esparsas são menos abundantes nas lavas *'a'ā* (~ 20%) e ocorrem nas brechas de topo. Recentemente, alguns estudos têm demonstrado que diferentes padrões de vesiculação, incluindo aqueles contendo material de segregação, podem ser gerados em diferentes posições dentro de derrames básicos subaéreos, não sendo restritos a base e topo de lavas *pahoehoe* (Goff, 1996; Cashman & Kauahikaua, 1997; Self *et al.,* 1998; Caroff *et al.,* 2000; Farrell, 2010).

A identificação das propriedades petrofísicas de derrames básicos, incluindo formas, tamanhos e materiais de preenchimento das vesículas poderiam auxiliar na determinação de um possível reservatório vulcânico de óleo e gás. A alta heterogeneidade textural e estrutural das rochas vulcânicas quando comparada com as rochas clásticas e carbonáticas as tornam reservatórios secundários na indústria de óleo e gás. No entanto, reservatórios de hidrocarbonetos associados com rochas vulcânicas têm sido reportados no mundo todo (Jinglan *et al.,* 1999; Mitsuhata *et al.,* 1999; Wang *et al.,* 2003; Sruoga *et al.,* 2004; Wu *et al.,* 2006; Sruoga & Rubinstein, 2007; Feng, 2008; Lenhardt & Gotz, 2011; Gudmundsson & Lotveit, 2014).

Em virtude da grande extensão areal e volume da maioria das províncias continentais, os derrames têm sido mapeados com um controle estratigráfico regional, em que a composição química é utilizada para estabelecer, mesmo que indiretamente, a estratigrafia interna dessas províncias. Na Província Paraná-Etendeka, as rochas vulcânicas foram agrupadas nos tipos baixo e alto Ti (Bellieni *et*

al., 1984) e em magmas tipos (Peate *et al.,* 1992), pois acredita-se que derrames pertencendo a um determinado tipo de magma se comportarão como uma unidade estratigráfica homogênea (Fodor *et al.,* 1985; Bellieni *et al.,* 1986; Hawkesworth *et al.,* 1986; Petrini *et al.,* 1987; Piccirillo *et al.,* 1989).

Uma importante questão ainda em debate é a origem dos magmas da Província Paraná-Etendeka e o papel da contaminação crustal. Este processo de contaminação tem sido bem documentado para os basaltos baixo Ti da Província Paraná-Etendeka (Cox & Hawkesworth, 1985; Mantovani *et al.,* 1985; Petrini *et al.,* 1987; Hawkesworth *et al.,* 1988; Piccirillo *et al.,* 1989; Peate & Hawkesworth, 1996; Ewart *et al.,* 1998), embora ainda sejam escassos os estudos quantitativos do grau dessa contaminação bem como dos possiveis contaminantes no sul da Província Paraná.

1.1 Objetivos

O objetivo geral desta tese é investigar detalhadamente os derrames da Formação Serra Geral na ombreira sul da “Sinclinal” ou calha de Torres para compor um novo arcabouço estratigráfico em escala de detalhe. Os objetivos especificos consistem em:

1) Aplicar o método de análise de fácies em sequências vulcânicas básicas de platô continental, propondo um esquema de litofácies simples e útil para organização dos derrames do perfil Santa Cruz do Sul-Herveiras com base nas estruturas de segregação, texturas e características de superfície;
2) Definir os parâmetros que devem ser utilizados para a definição das litofácies vulcânicas, tais como notação cientifica e código de litofácies, bem como os critérios para se agrupar as diferentes litofácies em associações de litofácies;
3) Estabelecer o significado do empilhamento dos ciclos vulcânicos na evolução estratigráfica da bacia;
4) Testar a eficácia do método gamaespectrométrico na individualização de fácies vulcânicas, baseados na resposta dos radionuclídeos K, U e Th presentes nos derrames básicos e ácidos;
5) Discutir a paleotopografia e avaliar os estilos de *emplacement* dos

derrames da Província Paraná através do estudo das morfologias;

6) Estabelecer os contrastes petrográficos entre as sucessões de derrames e seu reflexo nas morfologias *pahoehoe* e *rubbly*;
7) Identificar os padrões de vesiculação e estruturas de segregação que ocorrem em escala mesoscópica e fornecer os processos de formação dessas estruturas;
8) Fornecer estimativas das espessuras dos derrames, com base nas estruturas de segregação que são preservadas, bem como definir uma posição aproximada dentro do derrame em que determinadas estruturas ocorrem;
9) Identificar os tipos de porosidades existentes nos derrames *pahoehoe* e *rubbly*, e fornecer os dados quantitativos da contribuição dessas porosidades para um possível reservatório vulcânico nessa região;
10) Discutir as variações geoquímicas e isotópicas de Sr-Nd-Pb dos derrames basálticos dentro do magma-tipo Gramado a partir de uma estratigrafia de escala local;
11) Discutir a petrogênese dos magmas que originaram os derrames básicos dos perfis Santa Cruz do Sul-Herveiras, Lajeado e Morro da Cruz;
12) Avaliar qualitativa e quantitativamente o papel da contaminação crustal na região estudada e os possíveis contaminantes envolvidos para uma melhor compreensão da evolução geológica da bacia.

1.2 Área de estudo e amostragem

Análises macroscópicas, microscópicas, geoquímicas e isotópicas foram realizadas em amostras coletadas com espaçamento regular de 5 a 10 m em três perfis, os quais representam seções verticais completas da ombreira sul da calha de Torres. O principal perfil está localizado ao longo da estrada RSC-153, entre os municipios de Santa Cruz do Sul e Herveiras (coordenadas UTM: 342022/ 6728123 e 340138/ 6734162). Nesse perfil foram coletadas 22 amostras da base, núcleo e topo dos derrames para análise geoquímica, sendo que nove dessas também foram selecionadas para análises isotópicas de Sr-Nd-Pb.

O segundo perfil está localizado no Parque Natural do Morro da Cruz (coordenadas UTM: 363241/ 6710664), distante aproximadamente 50 km a sudeste do perfil principal. Desse perfil, três amostras foram selecionadas para análise geoquímica, sendo que em duas foram realizadas análises isotópicas.

O terceiro perfil está localizado próximo ao municipio de Lajeado, ao longo das estradas BR-386 e RS-227 (coordenadas UTM: 399230/ 6731618 e 386610/ 6763520). Esse perfil está distante cerca de 100 km E-NE do perfil de Santa Cruz do Sul. Cinco amostras foram coletadas desse perfil para análise geoquímica, sendo que duas delas também foram utilizadas para obtenção de análises isotópicas.

1.3 Métodos de investigação utilizados

1.3.1 Revisão bibliográfica

Envolveu a compilação de publicações referentes às áreas de estudo e assuntos relacionados ao tema, reunindo assim um conjunto de informações úteis sobre os métodos a serem utilizados no decorrer deste trabalho para que os objetivos propostos fossem alcançados. Essa etapa de revisão da literatura permitiu a construção de estratégias para levantamento de perfis geológicos e comparação das feições e estruturas observadas na área de estudo com aquelas descritas em regiões com contexto geológico similar.

1.3.2 Trabalhos de campo

As atividades de campo foram indispensáveis para a aquisição de dados nos derrames basálticos e permitiram uma melhor observação da grande maioria de suas feições e estruturas. Apesar das rochas basálticas serem bastante suscetíveis à alteração intempérica, especialmente nas porções de topo vesiculado, os afloramentos selecionados foram adequados para a concretização do trabalho.

As campanhas de campo foram divididas em seis etapas, sendo que cada uma teve duração de aproximadamente cinco dias. A etapa de descrição das estruturas e estruturas foi realizada nos afloramentos visitados, e em laboratório, utilizando amostras coletadas. É importante salientar que para a realização do estudo foi necessária a construção de secões verticais em escala de afloramento bem como a aquisição de fotografias de campo para a montagem de fotomosaicos e

croquis. Esse método utilizado em campo foi adaptado das técnicas de associação de elementos arquiteturais de Miall (2000) e Farrell (2010) e teve por objetivo final compor a arquitetura de fácies da região.

Análise no campo

Etapa 1: Acesso a área de estudo para seleção dos afloramentos disponíveis com o menor grau de alteração possível;

Etapa 2: Confecção de seções verticais (*graphic log*) paralelamente a aquisição de fotografias, semelhante ao método de análise de fácies vulcanoclásticas e sedimentares clásticas, onde no eixo das ordenadas (Y) foi inserida a espessura e no eixo das abscissas (X) os tamanhos dominantes dos grãos (no caso das rochas efusivas foram utilizados termos referentes a granulação: vidro, granulação fina, média e grossa).

Etapa 3: Seleção de um código de litofácies para ser utilizado nas seções verticais. Os códigos utilizados nesse estudo foram baseados em McPhie *et al.* (1993), Branney & Kokelaar (2002) e Caroff *et al.* (2000).

Nota: a simbologia deve ser selecionada de acordo com os tipos de rocha que se está trabalhando e a variabilidade das litofácies mapeadas.

Análise pós-campo

Etapa 4: Sobreposição de todas as fotos digitais em um programa gráfico (*Adobe Photoshop ou Autostitch*) gerando fotomosaicos que permitem auxiliar no mapeamento lateral dos cortes de estradas;

Nota: Se são observadas curvas/ondulações no afloramento, esses programas não podem ser utilizados, pois não conseguem normalizar grande parte dessas curvas. Se o afloramento apresentar uma pequena extensão lateral (500 m – 1 km), o programa Autostitch é preferido.

Etapa 5: Impressão de três fotomosaicos com a adição de *overlays* sobre os mesmos;

Etapa 6: Traçar diretamente sobre o *overlay* ressaltando a geometria externa dos derrames (lobos, lentes, lobados, etc) e o contato entre os lobos e os derrames mais espessos;

Etapa 7: Digitalização nos programas gráficos de seis croquis, três seções verticais e seus respectivos *overlays* fotointerpretados;

Etapa 8: Identificação da sucessão dos derrames a partir dos croquis e seções verticais digitalizados;

Etapa 9: Correlação dos derrames com os perfis verticais assegurando uma compreensão espacial e temporal da região (3D);

Etapa 10: Definição das litofácies existentes baseadas na variabilidade lateral e vertical das feições dos derrames, sendo que por fim foram definidas as associações de fácies.

1.3.3 Gamaespectrometria

Os dados de gamaespectrometria para K, U, Th e contagem total com 72 medidas foram adquiridos nos derrames básicos e ácidos dos afloramentos estudados, onde se pretendeu testar o uso do método gamaespectrométrico na individualização das fácies vulcânicas. Estudos realizados por Marques (1988) permitiram a comparação dos dados de U e Th em amostras de rochas ácidas, intermediárias e básicas da Bacia do Paraná. Análises dos teores de radionuclídeos em rochas da Austrália permitiram estabelecer uma correlação desses teores nas diferentes rochas ígneas (Dickson & Scott, 1997).

O equipamento utilizado foi o Explorium Radiation Detective Systems - Portable Gama Ray Spectrometer- software version RS-125/230 Super-Spec do Programa de Pós-graduação em Geociências da UFRGS. Os dados de K, U, Th e contagem total foram essenciais para: 1) separação de fácies tabulares simples de composta dos basaltos *pahoehoe* da Formação Serra Geral; 2) identificação de intrafácies dos basaltos *pahoehoe* decorrentes de variações nos padrões de vesiculação; 3) separação dos derrames básicos *rubbly* e *pahoehoe*, e estes dos derrames ácidos.

1.3.4 Descrições macroscópicas e microscópicas

Para os estudos macro e microscópicos foram coletadas 49 amostras nos três perfis, sendo que a primeira etapa da descrição macroscópica foi realizada ainda no campo, com o auxilio de uma lupa de mão com aumento de 10 vezes. A segunda etapa foi realizada no laboratório de microscopia da Universidade Federal do Rio

Grande do Sul, com o auxilio de uma lupa da marca Carls Zeiss Jena, cujos aumentos variam de 10 a 100 vezes.

Posteriormente, 41 das 49 amostras coletadas foram enviadas ao laboratório Spectrum Petrographics, localizado na cidade de Vancouver, Estados Unidos para confecção de lâminas polidas e impregnadas.

A etapa de petrografia envolveu a descrição de lâminas polidas utilizando um microscópio Leitz Wetzlar com cinco possibilidades de lentes ópticas, cujos aumentos vão desde 3,5 até 100 vezes. A análise microscópica teve por objetivo identificar as fases minerais e texturas de forma a estabelecer a ordem e a história de cristalização, bem como o *emplacement* desses derrames. A descrição petrográfica foi realizada através do *software Hardledge* (Lorenzatti *et al.,* 2011), que permite organizar os dados de acordo com mineralogia primária, texturas principais e subordinadas, bem como classificar a rocha a partir da contagem modal de 300 pontos. Essa quantificação é realizada com base no método Gazzi-Dickinson (Gazzi, 1966; Dickson, 1970; Zuffa, 1980), que consiste em uma análise estatística tradicionalmente utilizada para estimativa dos constituintes mineralógicos dispostos ao longo de linhas, a intervalos regulares sobre as lâminas. O fato das lâminas serem impregnadas com resina *epoxy* azul possibilitou a identificação e quantificação dos tipos de poros existentes nesses basaltos, os quais são imprescindíveis para estudos de porosidade e permeabilidade de rochas vulcânicas.

1.3.5 Geoquímica em rocha total

Nesta etapa foram adquiridos 30 dados químicos de rocha total para se investigar os contrastes entre derrames *pahoehoe* e *rubbly* da Formação Serra Geral. Porções de base, meio e topo dos derrames *pahoehoe* também foram analisadas para se investigar diferenças químicas internas nestes tipos de derrames. As amostras foram encaminhadas para o laboratório comercial Acme Analytical Laboratories Ltda, com matriz em Vancouver (Canadá).

A Acmelabs utilizou o pacote Grupo 4A + 4B para análise litogeoquímica de óxidos maiores, determinados por Inductively Coupled Plasma Atomic Emission Spectrometry (ICP-AES), e para análise de elementos traços e terras raras (ETR), determinados por Inductively Coupled Plasma Atomic Mass Spectrometry (ICP-MS). Esses procedimentos analíticos são descritos em detalhes no *folder* da empresa,

disponível no site www.acmelab.com, que inclui também os limite de detecção e a precisão analítica para cada elemento. A análise total de uma amostra requer 10 mg de amostra pulverizada.

Os resultados geoquímicos obtidos foram processados utilizando o *software GeoChemical Data toolkit* versão 2.3 (disponível em http://www.gcdkit.org/download) e posteriormente plotados em diagramas de classificação.

1.3.6 Geoquímica isotópica

Foram selecionadas 13 amostras para os estudos isotópicos de Sr, Nd e Pb, cujas análises foram realizadas no Laboratório de Geologia Isotópica da Universidade Federal do Pará (Pará-Iso UFPA) sob coordenação do Prof. Dr. Jean Michel Lafon. O equipamento utilizado foi o espectrômetro de massa ICP multi-coletor Thermo-Finnigan Neptune equipado com um sistema de nove coletores de íons em modo Faraday.

Para o procedimento de separação dos isótopos de Sr-Nd-Pb, aproximadamente 100 mg de amostra de rocha foi misturada a um *spike* de ^{149}Sm-^{150}Nd, e então dissolvida nos ácidos HNO_3, HCl and HF em bombas de Teflon Savillex® em forno microondas. Um procedimento cromatográfico de troca iônica de duplo estágio foi utilizado para a purificação dos elementos Pb, Sr, Nd e Sm. A primeira etapa consistiu na elutriação das amostras em colunas de Teflon preenchidas com a resina catiônica (Biorad Dowex AG 50W-X8) usando os ácidos HCl e HNO_3. Pb é coletado após elutriação com 3,9 ml de HCl 2N e Sr coletado após 13 mL de HCl 2N. O grupo dos ETRs foi extraído após elutriação com 2mL de HCl 2N e 12 mL de HNO_3 3N.

No estágio seguinte, os elementos Sm e Nd foram separados dos outros ETRs com o objetivo de evitar interferências isobáricas dos ETRP (Yang *et al.,* 2012) e a presença de elementos que tornem a ionização instável ou que interfiram na eficiência da ionização de Sm e Nd. A solução de ETR foi adicionada a colunas de Teflon preenchidas pela resina Eichrom® Ln, sendo que a fração de Nd foi coletada após elutriação de 7,3 mL de HCl 0,2N, e o Sm foi coletado após adição de 5 mL de HCl 0,2N e 7 mL de HCl 0,3N.

Para a segunda etapa de separação do Sr, a solução da amostra foi carregada em colunas de Teflon preenchidas pela resina Eichron® Ln, no qual o Sr

é coletado após adição de 2 mL de HNO_3 3,5N. Para a segunda separação cromatográfica de Pb, a solução de amostra foi adicionada à colunas de Teflon preenchidas por resina Eichrom® Ln, onde foram adicionados 3 mL de HCl 2N. O Pb foi coletado após adição de 3 mL de HCl 6N. A fração de Pb coletada na segunda separação foi dissolvida em 500μL de HNO3 3% +Tl (tálio) 50 ppb e então analisada. Os elementos Sr, Sm e Nd foram dissolvidos para análise em 2 mL de HNO_3 3%.

Os cálculos de incerteza para as razões Sm/Nd e $^{143}Nd/^{144}Nd$ são baseados nas análises repetidas dos materiais de referências BCR-1 e La Jolla, respectivamente (Oliveira *et al.,* 2008). As razões isotópicas de Sr foram normalizadas para $^{86}Sr/^{88}Sr$= 0,1194. As composições isotópicas de Nd foram normalizadas para $^{146}Nd/^{144}Nd$= 0,7219, cuja constante de decaimento utilizada foi o valor revisado por Lugmair & Marti (1978) de 6,54 x $10^{-12.y-1}$. Mais detalhes dos procedimentos experimentais estão disponíveis em Krymsky *et al.* (2007), Oliveira *et al.* (2008) e Romero *et al.* (2013).

CAPÍTULO 2

Contextualização

2.1 Grandes Províncias Ígneas

As grandes províncias ígneas são referidas como “Large Igneous Provinces” (*LIPs*), termo proposto por Coffin & Eldholm (1994) para identificar uma variedade de províncias ígneas máficas com grande extensão territorial > 0,1Mkm^2, curta duração de *emplacement* (<1-5 Ma) e grande volume (≈10^6 km^3). As *LIPs* não se formam por processos clássicos de espalhamento de assoalho oceânico ou subducção (Coffin & Eldholm, 1994). Sua origem e *emplacement* resultam de eventos ígneos anômalos na história da Terra que resultaram em grandes acumulações de rochas ígneas vulcânicas e plutônicas em um curto espaço de tempo (Coffin & Eldholm, 1994).

A maioria das *LIPs* é composicional e volumetricamente dominada por rochas máficas (SiO_2 < 56%), que afloram como sucessões de lavas basálticas, em geral toleíticas e pobres em fenocristais. Contudo, volumes consideráveis de magmatismo ácido estão frequentemente associados às *LIPs* continentais. Em outros casos, as *LIPs* são dominantemente ácidas sendo denominadas de Grandes Províncias Ígneas Félsicas (*Silicic Large Igneous Provinces - SLIPs*) (Figura 1).

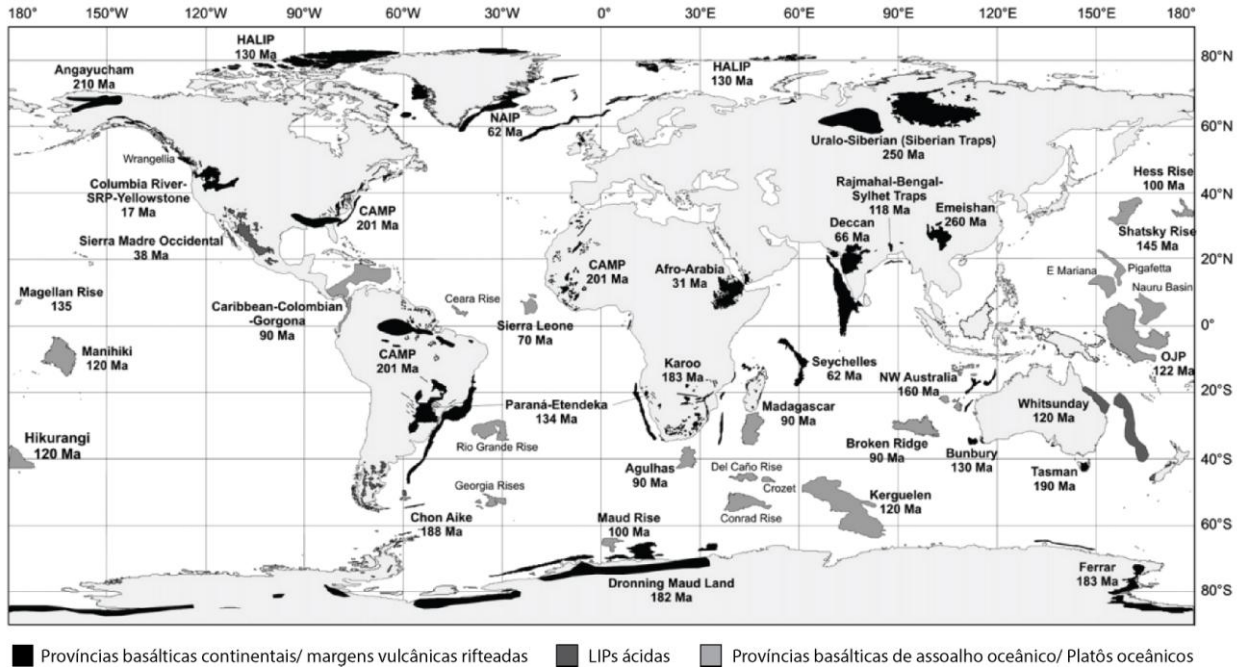

Figura 1. Distribuição global das grandes províncias ígneas (Bryan & Ernst, 2008).

A frequência dessas erupções e o volume total de magma liberado durante os principais pulsos magmáticos indicam que as *LIPs* são eventos excepcionais na história geológica da Terra e muitas vezes responsáveis por mudanças ambientais regionais ou globais incluindo, mudanças climáticas, eventos de extinção, mudanças topográficas regionais, e quebras de supercontinentes (Courtillot *et al.,* 1986; Rampino & Stothers, 1988; Courtillot, 1990, 1995, 1999; Glen, 1994; Rampino & Haggerty, 1996; Wignall, 2001, 2005; Courtillot & Renne, 2003; Self *et al.,* 2005; Kelley, 2007).

As *LIPs*, tanto básicas quanto ácidas, foram definidas ou caracterizadas por um conjunto de atributos além de extensão: 1) idade (Arqueano, Proterozoico, Fanerozoico); 2) volume; 3) contexto crustal (continental *versus* oceânico); 4) contexto tectônico; 5) duração ou rapidez de colocação do magma; 6) caráter intrusivo ou extrusivo (Sheth, 2007); 7) composição (ácidas ou básicas; Bryan & Ernst, 2006).

A base de dados no qual o termo LIP foi definido se resume quase que exclusivamente aos registros bem preservados do Mesozoico e Cenozoico que ocorrem tanto em continentes quanto oceanos, em contextos puramente intraplaca e ao longo de limites de placas. A classificação de *LIPs* inclui províncias basálticas continentais; margens vulcânicas passivas ou rifteadas; platôs oceânicos e basaltos de cadeias mesoceânicas (Tabela 1; Coffin & Eldholm, 1992, 1994, 2005). Uma lista completa com as informações de todas as *LIPs*, incluindo fragmentos de *LIPs* e as S*LIPs* pode ser consultado na Tabela 1.2 de Ernst (2014).

Nome da LIP	Tipo	Localização	Idade (Ga)	Área (A) Volume (V) (Mkm^2 e Mkm^3)	Referências selecionadas
Columbia River	C	América do Norte	0,02	A= 0,24	Reidel *et al.* (2013)
Afro-Arabian	C	Arabian Penn. África	0,03	A= 2	White & McKenzie (1989); Avni *et al.* (2012)
Sierra Madre Ocidental	A	Sudoeste EUA, México	0,03	A= 0,40 V= 0,39	Bryan & Ferrari (2013)
Província Ignea do Atlântico Norte	C	Greenland/Norte do Canadá e Europa (UK)	0,06	A= 1,30	White & McKenzie (1989); Storey *et al.* (2007); Jerram *et al.* (2009)
Deccan	C	India	0,07	A= 1,80	Hooper *et al.* (2010); Sheth & Vanderkluysen (2014)
Kerguelen- (Broken Ridge)	O	Oceano Índico	0,12	V= 9,10	Wallace *et al.* (2002)
Whitsunday	A	Austrália	0,09-0,12	V= 2,20	Pirajno & Hoatson (2012)
Ontong Java+Bacia Nauru	O	Oceano Pacifico	0,12	A= 4,27 V= 58	Ingle & Coffin (2004)
Paraná-Etendeka	C	América do Sul e África	0,13	A= 2	Peate (1997); Thiede & Vasconcelos (2010)
Karoo, Ferrar	C/A	África, América do Sul, Antarctica	0,18	V= 5	Neumann *et al.* (2011); Svensen *et al.* (2012); Storey *et al.* (2013)
Chon Aike	A	América do Sul, Antarctica	0,15-0,18	V= 0,23	Pankhurst *et al.* (1998, 2000)
Siberian Trap	C	Ásia	0,25	A= 7 V= 4	Sobolev *et al.* (2011); Ivanov *et al.* (2013)
Gawler Range	C/A	Sul do Cráton Australiano	1,59	A= 0,131	Pirajno & Hoatson (2012)
Uatumã	A	Cráton Amazônico	1,89-1,87	A= 1,50	Klein *et al.* (2012); Barreto *et al.* (2014a)

Tabela 1. Idade, extensão areal e volume das principais *LIPs* espalhadas pelo mundo. Abreviações: C= continental, O= platô oceânico, A= ácida (Ernst, 2014).

Desde a primeira classificação das *LIPs* (Coffin & Eldholm, 1994) houve um progresso substancial no sentido de esclarecer outros registros que se formaram no Paleozoico, Paleoproterozoico e Arqueano (Ernst & Buchan, 1997, 2001, 2003; Arndt *et al.,* 2001; Tomlinson & Condie, 2001; Isley & Abbott, 2002). No entanto, em *LIPs* antigas, grande parte do registro de rochas vulcânicas desapareceu em decorrência da erosão. Assim, a classificação das *LIPs* mais antigas tem sido baseada principalmente na extensão areal e volume inferido das rochas intrusivas.

Recentemente, Bryan & Ernst (2008) propuseram uma revisão na definição de *LIPs* e incluíram *LIPs* mais antigas, no qual enxames de diques continentais e províncias intrusivas máficas-ultramáficas são dominantes. Também foram incluídos *greenstone belts* de rochas toleíticas e komatiiticas arqueanas, além de *LIPs* ácidas (Figura 2).

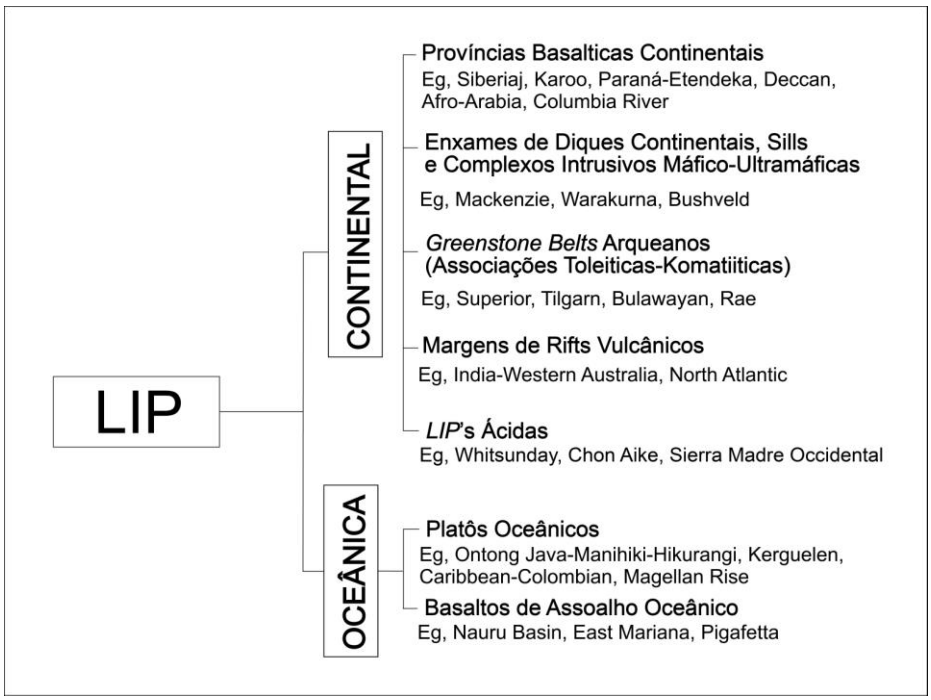

Figura 2. Classificação das grandes províncias ígneas incluindo *LIPs* antigas e ácidas (traduzido de Bryan & Ernst, 2008).

Diferentemente das grandes manifestações vulcânicas básicas, as erupções vulcânicas ácidas de grande volume são associadas a diversos regimes tectônicos e não são exclusivas de eventos *LIPs* (Thordarson *et al.,* 2009). As rochas ácidas em *LIPs* são, em geral, descritas como fluxos piroclásticos de alta temperatura (Petrini *et al.,* 1989; Roisenberg, 1989; Whittingham, 1989; Milner *et al.,* 1992, 1995; Roisenberg & Viero, 2000; Bryan *et al.,* 2002; Ukstins Peate, 2005; Bryan, 2007). Por outro lado, estes depósitos também são interpretados como lavas ácidas riolíticas com ampla extensão areal e originadas por uma efusão contínua (Bellieni *et al.,* 1986; Comin-Chiaramonti, 1988; Henry & Wolff, 1992; Umann *et al.,* 2001; Janasi *et al.,* 2007; Luchetti, 2010; Lima *et al.,* 2012a).

2.2 Províncias Basálticas Continentais

Entre os diferentes tipos de *LIPs*, destacam-se as grandes províncias basálticas continentais (PBCs), que em geral constituem imensos platôs que antecedem a quebra dos supercontinentes e a formação de riftes (White & McKenzie, 1989; Coffin & Eldhom, 1994).

As PBCs podem ser definidas como imensas manifestações magmáticas colocadas sobre áreas continentais, razão pela qual são frequentemente consideradas como evidências de plumas mantélicas (White & McKenzie, 1995). Muitos desses derrames extravasaram sobre um curto espaço de tempo, na ordem de 1 Ma (Bryan & Ernst, 2008), e são aparentemente sincrônicos com as grandes crises climáticas globais e extinções em massa. Essas províncias estão distribuídas em todos os continentes no globo, com expressão areal significativa, destacando-se as Províncias do Deccan, Paraná-Etendeka, Columbia River, Siberian Traps e Karoo (Figura 1, Tabela 1).

Em muitas PBCs os basaltos ocorrem associados com magmas ácidos (riolitos), com raras composições intermediárias. Essa bimodalidade levou diversos autores a propor que os magmas ácidos são gerados pela fusão parcial de dioritos e rochas gabróicas alojadas como *underplated* na base da crosta continental (Bryan *et al.,* 2010).

Os métodos de investigação dessas províncias são em geral fundamentados nos estudos pioneiros da PBC Columbia River, localizada no noroeste USA, que apresenta a menor extensão areal, dentre as PBCs existentes, em torno de ~0.234 Mkm^3 (Swanson *et al.,* 1975; Reidel *et al.,* 1989; Tolan *et al.,* 1989; Hooper, 1997; Self *et al.,* 1998; Camp *et al.,* 2003; Hooper *et al.,* 2007). Contudo, diversos estudos vêm sendo desenvolvidos atualmente em outras PBCs, tais como no Deccan, Paraná-Etendeka e Etiópia (Jerram *et al.,* 1999; Jerram, 2002; Waichel *et al.,* 2006a, 2006b, 2008, 2012; Jay & Widdowson, 2008; Self *et al.,* 2008; Chenet *et al.,* 2009; Brown *et al.,* 2011; Lima *et al.,* 2012a, 2012b; Barreto *et al.,* 2014b; Rossetti *et al.,* 2014). As PBCs, em geral, são claramente associadas com tectônicas extensionais que aparecem como consequência de estiramento litosférico associado à subida de material mantélico quente profundo. Em geral, os magmas PBCs são toleiíticos e com composições mais evoluídas, exibindo conteúdos baixos de MgO, Ni e Mg#,

atribuídos a um fracionamento significativo de líquidos picriticos primários (Cox, 1980; Garfunkel, 2008).

É frequente em PBCs, a presença de basaltos baixo e alto Ti (BTi e ATi), cuja distinção reflete basicamente os níveis de elementos incompatíveis (e.g. Marsh *et al.,* 2001; Jourdan *et al.,* 2007; Bryan & Ernst, 2008). Além disso, existe uma típica provincialidade na distribuição de suítes BTi e ATi (e.g. Paraná-Etendeka, Karoo, e Emeishan). O caráter BTi dos magmas basálticos toleiiticos tem sido comumente interpretado como reflexo da contaminação crustal por manto litosférico subcontinental e/ou crosta continental (e.g. Carlson, 1991; Peate,1997; Ewart *et al.,* 1998, 2004), ou por condições de altos graus de fusão parcial do manto ou fusão a profundidades mais rasas (Arndt *et al.,* 1993; Xu *et al.,* 2004). Em contrapartida, as suítes máficas ATi comumente exibem maiores similaridades geoquímicas e isotópicas com basaltos de ilhas oceânicas (OIBs – geoquímica intraplaca) e são relacionadas a manto astenosférico relativamente não contaminado ou com um componente de pluma (e.g. Arndt *et al.,* 1993; Zhao *et al.,* 1994; Ewart *et al.,* 1998, 2004).

Considerando que os magmas BTi e ATi têm histórias petrogenéticas distintas, Bryan *et al.* (2010) propõem um modelo para a evolução dos magmas básicos e ácidos das PBCs. Esses autores sugerem que em pressões mais elevadas ocorrem processos como cristalização fracionada e assimilação crustal, enquanto que em profundidades mais rasas são comuns complexos de *sills* colocados previamente à erupção (Figura 3).

Conforme observado na Figura 3, na trajetória A os magmas basálticos mostram pouca ou nenhuma evidência para armazenamento crustal ou assimilação, preservando as assinaturas isotópicas e geoquímicas de manto. A transferência desses magmas para a superfície seria através de fissuras diretamente das regiões fontes do manto superior. Alternativamente esses magmas poderiam ter residido temporariamente em reservatórios no manto superior ou em *underplate* máfico, evitando dessa forma oportunidades para assimilação crustal.

Nas trajetórias B1 e B3 é comum que o grande volume de magmas basálticos BTi seja submetido a armazenamento em profundidades crustais inferiores e superiores resultando em assimilação crustal, cristalização e desgaseificação para produzir lavas basálticas com conteúdos de MgO menor, e andesito basálticos

afíricos ou com fenocristais de plagioclásio. Na trajetória B2 os basaltos são do tipo ATi e possuem evidências para armazenamento crustal, embora sejam gerados pela fusão de intrusões máficas (*underplate* máfico), as quais diluem os indicadores geoquímicos de contaminação crustal, sendo dominantes os processos de cristalização fracionada e mistura de magmas.

Na trajetória C, os riolitos de alta temperatura e grande volume que ocorrem comumente nas *LIPs* continentais são muitas vezes explicados por processos AFC de grande escala. Esse processo envolveria fusão de granulito crustal inferior e/ou refusão de *underplate* basáltico com adicional *input* de magmas ácidos e básicos e prolongamento da cristalização fracionada para gerar magmas ácidos pobres em cristais, anidros e de alta temperatura. Essas erupções na superfície são expressas por meio de estruturas *sag* regionais (Ewart *et al.,* 2002) ou condutos fissurais, no qual são ausentes feições de caldeiras devido os reservatórios magmáticos de alta temperatura residirem em níveis crustais profundos.

Na trajetória C1 são descritos os riolitos BTi com maior envolvimento crustal, onde ocorre fusão crustal inferior e assimilação em resposta ao *underplating* basáltico com recarga máfica adicional. Além disso, esses magmas podem ficar armazenados nas porções médias e superiores da crosta, onde ocorre assimilação de materiais crustais graníticos e cristalização fracionada. Na trajetória C2 são comuns os riolitos ATi que possuem envolvimento crustal mínimo, onde ocorre fracionamento ou refusão de basaltos ATi próximo ao limite manto-crosta com adicional recarga de magma máfico. Além disso, pode ocorrer armazenamento em níveis crustais médios onde haveria mistura de magma ácido ou contaminação resultante de assimilação crustal ou interação com magmas ácidos que não extravasaram.

Ignimbritos riolíticos de grande volume e temperatura baixa, rico em cristais são posicionados na trajetória D1. Esses ignimbritos são encontrados principalmente em *LIPs* ácidas (Bryan, 2007), nos ambientes de margens continentais extensionais, cujo processo de formação de batólitos na crosta superior ocorre através de intrusões rasas e *underplating* de magmas máficos basálticos que teriam fornecido o *input* termal e de voláteis necessários para desencadear as erupções das câmaras crustais superiores e o desenvolvimento de caldeiras bem definidas. Na trajetória D2 são descritas intrusões de basaltos em profundidades crustais superiores que foram

geradas rapidamente e extravasaram volumes moderados de riolitos pobres em cristais através da refusão de rochas plutônicas altamente diferenciadas e solidificadas, as quais foram formadas durante as fases precoces do magmatismo no evento *LIP*.

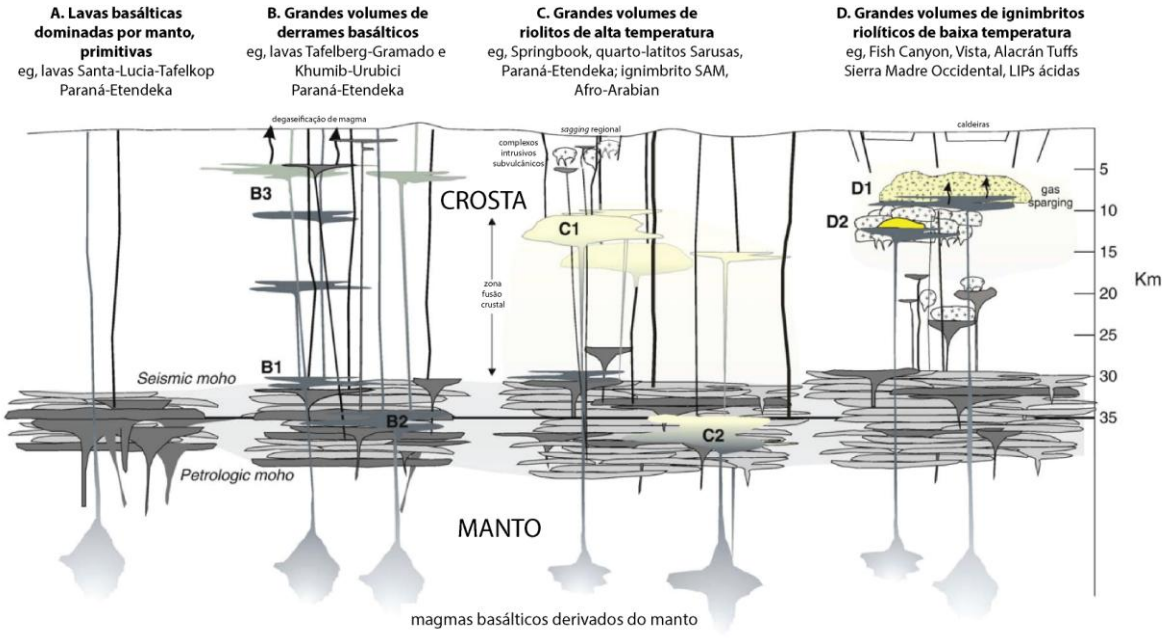

Figura 3. Visão crustal conceitual dos quatro membros finais de caminhos petrogenéticos para erupções de grande magnitude (basálticas e ácidas) principalmente em *LIPs* continentais (traduzido de Bryan *et al.,* 2010).

2.3 Província Paraná-Etendeka

A Província Paraná-Etendeka é uma das maiores PBCs do planeta, com um volume preservado em torno de $1x10^6$ km^3 (Cordani & Vandoros, 1967; Erlank *et al.,* 1984; Peate, 1997), cuja atividade vulcânica está concentrada entre 135 e 130 Ma (Turner *et al.,* 1994; Milner *et al.,* 1995; Renne *et al.,* 1996). Aproximadamente 95% dessa PBC (Paraná) aflora na América do Sul, enquanto os 5% restantes (Etendeka) estão na Namíbia, África. Quando da formação dessa PBC, essas duas províncias magmáticas estavam interligadas, o que permite uma correlação estratigráfica e de idade entre ambas (Figura 4, Figura 5).

Os estudos na Província Paraná-Etendeka têm enfatizado principalmente os aspectos geoquímicos (Bellieni *et al.,* 1984; Mantovani *et al.,* 1985; Melfi *et al.,* 1988; Peate *et al.,* 1992; Peate, 1997) e geocronológicos (Turner *et al.,* 1994; Renne *et al.,*

1995; Janasi *et al.,* 2011), sendo que os mais recentes têm enfatizado o arcabouço estratigráfico e a arquitetura interna e externa, fundamentada na caracterização dos morfotipos de derrames, associações de fácies, padrões texturais, paleotopografia e taxas de efusão (Jerram *et al.,* 1999; Jerram, 2002; Lima *et al.,* 2012a, 2012b; Waichel *et al.,* 2012; Barreto *et al.,* 2014b; Rossetti *et al.,* 2014).

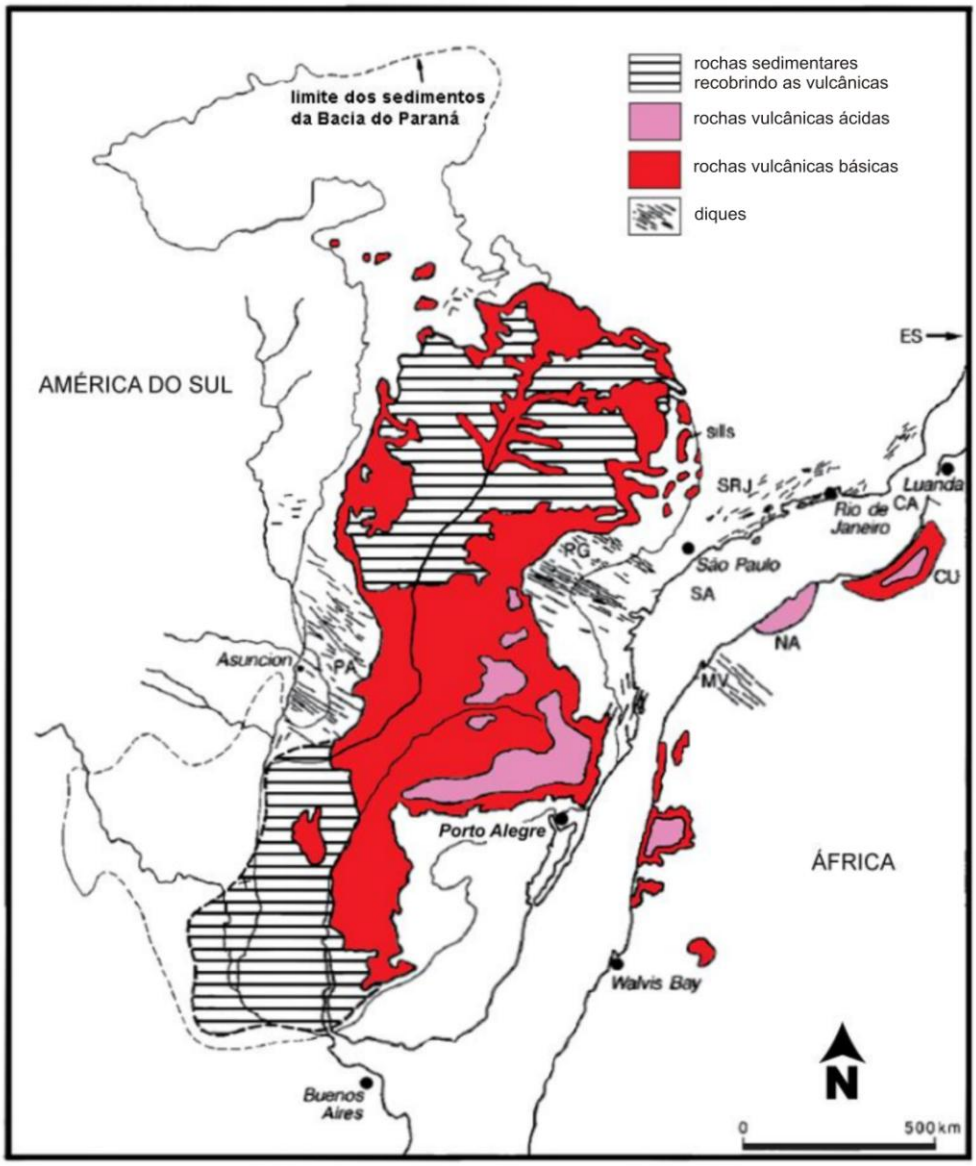

Figura 4. Reconstrução da PBC Paraná-Etendeka durante a fase inicial de abertura da porção sul do Oceano Atlântico, mostrando a grande extensão desse vulcanismo na Província Paraná quando comparado com a porção remanescente na África (Peate, 1997).

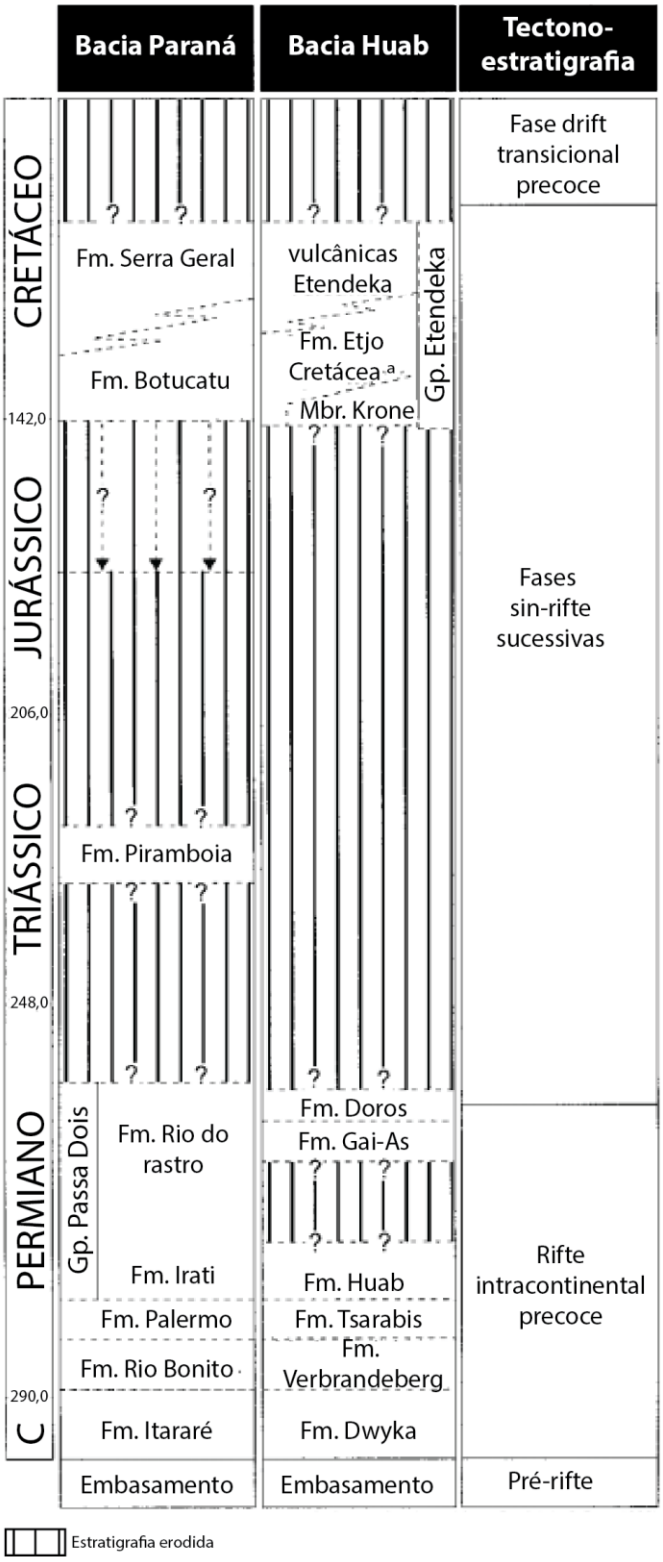

Figura 5. Correlação esquemática geral da Província Paraná-Etendeka com as Bacias do Paraná, sul do Brasil, e Bacia Huab, NW da Namíbia (traduzido de Jerram *et al.,* 1999).

CAPÍTULO 3

Estado atual da arte

3.1 Morfologias de lavas subaéreas e implicações nas taxas de efusão, paleotopografia e mecanismos de *emplacement*

A identificação da morfologia e das características físicas de lavas em PBCs fornece informações sobre os mecanismos de *emplacement* desses derrames, o qual permite a reconstrução da arquitetura das fácies vulcânicas e auxilia na interpretação da história evolutiva do vulcanismo dessas províncias (Self *et al.,* 1997; Jerram, 2002; Bondre *et al.,* 2004; Single & Jerram 2004; Waichel *et al.,* 2006a, 2006b, 2012; Hartmann *et al.,* 2010; Lima *et al.,* 2012b; Barreto *et al.,* 2014b; Rossetti *et al.,* 2014).

3.1.1 Tipos de derrames básicos subaéreos

Lavas basálticas subaéreas foram divididas em dois tipos (*end-members*): *pahoehoe* e *'a'ā* (Dutton, 1884; MacDonald, 1953). Esta subdivisão fundamentou-se a partir da morfologia de superfície e estruturas internas dos derrames (Figura 6). Entre esses dois tipos, também foram identificados tipos de lavas basálticas transicionais (Duraiswami *et al.,* 2003, 2008).

Lavas *pahoehoe* e *'a'ā* possuem mecanismos de *emplacement* distintos, que determina diferenças nas feições de superfície, estruturas internas e padrões de vesiculação. Rowland & Walker (1990) atribuem essas diferenças a taxa de fluxo volumétrico (taxa de efusão). Loock *et al.* (2010) discutem que lavas *pahoehoe* podem se transformar em *'a'ā* ou mesmo em lavas transicionais quando é ultrapassada a zona de transição (TTZ; Figura 7). Essa mudança ocorre devido ao aumento da taxa de deformação por cisalhamento ou da viscosidade aparente, a medida que os derrames *'a'ā* são gerados em um sistema aberto que expõe a lava para a atmosfera, a qual resfria rapidamente com a desvolatização.

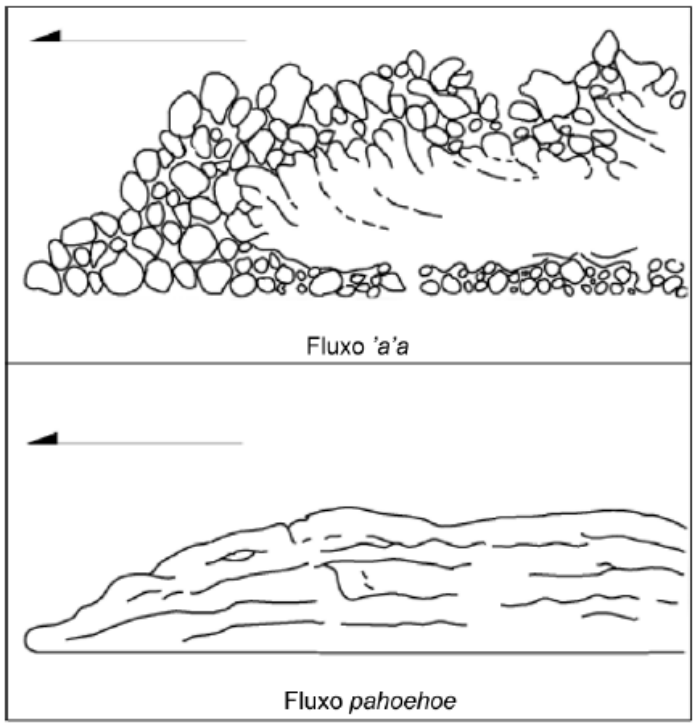

Figura 6. Morfologia característica de fluxos *'a'ā* e *pahoehoe*. A seta indica a direção de movimento do fluxo (traduzido de Lockwood & Lipman, 1980).

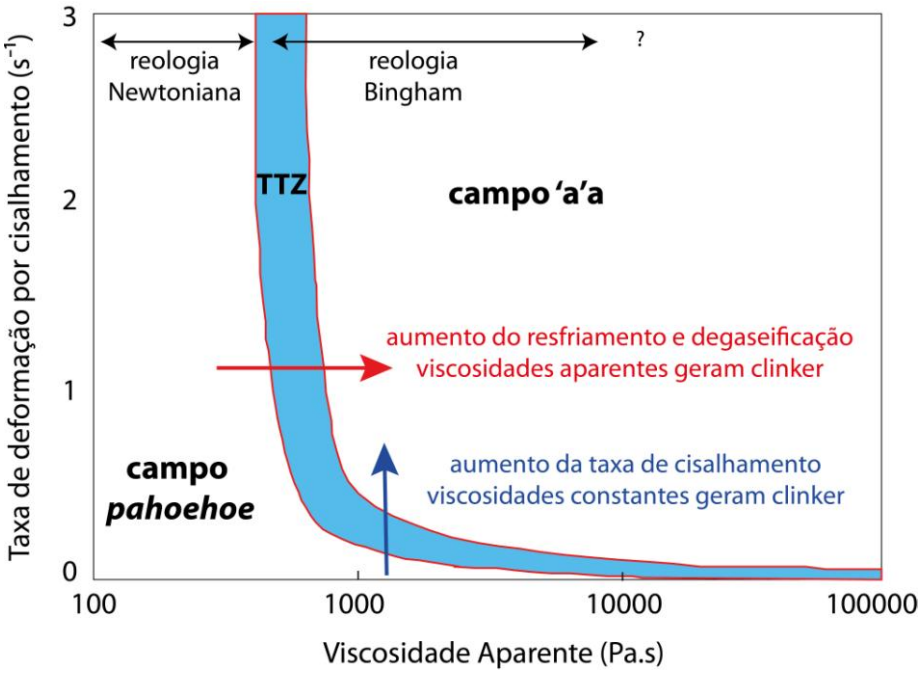

Figura 7. Diagrama da taxa de deformação por cisalhamento *vs.* viscosidade Newtoniana aparente, mostrando as relações aproximadas dos campos de estabilidade para as lavas *pahoehoe* Hawaiianas e os fluxos *'a'ā*, incluindo a zona de transição (TTZ) (traduzido de Loock *et al.,* 2010).

Derrames pahoehoe

Este tipo de derrame possui uma estruturação interna dividida em crosta superior, núcleo e crosta inferior, cujas superfícies são lisas, onduladas ou em corda (MacDonald, 1953; Aubele *et al.,* 1988).

Este tipo morfológico se desenvolve a partir de baixas taxas de efusão (< 5 – 10 m^3/s; Rowland & Walker, 1990) e paleotopografias planas (< 5º) que permitem a formação de uma crosta externa de resfriamento. Essa crosta preserva a estrutura interna do sistema (em geral 1100º C), com uma perda de calor por condução muito lenta (~1º C por km) quando transportada ao longo de tubos (Keszthelyi, 1995). Estima-se que este tipo de derrame pode se deslocar por até dezenas a centenas de quilômetros de distância da sua fonte, em superfícies horizontalizadas (<5º), antes da lava solidificar completamente (em torno 1000ºC - 900ºC).

A dinâmica dos derrames *pahoehoe* envolve inicialmente um avanço lento dos lobos com pequena espessura onde se forma rapidamente uma crosta superior fina, de comportamento plástico, devido ao resfriamento da lava em contato direto com a atmosfera. Com o contínuo resfriamento da lava, a crosta externa tende a espessar e se tornar mais rígida, aumentando consequentemente sua capacidade de reter o fluxo de lava, o que causa a inflação devido à recarga constante de lava vinda da fonte (Hon *et al.,* 1994; Self *et al.,* 1998). Quando a inflação se torna maior do que a capacidade da crosta de retê-la, o lobo se rompe, gerando um próximo. A repetição deste processo produz uma sucessão de lobos inflados interligados, com morfologia externa tabular, formando *sheet flows* se a topografia assim permitir (Hon *et al.,* 1994) (Figura 8A).

Segundo observações no Havaí, a formação de *sheet flows* ocorre em terrenos com inclinação de no máximo 2º, e geralmente menores do que 1º. Terrenos com inclinações mais altas originariam lobos alongados que não coalesceriam lateralmente, o que favoreceria a formação de fluxos canalizados ao invés de *sheet flows* (Hon *et al.,* 1994). Diante dessas possibilidades, a identificação de fluxos inflados fornece informações fundamentais sobre o paleorelevo, que é fundamental para entender a morfologia dos edifícios vulcânicos (Cashman & Kauahikaua, 1997).

Lavas *pahoehoe* são descritas na maioria das PBCs como os primeiros derrames a extravasarem com baixas taxas de efusão horizontalizando o

paleorelevo (Jerram *et al.,* 2000; Jerram & Widdowson, 2005). Dependendo do local, as lavas podem se acumular entre os obstáculos topográficos gerando derrames espessos do tipo *ponded pahoehoe*.

Na PBC Paraná-Etendeka, os primeiros derrames se colocaram nas interdunas de grandes *ergs* ativos (Scherer, 2002), tornando-se canalizados, e consequentemente, bastante espessos (Jerram *et al.,* 1999, 2000; Waichel *et al.,* 2012). Após o preenchimento das depressões, observam-se lavas *pahoehoe* com morfologias composta anastomosada (derrames *pahoehoe* compostos) e tabular clássica (derrames *pahoehoe* simples; Jerram, 2002; Waichel *et al.,* 2012). Os derrames *pahoehoe* compostos podem ser muitas vezes delimitados em escala de afloramento, onde exibem uma crosta fina vítrea que os envolve, cujo topo é caracterizado por grande vesiculação e a base é marcada por *pipe v*esículas (lobos do tipo P), sendo que algumas vezes os derrames exibem vesiculação generalizada (lobos do tipo S - *spongy*) (Figura 8B).

Figura 8. A) *Sheet flows* formadas no Hawaii, os quais são caracterizados por lobos *pahoehoe* inflados coalescidos lateralmente, cujos superfícies são lisas e em corda (extraído de Google imagens); B) derrame *pahoehoe* da Formação Serra Geral (região de Santa Cruz do Sul, RS) marcado no topo por uma superfície lisa e intensa vesiculação (lobo tipo S), o qual é sobreposto por um derrame *pahoehoe* com *pipe* vesículas (seta amarela) na base (lobo tipo P).

Derrames ‘a’ā

Este tipo de derrame possui o topo e a base de escórias, com vesículas alongadas e reentrâncias das zonas escoriáceas na porção central maciça, a qual é gerada pela súbita desvolatização e resfriamento (MacDonald, 1953; Kilburn, 1990).

Derrames *‘a’ā* são formados quando a lava é transportada em canais abertos, em geral associados a altas taxas de efusão (MacDonald, 1953; Pinkerton & Sparks, 1976; Rowland & Walker, 1990), ou a grandes taxas de deformação durante o fluxo (*shear rates*) causadas por paleorelevos acentuados (Hon *et al.,* 2003). Sob estas condições, as crostas externas dos derrames não se estabilizam e tendem a se romper e fragmentar continuamente em brechas *clinker*, se as tensões de cisalhamentos ultrapassarem o limiar dúctil-frágil (Kilburn, 1990; Cashman *et al.,* 1999; Soule & Cashman, 2005; Loock *et al.,* 2010). A brecha *clinker* do topo desses derrames seria transportada para frente da lava e incorporada a camada *clinker* da base, em um movimento análogo ao de uma esteira (Figura 9A). Essa hipótese de movimento *caterpillar* foi originalmente definida para os derrames do Hawaii que possuem declives acima de 4º (MacDonald, 1953).

Estudos recentes têm apontado que a hipótese de movimento análogo a uma esteira também pode ser aplicado em algumas PBCs (Brown *et al.,* 2011; Duraiswami *et al.,* 2014). Em outros exemplos de PBCs, o paleorelevo horizontalizado pelos derrames *pahoehoe* antecessores não permite o *emplacement* de lavas *‘a’ā* (Thordarson, 2006; Waichel *et al.,* 2012).

O resfriamento rápido dos derrames *‘a’ā* resulta em uma perda de calor de 2°C/km a 5°C/km, que aumenta a viscosidade aparente e a taxa de deformação por cisalhamento durante o escoamento (Loock *et al.,* 2010), levando a uma maior cristalinidade (quantidade de cristais) nos seus núcleos (MacDonald, 1953). Essa ineficiência termal do seu sistema de transporte restringe o deslocamento desses derrames por longas distâncias, o que poderia ser um bom indicador de proximidade com a fonte (MacDonald, 1953; Pinkerton & Sparks, 1976; Rowland & Walker, 1990; Self *et al.,* 1997; Brown *et al.,* 2011).

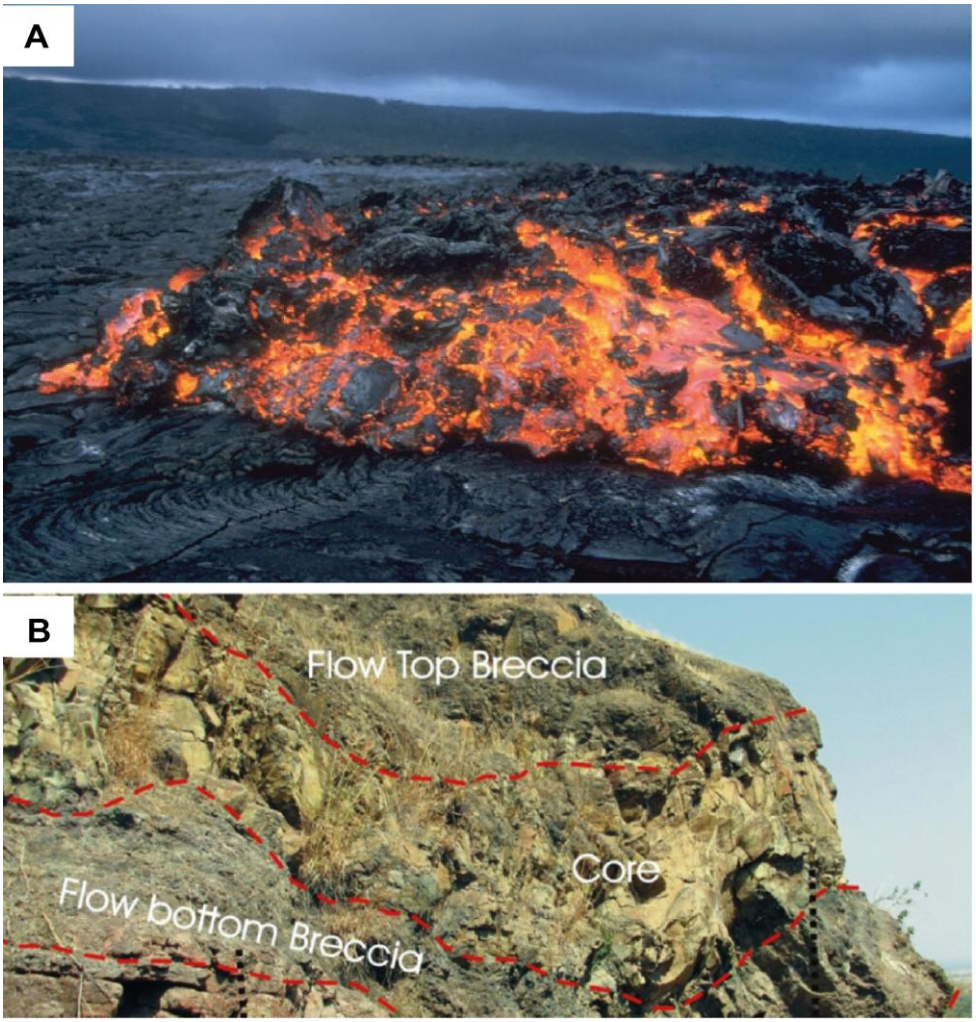

Figura 9. A) Frente de uma lava hawaiiana do tipo *'a'ā* sobre terreno mais antigo formado por lava *pahoehoe* com superfície em corda (extraído de USGS); B) derrame *'a'ā* exposto na Província continental Deccan, destacando-se base e topo brechados e núcleo maciço (extraído de Duraiswami *et al.,* 2014).

Derrames transicionais

Algumas lavas basálticas ocorrem entre os tipos *'a'ā* e *pahoehoe*. Estes morfotipos transicionais também têm sido referidos como *slabby pahoehoe*, *toothpaste pahoehoe, hummocky pahoehoe* e *rubbly pahoehoe* (Figura 10). Exemplos desses tipos de lavas estão bem documentados nas PBCs Paraná-Etendeka e Deccan (Managave, 2000; Keszthelyi *et al.,* 2001; Duraiswami *et al.,* 2003, 2008, 2014; Bondre *et al.,* 2004; Waichel *et al.,* 2006a, 2006b; Bondre & Hart, 2008; Barreto *et al.,* 2014b; Rossetti *et al.,* 2014).

Lavas *pahoehoe* do tipo pasta de dente (*toothpaste pahoehoe;* Rowland &

Walker, 1987) exibem sulcos (ranhuras) longitudinais, orientados paralelamente à direção de movimentação da lava ou mostram uma superfície recoberta por pequenos espinhos e ondulações transversais de escala maior que as superfícies em cordas (Figura 11A). Este tipo de lava se assemelha aquelas *'a'ā* proximais.

Lavas pahoehoe em placas (*slabby pahoehoe*; Peterson & Tilling, 1980; Rowland & Walker, 1987) são formadas quando fragmentos de superfícies em corda são englobados durante o movimento da lava subjacente (Figura 11B). A ocorrência de lavas *pahoehoe* em placas pode estar relacionada aos estágios iniciais da transição de derrames *pahoehoe* para *'a'ā* ou à geração de lobos (*breakouts*) que emergem da porção frontal de derrames mais espessos (Hon *et al.,* 1994).

Lavas *rubbly pahoehoe* (Keszthelyi & Thordarson, 2000) são divididas, em geral, em quatro partes: 1) crosta basal vesiculada e suavemente preservada, 2) núcleo maciço afanítico com disjunções curvi-planares, 3) porção superior do núcleo vesiculada que transiciona para 4) topo com superfície *rubbly* brechada e escoriácea (Figura 11C, 11D).

Tipo de lava	Definição	Desenho esquemático	Referências relacionadas	Significado
Pahoehoe	Um termo havaiano que significa lava básica não fragmentada e ondulada que possui superfícies em corda, onduladas, lobadas ou suaves. Lavas *pahoehoe* são compostas de diversas unidades.	Unidades múltiplas constituindo lavas pahoehoe 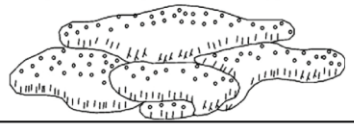	Macdonald (1953) Walker (1993) Self *et al.* (1998) Jay *et al.* (2009) Vye-Brown *et al.* (2013a,b)	Estas feições de superfície ocorrem devido a movimentação da lava fluida abaixo da crosta da superfície congelada. Este é um tipo de lava composta.
Hummocky pahoehoe	Uma variedade de lava *pahoehoe* que consiste em dedos de lavas, pequenos lobos e tumuli. A superfície desse tipo de lava é suave, bun-like e *hummocky*	Superfície hummocky suave 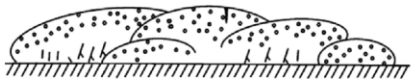	Swanson (1973) Bondre *et al.* (2004) Duraiswami (2009)	Este tipo de fluxo composto se forma ou sob taxas baixas de efusão ou devido a paleotopografia ondulada.
Sheet pahoehoe	Uma variedade de lava *pahoehoe* que consiste de grandes lobos tabulares e unidades espessas de lençóis de lavas. As unidades são empilhadas umas sobre as outras e formam uma geometria tabular plana.	Superfície plana, suavemente ondulada 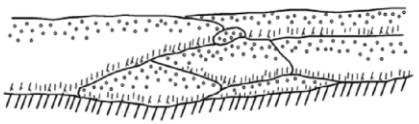	Aubele *et al.* (1988) Self *et al.* (1998) Duraiswami (2009)	Inflação e coalescência de lobos de lavas que originam *sheet* lobos com topos suavizados e típica estrutura interna em tripartite (crosta-núcleo-zona de *pipes* na base)
Slabby pahoehoe	Essas lavas contém uma série de placas regularmente espaçadas, com poucos metros de diâmetro e de espessura. Essas placas em geral estão quebradas e inclinadas graças ao movimento de massa ou drenagem da lava subjacente.	Superfície rompida com placas crustais 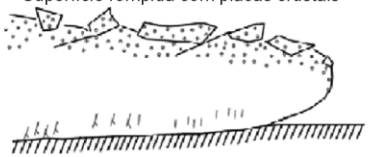	Peterson & Tilling (1980) Guilbaud *et al.* (2005)	Este é considerado um tipo de lava gradacional entre *pahoehoe* e *'a'ā*, o qual exibe característica predominante de lavas *pahoehoe*, embora com uma crosta de topo rompida (escoriácea)
Rubbly pahoehoe	Derrames com bases preservadas e crosta superior brechada constituem um tipo morfológico que difere em características daquelas típicas *pahoehoe* e *'a'ā*	Superfície brechada e base preservada 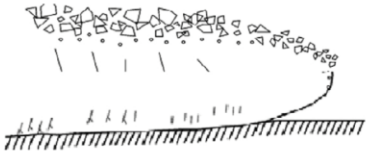	Managave (2000) Keszthelyi & Thordarson (2000) Guilbaud *et al.* (2005) Duraiswami *et al.* (2008)	Tipo de lava transicional entre pahoehoe e *'a'ā* que foi colocada sob taxas de efusão ligeiramente mais altas que aquelas das lavas *pahoehoe*
'A'ā	*'A'ā* é um termo havaiano que significa lava áspera e pedregosa. Esta representa uma dos três tipos de derrames básicos, cuja superfície é composta de lava *clinker* quebrada.	Superfície escoriácea irregular na base e topo 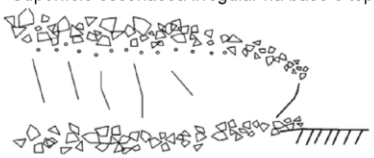	Macdonald (1953) Walker (1993)	Derrames *'a'ā* são geralmente os mais viscosos de todos os tipos morfológicos e avançam mais lentamente que os derrames *pahoehoe* sob mesmas condições de declividade

Figura 10. Classificação dos derrames básicos subaéreos baseados nas feições de superfície (traduzido de Duraiswami *et al.*, 2014).

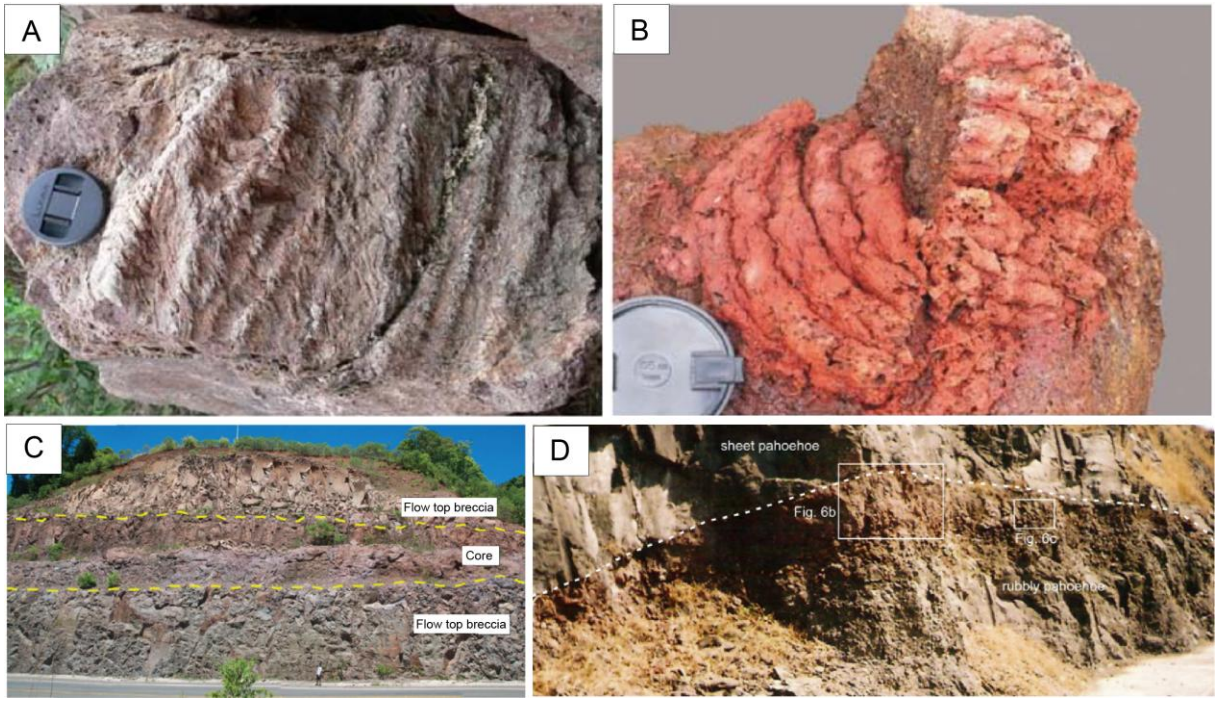

Figura 11. Tipos de derrames básicos transicionais. A) Derrame *pahoehoe* com superfície do tipo pasta de dente; B) derrame com processo de fragmentação da superfície em corda formando *pahoehoe* em placas (fotografias A e B extraídas de Waichel *et al.*, 2006b); C) contato entre dois derrame do tipo *rubbly pahoehoe* na Formação Serra Geral, na região de Santa Cruz do Sul-Herveiras (extraído de Barreto *et al.,* 2014b); D) exemplo de derrame do tipo *rubbly pahoehoe* descrito na Província Deccan (extraído de Duraiswami *et al.,* 2014).

3.2. Análise de fácies

Historicamente, a análise de fácies é um método muito utilizado em ambientes sedimentares (Walker, 1984; Miall, 2000), a qual está diretamente relacionada aos ambientes deposicionais. Esse método também pode ser bastante efetivo quando a análise é realizada em sucessões vulcânicas (McPhie & Allen, 1992; Jerram, 2002), a qual pode auxiliar no entendimento da estratigrafia vulcânica e consequentemente na história do vulcanismo de diferentes PBCs (Jerram *et al.,* 1999; Jerram, 2002; Single & Jerram, 2004; Farrell, 2010; Brown *et al.,* 2011; Waichel *et al.,* 2012).

3.2.1 Conceito de fácies

O método de fácies é uma forma conveniente de identificar, descrever e interpretar intervalos distintos e/ou associações de rocha, que são muitas vezes recorrentes em uma sucessão estratigráfica. Embora o uso de fácies seja comumente aplicado na sedimentologia (Walker, 1984, 1992; Miall, 2000; Dalrymple, 2010), ele pode e deve ser aplicado em sucessões vulcânicas.

Segundo Cas & Wright (1987) uma fácies é um corpo ou intervalo de rocha que possui características únicas que as distinguem de outras fácies ou intervalos de rocha. As características individuais de uma fácies podem ser baseadas em aspectos composicionais, texturais ou estruturais. Uma fácies é produto de um conjunto de condições em um dado ambiente deposicional, as quais podem ser físicas, químicas ou biológicas e incluem fatores como topografia, mecanismo de *emplacement* e taxas de efusão, transporte, clima, intemperismo, natureza dos materiais fonte, composição química do sistema e, em alguns casos, a influência da fauna e da flora.

Diferentemente das rochas sedimentares, muitos litotipos vulcânicos não exibem clara e inequívoca evidência de suas origens (McPhie *et al.,* 1993). Dessa forma, é recomendável iniciar a análise de uma sequência vulcânica priorizando-se a classificação litológica e de litofácies (Figura 12), antes de aplicar termos com implicações genéticas. Designações genéticas levam em consideração a geometria das fácies e associações de fácies em diferentes escalas, fornecendo informações sobre os processos de erupção e *emplacement*, especialmente para depósitos vulcanoclásticos (queda, fluxo, *surge*). Por outro lado, a classificação litológica fornece informações sobre a composição, componentes e tamanho de grão.

As fácies descritivas são geralmente referidas como litofácies, termo usado para se referir a determinados atributos observáveis, tais como padrões composicionais, texturais e estruturais observados em afloramentos e que podem indicar os estilos de erupção. A combinação entre estes atributos pode ser entendida e descrita a partir de um código de litofácies, p.ex Bma (maiúscula= basalto; m= maciço; a=afanítico).

Nomes descritivos para intrusões e lavas coerentes

Combinação ideal: (4) + (3) + (2) + (1)

alteração textura termo litofácies composição

ex: riolito bandado, granulação grossa com fenocristal de quartzo, sericitico

Condição minima: (2) + (1) ex: basalto maciço; riolito com disjunção em blocos

(3) + (1) ex: dacito afanítico; andesito com fenocristal de hornblenda

(4) + (1) ex: andesito epido-clorita; riolito com silica-sericita

(1) COMPOSIÇÃO

a) estimativa baseada na assembléia de fenocristais

* riolito: K-feldspato ± quartzo (± plagioclásio pobre em Ca ± fase ferromagnesiana: biotita, anfibólio, piroxênio, fayalita)

* dacito: plagioclásio ± fase ferromagnesiana: biotita, anfibólio, piroxênio ± quartzo (± K-feldspato)

* andesito: plagioclásio + fase ferromagnesiana: biotita, anfibólio, piroxênio (± olivina)

* basalto: piroxênio + plagioclásio rico em cálcio ± olivina

b) rochas afaníticas, estimativa baseada na cor

(2) LITOFÁCIES

* maciça ou foliação de fluxo, bandamento de fluxo, laminação de fluxo

* disjunção: colunar, colunar radial, concentrica, blocos, prismática, placas

* Pillows ou pseudo pillows

(3) TEXTURA

* porfiritica: a. fenocristais -tipo (quartzo.. piroxênio.. etc)
- abundância (pobremente... moderadamente... fortemente...)
- tamanho (fino <1mm, médio 1-5 mm, grosso >5 mm)
b. matriz - vítrea, criptocristalina, microcristalina, granulação muito fina

* afanítica: uniformemente microcristalina

*afirica: nenhum fenocristal presente

* vítrea: composta de vidro vulcânico

* não vesicular ou vesicular (ou amigdaloidal): espaçadamente... moderadamente... fortemente... púmicea escoriácea
* esferulítica, microesferulítica, rica em litófise

(4) ALTERAÇÃO

* mineralogia: clorita, sericita, silica, pirita, carbonato, feldspato, hematita...

* distribuição: disseminada, nodular, pintalgado, pervasiva, desigual

Figura 12. Esquema de nomes descritivos para lavas coerentes e intrusões (traduzido de McPhie *et al.,* 1993).

Branney & Kokelaar (2002) consideram uma litofácies vulcânica como resultante de um depósito, ou parte de um, que seja distinto dos demais por uma combinação de estratificação, tamanho de grão, seleção, fábrica e composição. Jerram (2002) utilizou o conceito de fácies proposto por Walker (1971, 1973) e assumiu que estilos diferentes de vulcanismo produziriam diferentes fácies com relações geométricas internas e externas também diferentes. Por outro lado, Farrell (2010) propôs um modelo de arquitetura de fácies, baseado na definição de Miall (2000), em que fácies consiste em um agrupamento de rochas colocadas (*emplacement*) sob condições similares.

3.2.2 Aplicação do método de fácies em sistemas vulcânicos

Análise de fácies em depósitos vulcânicos efusivos e explosivos é realizada com o objetivo de melhor compreensão do estilo das erupções, processos de *emplacement,* transporte, proximidade com a fonte e os processos subsequentes de retrabalhamento.

Nessa análise de fácies vulcânicas é levada em consideração a textura, composição, distribuição lateral e morfologia dos derrames, sendo que são aplicados métodos similares aos desenvolvidos em rochas sedimentares clásticas (Miall, 2000), incluindo levantamento de seções estratigráficas verticais e confecção de fotomosaicos para mapeamento horizontal das sucessões de derrames. As relações de fácies verticais fornecem informações sobre as relações estratigráficas no tempo, tais como aparentes deslocamentos do conduto ou mudanças no estilo de erupção (p. ex., mudanças na morfologia de *pahoehoe* para *'a'ā*), enquanto que as relações de fácies longitudinais permitem considerações sobre a evolução de uma erupção desde regiões proximais até distais.

Branney & Kokelaar (2002) alertam que litofácies não podem ser definidas com base unicamente na granulometria, pois cada litofácies possui uma escala de variação no tamanho do grão e seleção, e, além disso, determinadas características se sobrepõem com aquelas de outras litofácies. Dessa forma, esses autores sugerem utilizar uma combinação de características para definir uma litofácies.

A técnica da seção vertical (*graphic logging*) consiste em uma representação esquemática das sequências vulcânicas que fornece a aparência atual do depósito. Essa seção registra variações nas texturas, estruturas, tamanho de grão e relações

de contato (McPhie *et al.,* 1993). O formato da seção vertical para rochas vulcânicas efusivas é adaptado daquele utilizado em rochas sedimentares: o eixo vertical indica a espessura, e o eixo horizontal mostra a granulação da rocha.

Fácies vulcânicas, assim como as sedimentares, podem ser definidas em qualquer escala, variando desde regional, onde as fácies são agrupadas em grupos, formações e/ou membros, até uma escala mais detalhada, onde as fácies variam desde aquelas definidas em escala de afloramento até intrafácies (Cas & Wright, 1987; Single & Jerram, 2004; Németh & Martin, 2007). Dessa forma, a subdivisão de uma sucessão estratigráfica em fácies vulcânicas dependerá especialmente do grau de detalhe desejado, que em parte é controlado pelos objetivos do estudo e informação geológica disponível.

Em uma análise de fácies vulcânica, conforme destacado anteriormente, deve-se evitar denominações com conotação genética ou designações interpretativas que podem prejudicar a determinação correta da gênese da fácies (McPhie *et al.,* 1993; Cas & Wright, 1987). Por outro lado, não existe uma nomenclatura padrão que possa ser aplicada para todos os depósitos vulcânicos sem implicações genéticas (Németh & Martin, 2007).

A maioria das litofácies não fornece de forma isolada uma indicação de ambiente particular. Dessa forma, devem-se agrupar as litofácies em associações de litofácies e sucessão de litofácies (Branney & Kokelaar, 2002; Dalrymple, 2010). O termo sucessão de litofácies é definido como uma sucessão vertical de litofácies, caracterizada por uma mudança progressiva de um ou mais parâmetros, tais como granulação, estruturas, texturas. Essas combinações permitem gerar um modelo de fácies, indicativo do sistema deposicional (*emplacement*) ou estilo eruptivo (Figura 13).

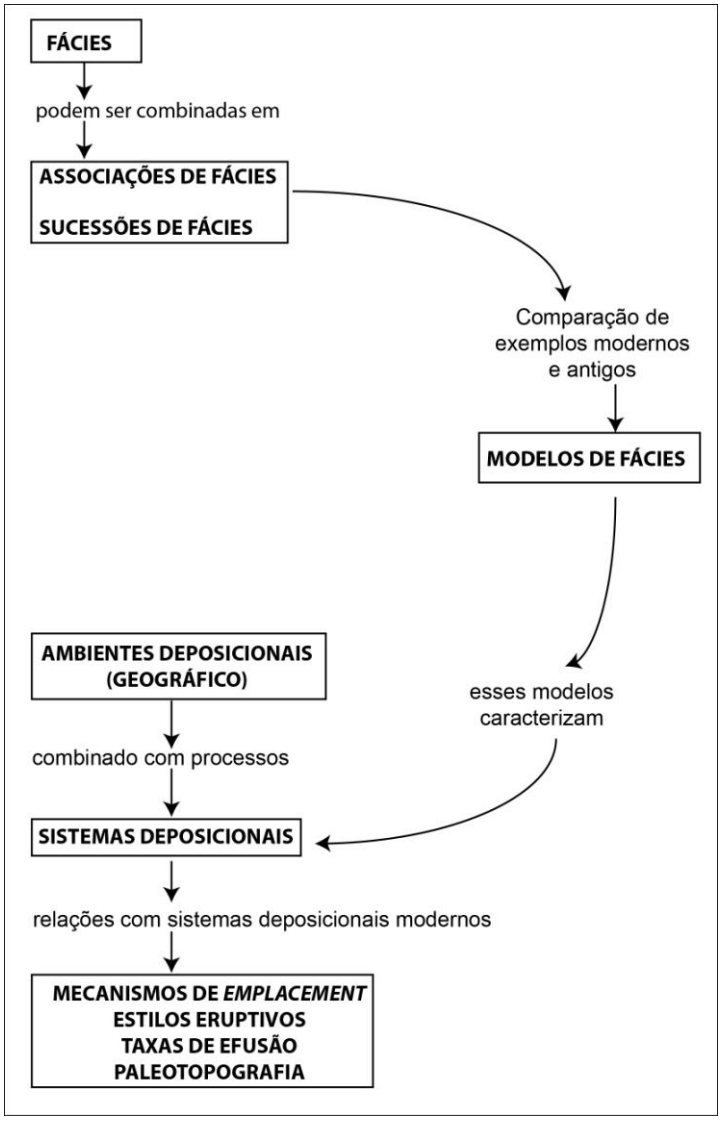

Figura 13. Fluxograma das etapas a serem seguidas na análise de fácies (modificado de Walker, 1992).

3.2.3 Arquitetura de fácies vulcânicas em PBCs

O conceito de arquitetura de fácies proposto para a investigação de bacias sedimentares, considera que os padrões de empilhamento são causados por interrelações entre as variações eustáticas, taxas de subsidência e de influxo sedimentar. Nos sistemas vulcânicos, a arquitetura de fácies considera a periodicidade e taxas de erupções, a subsidência, a paleotopografia e os hiatos temporais entre os derrames como determinantes nos padrões de empilhamento. As sucessões de fácies vulcânicas podem ser também lateralmente correlacionadas, o que pode auxiliar na identificação do estilo vulcânico, modelo eruptivo, duração,

periodicidade da sucessão e dessa forma compreender a história evolutiva do vulcanismo na bacia (Jerram & Widdowson, 2005).

Jerram (2002) propôs uma terminologia para a arquitetura de fácies em basaltos subaéreos, partindo de dois membros finais: fácies tabular clássica e fácies composta anastomosada. A primeira constitui a arquitetura de um derrame simples, com geometria em camada tabular, separada por paleossolos ou outros indicadores, os quais foram estabelecidos sob condições não turbulentas e taxas de efusão baixas. A fácies composta anastomosada consiste de vários fluxos de lobos *pahoehoe* gerados em condições de taxas de efusão bem mais baixas (Figura 14).

Farrell (2010) propôs um modelo de arquitetura de fácies para uma sequência vulcânica do British Columbia, no qual quatro elementos arquiteturais são representados: 1- tabular clássico; 2- composto anastomosado; 3- *foreset* acamadado; 4- transicional-misto (Figura 15).

Waichel *et al.* (2012) reconheceram nas sucessões vulcânicas da Sinclinal de Torres, sul da Província Paraná, as fácies vulcânicas descritas por Jerram (2002) e propuseram mais dois membros finais (Figura 16), sendo eles fácies lobada/escoriácea (lavas *'a'ā*) e fácies de domo de lava (domos ácidos).

As arquiteturas de fácies propostas por Jerram (2002), Farrell, (2010) e Waichel *et al.* (2012) para fácies vulcânicas basearam-se na análise de elementos arquiteturais definida por Miall (2000), priorizando a morfologia externa dos derrames. Adicionalmente, Single & Jerram (2004) interpretaram as fácies em escala de detalhe, propondo um esquema de classificação de intrafácies.

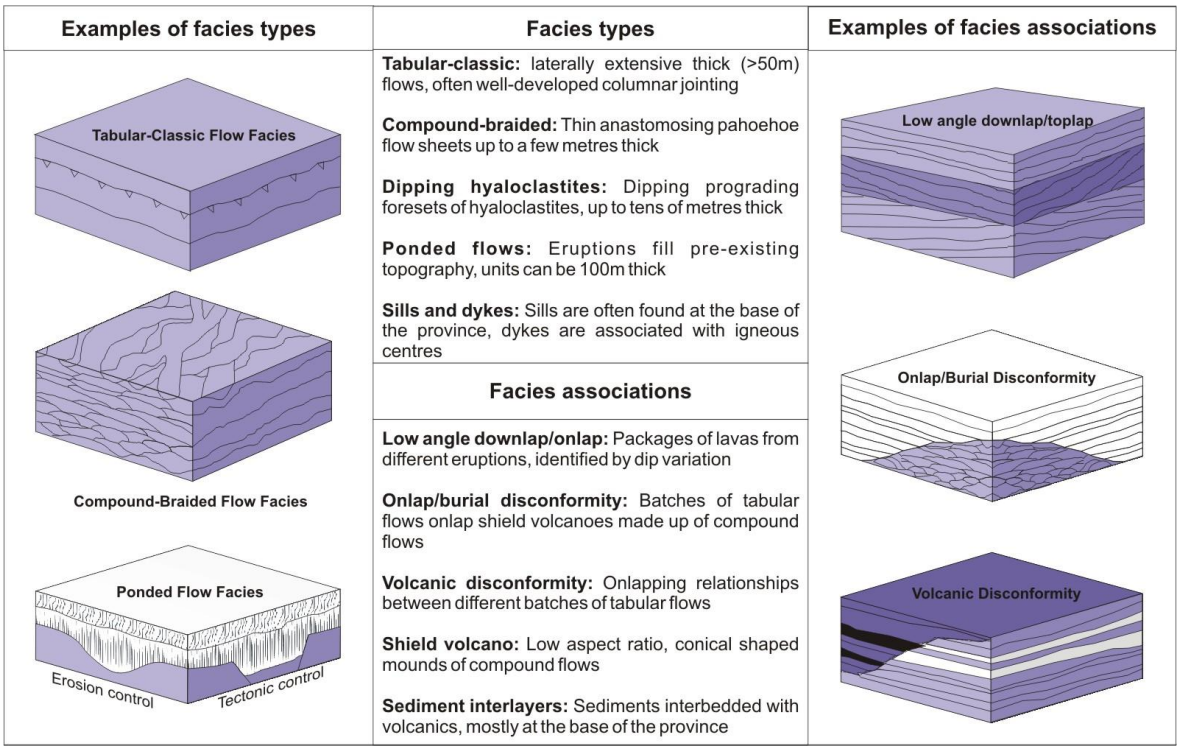

Figura 14. Tipos de fácies e associações de fácies mapeadas em PBCs (baseado em Jerram, 2002).

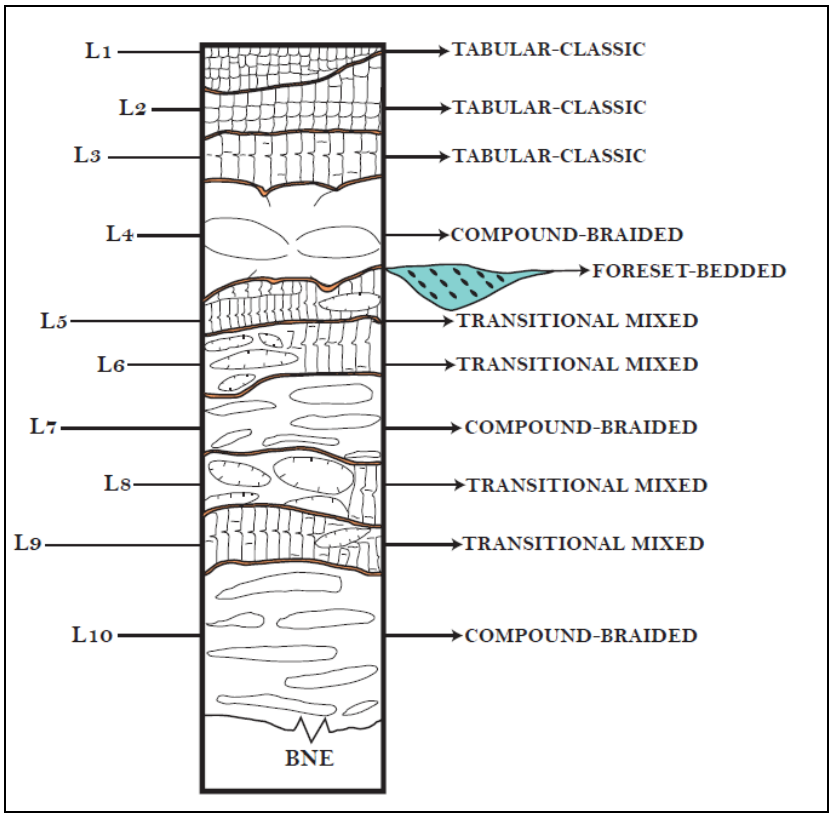

Figura 15. *Log* estratigráfico ilustrando os quatro elementos arquiteturais propostos para uma sequência vulcânica do British Columbia (extraído de Farrell, 2010).

Arquitetura da Fácies Vulcânica	Bloco Diagrama	Tipo de Derrame (Predominante)	Espessura Média (por derrame)	Espessura máxima
Derrames Tabulares	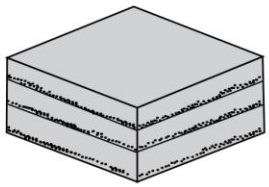	derrames tabulares ácidos	~20 m	~150m
Tabular/ Lobular Escoreácea	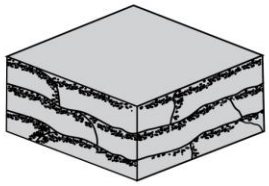	derrames *'a'a*	10 -15 m	~250 m
Domos de Lava	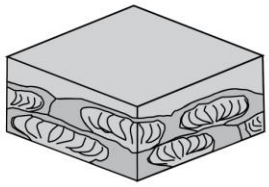	domos ácidos	até 30 m	~150 m
Tabular Clássica	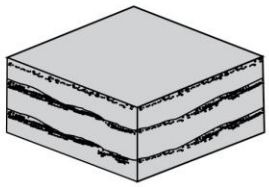	derrames *pahoehoe* simples	10 - 20 m	~500 m
Composta Anastomosada	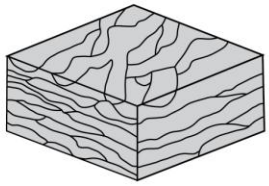	derrames *pahoehoe* compostos (área de duna) derrames p*ahoehoe* ponded (áreas de interdunas)	0,3 - 1,0 m até 40 m	100-200 m

Figura 16. Quadro esquemático das arquiteturas de fácies vulcânicas descritas na "Sinclinal" ou calha de Torres, sul da Província Paraná (traduzido de Waichel *et al.,* 2012).

3.3 Padrões de vesiculação e estruturas de segregação em derrames basálticos

Em geral, a investigação dos padrões de vesiculação tem um papel coadjuvante no estudo de basaltos, onde são genericamente vinculados aos topos dos derrames *pahoehoe* (MacDonald, 1953; Hon *et al.,* 1994; Self *et al.,* 1998). Contudo, estudos recentes constataram que o reconhecimento de alguns padrões de vesiculação e associadas estruturas de segregação fornece informações sobre

as espessuras dos derrames e estilos de *emplacement* (Goff, 1996; Caroff *et al.,* 2000). Além disso, essas estruturas de segregação atuam como bons marcadores de base, núcleo e topo dos derrames (Figura 17).

Os padrões de vesiculação são distintos entre os diferentes tipos morfológicos de lavas e relativamente constantes dentro de cada tipo, tornando possível a sua utilização na identificação dos derrames. Nos basaltos *'a'ā* as vesículas são pouco abundantes (< 20% do volume) e concentradas nas escórias de base e topo, as quais tendem a ser alongadas, irregulares e distorcidas, devido o rompimento do topo desses derrames com o resfriamento e desvolatização rápidos (MacDonald, 1953). Em contrapartida, nos basaltos *pahoehoe* as vesículas são mais abundantes (20 a 60% do volume), como resultado da formação de uma crosta externa durante o *emplacement*, que promove um resfriamento lento da lava, possibilitando o aprisionamento de voláteis.

Em geral, o padrão de vesiculação varia dentro da estruturação interna dos derrames *pahoehoe* (Figura 18). Em derrames *pahoehoe* compostos, os lobos "esponjosos (tipo S; Walker, 1989) apresentam vesículas esféricas distribuídas por todo o núcleo. Lobos do tipo P apresentam *pipe* vesículas na base e um núcleo tipicamente maciço microvesiculado, cuja concentração de vesículas aumenta em direção ao topo (Wilmoth & Walker, 1993). Lobos do tipo S se formam quando a inflação é mínima, enquanto lobos do tipo P invariavelmente geram fluxos inflados (Self *et al.,* 1998). No núcleo dos derrames inflados (*pahoehoe* simples) são preservados cilindros e proto-cilindros ricos em vesículas, *pods*, camadas de vesículas tipo S2 e vesículas gigantes. Em contrapartida, no topo dos derrames, apenas camadas de vesículas tipo S1 e vesículas do tipo V1 são preservadas (Figura 17). A Figura 18 ilustra a evolução dos padrões de vesiculação em lavas *pahoehoe*.

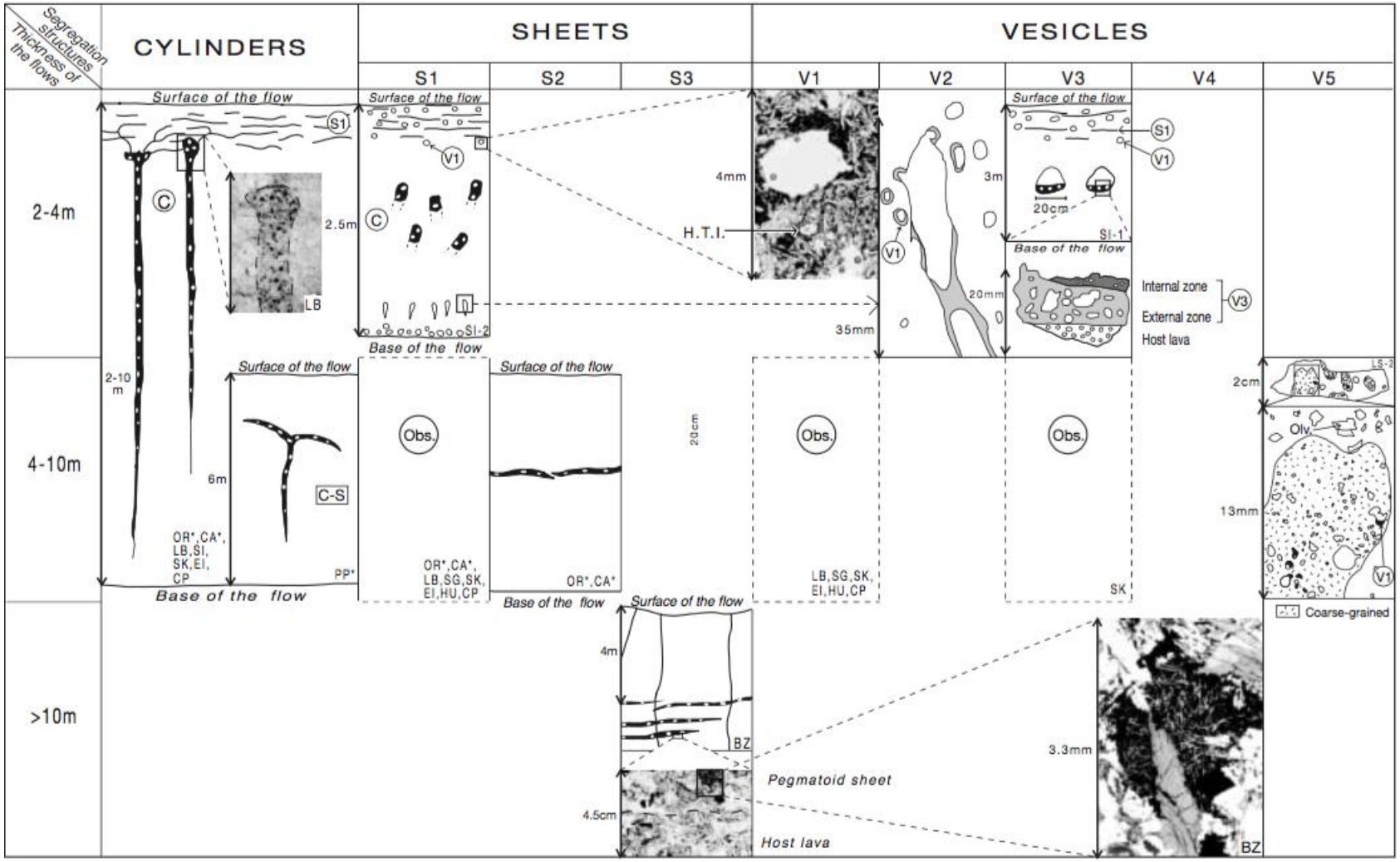

Figura 17. Ilustração e classificação dos tipos de estruturas de segregação mapeados em derrames (extraído de Caroff *et al.,* 2000).

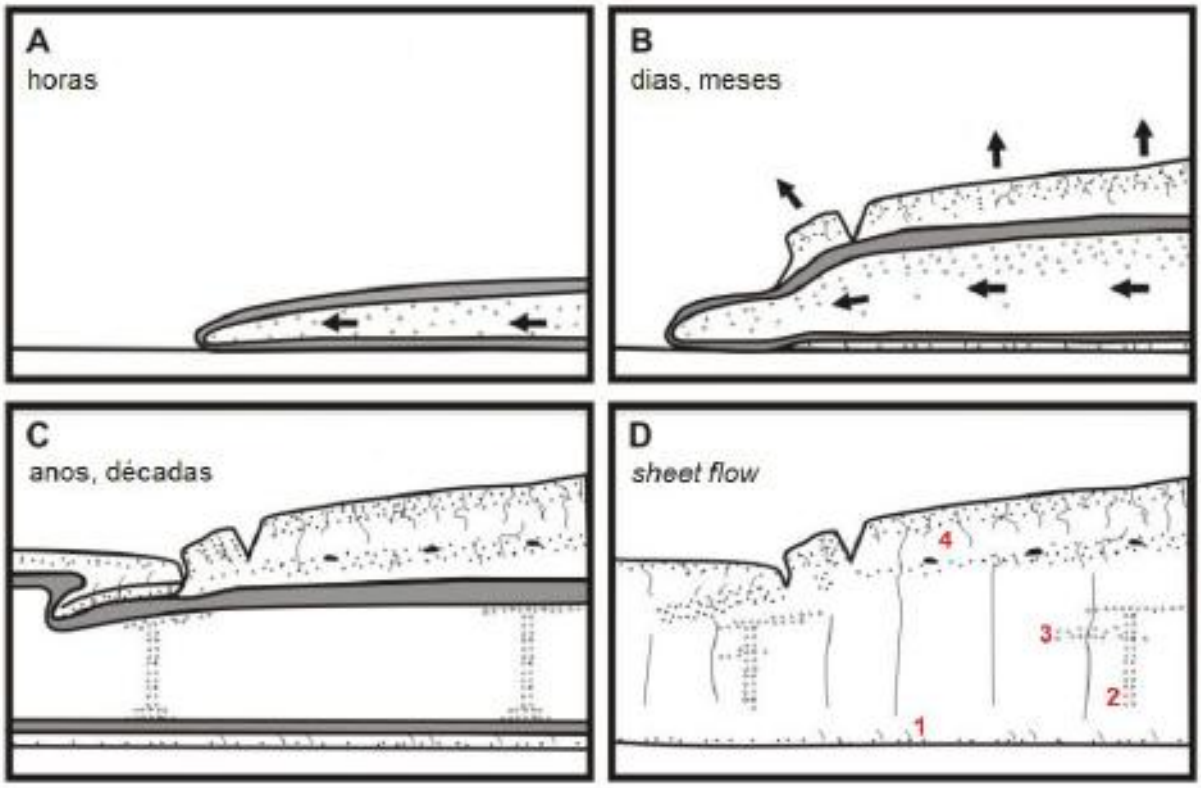

Figura 18. Esquema genérico da inflação de um derrame *pahoehoe* e os padrões de vesiculação formados (baseado em Self *et al.,* 1996). A) Avanço do lobo e formação de crosta plástica; B) formação de crosta rígida e topo vesiculado, com a inflação e geração de um novo lobo; C) espessamento da crosta rígida e formação de diferentes padrões de vesiculação; D) derrame totalmente cristalizado – 1) *pipe vesicles*; 2) *vesicle cylinders*; 3) *sheet vesicles*; 4) crosta superior vesiculada.

CAPÍTULO 4

Contexto geológico regional da Bacia do Paraná

A Bacia do Paraná é uma província geológica Fanerozoica situada no sudeste da Plataforma Sul-Americana. Constitui uma depressão de aproximadamente 1.600.000 km^2 alongada na direção NNE-SSW, abrangendo partes do Brasil, Argentina, Paraguai e Uruguai. Zalán *et al.* (1987), classificou esta bacia como do tipo flexural de interior cratônico, de natureza policíclica, com história geológica do Ordoviciano ao Cretáceo, sendo sugerido por Milani & Ramos (1998) um rifte precursor referente ao início da subsidência. Milani *et al.* (2007) reconheceram no registro estratigráfico da Bacia do Paraná, seis unidades de ampla escala ou Supersequências (Figura 19; Vail *et al.,* 1977): Rio Ivaí (Ordoviciano-Siluriano), Paraná (Devoniano), Gondwana I (Carbonífero-Eotriássico), Gondwana II (Meso a Neotriássico), Gondwana III (Neojurássico-Eocretáceo) e Bauru (Neocretáceo). A Supersequência Gondwana III compreende os sedimentitos eólicos da Formação Botucatu e as rochas magmáticas ácidas e básicas da Formação Serra Geral (Figura 20).

A Bacia do Paraná possui uma série de estruturas tectônicas (arco de Ponta Grossa, Sinclinal de Torres, arco de Rio Grande), sendo dividida por grandes zonas de falhas, refletidas em anomalias geofísicas lineares e em rupturas de relevo, além de arqueamentos e flexuras (Figura 21). Embora a Bacia do Paraná seja dividida em grandes lineamentos, poucos estudos focam sistematicamente nestes segmentos.

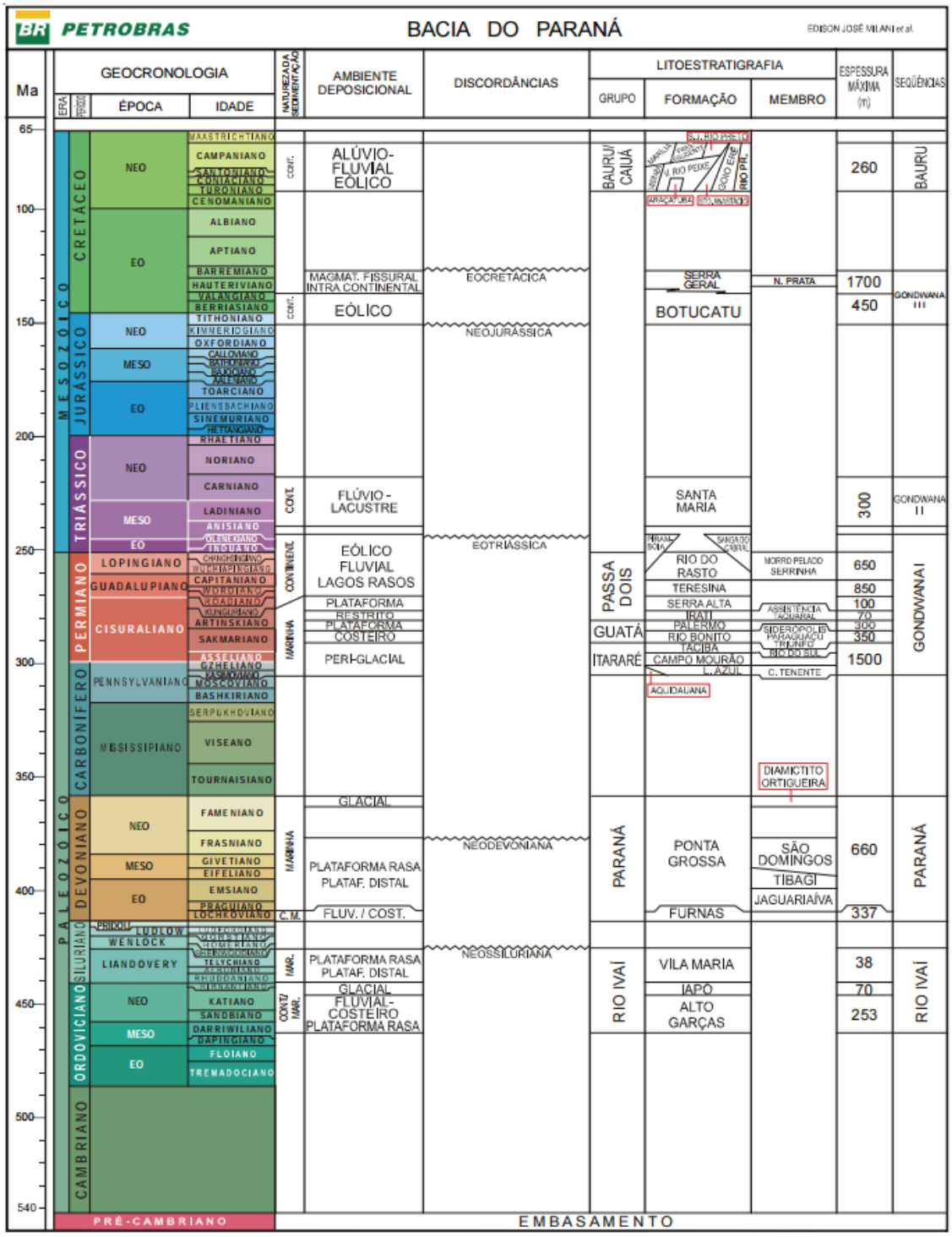

Figura 19. Carta estratigráfica da Bacia do Paraná (extraído de Milani *et al.,* 2007).

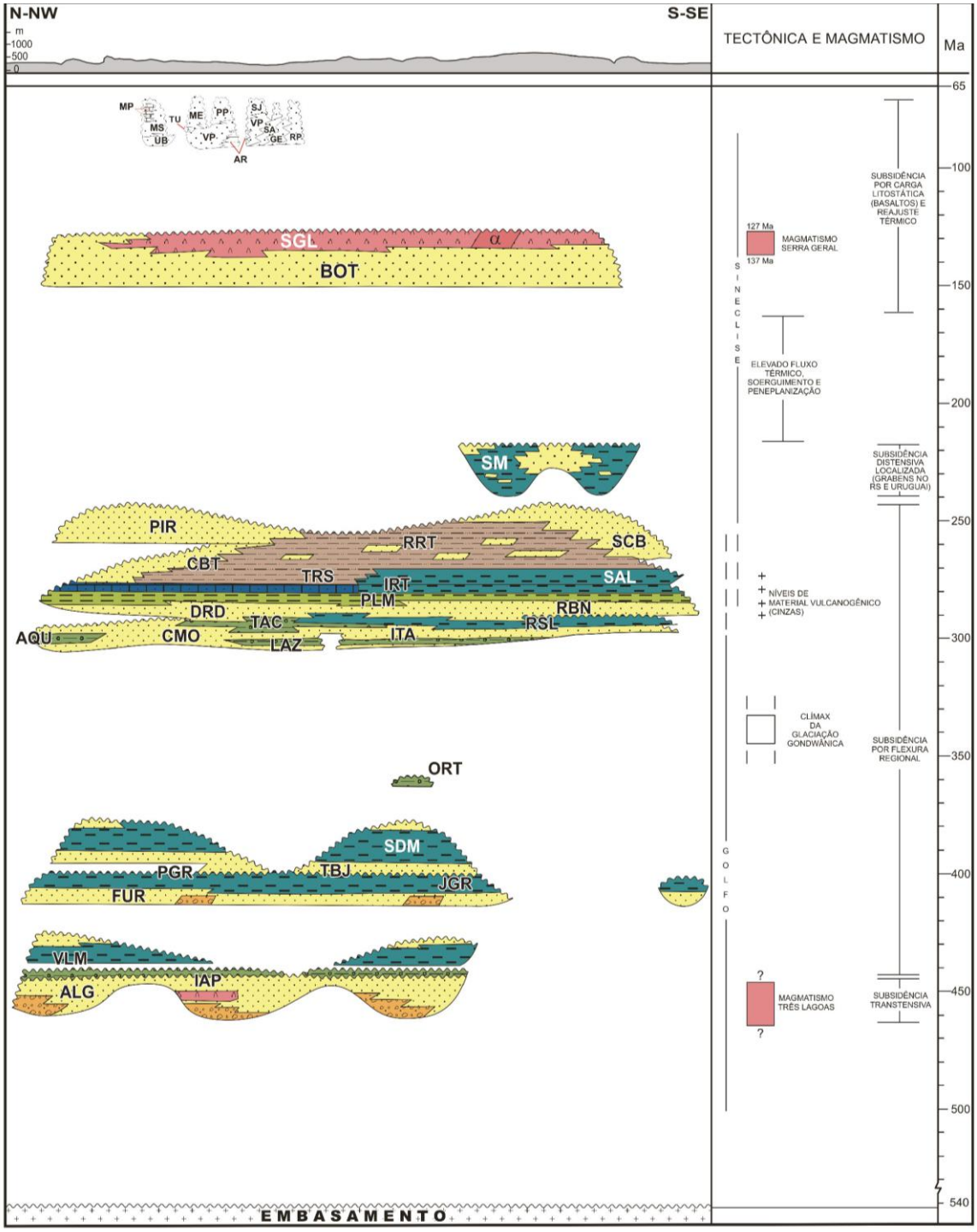

Figura 20. Coluna litoestratigráfica da Bacia do Paraná, mostrando a distribuição espaço-temporal das principais unidades estratigráficas ao longo de uma seção NNW-SSE (extraído de Milani *et al.*, 2007).

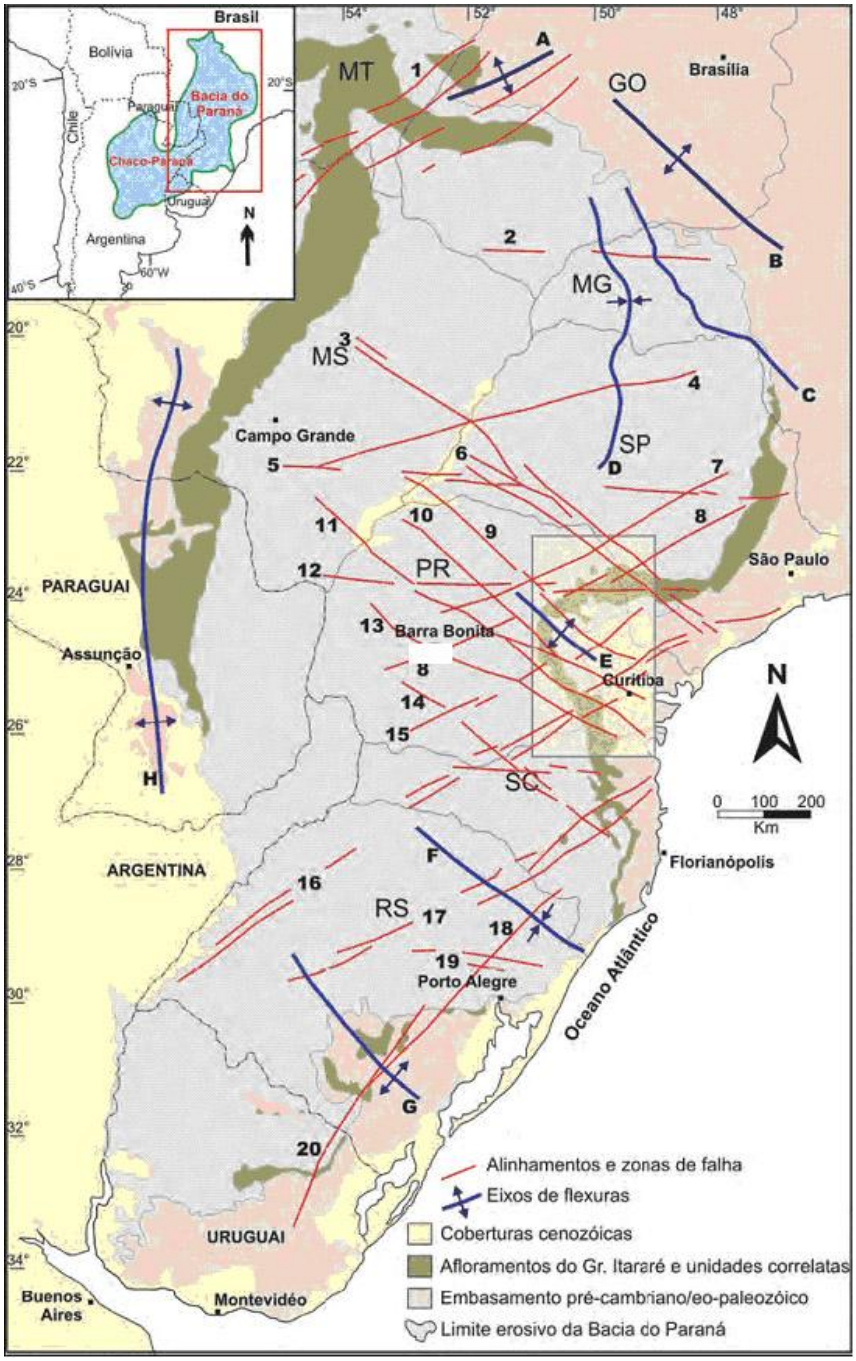

Figura 21. Mapa de localização da Bacia do Paraná e os principais elementos tectônicos definidos por Zalán *et al.* (1987): 1) Transbrasiliano; 2) Cassilândia; 3) Guapiara; 4) Araçatuba; 5) Moji-Guaçu/Dourados; 6) Santo Anastácio; 7) Guaxupé; 8) Jacutinga; 9) São Jerônimo/ Curiúva; 10) Rio Alonzo; 11) Cândido de Abreu/Campo Mourão; 12) São Sebastião; 13) Rio Piquiri; 14) Caçador; 15) Taxaquara; 16) Lancinha/Cubatão; 17) Blumenau/Soledade; 18) Leão; 19) Bento Gonçalves; 20) Açotea; a) Arco de Bom Jardim de Goiás; b) Arco do Alto Paranaíba; c) Flexura de Goiânia; d) Baixo de Ipiaçu/Campina Verde; e) Arco de Ponta Grossa; f) Sinclinal de Torres; g) Arco do Rio Grande; h) Arco de Assunção.

Atualmente estudos mais detalhados vêm sendo desenvolvidos no segmento denominado pela Petrobrás de Sinclinal de Torres. Na realidade trata-se de uma calha posicionada entre os altos de Florianópolis e Rio Grande. Nesse contexto, a expressão sinclinal de Torres não tem implicação genética sobre a origem desta calha. Estudos recentes indicam que esta é uma grande estrutura orientada com direção NW-SE, localizada na margem brasileira sul, a qual pode ser dividida em calha principal, zona intermediária e ombreira sul (Figura 22), onde cada zona da ST possui evolução estratigráfica e espessura distintas (Lima *et al.,* 2012a, 2012b; Waichel *et al.,* 2012; Barreto *et al.,* 2014b; Rossetti *et al.,* 2014). A estratigrafia da ST foi subdividida em 1) *paleoerg* Botucatu, 2) episódio vulcânico básico I, 3) episódio vulcânico básico II, 4) vulcânicas ácidas, 5) episódio vulcânico básico III, 6) episódio vulcânico ácido II (Waichel *et al.,* 2012).

Historicamente, as pesquisas na Bacia Paraná têm enfatizado os aspectos geoquímicos (Bellieni *et al.,* 1984; Mantovani *et al.,* 1985; Melfi *et al.,* 1988; Peate *et al.,* 1992; Peate, 1997) e geocronológicos (Turner *et al.,* 1994; Renne *et al.,* 1995; Janasi *et al.,* 2011; Florisbal *et al.,* 2014), sendo raras e recentes as pesquisas relacionadas a estratigrafia e morfologias de derrames, fácies e associações de fácies, estruturas e texturas, implicações da paleotopografia e taxas de efusão para mudança no estilo de *emplacement* das lavas (Jerram *et al.,* 1999; Jerram, 2002; Lima *et al.,* 2012b; Waichel *et al.,* 2012).

Embora os derrames básicos colocados na ST tenham sido considerados como uma pilha de derrames monótonos, com o mapeamento das sucessões vulcânicas realizado na ombreira sul da ST é possivel individualizar derrames com morfologias distintas, tais como *pahoehoe*, *'a'ā* e *rubbly* (Waichel *et al.,* 2006a, 2006b, 2012; Lima *et al.,* 2012b; Barreto *et al.,* 2014b; Rossetti *et al.,* 2014).

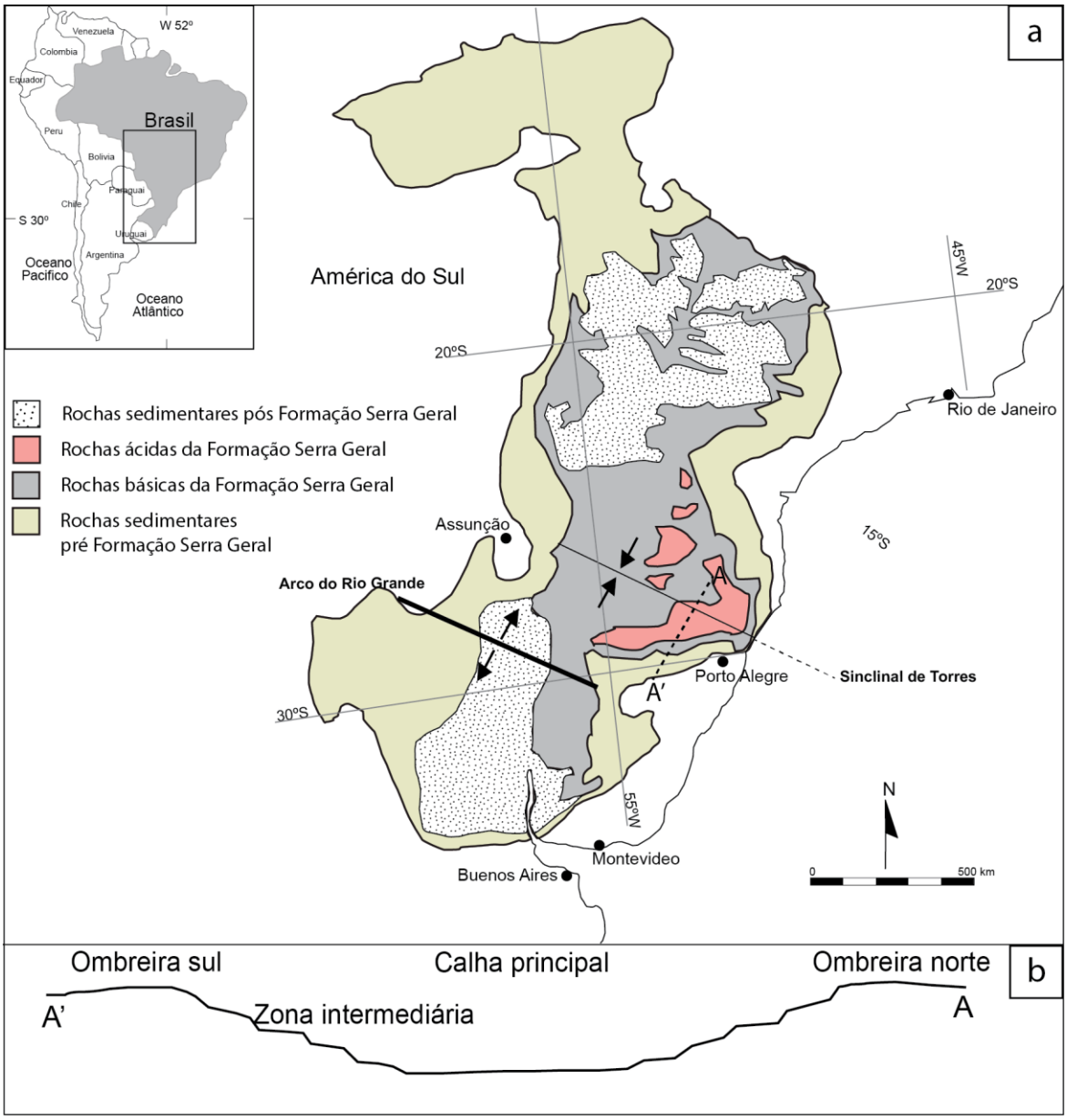

Figura 22. Mapa geológico da Bacia do Paraná com a localização da “Sinclinal” ou calha de Torres (traduzido de Waichel *et al.,* 2012).

4.1 Grupo São Bento

White (1908) propôs pela primeira vez na Bacia do Paraná a Série São Bento, a qual dividiu em três unidades: Rochas eruptivas Serra Geral, arenitos São Bento e camadas vermelhas do Rio do Rasto. Oppenhein (1934) analisou o comportamento estratigráfico da Série São Bento e subidividiu-a em: derrame basáltico Serra Geral, Arenito do Botucatu, e arenitos e argilas vermelhas do grupo Rio do Rasto. Nessa

revisão estratigráfica, Opphenheim (1934) confirma a denominação de arenito Botucatu como uma unidade própria e em discordância com os sedimentitos sotopostos.

As primeiras manifestações vulcânicas da Província Paraná-Etendeka indicam a interação entre sedimentos e lavas e a formação de um litotipo “misto” que pode conter diferentes proporções destes constituintes. Rochas geradas por esta interação são denominadas de peperitos (Petry *et al.,* 2007; Waichel *et al.,* 2008). Estes, em geral, são originados pela mistura entre sedimentos com água (não consolidados) e magma. Peperitos em ambientes áridos indicam que os processos de formação desses são diversos e nem sempre necessitam de água na fração sedimentar. Este é o caso da interação entre os sedimentos eólicos da Formação Botucatu e as primeiras manifestações de lavas básicas da Formação Serra Geral.

Essas formações pertencentes ao Grupo São Bento cobrem, no Estado do Rio Grande do Sul, uma área superior a 150.000 km^2 atingindo uma espessura máxima de 800 m (Figura 23). As espessuras da Formação Botucatu são variadas (< 100 m), estando inclusive ausentes por não deposição na porção central do Estado no Rio Grande do Sul, onde os derrames vulcânicos estão dispostos diretamente sobre os depósitos triássicos.

Trabalhos pioneiros (e.g. Gordon Jr., 1947; Sanford & Lange, 1960; Bortoluzzi, 1974; Schneider *et al.,* 1974) sugeriram um contato discordante, mas atualmente é consenso de que não existe um hiato temporal, entre os arenitos eólicos e os derrames básicos (e.g. Almeida, 1953; Scherer *et al.,* 2000). A continuidade temporal entre a sedimentação e o magmatismo é marcada por um decréscimo dos depósitos eólicos e um aumento do volume de rochas vulcânicas em direção ao topo do Grupo São Bento (Soares, 1975).

Por outro lado, a interdigitação entre os arenitos eólicos e os derrames vulcânicos constitui um problema de natureza litoestratigráfica que merece uma reflexão mais detalhada. Onde deveria ser demarcado o contato entre as Formações Botucatu e Serra Geral? Os arenitos intercalados com as rochas vulcânicas seriam ainda pertencentes à Formação Botucatu ou já passariam a ser denominados de Serra Geral?

Estudos recentes (e.g. Milani *et al.,* 1998; Scherer, 2002) defendem a manutenção dos nomes "Botucatu" e "Serra Geral" para designar duas unidades

litoestratigráficas independentes, distanciando-se, portanto, da proposição de Almeida (1953). A Formação Botucatu refere-se à seção contínua de arenitos encontrados abaixo dos primeiros derrames vulcânicos. A Formação Serra Geral, por sua vez, deve ser restrita ao intervalo constituído dominantemente por depósitos vulcânicos, que ocasionalmente apresentam intercalações de arenitos eólicos, aproximando-se, desta forma, da proposição de Gordon Jr. (1947). A restrição do nome Botucatu aos arenitos subjacentes às lavas vem do fato destes constituírem um pacote litológico homogêneo, rastreado por uma grande extensão lateral, o que não é verificado com sedimentos interacamadados com as lavas, cuja distribuição é descontínua e fortemente condicionada pelo vulcanismo Serra Geral.

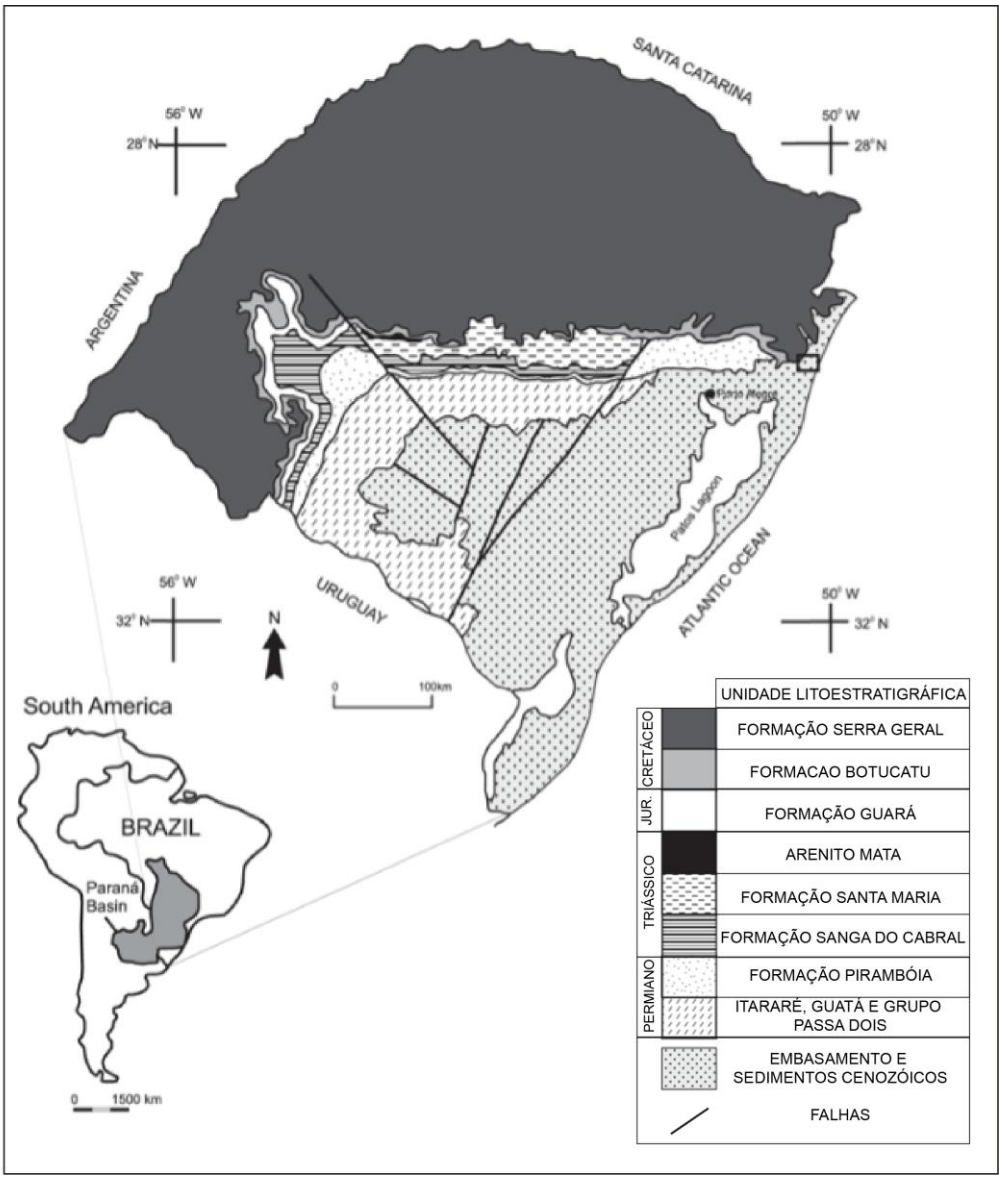

Figura 23. Mapa geológico do Rio Grande do Sul (extraído de Silva *et al.,* 2006).

4.1.1 Formação Botucatu

Grande parte da Formação Botucatu (FB) consiste de depósitos eólicos, dominantemente *sets* e *cosets* de estratos cruzados (Mountney *et al.,* 1998; Scherer, 1998, 2002). Os depósitos eólicos têm uma espessura de até 100 m, porém em algumas regiões, os mesmos são ausentes devido a não deposição. A espessura dessa formação é bastante variável, refletindo a própria paleotopografia no momento da deposição, já que o *erg* ativo Botucatu possuía dunas de até 100 m de espessura. Scherer (2002) concluiu que a FB se trata de um sistema eólico seco, evidenciado pela acumulação de dunas eólicas com ausência de interdunas úmidas.

A idade de deposição da FB, em torno do Jurássico Superior-Cretáceo inferior (Bonaparte, 1996) foi definida com base na identificação de icnofósseis vertebrados dentro dos estratos eólicos. Contudo, a relação entre os arenitos eólicos e os derrames da Formação Serra Geral, aliados a ausência de superfícies limitantes dentro da sucessão eólica sugere que a FB, pelo menos na porção sul da Bacia do Paraná representa um curto intervalo de sedimentação, em torno de algumas centenas de milhares de anos antes do inicio da atividade vulcânica (Scherer, 2002).

4.1.2 Formação Serra Geral

A Formação Serra Geral (FSG) foi proposta e introduzida como unidade estratigráfica por White (1908). Consiste de uma sucessão de rochas vulcânicas com uma espessura máxima de aproximadamente 1700 m no centro da Bacia do Paraná (Almeida, 1986), em que predominam basaltos e andesitos basálticos de afinidade toleítica (mais de 90% em volume). Rochas efusivas de composição ácida são predominantes no topo dessa sequência vulcânica, principalmente nos Estados do Rio Grande do Sul e Santa Catarina (Melfi *et al.,* 1988; Lima *et al.,* 2012a, Waichel *et al.,* 2012; Polo & Janasi, 2014). Uma intensa atividade intrusiva também foi evidenciada nessa região, representada por soleiras e diques que seguem, em geral, as maiores descontinuidades estruturais da bacia.

As rochas básicas e ácidas da FSG foram divididas geoquimicamente em dois grupos com base nos conteúdos de TiO_2: basaltos ATi (> 2%) e basaltos BTi com teores inferiores a 2% (Bellieni *et al.,* 1984; Mantovani *et al.,* 1985). A abundância de elementos maiores e razões entre elementos traços levou Peate *et al.* (1992) a

subdividirem a sequência vulcânica básica em seis tipos de magmas. Na subprovíncia ATi, foram definidos os magmas-tipo Urubici, Pitanga e Paranapanema, enquanto na subprovíncia BTi, os magmas definidos são Gramado, Esmeralda e Ribeira (Figura 24). As rochas vulcânicas ácidas foram divididas em dois tipos principais: 1) Palmas, que aflora na porção sul da província e exibe afinidades com os basaltos BTi; 2) Chapecó, que aflora na porção centro-norte da província e está relacionado aos basaltos ATi. Esses dois tipos de magmas ácidos são ainda subdivididos em vários subtipos (Peate, 1997; Nardy *et al.,* 2008).

Datações obtidas pelo método $^{40}Ar/^{39}Ar$ indicam idades para o magmatismo Serra Geral entre 138-125 Ma, com o clímax entre 133-129 Ma (Renne *et al.,* 1992; Turner *et al.,* 1994; Milner *et al.,* 1995; Mincato, 2000). Recentemente, foi obtida uma idade $^{238}U/^{206}Pb$ de 134,3 ± 0,8 Ma (Janasi *et al.,* 2011), que é semelhante, se considerada a incerteza do método, às datações $^{40}Ar/^{39}Ar$ (135-134 Ma) disponíveis para os basaltos (tipos Gramado e Esmeralda) e lavas ácidas BTi (tipo Palmas) do Sul do Brasil, que são supostamente mais antigos. Essa superposição nas idades obtidas pode estar refletindo a curta duração desse vulcanismo, indicando uma expressiva taxa de efusão num curto espaço de tempo ou uma taxa de efusão menor, porém permanente no tempo.

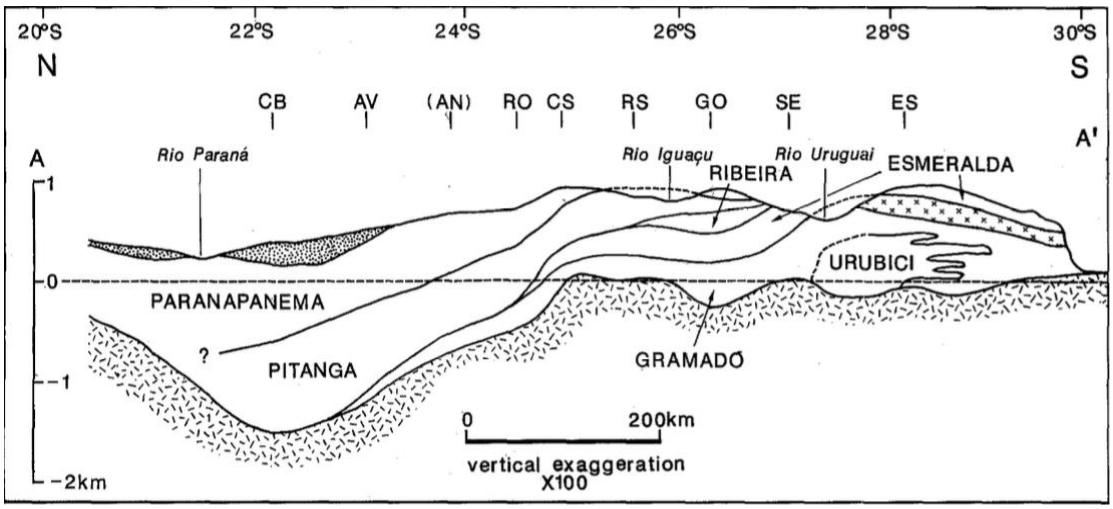

Figura 24. Seção esquemática N-S ilustrando a estratigrafia química da Bacia do Paraná definida pelos distintos tipos de magmas (extraído de Peate *et al.,* 1992).

4.2 Processos envolvidos na gênese dos magmas alto e baixo Ti e as correlações quimioestratigráficas do magmatismo Serra Geral

Os estudos nas PBCs ao longo das décadas têm se concentrado, sobretudo, nas discussões sobre a gênese dos magmas BTi e ATi (Anderson, 2005; Sheth, 2005) e nas correlações regionais quimioestratigráficas (Milner *et al.,* 1992, 1995; Peate *et al.,* 1992; Peate, 1997).

Nesse contexto, ainda existem muitas controvérsias sobre os processos envolvidos na gênese dos basaltos da PIP. Uma das hipóteses é que as composições basálticas devem refletir uma fonte por pluma mantélica astenosférica profunda denominada de Tristão da Cunha (Richards *et al.,* 1989; White & McKenzie, 1989; Gibson *et al.,* 1995; Milner & Le Roex, 1996; Courtillot *et al.,* 1999). Contudo, o papel da pluma mantélica como principal fonte para a geração dos líquidos da PIP foi descartado com base em isótopos de Sr-Nd-Pb e geoquímica de elementos maiores e traços (Peate & Hawkesworth, 1996; Marques *et al.,* 1999). Esses autores propuseram que os derrames foram originados por fusão de manto litosférico heterogêneo, assumindo que essa pluma poderia ter atuado apenas como fonte de calor.

Um modelo alternativo não relacionado a plumas e utilizando geoquímica, isótopos, paleomagnetismo e dados de anomalias de geoides propõe que o magmatismo da PIP foi ocasionado por uma grande anomalia termal, localizada na costa oeste da África, em que essa provincia permaneceu estacionada por aproximadamente 50 Ma (Ernesto *et al.,* 2002).

Outra hipótese petrogenética para explicar a gênese dos magmas da PIP, baseada em dados isotópicos de Re-Os, considera uma possível influência de manto litosférico subcontinental relacionado a pluma Tristão da Cunha (OIB – basaltos de ilha oceânica) (Rocha-Júnior *et al.,* 2012). Esses autores identificaram que uma fusão exclusiva de manto litosférico sub-continental antigo ou de uma pluma mantélica não explicariam satisfatoriamente todas as características isotópicas e químicas da PIP e nesse caso, o componente astenosférico envolvido na geração da província deveria ter sido enriquecido por fluidos e/ou magmas relacionados a processos de subducção. Rocha-Júnior *et al.,* (2013) baseados em elementos traços e razões isotópicas de Sr-Nd-Pb interpretaram que os basaltos ATi

foram derivados de magmas que se originaram de uma fonte sub-litosférica metassomatizada por piroxenito.

Além da discussão sobre a gênese dos magmas da PIP, diversos autores já enfatizaram que a contaminação crustal tem sido claramente um processo importante na evolução do magmatismo BTi para o sul da PIP, sul do Brasil e seu equivalente na Provincia Etendeka, noroeste da África (Mantovani *et al.,* 1985; Petrini *et al.,* 1987; Mantovani & Hawkesworth, 1990; Peate & Hawkesworth, 1996).

Dessa forma, quando os magmas-tipo da PIP são distinguidos com base nas razões isotópicas de Sr (Cordani *et al.,* 1980, 1988; Peate *et al.,* 1992; Garland *et al.,* 1995), percebe-se que os valores mais elevados referem-se ao tipo Gramado (0,7075 – 0,7167), seguido pelo Esmeralda (0,7046 – 0,7086), Ribeira (0,7055 – 0,7060), Paranapanema (0,7055 – 0,7063), Pitanga (0,7055 – 0,7060) e Urubici (0,7048 –0,7065). Desta forma, as mais altas razões de Sr são conferidas aos basaltos do tipo BTi, reforçando a hipótese de processos de contaminação crustal significativos na porção sul da bacia (Tabela 2).

Grupo	Tipo de magma	Localização na Província Paraná	TiO_2 (%)	Ti/Y	Ti/Zr	$^{87}Sr/^{86}Sr_i$
Baixo-Ti	Gramado	Sul	0,7-1,9	<310	< 70	0,7075-0,7167
	Esmeralda	Sul	1,1-2,3	<310	> 60	0,7046-0,7086
	Ribeira	Norte	1,5-2,3	<310	> 65	0,7055-0,7060
	Urubici	Sul	> 3,3	> 500	> 57	0,7048-0,7065
Alto-Ti	Pitanga	Norte	> 2,9	> 350	> 60	0,7055-0,7060
	Paranapanema	Norte	1,7-3,2	> 330	> 65	0,7055-0,7063

Tabela 2. Comparativo das principais características composicionais e isotópicas dos tipos de magmas individualizados na sequência básica da Província Paraná (Peate, 1997).

Para melhor entender como essas fontes magmáticas e os processos têm variado durante a evolução da PIP, foram necessários estudos quimioestratigráficos que têm o papel fundamental de investigar a estrutura interna e a sucessão dos derrames na pilha vulcânica (Cordani *et al.,* 1988).

A abordagem quimioestratigráfica do magmatismo Serra Geral advém da concepção inicial de que grandes derrames de lava possuiam uma estratigrafia

simples denominada *layer cake* (Jerram, 2002). Considerando o volume grande de magmatismo na Bacia do Paraná, os derrames basálticos têm sido mapeados a partir de um controle estratigráfico em escala regional, cujas composições químicas são usadas como o meio mais efetivo de organizar os derrames da província como um todo.

Para facilitar na construção dessa estratigrafia química, as sucessões de derrames foram divididas em seis tipos de magma distintos (Peate *et al.,* 1992): Paranapanema, Pitanga e Ribeira com razões Ti/Y > 300 e localizados no norte da PIP, enquanto os tipos Gramado, Esmeralda e Urubici predominam no sul da província com razões Ti/Y < 300 (Figura 25). Essa quimioestratigrafia suporta a hipótese de que os derrames que pertencem a um tipo de magma particular se comportariam como uma unidade estratigráfica relativamente coerente.

Segundo a quimioestratigrafia proposta para a Bacia do Paraná (Peate *et al.,* 1992), os basaltos BTi do tipo Gramado correspondem às primeiras manifestações do vulcanismo que ocorreram sobre o sistema eólico ativo da FB, preservando localmente morfologias originais de dunas e feições sedimentares na porção sul da PIP (Scherer, 2002; Waichel *et al.,* 2008, 2012). Estas manifestações foram seguidas pelos basaltos do tipo Esmeralda que exibem em direção ao topo, intercalações com rochas vulcânicas ácidas do tipo Palmas (Bellieni *et al.,* 1986; Garland *et al.,* 1995; Nardy, 1995; Nardy *et al.,* 2008; Waichel *et al.,* 2012). O magmatismo ATi inicia com a efusão de um volume pequeno de lavas félsicas do tipo Chapecó que se sobrepõem diretamente aos arenitos eólicos da FB na porção norte da PIP (Piccirillo *et al.,* 1987; Janasi *et al.,* 2007; Luchetti, 2010) ou recobrem as rochas vulcânicas dos tipos Esmeralda e Palmas na porção central da PIP (Nardy, 1995; Nardy *et al.,* 2008). Os basaltos ATi dos tipos Pitanga e Paranapanema representam as últimas manifestações vulcânicas da PIP, os quais recobrem as porções norte e oeste da Bacia do Paraná (Peate *et al.,* 1992; Peate, 1997) (Figura 25).

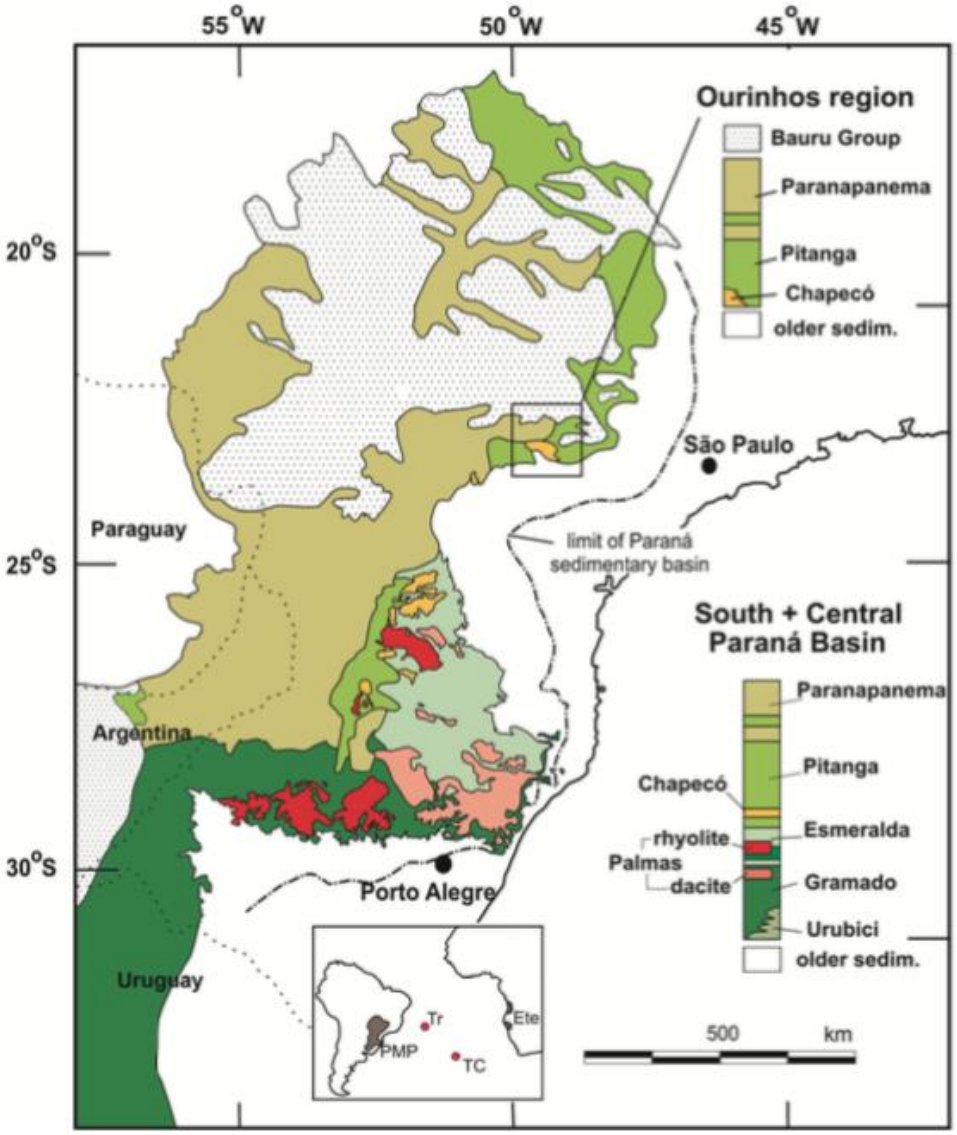

Figura 25. Mapa da Província Paraná-Etendeka com ênfase na Bacia do Paraná, mostrando a distribuição geográfica dos tipos de basaltos BTi e ATi e as rochas vulcânicas ácidas associadas (extraído de Polo & Janasi, 2014).

CAPÍTULO 5

Apresentação dos artigos científicos

5.1 Artigo 1

TÍTULO: Lithofacies analysis of basic lava flows of the Paraná Igneous Province in the south hinge of Torres Syncline, Southern Brazil.

AUTORES: Carla Joana Santos Barreto

Evandro Fernandes de Lima

Claiton Marlon Scherer

Lucas de Magalhães May Rossetti

PUBLICADO: Agosto de 2014, v. 285, p. 81-99.

PERIÓDICO: Journal of Volcanology and Geothermal Research

Esse artigo cientifico teve como objetivo propor um esquema de litofácies vulcânicas útil e simples para organização dos derrames da região de Santa Cruz do Sul-Herveiras. Os parâmetros para dividir os derrames em litofácies foram baseados nos padrões de vesiculação e estruturas de segregação, bem como nas texturas e características de superfície. As litofácies vulcânicas deveriam auxiliar na identificação dos processos que ocorreram dentro da sucessão de derrames básicos. A organização dos derrames em associações de fácies permite registrar os episódios que ocorreram durante a evolução do vulcanismo da ombreira sul da ST, incluindo a reconstrução da paleotopografia e avaliação dos estilos de *emplacement* dos derrames da PIP.

O método da análise de fácies aplicado na ombreira sul da ST, no perfil Santa Cruz do Sul-Herveiras provou ser uma ferramenta importante para estabelecer modelos evolutivos para essa região, elencando episódios vulcânicos distintos. Dessa forma, os derrames foram subdivididos em 16 litofácies e agrupados em três associações de litofácies: (1) *pahoehoe* composto precoce (2) *pahoehoe* simples precoce (3) *rubbly* simples tardio.

Nesse artigo foi apresentado um mapa geológico com escala de 1:50.000 separando de forma pioneira os diferentes tipos de derrames básicos e as lavas

ácidas da FSG na área estudada. Com os dados de gamaespectrometria também foi possível realizar essa separação, sendo que os derrames *pahoehoe* compostos e simples apresentaram os valores mais baixos de contagem total, seguidos pelo aumento desses valores em direção aos derrames *rubbly* simples. As lavas ácidas apresentaram aumentos significativos nos valores da contagem total em relação aos derrames básicos.

Os resultados obtidos nesse artigo sugerem que o início do vulcanismo na região de Santa Cruz do Sul-Herveiras foi marcado por lavas *pahoehoe* compostas (~2 m espessura) com olivina, indicando baixas taxas de efusão com um aporte de lavas colocadas de forma intermitente e sem erosão termal sobre as areias da FB. Derrames *pahoehoe* simples (~ 2-6 m espessura), mais diferenciados, também extravasaram sob baixas taxas de efusão, embora a alimentação desses magmas tenha se mantido mais constante, permitindo que os derrames se espessassem pelo processo de inflação. Os derrames *pahoehoe* foram sucedidos na estratigrafia pelos basaltos e andesitos basálticos com morfologia do tipo *rubbly*, caracterizados por um *emplacement* sob altas taxas de efusão, originando derrames mais espessos (~50 m), e vertical e lateralmente homogêneos.

Journal of Volcanology and Geothermal Research 285 (2014) 81–99

Contents lists available at ScienceDirect

Journal of Volcanology and Geothermal Research

journal homepage: www.elsevier.com/locate/jvolgeores

Lithofacies analysis of basic lava flows of the Paraná igneous province in the south hinge of Torres Syncline, Southern Brazil

Carla Joana Santos Barreto *, Evandro Fernandes de Lima, Claiton Marlon Scherer, Lucas de Magalhães May Rossetti

I, Universidade Federal do Rio Grande do Sul, Programa de Pós-Graduação em Geociências, Av. Bento Goncalves, 9500, CEP 91501-970, caixa postal 15001, Porto Alegre, RS, Brazil

ARTICLE INFO

Article history:
Received 17 March 2014
Accepted 8 August 2014
Available online 20 August 2014

Keywords:
Continental basaltic provinces
Lava morphologies
Pahoehoe lava flows
Rubbly lava flow
Lithofacies analysis of basaltic lavas

ABSTRACT

The Paraná igneous province records the volcanism of the earlier Cretaceous that preceded the fragmentation of the Gondwana supercontinent. Historically, investigations of these rocks prioritized the acquisition of geochemical and isotopic data, considering the volcanic pile as a monotonous succession of tabular flows. This work provides a detailed analysis of the emplacement conditions of these basic volcanic rocks, applying the facies analysis method integrated to petrographic and geochemical data. The Torres Syncline is a NW–SE tectonic structure, located in southern Brazil, where a thick sequence of the Paraná–Etendeka volcanic rocks is well preserved. This study was performed in the south hinge of the syncline, where the basaltic lava flows are divided into three lithofacies associations: early compound pahoehoe, early simple pahoehoe and late simple rubbly. The first lavas that erupted were more primitive compound pahoehoe flow fields composed of olivine basalts with higher MgO contents and covered the sandstones of the Botucatu Formation. The emplacement of compound pahoehoe flow fields is possibly related to intermittent low effusion rates, whereas the emplacement of simple pahoehoe is related to sustained low effusion rates with continuous supply. The thick simple rubbly lavas are associated with high effusion rates and were formed during the main phase of volcanism in the area. The absence of paleosoils between the lavas and lithofacies associations suggests that the successive emplacement of the lava flows occurred in a relatively short time gap. Geochemically, the lithofacies associations are low-TiO_2 and belong to Gramado magma type. The lavas of the south hinge of the Torres Syncline have a similar evolution when compared to other Continental Basaltic Provinces with earlier compound flows at the base and thicker simple flows in the upper portions.

1. Introduction

Large igneous provinces (LIPs) represent anomalous events in the Earth's history. In a relatively short time span, huge volumes of lavas and intrusions were generated and accumulated (Coffin and Eldholm, 1994; Storey et al., 2007; Bryan and Ernst, 2008). A portion of LIPs are continental basaltic provinces (CBPs), which, according to $^{40}Ar/^{39}Ar$ geochronological studies (Siberian Plateau, Karoo/Ferrar, Deccan, Columbia River, Paraná–Etendeka), were built from volumes on the order of 10^5–10^7 km^3 in short time intervals (~10^5–10^6 years). Typically, the volcanic sequences of these provinces are reported as a thick homogeneous volcanic pile.

The morphology of lava flows in CBPs is indispensable to the interpretation of lava flow dynamics with the determination of paleotopography conditions, the mechanism involved in their emplacement and the determination of the related environmental consequences (Self et al., 1997). Flood basalts are often subdivided into stratigraphic packages by variations in the geochemical signatures across lava fields in both vertical and lateral spaces (Saunders et al., 1997; Marsh et al., 2001) and less commonly by volcanic units. The detailed internal organization of flood basalt stratigraphy has often been neglected, and our understanding of the physical geometries present within flood basalts has suffered accordingly. The development of facies and architecture of facies is limited to few recent studies (e.g., Self et al., 1997; Jerram et al., 2000; Planke et al., 2000; Jerram, 2002; Single and Jerram, 2004; Waichel et al., 2012; Duraiswami et al., 2014; Rossetti et al., submitted for publication).

For this reason, it is essential to understand the internal and external shape of flood basalts and the internal variability of facies and rock properties, concentrating on the lava flow stacking patterns and the visible internal heterogeneities preserved within individual flows (Planke et al., 2000; Jerram and Robbe, 2001; Jerram, 2002).

To quantify the internal facies heterogeneities, this study devised a simple and useful volcanic lithofacies scheme for the flood basalts of the Santa Cruz do Sul-Herveiras section (southern Brazil), with emphasis on the vesiculation patterns and their segregation structures, textures and surface characteristics. Based on this scheme, the goals are

* Corresponding author. Tel.: +55 51 33087380.
E-mail address: carlabarreto.geo@hotmail.com (C.J.S. Barreto).

http://dx.doi.org/10.1016/j.jvolgeores.2014.08.008
0377-0273/

identify distinct volcanic episodes that occurred during the evolution of volcanism and determine the stratigraphy and lithofacies associations of the south hinge of the Torres Syncline in the Paraná CBP (Fig. 1). Furthermore, the proposed lithofacies associations are organized to reconstruct the paleotopography and evaluate the emplacement styles of the lava flows of the Paraná province.

2. Geological setting

The cratonic Paraná Basin has an elliptical shape with N–S direction that covers an area of ca. 917,000 km^2 in central-eastern South America (Frank et al., 2009; Fig. 1). The basin comprises a thick Upper Ordovician/Upper Cretaceous volcano-sedimentary succession, divided into six supersequences by Milani (1997): Rio Ivaí (Upper Ordovician–Lower Silurian), Paraná (Devonian), Gondwana I (Upper Carboniferous–Lower Triassic), Gondwana II (Middle–Upper Triassic), Gondwana III (Upper Jurassic–Lower Cretaceous) and Bauru (Upper Cretaceous). The supersequences are separated by regional unconformities.

The Gondwana III supersequence comprises an aeolian sandstone deposit at the base (Botucatu Formation) overlapped by a volcanic pile (Serra Geral Formation) covering an area of more than 1,300.000 km^2 in Brazil, Paraguay, Uruguay and Argentina. The sequence of aeolian sands overlapped by volcanic rocks is also present in well-exposed sections in the Huab basin in NW Namibia (Jerram et al., 2000).

The Botucatu Formation and its Etendeka equivalent Twyfelfontein consist of aeolian deposits, where sets and cosets of cross-strata are dominant (Mountney et al., 1998; Scherer, 1998). The aeolian deposits of the Botucatu Formation reach 400 m thick but are absent in some regions due to non-deposition. Scherer (2000, 2002) interpreted the Botucatu Formation as the record of a dry aeolian system as indicated by the accumulation of aeolian dunes without development of wet interdune facies.

The Serra Geral Formation (SGF) is a succession of volcanic rocks with a maximum thickness of approximately 1700 m in the center of basin (São Paulo state- Brazil; Almeida, 1986). This stratigraphic unit is composed mostly of tholeiitic basalts and basaltic andesites with minor rhyolites and rhyodacites in the upper portion (Melfi et al., 1988). The first pahoehoe lavas advanced over the unconsolidated sediments of Botucatu Formation and generate features of interaction such as peperites and lava prints (Scherer, 2002; Petry et al., 2007; Waichel et al., 2008). The confinement of early lava flows by the topography of the dunes favored the formation of ponded pahoehoe flow units (Jerram et al., 2009; Waichel et al., 2012).

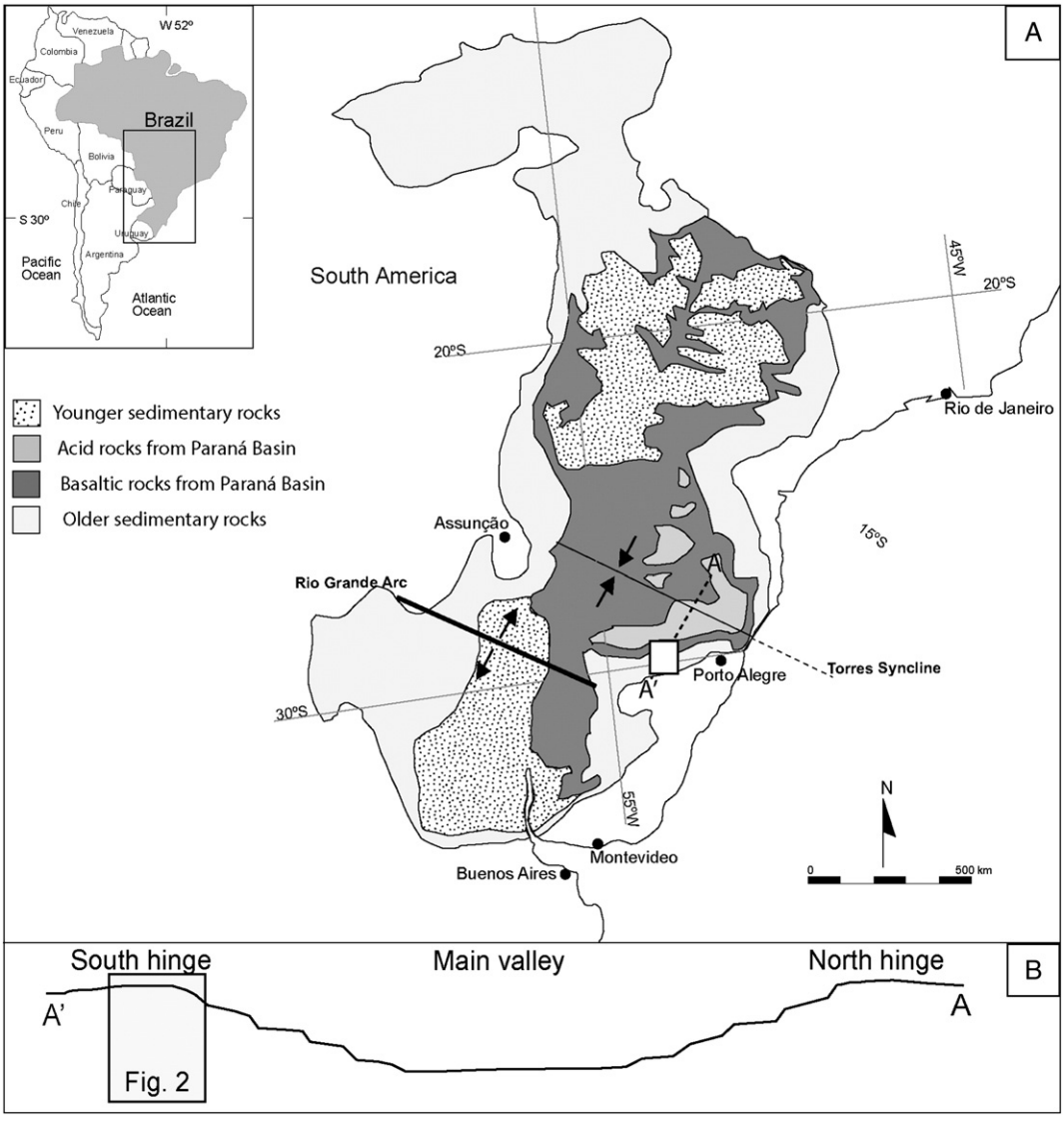

Fig. 1. A) Simplified geological map of Paraná Basin, highlighting the Torres Syncline structure; B) location of the studied area into the south hinge of syncline. Source: modified from Waichel et al. (2012).

The basaltic rocks of the SGF were divided into two groups based on TiO_2 contents: high-Ti basalts—HTi ($TiO_2 > 2\%$) occur in the north and central parts of the Paraná basin and the low-Ti basalts—LTi ($TiO_2 < 2\%$) that occur dominantly in the southern part (Bellieni et al., 1984; Mantovani et al., 1985).

Many large tectonic structures found in the Paraná Basin (e.g., Ponta Grossa arc, Torres Syncline, Rio Grande arc) have influenced the current limits of the basin, and, if active during the syn-volcanic subsidence process, induced the formation of sub-basins, which had an important role in the structural evolution of the Paraná Basin. These tectonic structures evolved since the Devonian and were particularly active in the Triassic–Jurassic periods (Fúlfaro et al., 1982).

The Torres Syncline is a large structure oriented NW–SE and located in the south Brazilian margin. It constitutes the eastmost outcrops of volcanic rocks in South American side of the Paraná–Etendeka CBP (Fig. 1). The syncline has been divided into three regions—a main valley, an intermediate zone and a south hinge, where each region displays distinct stratigraphy and total thickness reflecting the structural evolution of the syncline (Waichel et al., 2012). According to Waichel et al. (2012), the stratigraphy of the Torres Syncline can be divided into 1) Botucatu paleoerg, 2) Basic volcanic episode I, 3) Basic volcanic episode II, 4) Acidic volcanic, 5) Basic volcanic episode III and 6) Acidic volcanic episode II.

The lava flows belonging to the SGF inside the Torres Syncline have been previously considered to be monotonous flat lying basaltic lava flows. Waichel et al. (2006a, 2006b) were some of the first researchers to identify that there are fundamental differences in basaltic lava flow morphologies of the central portion of the Paraná CBP. Recent studies have identified pahoehoe, ´a´ā and rubbly lava flows in the south of this province at the Torres Syncline (Lima et al., 2012; Waichel et al., 2012; Rossetti et al., submitted for publication).

3. Study area and methodology

The study area is located in the Rio Grande do Sul state, southern Brazil, in the road section between the localities of Santa Cruz do Sul and Herveiras. This area is bounded between latitudes 29°30′ to 29°35′ and longitudes 52°30′ to 52°45′ W. There are excellent exposures in these road cuts where features related to lava morphology and internal structures can be observed. The systematic mapping of the lava flows allows the construction of an isopach geologic map at a 1:50.000 scale (Fig. 2), where the contacts of different volcanic rocks were based on elevation curves. Similar contacts were also observed in other profiles of the Torres Syncline (Waichel et al., 2012; Rossetti et al., submitted for publication). The geologic map was built to provide a new stratigraphic framework for the present investigation because, previously, all of the basaltic rocks of the Serra Geral Formation were included in a single unit.

3.1. Field mapping procedures

For assessment of the internal volcanic organization of the lava flows, good quality outcrops are required, in which the morphology of the lavas could be traced, the contacts outlined and is provided complete vertical sections of representative lava flows with regards to

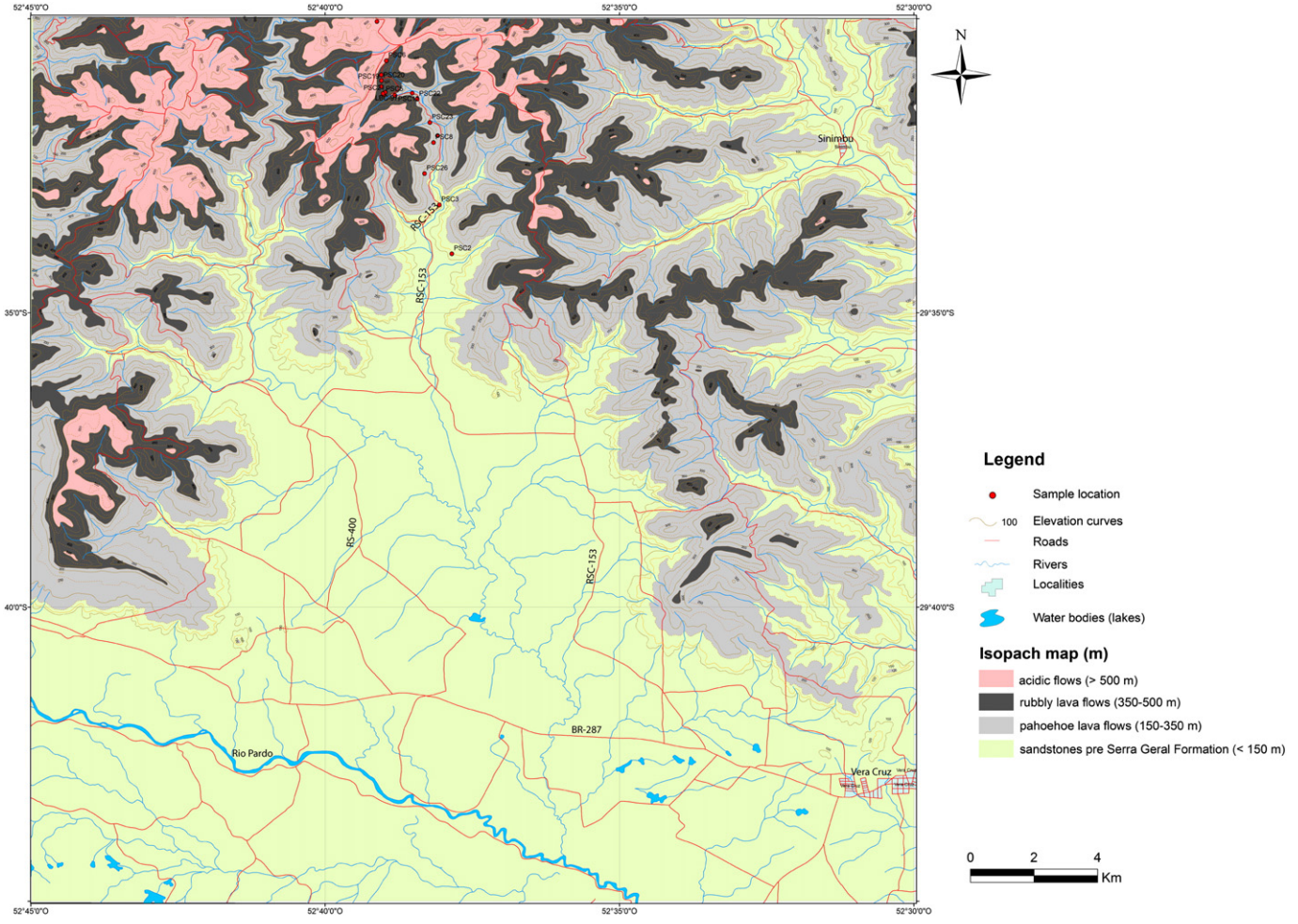

Fig. 2. Geological map of the Santa Cruz do Sul-Herveiras region with the location of the rock samples.

segregation structures, jointing and sampling for petrographic descriptions and whole-rock chemistry.

The basic lava succession is well exposed in sections along the RSC-153 road in the Santa Cruz do Sul-Herveiras profile, in the south hinge of the Torres Syncline. High-resolution graphic logging as outlined in McPhie et al. (1993), Miall (2000) and Farrell (2010) was undertaken along the study section to produce composite graphic logs. Lateral panels constructed from photomontages of the selected outcrops were used to define the two-dimensional (2D) geometries of the lava flows. Facies were defined mainly based on their primary attributes, such as bedding, lithology, texture, structure and vesiculation patterns. The facies described in the field were grouped in facies associations, which allow reconstruction of the paleotopography, evaluation of the emplacement conditions and understanding of the volcanism evolution.

3.2. Gamma ray spectrometric

The gamma-ray data for K, U, Th and total count with 70 measurements were acquired in the basic and acid lava flows of the study area. The equipment used was the Explorium Radiation Detective Systems Portable Gama Ray Spectrometer, model RS-125/230, belonging to the Postgraduate program in Geosciences from Federal University of Rio Grande do Sul.

This method allows distinct lava flows according to their differentiation degree, on basis in the K, U and Th radiogenic elements, where the contents increase toward the more differentiated lavas. Slightly compositional variations along the volcanic succession can be traced, mainly in the change from basic pahoehoe to rubbly flows, and these for acid lavas.

3.3. Petrography

The petrographic studies of twenty-six samples were aimed at mineralogical and textural identification and classification of the basic rocks from the study area. Pahoehoe flows were identified in the lower portions of the Torres Syncline, rubbly flows in the intermediate and acid flows in the upper part of the volcanic sequence. Furthermore the distinct volcanic textures from pahoehoe and rubbly were described. The acid lava petrography is outside of this study.

3.4. Whole-rock geochemistry

Twenty-one whole-rock chemical analyses were performed at ACME Analytical Laboratories Ltd., Vancouver, Canada, with the application of the 4A and 4B analytical routines. The former yielded the total contents of the main oxides and several trace elements by means of inductively coupled plasma atomic emission spectroscopy (ICP-AES). The 4B routine yielded the concentrations of rare earth and refractory elements by means of ICP-mass spectrometry (MS). In both routines, 0.2 g of powdered sample was used. All of the results are provided in Table 3.

4. Terminology of lithofacies and its use in volcanic environments

According to Miall (2000), the word facies can be used in a descriptive and interpretative sense, where the descriptive facies can be defined as lithofacies. The lithofacies term is used to refer to certain observable attributes in sedimentary-rock bodies that can be interpreted in terms of depositional processes.

The definition of lithofacies proposed by Miall (2000) may also be applied to volcanic rocks, where the lithological, textural and structural attributes observable in outcrop scale can be interpreted in terms of effusion rate and eruption conditions or emplacement style (Selley, 1978; Walker, 1984; Cas and Wright, 1987). Lithofacies analysis is a useful approach to unravel the eruption history and the evolution of volcanism in old terrains, where the volcanic sequences have undergone overprinting of the original stratigraphic and structural features by weathering.

Lithofacies may be defined very broadly to encompass mappable stratigraphic units, or they can involve a fine and detailed description obtainable in centimeter-by-centimeter logging. In order to understand the lava flow types and dynamic of emplacement, a relatively fine degree of description and subdivision is required.

Shorthand descriptive classification schemes are generally developed from fluvial systems (e.g., Miall, 1986). The use of these schemes should facilitate the understanding of the field geology, and for this reason the facies schemes should be kept as simple as possible.

A lithofacies code of at least two letters must be adopted to facilitate the documentation and quick field and laboratory identification (Miall, 1996, 2000). Primary lithological descriptors are given by capital letters and subsequent lower-case letters indicate texture, structure and vesiculation patterns. In the case of volcanic rocks, the lithofacies are not defined on the basis only on grain size or rock-type, because each lithofacies exhibits a range of characteristics, which could overlap with those of other lithofacies. Therefore, it is best to use a combination of features to define a lithofacies (Branney and Kokelaar, 2002).

Unlike sedimentary lithofacies, the change of volcanic lithofacies is transitional, without a well-defined threshold, where each lithofacies is a result of different depositional processes, which are likely influenced by many small-scale local factors.

The individual lithofacies can be grouped in facies associations, which can be defined in the sedimentary context as a group of facies genetically related to one another and which have some environmental significance (Collinson, 1969). The volcanic lithofacies can also be grouped into lithofacies associations, and represent a set of volcanic processes that occur in specific area and that are associated with different lava flow units, where each flow-unit is separated by a cooling unit.

5. Lithofacies analysis in the Santa Cruz do Sul-Herveiras section

Table 1 lists the lithofacies descriptions in the Santa Cruz do Sul-Herveiras section, the codes used for note taking and the interpretation of the process responsible for the formation of each one.

The criteria used to identify the lithofacies in outcrops include (1) change in the internal textures and structures, (2) change in the surface features of the lava flows and (3) change in the vesiculation patterns, where different processes are responsible by the formation of distinct segregation structures. The field scale photographs of each individual lithofacies are shown in Figs. 3 and 4.

6. Lithofacies associations in the Santa Cruz do Sul-Herveiras section

Despite this study has established several lithofacies, the paleoenvironment and emplacement processes and volcanic event sequences cannot be interpreted from a single volcanic lithofacies because different processes may produce similar lithofacies. Therefore, to achieve a correct interpretation and paleoenvironmental reconstruction, representative volcanic sequences and lithofacies associations need to be established. The basic volcanic rocks of the SGF (Santa Cruz do Sul-Herveiras section) are categorized into three distinct lithofacies associations (Table 2): 1) early compound pahoehoe, 2) early simple pahoehoe, and 3) late simple rubbly.

6.1. Early compound pahoehoe lithofacies association

This lithofacies association comprises the basal sequences of the studied section and is characterized by the smaller unit-flows with limited aerial extent (Fig. 5A, B) and individual thickness ranging from 50 cm to 2 m (Table 2), where the overall thickness of individual lobes set reach 3 m. There are some locally interleaved extensive lava sheets with thickness from 2 to 3 m displaying a simple morphology

Table 1
Summary of lithofacies description and interpretation of the mafic lava flows of the Santa Cruz do Sul-Herveiras section.

Lithofacies code	Lithofacies	Position within lava flow	Interpretation
Bpv	Vesiculated basalt with pipe vesicles	Base	Frozen-in upward-rising gas bubbles formed perpendicular to the solidification front
Bcs	Basalt with C-S cylinder sheets	Lower half of the flow	Vesicle cylinders end within of top horizontal vesicle sheets. Solidification fronts advance more slowly in a later stage
Bproc	Basalt with proto cylinder	Lower half of the flow	Accumulation of vapor and differentiated melt causes the formation of vertical trail of vesicles with small size and indistinct limits
Bvc	Basalt with vesicle cylinder	Core	Residual liquids generated within the lower solidification zone move into vesicle-rich low-density areas, through of gas filter-pressing mechanisms that migrate toward the top of the flow after the host lava ceased all movement
Bmvph	Microvesiculated massive basalt with phaneritic texture	Core	Slower crystallization. Mechanism of endogenous transfer (inflation) within a visco-elastic crust in an insulated environment, which is responsible by the coarser granular texture
Bchvs	Basalt with core horizontal vesicle sheets	Core	Last body of differentiated liquid to form in the flow when the solidification fronts advance more slowly. Form only after the flow has stagnated and is no longer inflating
Bgv	Basalt with giant domed segregation vesicles	Upper half of the core	Coalescence of bubbles of different sizes by mass transfer above the lower solidification front
Bpod	Basalt with pods filled by segregation vesicles	Upper half of the core	Accumulation zone of segregation vesicles frozen-in upward-rising gas bubbles
Bthvs	Basalt with top horizontal vesicle sheets	Within or just below the chilled crust	Cooling front progressing downward into the lava accompanying inflation. Fluctuations of pressure and/or flux during active inflation
Bvt	Basalt with vesiculated crust top	Upper crust	The skin confines just below it gas bubbles risen from the underlying fluid
Bros	Ropy basalt surface	Upper crust	Flexible skin is deformed by the motion of the lava
Bbss	Smooth bilowry basalt surface	Upper crust	After the initial burst of liquid lava, the top of the flow becomes smooth continuous flexible skin of cooler lava and freeze the surface
Bsvb	Slighter vesiculated flow base with elongated and stretched vesicles	base	Smooth emplacement of lavas over flat surface
Bam	Aphanitic and hypocrystaline massive basalt	core	Faster cooling and crystallization with degassing. Initial emplacement through endogenous growth that enabled the thickening
Bsv	Aphanitic massive basalt with sparse centrimetric vesicles	Upper half of the core	Increase of the vesicularity upward to flow-top breccias
Brt	Flow-top breccia	Upper crust	Inflation and accumulation of volatiles due to tensile stresses led to degassing and rupturing, while the increase in the effusion rates promote to brecciation

(Fig. 5A), despite the dominating compound morphology in this early stage of volcanism.

There are S- and P-type lobes with smoother reliefs, where the S-type lobes (spongy; Walker, 1989) are characterized by lack of pipe vesicles, microvesiculated massive cores (Bmvph; Fig. 5D) and homogenous distribution of large amount millimetric vesicles (~1–5 mm) toward the center that decrease in size toward the periphery (Fig. 5D). The P-type lobes (pipe vesicles; Wilmoth and Walker, 1993) are more common and exhibit vesicles in the shape of tubes (pipes) at the base (Bpv; Fig. 5A, B, C, E), microvesiculated massive cores (Bmvph; Fig. 5B, C, E) and vesiculated tops (Bvt; Fig. 5C, E). The upper crusts of both lobes are essentially thin glassy rinds, with smooth (Bbss) and ropy (Bros) surfaces, where they often display a red to orange color due to oxidation (Fig. 5D, E).

This lithofacies association is interpreted as compound pahoehoe flows, where the lobes are the smallest coherent package of lava (Self et al., 1998). These compound pahoehoe lobes are result of low effusion rates with intermittent lava supply and minimum inflation. The lobe sets filled the pre-existing topography controlled by the accommodation space available. The term compound lava proposed by Walker (1952) is recommended for lavas divisible into flow-units that may be related to the same eruptive event, where each flow-unit (pahoehoe lobe) has a significantly and solidified cooled top (semi-solid carapace) before another flow-unit superposed it. Typical features of the compound pahoehoe lavas include concentration of vesicles in the uppermost third portion and a zone of pipe vesicles along the base in P-type pahoehoe lobes. In general, the compound pahoehoe lavas scattered in nearly horizontal surfaces tend to adopt individual lobate shapes and the set of lobes generates a flat topography.

6.2. Early simple pahoehoe lithofacies association

This lithofacies association consists of sheet flows laterally extensive with individual thickness between 1 and 6 m and the whole thickness of these flows reaching up to 100 m, forming a flat topography (Fig. 6B).

These thicker lava flows exhibit mainly in the core the greatest amount of vesiculation patterns and their segregation structures, (Fig. 6A). Slightly coarse segregation material fills these structures, which display abrupt contact with the host lava (Fig. 6A, C, D).

Pipe vesicles (2–13 cm long, 1 cm wide; Bpv) filled with secondary minerals such as zeolites and quartz generally mark the basal zone (Fig. 6A, C, E).

The interface base-core is marked by proto-cylinders (up to 28 cm long; Bproc) that form a vertical trail of vesicles with indistinct limits (Fig. 6A), which are generated through the same process of formation of vesicle cylinders.

The coarse-grained massive core (Bmvph) is microvesiculated (Fig. 6A, C, D) and locally exhibits levels of oxidized entablature with planar–curvilinear fractures that present similar coarse-grained texture and composition. Several vesiculation patterns occur in the core: vesicle cylinders (0.02–2 m long, 2–6 cm wide; Bvc; Fig. 6A, C, D), cylinder-sheets (10–25 cm wide; Bcs; Fig. 6A, D) and core horizontal vesicle sheets (2–10 cm wide; Bchvs; Fig. 6A, D).

The upper vesiculated crust–core interface is transitionally marked by giant vesicles (reach 1 m wide; Bgv) filled with zeolite and quartz (Figs. 3G, 6A) and pods (15–30 cm wide; Bpod) that encompass segregation vesicles <1 cm (Fig. 6C). The flow tops are highly vesicular (>50%) reaching up to 3 m thick with a complete range of vesicle shapes and sizes. It is common a typical gradation in vesicles distribution, with a large number of minor vesicles (2–5 mm) at the upper portion and a minor number of larger vesicles (1–5 cm) at the inner portion (fining up). Most vesicles are spherical, some are domed, and others are flat and elongated (Fig. 6A, C, E). In general, these upper crusts display top horizontal vesicle sheets that range from 2 to 10 cm thick (Bthvs; Fig. 6A, E). The thin external portion also displays smooth and ropy surfaces (Bbss and Bros; Fig. 4B, C) with elongated vesicles pointing to different directions of the flow.

Based on lava flow characteristics aforementioned such as higher thickness and large amount of segregation structures, this lithofacies

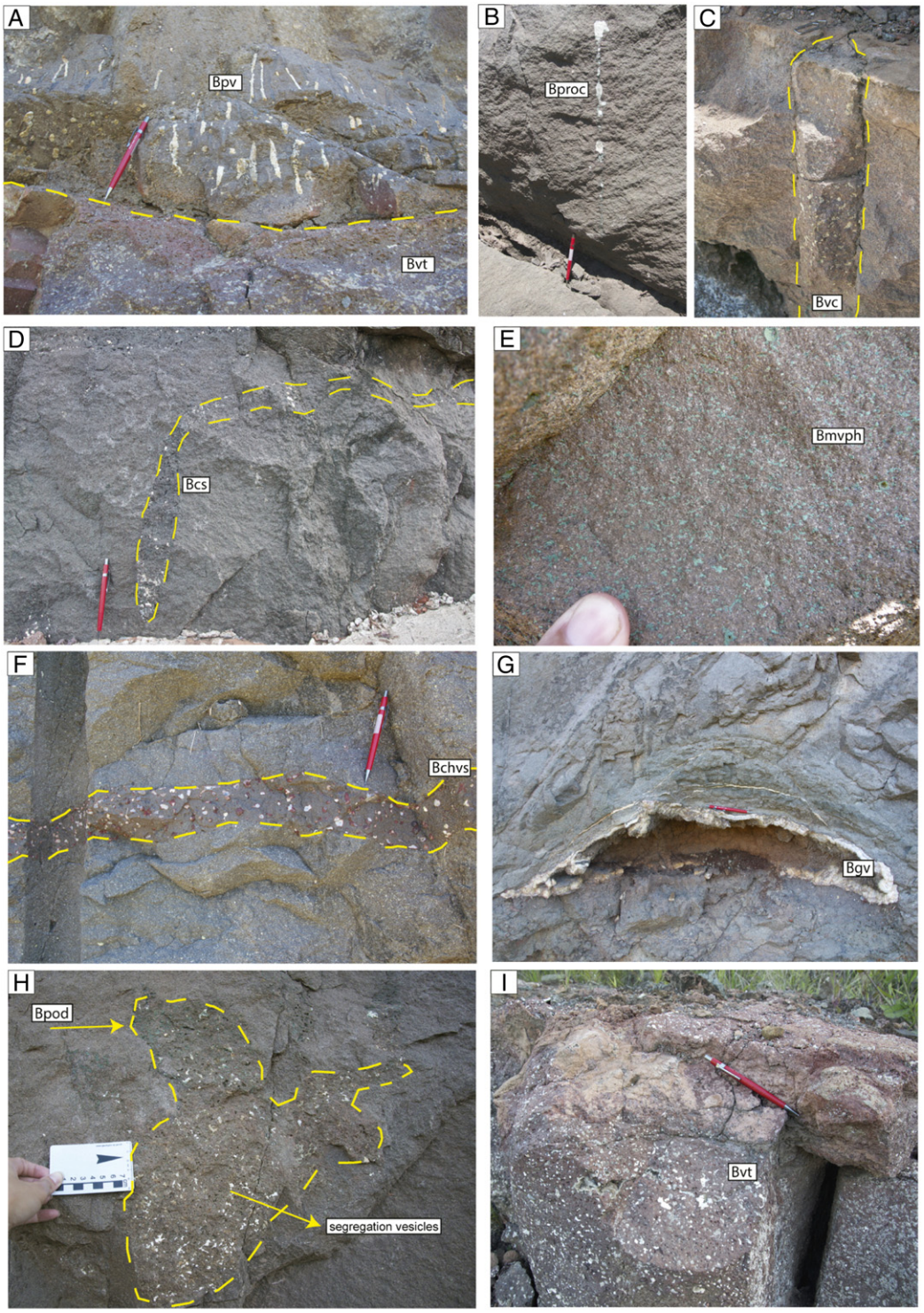

Fig. 3. Volcanic lithofacies defined for simple and compound pahoehoe lavas of the study area. A) Contact between vesiculated top (Bvt) of the underlying lava flow and the basal portion of the overlying lava flows marked by pipe vesicles (Bpv); B) proto-cylinders (Bproc); C) vesicle cylinders (Bvc); D) cylinder sheets (Bcs); E) massive phaneritic basalt core (Bmvph); F) core horizontal vesicle sheets (Bchvs); G) domed giant vesicles (Bgv) in the upper half of the core; H) pods (Bpod) with large concentration of segregation vesicles; I) vesiculated upper crust (Bvt).

association can be interpreted as simple pahoehoe lava flows, which are product of low effusion rates with sustained lava supply, where the inflation process was dominant, originating a flat topography with tabular shape. These lavas solidified under a semi-solid carapace, which allowed an inflation of this crust with the internal pressure of volatiles, promoting lava spreading, thickening of external surfaces and transport for long distances. To form these flows, a horizontal paleotopography (<5° declivity) is required. The simple pahoehoe lava flows consist of a series of massive alternating layers, where the boundary between the upper portion of one unit and the basal part of the succeeding unit cannot normally be seen. On occasion, the time interval between the superposition of units (lava

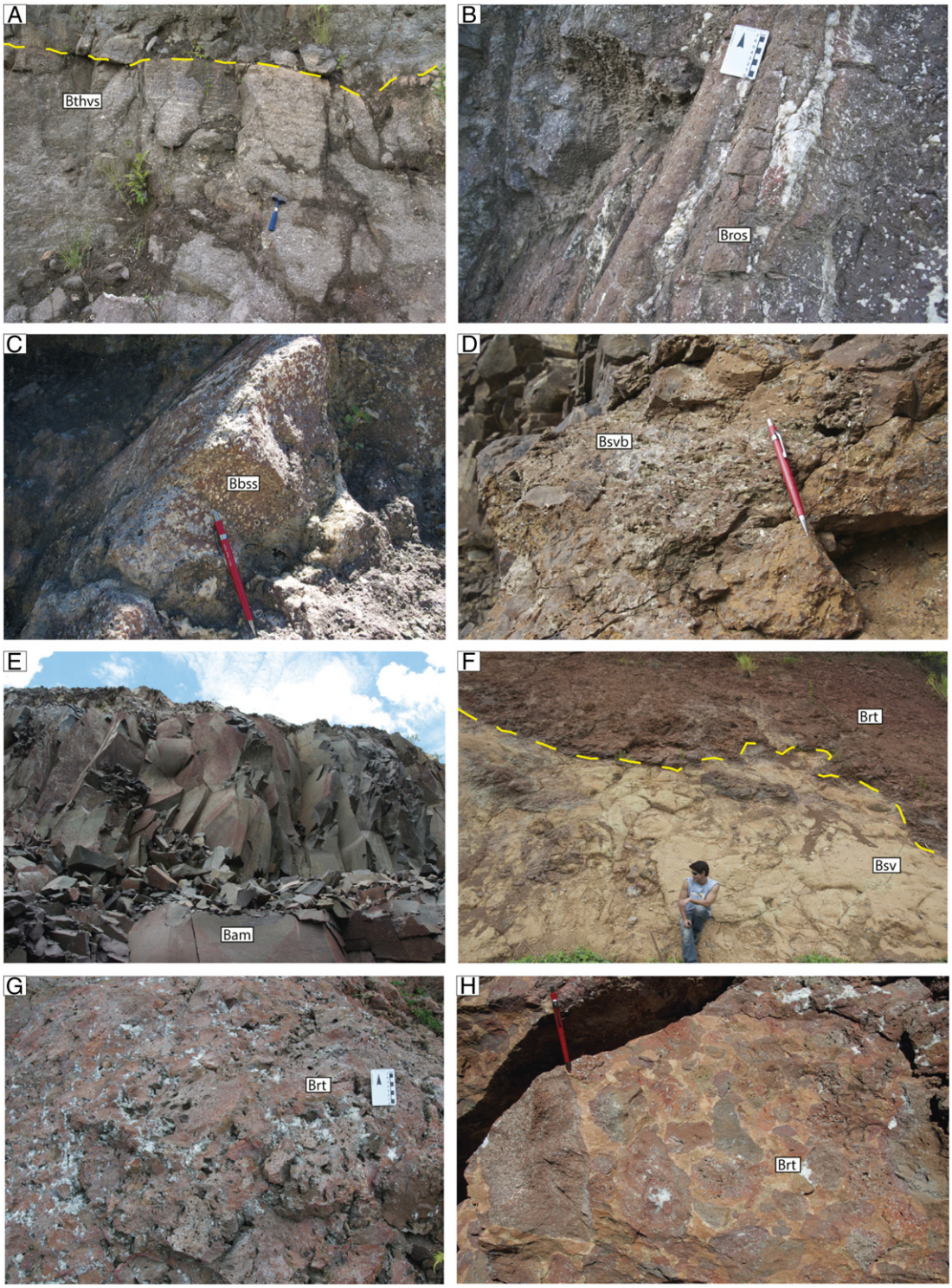

Fig. 4. Volcanic lithofacies defined for the upper crust of pahoehoe lavas, and for rubbly lava flows. A) Top horizontal vesicle sheets (Bthvs) observed in simple pahoehoe; B) ropy surface (Bros) that occur in both compound and simple pahoehoe lavas; C) billowy smooth surface (Bbss) of the compound and simple pahoehoe lavas; D) vesiculated base (Bsvb) of the rubbly lavas; E) massive aphanitic core (Bam) of the rubbly lavas; F) transition between vesiculated zone of the upper half of the core (Bsv) and flow-top breccias (Brt); G) flow-top breccias (Brt) with sub-rounded to sub-angular fragments enclosed in red/brown very fine coarse matrix; H) fragments of the top breccia (Brt) enveloped in a sandstone matrix.

flows) is too short in that no significant cooling of one unit occurs before it is buried. Thus, the whole lava layers cool as a single cooling unit, which is revealed by the distribution of layers or bands of vesicles that tend to be parallel with the margins of the external surface (Walker, 1952). Walker (1952) proposed the term simple for lavas not easily divisible into flow-units, and this term has been employed to characterize pahoehoe lavas with near horizontal upper and lower surfaces and broad flow fronts with large lateral extensions defined as single eruptive units (Walker, 1971; Keszthelyi et al., 1999; Bondre et al., 2004).

Table 2
Lithofacies associations of the study area.

Lithofacies association	Description	Interpretation	Scheme
Late simple rubbly	Rubbly lava flows exhibit individual thickness of 50 m including a centimetric vesiculated base (Bsvb), a aphanitic core (Bam) of 30 m that have transition for a massive zone with sparse vesicles (Bsv) and to flow-top breccias (Brt) around 20 m thick.	Rubbly lava flows were initially accomodated endogenously within the sheets, enabling them thicken due to inflation process, which is related to increase in the effusion rate. This was possible by insulating effect of brecciated upper crusts	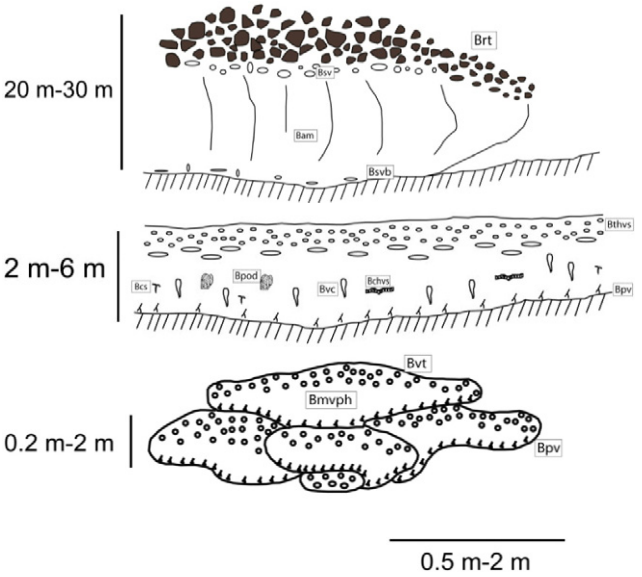
Early simple pahoehoe	Pahoehoe sheets with individual thickness from 2 m to 6 m. These flows exhibit the largest number of segregation structures (Bpv, Bcs, Bproc, Bvc, Bmvph, Bchvs, Bgv, Bpod, Bthvs, Bros, Bbss)	These flows were formed under low effusion rate with sustained lava supply, where the inflation process is dominant. Their emplacement results in flat terrains. Lavas solidified under a semi-solid carapace that allows a thickening of lobes.	
Early compound pahoehoe	P- and S-type lobes with thickness up to 2 m are arranged in the following lithofacies: a base with pipe vesicles (Bpv) in the case of P-type lobe, a hollocrystalline and microvesiculated massive core (Bmvph) and a vesiculated crust top (Bvt). The thin glassy surfaces can be smoothy (Bbss) or ropy (Bros)	Compound pahoehoe lavas were emplaced under low effusion rate with intermittent lava supply, and minimum inflation. Lavas filled the pre-existing topography controlled by available accomodation space. Lavas solidified under a semi-solid carapace	

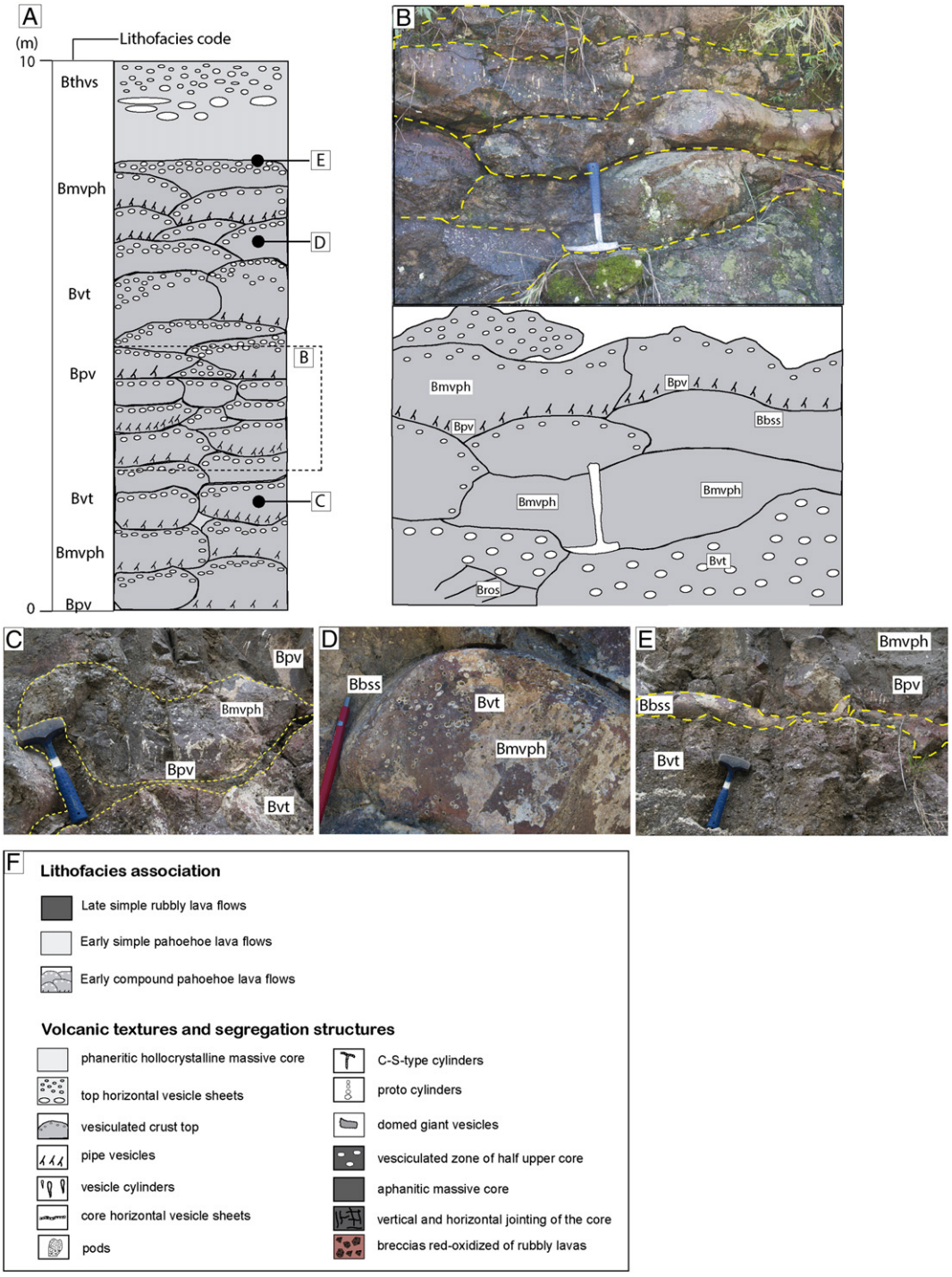

Fig. 5. A) Log showing the relation of the lithofacies in the early compound pahoehoe lithofacies association; B) overlapping of multiples S- and P-type lobes; C) overlapping of lobes, where the contact is marked by vesiculated top (Bvt) of the underlying and the base with pipe vesicles (Bpv) of the overlying; D) S-type lobe with microvesiculated massive phaneritic core (Bmvph), vesiculated top (Bvt) and billowy smooth surface (Bbss); E) contact of three lobes, where the underlying is marked by vesiculated top (Bvt), the middle exhibit billowy smooth surface (Bbss) and the overlying display pipe vesicles in the base (Bpv); F) explanation of symbols used in the volcanic logs of this paper. See Table 1 for the lithofacies codes and their interpretations.

6.3. Late simple rubbly lithofacies association

This lithofacies association is less complex in terms of vesiculation patterns and textures (Fig. 7A) and is distributed in the upper portion of the volcanic sequence (Fig. 10A). These flows characterize a thicker tabular geometry (individual thickness around 50 m; Fig. 7B) than the previous lavas. The internal structure of these flows is divided into four parts as described in the literature: a smooth vesiculated base (Bsvb), aphanitic massive core with planar–curvilinear joints (Bam), upper vesiculated portion (Bsv), and a brecciated rubbly top (Brt) (Fig. 7A).

A thin vesicular zone with thickness ranging from 7 to 18 cm characterizes the basal portion of these lava flows (Bsvb), where spherical and elongated/stretched vesicles occur with diameters from 1 mm to 1 cm filled by zeolite and quartz (Fig. 7D). Pipe vesicles were not observed in any of the locations.

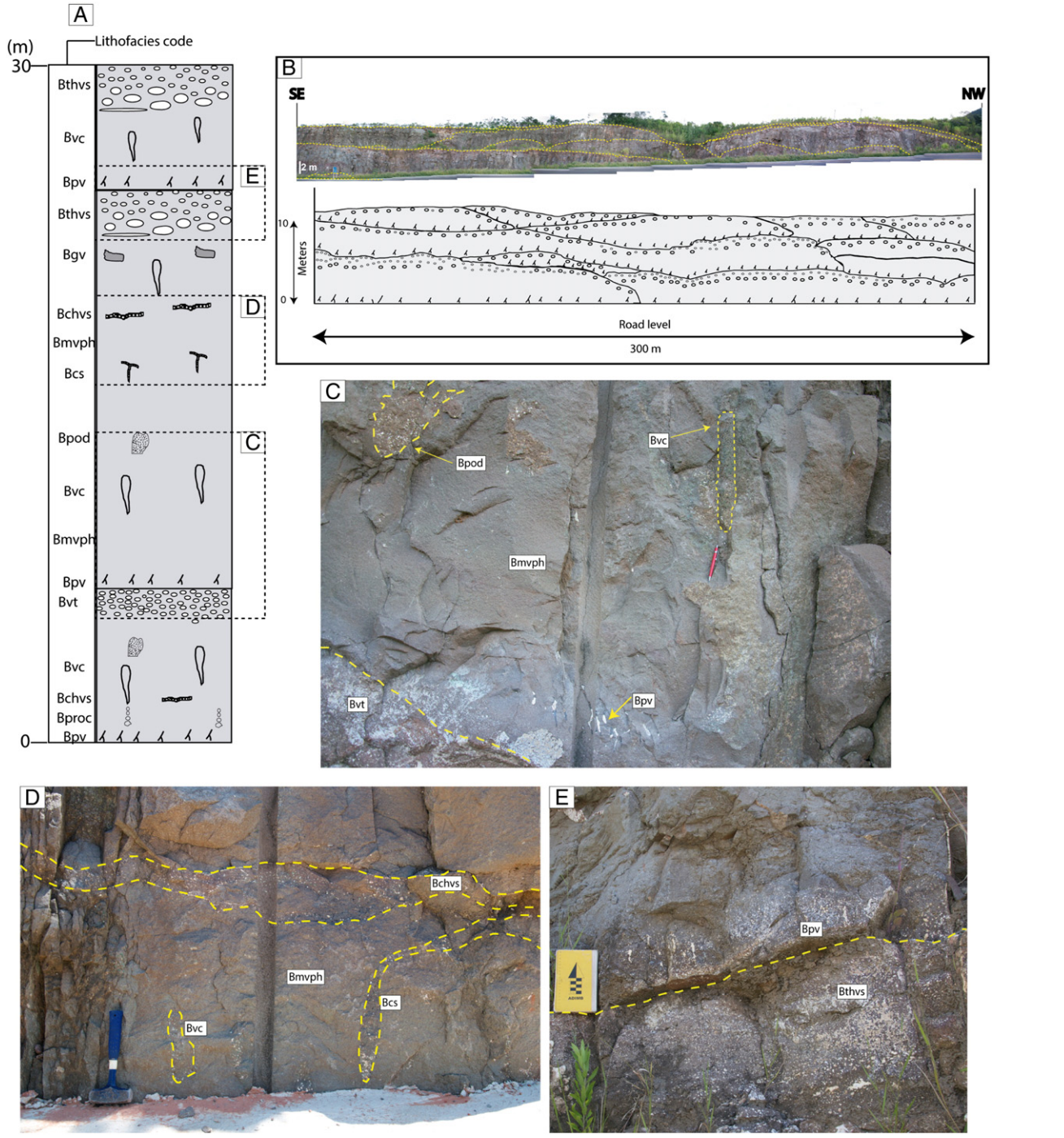

Fig. 6. A) Log showing the relation of the lithofacies in the early simple pahoehoe lithofacies association. B) Lateral outcrop panel showing the relation between the different pahoehoe sheets; C) transition between the lithofacies from the vesiculated top (Bvt) of the underlying lava flow, with pipe vesicles in the base (Bpv) of the overlying lava flow, microvesiculated phaneritic massive core (Bmvph), vesicle cylinders (Bvc) and pods (Bpod); D) transition of different lithofacies in the core of the lava flow, with vesicle cylinders (Bvc), S-C-type cylinders (Bcs) and core horizontal vesicle sheets (Bchvs); E) contact between top horizontal vesicles sheets (Bthvs) of the underlying lava flow and pipe vesicles in the base (Bpv) of the overlying lava flow. See Fig. 5F for explanation of symbols and Table 1 for lithofacies codes and their interpretations.

The massive core (Bam) has an average thickness of 30 m and a horizontal and vertical jointing pattern with conchoidal and curvilinear cooling fractures typical of finer-grained aphanitic and hypocrystalline basalts (Fig. 7A, B, E, F).

Vesicularity in the lava core does change significantly upward, where contorted and spherical, stretched/elongated vesicles (diameters between 0.5 and 3 cm) are sparsely distributed in the upper half of the core of these flows (Bsv; Fig. 7G), with their size increasing toward the flow-top breccias (reach 6 cm next to the top).

The top of these flows (Brt) is 20 m thick and directly overlies the vesiculated zone (Fig. 7G). The top is composed of breccias, which consist of an unsorted chaotic assemblage of fragments with a pinkish red color, highly oxidized with massive portions and vesiculated of basalts (up to 60% of vesicles), where the fragments are sub-rounded to sub-angular and range between 5 and 30 cm in size (Figs. 4G, 4H). The oxidized fragments of these breccias suggest that the original crusts were previously formed and later fragmented. The first tops display reddened vesicular fragments of various sizes that are enveloped in a sandstone matrix

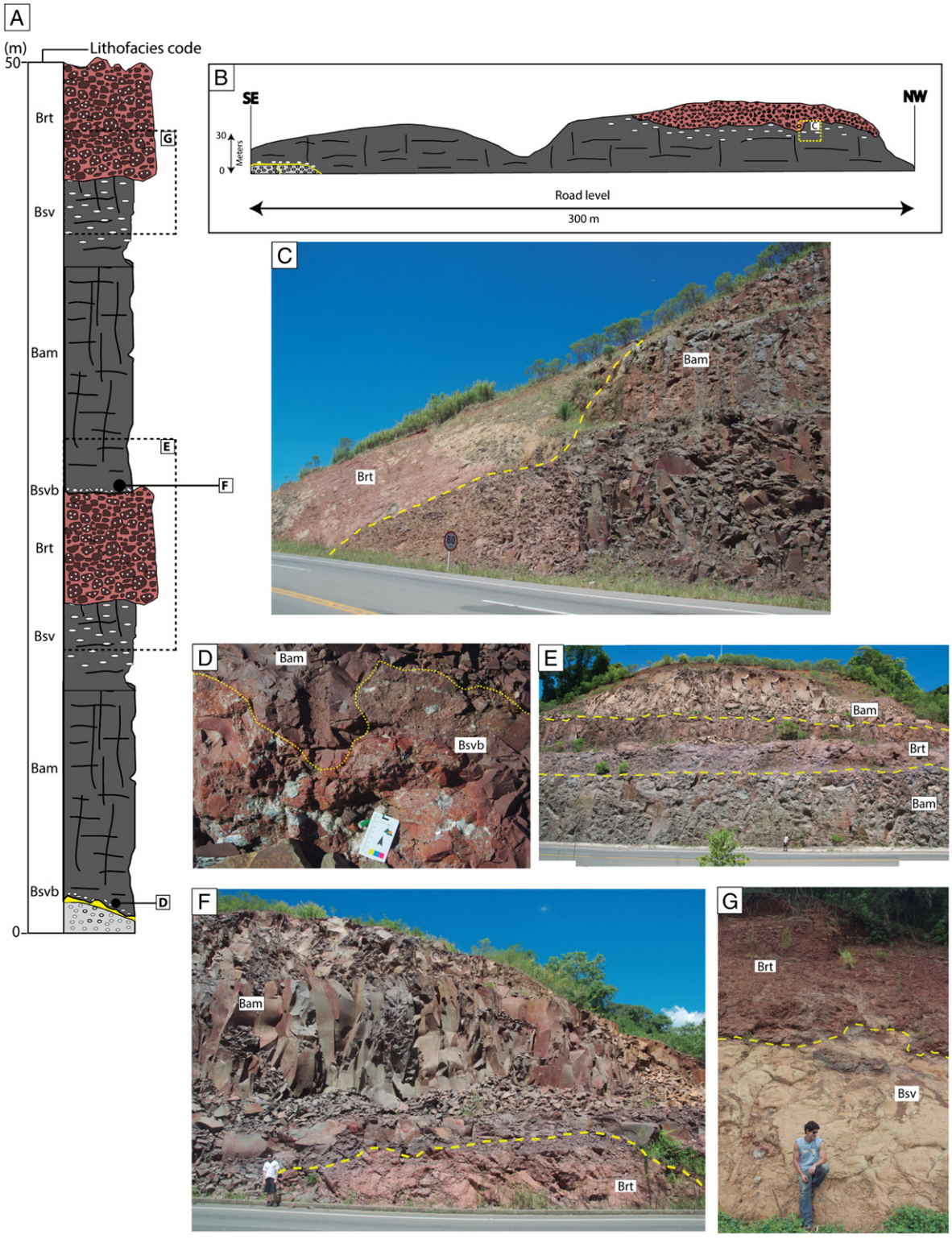

Fig. 7. A) Log showing the relation of the lithofacies in the late simple rubbly lithofacies association. B) Lateral outcrop panel showing the relation between the different lithofacies; C) contact of aphanitic massive core (Bam) and flow-top breccias (Brt); D) contact of vesiculated base (Bsvb) and massive core (Bam); E) contact between two rubbly lava flows, where occur the transition from (Bam) to (Brt) lithofacies in the underlying lava flow, which is overlapped by the massive core (Bam) of the overlapping flow; F) contact of flow-top breccias (Brt) of the underlying lava flows and massive core (Bam) of the overlapping lava flow; G) contact between vesiculated portion of upper half of the core (Bsv) and flow-top breccias (Brt). See Fig. 5F for explanation of symbols and Table 1 for lithofacies codes and their interpretations.

(Fig. 4H), whereas the top fragments of the overlying flows are enclosed in a deep red/brown very fine coarse matrix of rock flour that is invariably altered and friable (Fig. 4G).

The vesicles within the fragments are spherical, stretched, elongated and have different orientations (Fig. 4G, H). Their sizes range from one fragment to the other, in general, with diameters <1 cm for spherical vesicles and up to 5 cm for the stretched vesicles; most vesicles are filled with secondary minerals such as zeolites and quartz.

This lithofacies association is interpreted as simple rubbly lavas, which were initially accommodated endogenously within the sheets,

enabling them to thicken due to a possible inflation process related to an increase in the effusion rate. The inflation in rubbly flows is possible because of the insulating effect of the brecciated upper crusts.

In the literature, rubbly pahoehoe has been defined for lavas with an internal structure of four parts: autobrecciated top, coherent vesicular upper crust, dense but jointed core and lower glassy vesicular crust (Keszthelyi, 2000; Keszthelyi and Thordarson, 2000). The flows tops are composed of fragments of pahoehoe (Keszthelyi, 2000), whereas the base is smooth and also typical of pahoehoe flows. In this study, the term rubbly flow instead of rubbly pahoehoe flow is justified because its petrographic patterns (discussed below) are very different from classical pahoehoe, which reflects a distinct emplacement style and cooling history.

7. Petrography

7.1. Pahoehoe lava flows

Plagioclase, augite, opaque minerals, and apatite constitute the primary mineral components of these flows. Subordinate highly altered olivine crystals occur restricted to early compound pahoehoe lobes.

The base of the pahoehoe lavas is aphanitic and hypocrystalline, which predominate aphyric, intersertal, vesicular and amygdaloidal textures (Fig. 8A, B). The intersertal texture consists of augite, olivine, and plagioclase microphenocrysts, plagioclase microlites and acicular augite embedded in a mesostasis replaced by fine-grained iron oxide and smectite. Some vesicles are rounded with celadonite and partially to completely filled by zeolite forming the amygdales (Fig. 8B). Other vesicles are subordinately filled with carbonate (Fig. 8B), chalcedony, and subhedral and anhedral aggregate of quartz crystals. Most of the plagioclase crystals are subedric, clear to be highly replaced by albite plus zeolite, and range from microphenocrysts to microlites. Olivine crystals in compound pahoehoe lavas ranging in size from 0.73 to 0.34 mm are found in various stages of alteration. Usually, the olivine is altered to a green microcrystalline aggregate identified as bowlingite, which is a mixture of smectite–chlorite and serpentine minerals. Moreover, in some rocks is common for the olivine to be completely altered to iron oxide and a dark orange–brown platy mineral was classified as iddingsite (Fig. 8C).

For both simple and compound pahoehoe lava flows, the core displays holocrystalline (fine to medium-grained phaneritic) to aphyric textures (Fig. 8D). The intergranular texture predominates with augite crystals between plagioclase laths, and the subophitic texture with plagioclase laths with sizes ranging from 1.28 to 0.62 mm partially embedded in several augite crystals ranging from 0.7 to 0.34 mm (Fig. 8E). The diktytaxitic texture is very common in this portion of the lava flow and represents microvesicular pattern with small inter-mineral cavities filled with late minerals such as smectite and celadonite (Fig. 8F). Porphyritic, glomeroporphyritic, intersertal, vesicular and amygdaloidal textures are rare. The plagioclase phenocrysts occur mainly as laths with grain sizes ranging from very fine-to-fine. In many flows, they are relatively uniform in their concentration and display no alignment tendency.

The top of pahoehoe lava flows is aphanitic and hypocrystalline and displays the same textures of the base with higher amount of vesicles and amygdales (Fig. 8G, H). Some vesicles are outlined by chalcedony and filled with zeolites from different habits (prismatic, botroidal and fibrose). The cavities between crystals (diktytaxitic texture) are filled by smectites, which are a product of alteration of the mesostasis

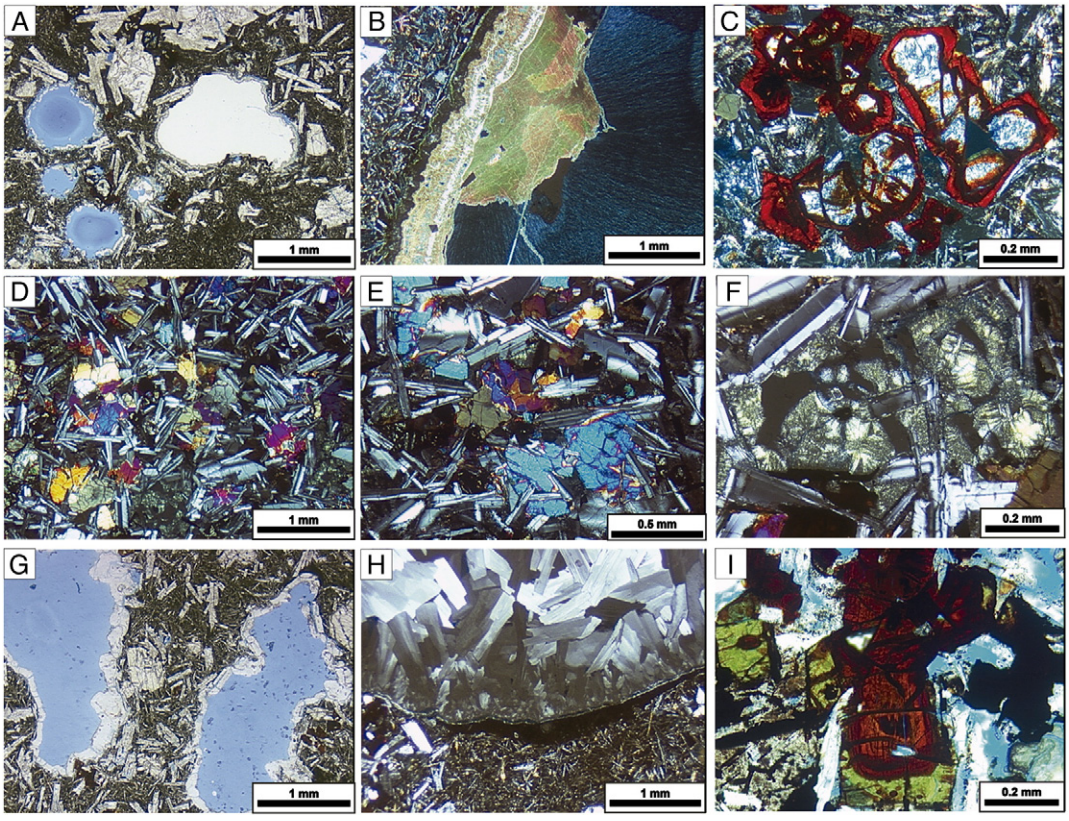

Fig. 8. Photomicrographs of the pahoehoe lava flows. A) Vesicular, amygdaloidal and intersertal textures of the base of lava flows; B) amygdaloidal texture of the base, where the vesicle is rounded by celadonite and filled by carbonate and zeolite; C) olivine crystals highly altered for iddingsite; D) fine to medium-grained texture of the massive core; E) intergranular texture with augite crystals between plagioclase laths and subophitic texture with plagioclase laths partially embedded in several augite crystals; F) microvesicular pattern observed mainly in the core of lava flows, where the small inter-mineral cavities are filled by late smectite; G) vesicular texture of the hypocrystalline top of pahoehoe lavas; H) amygdaloidal texture of pahoehoe top, which the vesicles are filled by prismatic zeolite; I) olivine crystals with core altered to iddingsite and rims replaced by bowlingite.

together with iron oxide. The plagioclase crystals are clear to be highly replaced by an exsolution of albite and zeolite. Most of the augite crystals are well preserved, although some have been partially altered to iron oxide. On the other side, the olivine crystals are highly altered to bowlingite and iddingsite, where the core of some crystals is totally altered to bowlingite and the rims were altered to iddingsite (Fig. 8I). The most external portion of the simple and compound pahoehoe lava flows is often holohyaline and oxidized.

7.2. Rubbly lava flows

The mineral composition of the rubbly lavas is the same as the pahoehoe: plagioclase, augite, opaque minerals, apatite and lacking olivine crystals.

The core of these lava flows is aphanitic, hypocrystalline and aphyric (Fig. 9A). They are composed predominantly of sub-equal proportions of plagioclase and augite in an intergranular relationship. Intersertal texture is common; where the mesostasis altered to fine-grained iron oxides encompass crystals of plagioclase and augite (Fig. 9B). Diktytaxitic texture is most clearly defined in coarsely crystalline rocks, where the cavities are relatively uniform in their distribution, such as pahoehoe lava flows. However, this texture is also observed in rubbly flows, where the intergranular open spaces are more scattered in their distribution and occupied by smectite (Fig. 9C). Anhedral grains of an opaque phase are scattered throughout the groundmass. The vesiculated zone marks the transition of core to the lower portion of the top and displays small fragments of vesiculated unsorted autobreccias.

The rubbly flow-top breccias are constituted by hypocrystalline vesicular basalt fragments with plagioclase microlites (Fig. 9D). Most of these fragments exhibit sizes ranging from 0.4 mm to 3 mm, where the spaces inter-fragments are cemented by zeolite and quartz (Fig. 9E). Although angular basalt fragments are common in the rubble, many fragments have undergone considerable rounding at the thin section (Fig. 9D, 9E) and field scales (Fig. 4G, H), where their edges appear to have been smoothened. The red material of the matrix is an admixture of fine-grained rock flour and altered glass. The vesicles have spherical and stretched shapes and are filled with zeolite (Fig. 9F).

8. Stratigraphy succession and relationship between the lithofacies associations of Santa Cruz do Sul-Herveiras volcanic sequence

The stacking patterns of the lava successions throughout the studied section are characterized by an up-sequence increase in flow individual thickness and increase in the brecciation of the flow top. The whole sequence of Santa Cruz do Sul-Herveiras section represents around ~472 m thick of volcanic rocks of the SGF, considering up to the acid flows of the Herveiras region. The gamma ray spectrometric method was essential to separate the lava flows through differentiation degree of the rocks (Fig. 10A).

The lowermost of the section is essentially formed by multiple compound pahoehoe lobes (early compound pahoehoe lithofacies association), which are in contact with sandstones of Botucatu Formation in elevation of 130 m (Fig. 10E). These lavas are followed in the stratigraphy by simple pahoehoe (early simple pahoehoe lithofacies association; Fig. 10D). Both lobes and simple pahoehoe lavas display spheroidal weathering and cooling fractures perpendicular to external crust pointing to inflation process.

The simple pahoehoe lavas are overlain by a smooth contact with rubbly flows (late simple rubbly lithofacies association) at an elevation of 350 m (Fig. 10C). The vesiculated basal zone of the rubbly lava flows is smooth and devoid of pipe vesicles, while the thick, dense and jointed core transitions to an upper vesiculated core and these are followed in the stratigraphy by irregular flow-top-breccias.

Successive acid lavas constitute the uppermost flows of the section and overlap rubbly lavas at elevations above 500 m (Fig. 10B). The acid lavas are massive, with horizontal and vertical jointing, and thicker than rubbly flows. These acid rocks were not inserted in the lithofacies scheme and lithofacies associations of the Santa Cruz do Sul-Herveiras section, because are outside the scope of this work.

Dykes and discontinuous sheets of sandstone reddish in color are common in the studied area. The sheets range from 20 mm to 7 cm thickness, mainly occurring between compound and simple pahoehoe lava flows. Sandstone sheets of 20 cm thick separate the top of pahoehoe and the base of rubbly lavas. On the other side, there are no sandstone sheets in the contact between the rubbly and acid flows, which indicates that the support of sand ended on the top of the volcanic sequence.

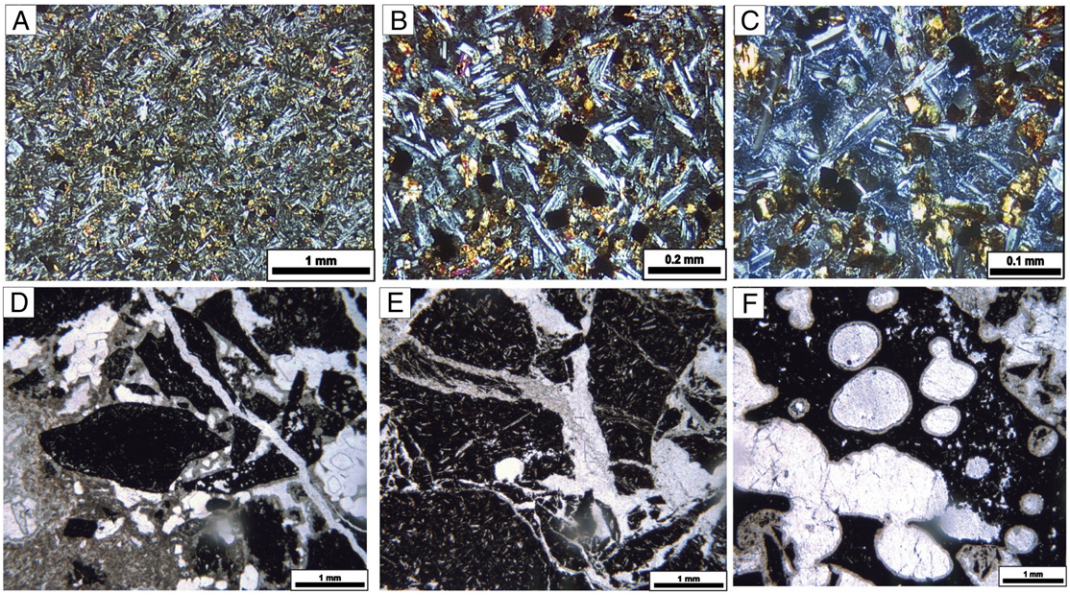

Fig. 9. Photomicrographs of the rubbly lava flows. A) hypocrystalline, aphyric core with very fine-grained texture; B) zoom on the intersertal texture; C) diktytaxitic texture in the core, where the open spaces between minerals are occupied by late smectite (blue resin); D) flow-top breccia of rubbly lavas with vesicular fragments of basalt; E) rounded fragments and inter-fragment spaces of the top breccias cemented by zeolite and quartz; F) spherical and stretched vesicles of fragments filled by zeolite.

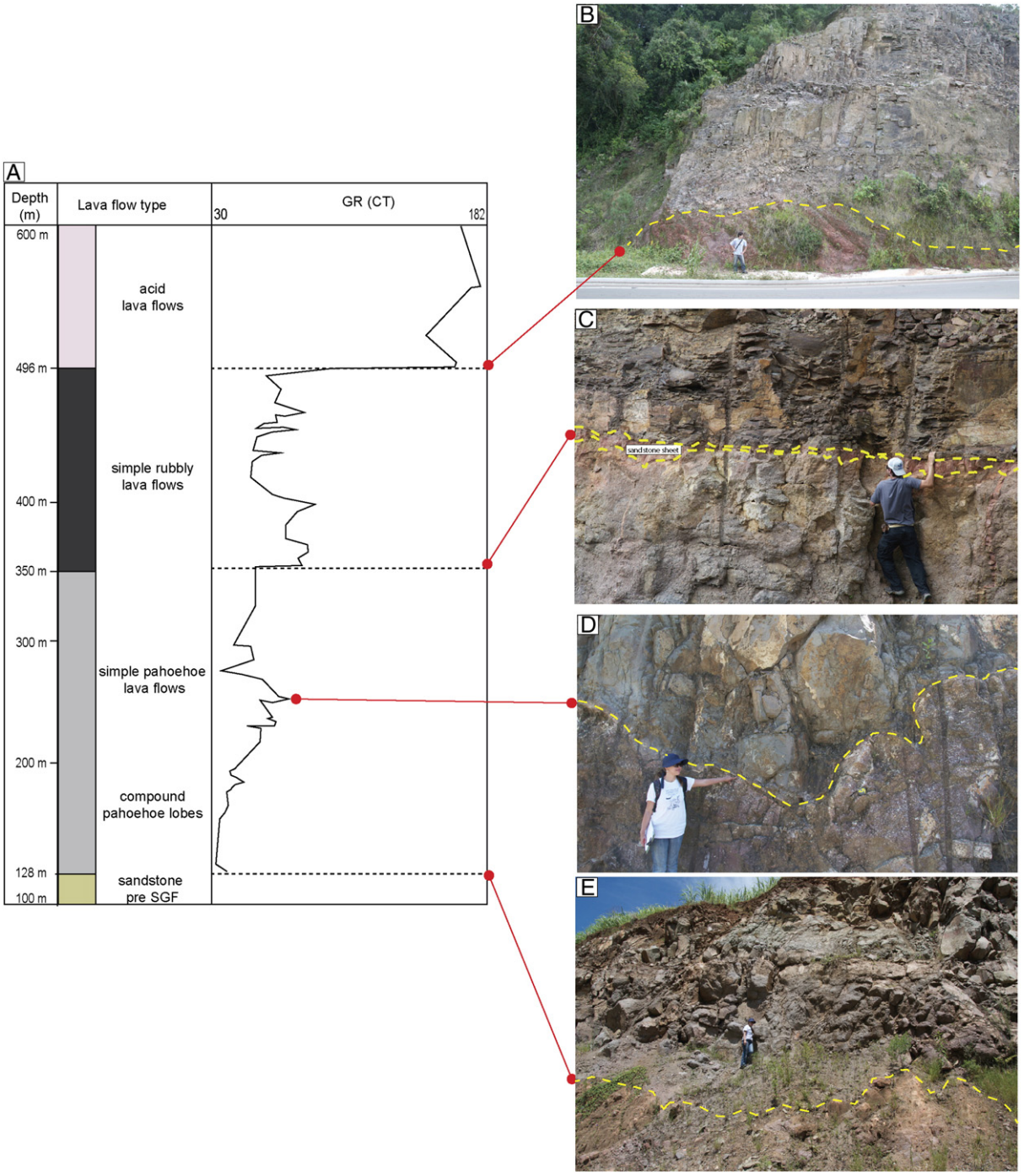

Fig. 10. A) Stratigraphic cross-section based on log correlations, displaying the lithofacies associations (datum: sandstones of Botucatu Formation at the base and acid lavas at the top), including the gamma ray spectrometric data obtained in the different rocks; B) change of late simple rubbly lithofacies association for acid lavas; C) relationship between late simple rubbly lithofacies association and early simple pahoehoe lithofacies association with a sandstone sheet between them indicating a time gap; D) contact between early simple pahoehoe and early compound pahoehoe lithofacies associations; E) contact between sandstone of Botucatu Formation and lobes of the early compound pahoehoe lithofacies association.

Fig. 10 represents the relationship between the different lithofacies associations along the studied stratigraphic section.

9. Geochemistry of basaltic rocks

The mafic rocks of the study area have SiO_2 contents ranging from 46.70 to 55.96 wt.% with FeO/MgO rates (Table 3) from 1.44 to 4.01, typical of tholeiitic rocks (Myashiro, 1974). The contents of TiO_2 smaller than 2% are compatible with the low-TiO_2 series (Bellieni et al., 1984; Mantovani et al., 1985), whereas the contents of high field strength (HFS) and rare earth elements (REE) are similar to the Gramado magma type (Peate et al., 1992).

In the early compound pahoehoe lithofacies association, the lava flows are more primitive, being petrographically olivine basalts, with contents of SiO_2 ranging from 46.70 to 50.34 wt.%, MgO from 5.58 to 7.30, and Ni 21.9 to 70.9 ppm.

We observed an overlap between the sample compositions of early simple pahoehoe and late simple rubbly lithofacies associations with

Table 3
Geochemical data of basalts from the Santa Cruz do Sul region.

Sample	PSC2C	PSC3A	PSC3B	PSC3C	PSC3D	PSC3F	PSC3L	PSC3M	PSC23	PSC3G	PSC3H	PSC3I	PSC3J	PSC3K	PSC22	PSC26	PSC4A	PSC4B	PSC5B	PSC20	PSC21
Morphology type	comp phh	comp phh	comp phh	comp phh	comp phh	comp phh	comp phh	comp phh	comp phh	simp phh	simp phh	simp phh	simp phh	simp phh	simp phh	simp phh	rub	rub	rub	rub	rub
OL	X	X	X	X	X	X	X	X	X												
Major elements																					
SiO2	49.45	50.40	48.30	46.70	48.83	49.05	48.19	49.48	47.97	50.39	50.02	52.34	49.51	50.02	51.21	53.20	55.96	55.46	53.83	52.22	50.16
TiO2	1.07	1.19	1.15	1.11	2.11	1.13	1.13	1.34	1.05	1.77	1.16	1.20	1.44	1.39	1.17	1.14	1.55	1.56	1.41	1.47	1.40
Al2O3	15.39	14.91	14.94	15.22	12.72	14.01	14.36	15.63	15.65	13.40	14.40	14.00	15.4	14.42	16.35	14.88	12.90	12.97	13.54	14.24	14.39
Fe2O3	11.72	11.07	10.61	10.89	13.34	10.51	10.97	12.37	10.97	12.83	10.54	10.83	12.51	12.08	10.27	10.68	13.66	13.69	13.03	13.09	13.03
MnO	0.16	0.17	0.15	0.17	0.21	0.15	0.14	0.17	0.20	0.18	0.16	0.14	0.17	0.14	0.15	0.17	0.18	0.19	0.17	0.20	0.18
MgO	5.96	6.37	6.19	7.30	6.28	6.40	6.87	5.58	6.60	5.14	4.59	3.94	4.79	4.38	5.12	5.45	3.06	3.11	4.37	4.77	5.48
CaO	10.42	10.48	9.29	10.74	8.17	7.81	9.30	9.29	10.63	8.63	7.34	7.12	8.63	7.46	9.55	8.91	6.57	6.57	8.04	8.63	9.34
Na2O	2.09	2.07	2.12	1.90	2.10	3.92	2.51	2.07	1.76	2.25	2.79	2.41	2.20	2.81	2.27	2.21	2.64	2.57	2.59	2.53	2.33
K2O	0.85	1.12	1.00	0.93	1.77	1.01	1.16	1.60	0.45	1.00	1.04	1.42	1.95	1.97	1.28	1.92	2.11	2.19	1.79	1.17	0.79
P2O5	0.15	0.21	0.21	0.20	0.37	0.21	0.20	0.18	0.15	0.33	0.23	0.18	0.19	0.18	0.21	0.17	0.21	0.20	0.19	0.20	0.18
LOI	2.50	1.70	5.70	4.60	3.80	5.50	4.90	2.10	4.40	3.80	7.40	6.20	3.00	4.90	2.20	1.10	0.90	1.30	0.80	1.20	2.50
Total	99.79	99.75	99.72	99.80	99.68	99.76	99.79	99.8	99.82	99.74	99.75	99.77	99.78	99.79	99.78	99.80	99.74	99.76	99.76	99.77	99.78
Fe2O3/MgO	1.77	1.56	1.54	1.34	1.91	1.48	1.44	1.99	1.49	2.24	2.06	2.47	2.35	2.48	1.80	1.76	4.01	3.96	2.68	2.47	2.14
Minor elements																					
Ba	350.0	420.0	542.0	301.0	621.0	524.0	279.0	282.0	213.0	380.0	395.0	341.0	320.0	326.0	396.0	358.0	381.0	404.0	315.0	330.0	278.0
Co	40.9	43.5	40.2	39.0	39.7	36.4	37.2	40.7	41.9	32.9	37.5	38.9	43.3	40.3	33.0	38.1	40.1	39.1	36.6	36.7	36.3
Ni	44	55	64	64	47	71	55	22	46	23	70	34	28	25	9	23	10	7	19	9	12
Sc	35.0	36.0	35.0	35.0	36.0	34.0	37.0	37.0	34.0	36.0	34.0	33.0	36.0	36.0	31.0	32.0	33.0	33.0	34.0	34.0	36.0
Rb	49	32	26	39	45	19	48	35	15	18	19	38	64	72	29	73	76	81	68	41	14
Sr	258	356	768	305	336	528	337	207	246	390	609	465	221	235	294	211	208	215	208	226	230
Ta	0.5	0.7	0.7	0.7	1.1	0.6	0.7	0.5	0.4	1.2	0.8	0.5	0.9	0.4	0.6	0.6	0.8	0.8	0.6	0.5	0.5
Nb	6.6	13.4	10.3	10.0	22.6	10.8	10.6	7.4	6.3	17.2	10.8	9.0	8.8	7.6	7.4	8.7	12.3	12.9	10.5	9.4	8.9
Th	3.6	2.9	2.6	2.3	5.2	2.2	2.7	4.5	3.4	4.5	2.7	4.1	5.1	4.2	4.5	5.9	7.4	7.1	5.8	5.7	4.6
U	0.6	0.7	0.5	0.3	0.8	0.5	0.4	1.0	0.7	0.7	0.4	1.2	1.2	0.9	1.3	1.1	1.8	1.4	1.6	1.5	1.0
Zr	115	131	117	107	221	112	119	124	114	189	119	117	140	134	139	144	171	168	137	148	129
Y	30.8	23.1	19.3	18.4	33.1	18.3	21.0	23.6	21.3	28.2	23.2	21.3	26.7	23.8	23.8	24.3	31.7	31.1	27.5	29.0	27.3
Pb	2.6	1.8	4.1	3.4	4.2	3.4	5.2	3.2	5.0	4.9	4.3	3.2	2.8	2.4	5.5	1.9	2.6	2.9	3.2	3.1	3.7
Hf	3.8	3.2	3.3	2.6	5.4	3.1	3.3	3.2	2.9	4.8	2.7	3.1	3.3	3.2	3.4	4.1	4.7	4.8	3.9	4.1	3.0
Ga	18.0	22.0	16.2	17.3	23.4	12.4	16.6	17.6	16.7	17.1	15.2	20.1	19.3	17.7	17.6	16.8	22.8	23.2	21.8	20.0	18.6
Cs	2.5	0.8	1.0	1.8	1.4	2.5	2.9	0.8	0.4	0.3	0.4	1.1	1.1	1.6	0.7	2.2	2.4	2.7	2.6	1.9	1.1
La	24.7	22.3	20.1	18.6	34.5	19.5	20.2	18.9	17.6	28.8	21.2	17.9	21.0	19.6	22.9	22.0	26.4	26.7	21.6	23.1	19.7
Ce	41.4	46.7	38.4	36.2	73.1	36.9	37.6	38.5	35.3	58.2	39.3	36.2	43.8	39.8	45.7	46.2	56.1	54.7	41.9	46.0	40.8
Pr	6.2	5.4	5.0	4.6	8.7	4.6	4.9	5.0	4.4	7.2	5.0	4.7	5.4	5.0	5.7	5.8	6.8	6.8	5.4	5.7	5.0
Nd	27.8	21.5	21.5	18.0	34.8	20.3	19.2	18.9	17.1	29.4	18.7	18.7	23.7	21.3	25.6	25.4	28.8	27.9	22.4	22.0	19.8
Sm	5.5	4.6	4.2	3.8	6.9	4.1	3.9	4.3	3.9	6.1	3.9	4.3	4.6	4.7	5.0	4.8	6.0	5.9	4.8	5.0	4.8
Eu	1.6	1.37	1.2	1.2	1.8	1.2	1.3	1.2	1.2	1.6	1.2	1.2	1.3	1.3	1.4	1.3	1.6	1.5	1.3	1.5	1.3
Gd	6.3	4.5	4.0	3.8	6.7	4.0	4.3	4.8	4.4	6.0	4.7	4.1	4.9	5.1	5.2	5.4	6.1	6.0	5.1	5.6	4.9
Tb	0.9	0.7	0.6	0.5	1.0	0.6	0.6	0.7	0.6	0.9	0.6	0.7	0.7	0.8	0.7	0.8	1.0	1.0	0.8	0.8	0.8
Dy	5.9	4.1	3.3	3.8	6.0	3.5	3.7	4.5	4.1	5.8	4.0	4.0	4.2	4.4	4.4	4.4	5.5	5.3	5.6	5.7	4.7
Ho	1.1	0.8	0.8	0.8	1.2	0.6	0.7	0.8	0.8	1.1	0.9	0.8	1.0	0.9	0.9	0.9	0.9	1.2	1.1	1.1	0.9
Er	3.2	2.2	2.4	2.00	3.2	1.7	2.2	2.4	2.2	3.0	2.4	2.1	2.4	2.7	2.4	2.5	3.1	3.2	3.3	2.7	2.9
Tm	0.4	0.3	0.3	0.3	0.5	0.3	0.3	0.4	0.3	0.4	0.3	0.3	0.3	0.4	0.3	0.4	0.5	0.4	0.4	0.4	0.4
Yb	2.8	2.1	1.9	1.7	3.1	1.8	2.0	2.4	2.0	2.6	2.1	2.3	2.4	2.6	2.6	2.4	3.4	2.7	2.9	2.9	2.5
Lu	0.4	0.3	0.3	0.3	0.5	0.3	0.3	0.3	0.3	0.4	0.3	0.3	0.4	0.4	0.4	0.4	0.5	0.4	0.4	0.4	0.4

OL = presence of olivine microphenocrysts.
comp phh = compound pahoehoe lava flows; simp phh = simple pahoehoe lava flows.
rub = rubbly lava flows.

SiO_2 ranging from 49.51 to 55.96 wt.% and MgO from 3.06 to 5.48 wt.% (Table 3), which suggests that different flow morphologies cannot be explained by changes in the chemical compositions.

10. Discussion

10.1. Emplacement model of basaltic lava flows at the Santa Cruz do Sul-Herveiras section based on lithofacies associations

Models of facies and facies associations in mafic volcanic systems are becoming increasingly more detailed as new data sets and approaches are developed (e.g., Self et al., 1998; Single and Jerram, 2004; Planke et al., 2005; Nelson et al., 2011; Waichel et al., 2012; Rossetti et al., submitted for publication).

On the basis of the aforementioned lithofacies analysis, the basaltic volcanic rocks in the south hinge of the Torres Syncline were grouped in three lithofacies associations aiming to reconstruct the paleotopography and evolution of the volcanism in this portion of the syncline.

The early compound pahoehoe lithofacies association consists of the earlier olivine-rich basalts that assume complex architectures of the compound pahoehoe lavas. These flows were erupted at low effusion rates, effused passively with no clear evidence of thermal erosion over the sandstone of Botucatu Formation, but intermittent lava supply with lobes stacked horizontally and vertically. These compound pahoehoe flows are not correlated over large distances, most likely due to little size of the sets of lobes, which filled the space available in the pre-existing topography.

The mode of emplacement of compound flows is ruled by insulating transport of lava from the vent to the flow front, which the lava is able to travel under a stable crust with minimal thermal loss. The flow propagates through lobe-by-lobe emplacement (Baloga and Glaze, 2003) and creates a flow field with an array of stacked lobes with different shapes and sizes, resulting in anastomosing architectures.

On the other side, thicker basaltic andesite lavas without olivine that effused under low effusion rates, although with sustained lava supply characterize the early simple pahoehoe lithofacies association.

The continuous low effusion rate allows simple pahoehoe lavas to undergo inflation process and the coalescence of lobes, where the lobe boundaries are indistinguishable and the flow field resembles a sheet-like flow. Evidence of inflation was found in the study area, often visible in the thin glassy crust that envelopes the lava flow behaving as insulations, in cooling fractures perpendicular to external crusts in a centripetal pattern, and in the subordinate presence of tumuli. The tumuli (concept proposed by Walker, 1991) must have developed initially as thin lobes, and the lava supply rates must have been initially low, but, at some point, a new pulse of lava result in an increased lava influx that led to consequent inflation and possibly merging of some lobes on top of the previously emplaced flows. Distinguishing tumuli in cross-sections, where the lobes are overlapping and amalgamated, can be challenging, mainly because of the absence of squeeze-ups.

The appearance of larger elongated vesicles, greater degree of curvilinear jointing in the core and flow-top breccias indicate a change of emplacement conditions and the transition from pahoehoe in the early eruptive event to rubbly lava flows in the later stages.

All the lava flows of late simple rubbly lithofacies associations are large sheet lobes with the absence of lateral variability in their segregation structures and textural characteristics. Rubbly individual flows cover areas larger than compound and simple pahoehoe and are substantially thicker with brecciated portions in the top. This might be attributed to the advancement of lava streams on shallow slopes under higher effusion rates resulting in rapid lava inflation and coalescence of lobes, accompanied by rapid volatile exsolution. The formation of these lavas through increase in the paleo-slope is ruled out because the former pahoehoe lavas of the sequence created a flat topography. In the absence of slopes to drive high flow velocities, typical of channeled ´a´ā flows, the mass eruption rate and its control on lava effusion rates become important, which facilitate the continuous tearing and brecciation of the rubbly upper crust.

The lithofacies association analysis suggests that in the south hinge of the Torres Syncline a single eruptive event occurred with directly superposed distinct volcanic episodes.

In the Paraná CBP, the short time span of volcanism ~ 1 Ma (ages obtained by ^{40}Ar–^{39}Ar and U–Pb baddeleyite/zircon methods; Turner et al. (1994); Stewart et al. (1996); Kirstein et al. (2001); Thiede and Vasconcelos (2010); Janasi et al. (2011)) and the absence of paleosoil horizons make it difficult the reconstruction of the flow fields formed during the eruption. However, some interflow sandstone layers (centimeters) that occur in the study area could suggest short hiatuses in the magma supply of the lava flows from the same volcanic event (Fig. 10C), although it is difficult to define the duration of the gap. These layers could be used for the individualization of the flow fields. However, further studies are needed to answer these remaining questions.

10.2. Mechanism of formation of rubbly flow morphology within the Serra Geral Formation and implications for the south hinge of the Torres Syncline

The inflation process as the main emplacement mechanism to explain compound and simple pahoehoe flows is relatively well understood and widely used. There are many examples of use of the inflation process for explain the emplacement conditions in Paraná–Etendeka province and in other CBPs (Jerram, 2002; Bondre et al., 2004; Passey and Bell, 2007; Duraiswami et al., 2008; Brown et al., 2011; Waichel et al., 2012; Vye-Brown et al., 2013; Duraiswami et al., 2014; Rossetti et al., submitted for publication). On the other side, transitional lava types in CBPs are more common than previously thought, although their study is relatively recent (Self et al., 1997; Duraiswami et al., 2008, 2014; Rossetti et al., submitted for publication).

The identification and systematic documentation of these transitional typologies are therefore important for constrain the emplacement dynamics of lava flows, which can aid in better understanding of flood basalt architecture and in building of a robust volcanic stratigraphy for ancient CBPs, such as the Paraná–Etendeka province.

Previous studies in the Paraná CBP have described thicker simple flows with brecciated tops as 'a'ā lava flows (Waichel et al., 2006a, 2006b; Hartmann et al., 2010; Lima et al., 2012; Waichel et al., 2012). In classical ´a´ā flows, there is evidence of partially resorbed breccias clasts in the interior of the flows and core material pushing up into the breccias (Keszthelyi, 2002). The clinker breccias of the base and top have fragments of angular basalt of different sizes and vesicle orientations. These characteristics are absent in the rubbly flows of south hinge of the Torres Syncline, where occur sub-rounded and angular vesicular fragments in the flow-top breccias, lack of basal breccias, and, further, a four-part structure, which is typical of rubbly flows instead of ´a´ā. The basal zones of the rubbly flows are usually smooth and vary in vesicularity. This indicates that shearing at the base of these flows was limited and did not lead to brecciation.

Continuous addition of new lava to the viscous zone of the stable upper vesicular crust will eventually lead to lava growth by inflation (Hon et al., 1994). This process was initially proposed for simple pahoehoe lavas, although similar models have been proposed for simple rubbly flows. In these cases, growth by inflation could be due to either pressurized lavas or pulses of higher fluxes (Rossi and Gudmundsson, 1996).

Thick simple rubbly flows are not expected to be the products of long-lasting eruptions with low effusion rates, because the thickening of the crust increases the tensile strength of the lobes, preventing inflation and instead promotes rupture, brecciation and stagnation. High effusion rates may account for rapid thickening of the flow but are unlikely to be maintained for a long time.

Emplacement models of rubbly lavas have been proposed for the Deccan Trapps (Keszthelyi et al., 2004; Guilbaud et al., 2005; Keszthelyi et al., 2006; Duraiswami et al., 2008). In these models, large

volumes of lava were initially accommodated endogenously within the sheets, enabling them thicken. This is possible due to the insulating effect of thickening upper crusts. Tensile stresses in the upper crusts related to inflation and accumulation of volatiles led to degassing and rupturing, whereas pulses in effusion rate and/or increasing viscosity could have led to brecciation.

One possibility to explain the inflation process in rubbly lavas is through multiple phases of crust formation and disruption. Keszthelyi et al. (2004) and Guilbaud et al. (2005) showed evidences for the Laki flow of an extended period of brecciation, and the proposed model was also adopted for the Deccan flows (Duraiswami et al., 2008). These multiple phases of brecciation could result from pulses or surges in effusion rates, which periodically led to increased supply to the flow interiors and enhanced shearing between the crust and the underlying fluid lava (Managave, 2000; Duraiswami et al., 2003; Keszthelyi et al., 2006). The disrupted crusts capped by new flow-top breccias of varying thickness would form breccia layers that could be reasonable insulators facilitating a possible inflation process. However, as earlier mentioned, the core of rubbly flows exhibits hypocrystalline finer textures, most likely as result of faster cooling and less efficient insulation compared with the upper crust of typical pahoehoe lava flows.

Bondre et al. (2004) also considered the possibility of initial inflation, but noted that typical features of inflated pahoehoe lobes are rarely observed. They observed that these flows have absence of associated smaller lobes, and are consistently thicker and much more extensive than the typical pahoehoe lobes from the earlier stratigraphic formations. They suggested that one of the reasons for this might be that simple rubbly flows were emplaced at higher effusion rates, which obviously inhibited the formation of toes and smaller lobes, generally associated with slowly emplaced pahoehoe flows.

10.3. Volcanic textures as result of different emplacement conditions of lava flows in the south hinge of the Torres Syncline

MacDonald (1953) was the first to highlight different lava morphologies through petrographic patterns, for which the greater crystallinity (abundance of crystals) of the ´a´ā cores was attributed to the more vigorous movement during emplacement. Kouchi et al. (1986) demonstrated experimentally that an increase in the internal movement of a basic magma promotes faster plagioclase nucleation (shear effect) and decrease the incubation time of these crystals. Sato (1995) stressed the lower abundance of plagioclase in the matrix and the coarser texture of the pahoehoe lavas compared with ´a´ā flows, despite the similar chemical composition of both types. Lima et al. (2012) concluded that the great abundance of plagioclase microlites in the matrix of the ´a´ā flows in comparison to pahoehoe is attributed to undercooling and devolatization of the ´a´ā lavas.

The mineralogy of the basaltic lava flows (pahoehoe and rubbly) in the study area is similar, being mainly composed of plagioclase and pyroxene, with subordinate opaque minerals and apatite, and olivine restricted to early compound pahoehoe lobes. The simple and compound pahoehoe lavas are texturally coarser, wherein the mechanism of endogenous transfer (inflation) within a visco-elastic crust in an insulated environment favors the formation the intergranular and ophitic holocrystalline textures in these flows. The base and top crust of the simple pahoehoe lava flows are amygdaloidal, with different generations of secondary zeolite filling spherical and stretched vesicles.

The finer textural pattern and the plagioclase abundance in the rubbly flows matrix could be explained by the higher effusion rate of these systems. The pre-eruptive condition of rapid magma ascension would promote the loss of volatiles in the upper portions, generating a convective pattern of the system with the undegassed portions (Kazahaya et al., 1994). This movement would accelerate the degassing process and increase the undercooling interval and the shear effect in the system. The combination of these processes could favor the rapid nucleation of plagioclase crystals with elongated and partially reabsorbed shapes. Many of the rubble fragments appear to have been rounded in thin sections as well as at the outcrop scale, suggesting the influence of syn-emplacement shearing and rotation of the fragments. The presence of diktytaxitic texture in the hypocrystalline and aphanitic core of the rubbly flows suggests that the entrapment of gas bubbles in this portion of the lava flow is not exclusive of pahoehoe lavas. This process forms open irregular cavities with angular shapes that have been subsequently filled by zeolites as result from the endomorphic alteration of the feldspar, which resembles the interstitial areas occupied by the glassy mesostasis in some basalts.

As mentioned before, the origin of different morphologies of basalt observed in the study area could be influenced by continuous increases in magma effusion rate, where the compositional factor could be ruled out because of the overlapping in the SiO_2 contents and in the Fe_2O_{3t}/MgO ratios of the simple pahoehoe and rubbly lavas.

11. Conclusions

This study identified the succession and evolution of mafic volcanism in the South hinge of the Torres Syncline in the Santa Cruz do Sul-Herveiras section, where the basaltic lava flows were divided into 16 lithofacies and grouped into three lithofacies associations: early compound pahoehoe, early simple pahoehoe and late simple rubbly.

The onset of volcanism in the south hinge of Torres Syncline is built up by a complex set of olivine-rich compound pahoehoe lavas that were effused with low effusion rates and an intermittent lava supply without thermal erosion over sands of Botucatu paleoerg. More evolved flows, without olivine (simple pahoehoe) are thicker and also effused with low rates, although with sustained lava supply, which predominates the inflation process. These flows are succeeded by rubbly lava morphologies, in which the effusion rates have increased, the thicker lava flows are more evolved, and are vertical and laterally homogeneous. Pahoehoe–rubbly transitions in the lava flow fields of the south of Torres Syncline have implications for emplacement dynamics, flood basalt architecture and volcanic stratigraphy. The lack of paleosols and minor occurrence of thin sandstone sheets suggest short time gaps, especially between the early simple pahoehoe and late simple rubbly lithofacies associations. After the emplacement of these mafic associations, acid lava flows in the SGF were identified, but they are outside the scope of this study.

The contrast between the petrographical patterns of the pahoehoe and rubbly lavas reflects different undercooling degrees, effusion rates and emplacement styles. The origin of different basalt morphologies observed in the study area could have been influenced to an increase in magma effusion rate, where the compositional factor can be ruled out due to overlap in the SiO_2 contents and in Fe_2O_{3t}/MgO ratios of the simple pahoehoe and rubbly lavas. Geochemically, all lavas are compatible with the low-TiO_2 series and belong to Gramado magma type.

The facies analysis method have proven to be an important tool to establish evolution models of volcanism, especially for CBPs, where it is possible divide lava flows into smaller rock units, lithofacies.

Acknowledgments

The authors acknowledge the financial support of the PRH PB-215 (Doctoral scholarship to Carla Barreto), FAPESP 2012/06082-6, CAPES FCT-33013, and CNPq 479784/20124 and 3038/20098 projects.

References

Almeida, F.F.M., 1986. Distribuição regional e relações tectônicas do magmatismo pós Paleozóico no Brasil. Rev. Bras. Geocienc. 16, 325–349.

Baloga, S.M., Glaze, L.S., 2003. Pahoehoe transport as a correlated random walk. J. Geophys. Res. 108 (B1), 2031. http://dx.doi.org/10.1029/2001JB001739.

Bellieni, G., Comin-Chiarmonti, P., Marques, L.S., Melfi, A.J., Piccirillo, E.M., Nardy, A.J.R., Roisenberg, A., 1984. High- and low-Ti flood basalts from the Paraná plateau (Brazil): petrogenetic and geochemical aspects bearing on their mantle origin. Mineralogie (Abh.) 150, 272–306.

Bondre, N.R., Duraiswami, R.A., Dole, G., 2004. Morphology and emplacement of flows from the Deccan Volcanic Province, India. Bull. Volcanol. 66, 29–45.
Branney, M.J., Kokelaar, P., 2002. Pyroclastic density currents and the sedimentation of ignimbrites. Geol. Soc. Lond. Mem. (27), 51–56.
Brown, R.J., Blake, S., Bondre, N.R., Phadnis, V.M., Self, S., 2011. ´A´ā lava flows in the Deccan Volcanic Province, India, and their significance for the nature of continental flood basalt eruptions. Bull. Volcanol. 73, 737–752.
Bryan, S.E., Ernst, R.E., 2008. Revised definition of Large Igneous Provinces (LIPs). Earth Sci. Rev. 86, 175–202.
Cas, R.A.F., Wright, J.V., 1987. Volcanic succession, modern and ancient: a geological approach to processes, products and successions, 1st ed., Chapman & Hall, London, p. 528, (March 31, 1987).
Coffin, M.F., Eldholm, O., 1994. Large igneous provinces: crustal structure, dimensions and external consequences. Rev. Geophys. 32 (1), 1–36.
Collinson, J.D., 1969. The sedimentology of the Grindslow Shales and the Kinderscout Grit: a deltaic complex in the Namurian of northern England. J. Sediment. Petrol. 39, 194–221.
Duraiswami, R.A., Dole, G., Bondre, N.R., 2003. Slabby pahoehoe from the western Deccan Volcanic Province: evidence for incipient pahoehoe—aa transitions. J. Volcanol. Geotherm. Res. 121, 195–217.
Duraiswami, R.A., Bondre, N.R., Managave, S., 2008. Morphology of rubbly pāhoehoe (simple) flows from the Deccan Volcanic Province: implications for style of emplacement. J. Volcanol. Geotherm. Res. 177, 822–836.
Duraiswami, R.A., Gadpallu, P., Shaikh, T.N., Cardin, N., 2014. Pahoehoe–a'a transitions in the lava flow fields of the western Deccan Traps, India-implications for emplacement dynamics, flood basalt architecture and volcanic stratigraphy. J. Asian Earth Sci. 84, 146–166.
Farrell, R.E., 2010. Volcanic Facies Architecture of the Chilcotin Group Basalts at Chasm Provincial Park, British Columbia. The University of British Columbia, Vancouver, (The Faculty of Graduate Studies (Geological Sciences). Thesis of master of Science).
Frank, H.T., Gomes, M.E.B., Formoso, M.L.L., 2009. Review of the areal extent and the volume of the Serra Geral Formation, Paraná Basin, South America. Pesqui. Geocienc. 36 (1), 49–57.
Fúlfaro, V.J., Saad, A.R., Santos, M.V., Vianna, R.B., 1982. Compartimentação e evolução tectônica da bacia do Paraná. Rev. Bras. Geocienc. 12, 590–611.
Guilbaud, M.N., Thordarson, T., Blake, S., 2005. Morphology, surface structures, and emplacement of lavas produced by Laki, A.D., 1783–1784. In: Manga, M., Ventura, G. (Eds.), Kinematics and dynamics of lava flows. Geol. Soc. Am. Special Paper. 396, pp. 81–102.
Hartmann, L.A., Wildner, W., Duarte, L.C., Duarte, S.K., Pertille, J., Arena, K.R., Martins, L.C., Dias, N.L., 2010. Geochemical and scintillo-metric characterization and correlation of amethyst geode-bearing Paraná lavas from the Quaraí and Los Catalanes districts, Brazil and Uruguay. Geol. Mag. 147, 954–970.
Hon, K., Kauahikaua, J., Denlinger, R., Mackay, K., 1994. Emplacement and inflation of pahoehoe sheet flows: observations and measurements of active lava flows on Kilauea volcano, Hawaii. Geol. Soc. Am. Bull. 106, 351–370.
Janasi, V.A., Freitas, V.A., Heaman, L.H., 2011. The onset of flood basalt volcanism, Northern Paraná Basin, Brazil: a precise U–Pb baddeleyite/zircon age for a Chapecó-type dacite. Earth Planet. Sci. Lett. 302, 147–153.
Jerram, D.A., 2002. Volcanology and facies architecture of flood basalts. In: Menzies, M.A., Baker, J., Ebinger, C.J., Klemperer, S.L. (Eds.), Volcanic rifted marginsGeol. Soc. Am. Special Paper. 362. GSA, Boulder, Colorado, pp. 121–135.
Jerram, D.A., Robbe, O., 2001. Building a 3-D model of a flood basalt: an example from the Etendeka, NW Namibia. Electron. Geosci. 6, 1.
Jerram, D.A., Mountney, N.P., Howell, J.A., Long, D., Stollhofen, H., 2000. Death of a sand sea: an active aeolian erg systematically buried by the Etendeka flood basalts of NW Namibia. J. Geol. Soc. Lond. 157, 513–516.
Jerram, D.A., Single, R.T., Hobbs, R.W., Nelson, C.E., 2009. Understanding the offshore flood basalt sequence using onshore volcanic facies analogues: an example from the Faroe–Shetland basin. Geol. Mag. 146 (3), 353–367.
Kazahaya, K., Shinohara, H., Saito, G., 1994. Excessive degassing of Izu-Oshima volcano: magma convection in a conduit. Bull. Volcanol. 56 (3), 207–216.
Keszthelyi, L., 2000. The brecciated lava flows of the Kerguelen Plateau: what are they? EOS Trans. Am. Geophys. Union 8, S 43.
Keszthelyi, L., 2002. Classification of the mafic lava flows from ODP Leg 183. In: Frey, F.A., Coffin, M.F., Wallace, P.J., Quilty, P.G. (Eds.), Proceedings of the Ocean Drilling Program. Scientific Results. 183, pp. 1–28.
Keszthelyi, L., Thordarson, T., 2000. Rubbly pahoehoe: a previously undescribed but widespread lava type transitional between aa and pahoehoe. Geol. Soc. Am. Abstr. Programs 32, 7.
Keszthelyi, L., Self, S., Thordarson, T., 1999. Application of recent studies on the emplacement of basaltic lava flows to the Deccan Traps. In: Subbarao, K.V. (Ed.), Memoir Geol. Soc. India. 43. Geological Society of India, Deccan Volcanic Province, pp. 485–520.
Keszthelyi, L.P., Thordarson, T., McEwan, A., H'a'ack, H., Guilbaud, M.-N., Self, S., Rossi, M.J., 2004. Icelandic analogs to Martian flood lavas. Geochem. Geophys. Geosyst. 5 (11), 1–32.
Keszthelyi, L., Self, S., Thordarson, T., 2006. Flood lavas on Earth, Io and Mars. J. Geol. Soc. Lond. 163, 253–264.
Kirstein, L.A., Kelley, S., Hawkesworth, C., Turner, S., Mantovani, M., Wijbrans, J., 2001. Protracted felsic magmatic activity associated with the opening of the South Atlantic. J. Geol. Soc. 158, 583–592.
Kouchi, A., Tsuchiyama, A., Sunagawa, I., 1986. Effect of stirring on crystallization kinetics of basalt: texture and element partitioning. Contrib. Mineral. Petrol. 93, 426–438.
Lima, E.F., Waichel, B.L., Rossetti, L.M.M., Viana, A.R., Scherer, C.M., Bueno, G.V., Dutra, G., 2012. Morphology and petrographic patterns of the pahoehoe and ´a´ā flows of the Serra Geral Formation in the Torres Syncline (Rio Grande do Sul state, Brazil. Rev. Bras. Geocienc. 42, 744–753.
Macdonald, G.A., 1953. Pahoehoe, ´a´ā, and block lava. Am. J. Sci. 251, 169–191.
Managave, S., 2000. The Geology Around Kurundwad. Unpublished M.Sc. Dissertation, University of Pune, pp. 104.
Mantovani, M.S.M., Atalla, L., Civetta, L., De Sousa, M.A., Innocenti, F., Marques, L.S., 1985. Trace element and strontium isotope constraints on the origin and evolution of Paraná continental flood basalts of Santa Catarina State, southern Brazil. J. Petrol. 26, 187–209.
Marsh, J.S., Ewart, A., Milner, S.C., Duncan, A.R., Miller, R. McG, 2001. The Etendeka Igneous Province: magma types and their stratigraphic distribution with implications for the evolution of the Paraná–Etendeka Flood Basalt Province. Bull. Volcanol. 62, 464–486.
McPhie, J., Doyle, M., Allen, R., 1993. Volcanic TEXTURES: A guide to the interpretation of textures in volcanic rocks, (Tasmania, 191 pp.).
Melfi, A.J., Nardy, A.J.R., Piccirillo, E.M., 1988. Geological and magmatic aspects of the Paraná Basin: an introduction. In: Piccirillo, E.M., Melfi, A.J. (Eds.), The Mesozoic Flood Volcanism of the Paraná Basin: Petrogenetic and Geophysical Aspects. IAG-USP, pp. 1–13.
Miall, A.D., 1986. Effects of Caledonian tectonism in Artic Canada. Geology 14, 904–907.
Miall, A.D., 1996. The Geology of Fluvial Deposits. Sedimentary Facies, Basin Analysis, and Petroleum Geology. Springer-Verlag, Berlin, Heidelberg, New York, London, Paris, Tokyo, Hong Kong 3 540 59186 9, (xvi + 582 pp.).
Miall, A.D., 2000. Principles of Sedimentary Basin Analysis, 3rd edition. Springer-Verlag Inc., New York, (616 pp.).
Milani, E.J., 1997. Evolução tectono-estratigráfica da Bacia do Paraná e seu relacionamento com a geodinâmica fanerozóica do Gondwana sul-ocidental. (Tese (Doutorado)) 2. Universidade Federal do Rio Grande do Sul, Porto Alegre, (199 pp.).
Mountney, N., Howell, J., Flinth, S., Jerram, D., 1998. Aeolian and alluvial deposition within the Mesozoic Etjo Sandstone Formation, nortwest Namibia. J. Afr. Earth Sci. 27, 175–192.
Myashiro, A., 1974. Volcanic rock series in island arc and active continental margins. Am. J. Sci. 274, 321–355.
Nelson, C.E., Jerram, D.A., Hobbs, R.W., Terrington, R., Kessler, H., 2011. Reconstructing flood basalt lava flows in three dimensions using terrestrial laser scanning. Geol. Soc. Am. 7 (1), 87–96.
Passey, S.R., Bell, B.R., 2007. Morphologies and emplacement mechanisms of the lava flows of the Faroe Islands Basalt Group, Faroe Islands, NE Atlantic Ocean. Bull. Volcanol. 70, 139–156.
Peate, D.W., Hawkeswort, C.J., Mantovani, M.S.M., 1992. Chemical stratigraphy of the Paraná lavas (South America): classification of magma types and their spatial distribution. Bull. Volcanol. 55, 119–139.
Petry, K., Jerram, D.A., Almeida, D.P.M., Zerfass, H., 2007. Volcanic sedimentary features in the Serra Geral Fm., Paraná Basin, southern Brazil: example of dynamic lava-sediment interactions in a arid setting. J. Volcanol. Geotherm. Res. 159, 313–325.
Planke, S., Symonds, P.A., Alvestad, E., Skogseid, J., 2000. Seismic volcanostratigraphy of large-volume basaltic extrusive complexes on rifted margins. J. Volcanol. Geotherm. Res. 105 (B8), 19335–19351.
Planke, S., Rasmussen, T., Rey, S.S., Myklebust, R., 2005. Seismic characteristics and distribution of volcanic intrusions and hydrothermal vents complexes in theVøring and Møre basins. In: Doré, A.G., Vining, B. (Eds.), Petroleum Geology: North-West Europe and Global Perspectives—Proceedings of the 6th Petroleum Geology Conference. Geol. Soc. London, pp. 833–844.
Rossetti, L.M.M., Lima, E.F., Waichel, B.L., Scherer, C.M., Barreto, C.J.S., 2014. Stratigraphical framework of basaltic lavas in Torres Syncline Main Valley, Southern Brazil. J. S. Am. Earth Sci. (submitted for publication).
Rossi, M.J., Gudmundsson, A., 1996. The morphology and formation of flow-lobe tumuli on Icelandic shield volcanoes. J. Volcanol. Geotherm. Res. 72 (3–4), 291–308.
Sato, H., 1995. Textural difference between pahoehoe and aa lavas of Izu-Oshima Volcano, Japan, and experimental study on population density of plagioclase. J. Volcanol. Geotherm. Res. 66, 101–113.
Saunders, A.D., Fitton, J.G., Kerr, A.C., Norry, M.J., Kent, R.W., 1997. The North Atlantic Igneous Province. In: Mahoney, J.J., Coffin, M.F. (Eds.), Large Igneous Provinces: continental, oceanic and planetary flood volcanism. Am. Geophys. Union Geophys. Monograph. 100, pp. 45–93.
Scherer, C.M.S., 1998. Análise Estratigráfica e Litofaciológica da Formação Botucatu (Cretáceo Inferior da Bacia do Paraná) No Rio Grande do Sul. Unpubl. Ph.D Thesis, Universidade Federal do Rio Grande do Sul, Porto Alegre.
Scherer, C.M.S., 2000. Eolian dunes of the Botucatu Formation (Cretaceous) in Southernmost Brazil: morphology and origin. Sediment. Geol. 137, 63–84.
Scherer, C.M.S., 2002. Preservation of aeolian genetic units by lava flows in the Lower Cretaceous of the Paraná Basin, southern Brazil. Sedimentology 49, 97–116.
Self, S., Thordarson, T., Keszthelyi, L., 1997. Emplacement of continental flood basalt lava flows. In: Mahoney, J.J., Coffin, M.L. (Eds.), Large Igneous Provinces: continental, oceanic, and planetary flood volcanism. AGU, Geophysics Monography. 100, pp. 381–410.
Self, S., Keszthelyi, L., Thordarson, T., 1998. The importance of pahoehoe. Annu. Rev. Earth Planet. Sci. 26, 81–110.
Selley, R.C., 1978. Ancient Sedimentar Environments, 2nd edn. Champman & Hall, London.
Single, R.T., Jerram, D.A., 2004. The 3D facies architecture of flood basalt provinces and their internal heterogeneity: examples from the Palaeogene Skye Lava Field. J. Geol. Soc. Lond. 161, 911–926.
Stewart, K., Turner, S., Kelley, S., Hawkesworth, C., Kirstein, L., Mantovani, M., 1996. 3-D, ^{40}Ar–^{39}Ar geochronology in the Parana continental flood basalt province. Earth Planet. Sci. Lett. 143, 95–109.

Storey, M., Duncan, R.A., Tegner, C., 2007. Timing and duration of volcanism in the North Atlantic Igneous Province: implications for geodynamics and links to the Iceland hotspot. Chem. Geol. 241 (3–4), 264–281 (the Great Plume Debate: Testing the Plume Theor).

Thiede, D.S., Vasconcelos, P.M., 2010. Parana flood basalts: rapid extrusion hypothesis confirmed by new $^{40}Ar/^{39}Ar$ results. Geology 38, 747–750.

Turner, S., Regelous, M., Kelley, S., Hawkesworth, C., Mantovani, M., 1994. Magmatism and continental break-up in the South Atlantic: high precision $^{40}Ar–^{39}Ar$ geochronology. Earth Planet. Sci. Lett. 121, 333–348.

Vye-Brown, C., Self, S., Barry, T., 2013. Architecture and emplacement of flood basalt Flow fields: case studies from the Columbia River Basalt Group, NWUSA. 75 (3), 1–21.

Waichel, B.L., Lima, E.F., Lubachesky, R., Sommer, C.A., 2006a. Pahoehoe flows from the central Paraná Continental Flood Basalts. Bull. Volcanol. 68, 599–610.

Waichel, B.L., Lima, E.F., Sommer, C.A., 2006b. Tipos de Derrame e Reconhecimento de Estruturas nos Basaltos da Formação Serra Geral: Terminologia e Aspectos de Campo. Pesqui. Geocienc. 33 (2), 123–133.

Waichel, B.L., Scherer, C.M.S., Frank, H.T., 2008. Basaltic lava flows covering active aeolian dunes in the Paraná Basin in southern Brazil: features and emplacement aspects. J. Volcanol. Geotherm. Res. 171, 59–72.

Waichel, B.L., Lima, E.F., Viana, A.R., Scherer, C.M., Bueno, G.V., Dutra, G., 2012. Stratigraphy and volcanic facies architecture of the Torres Syncline, Southern Brazil, and its role in understanding the Parana–Etendeka Continental Flood Basalt Province. J. Volcanol. Geotherm. Res. 215–216, 74–82.

Walker, G.P.L., 1952. Compound and Simple Lava Flows and Flood Basalts. Imperial College, London, pp. 579–590, (SW7 2 BP).

Walker, G.P.L., 1971. Compound and simple lava flows and flood basalts. Bull. Volcanol. 35, 579–590.

Walker, R.G., 1984. General introduction: facies, facies sequences and facies models, In: Walker, R.G. (Ed.), Facies Models, 2nd edition Geol. Assoc. Canada, St. Johns, pp. 1–9.

Walker, G.P.L., 1989. Spongy pahoehoe in Hawaii: a study of vesicle distribution patterns in basalt and their significance. Bull. Volcanol. 51, 199–209.

Walker, G.P.L., 1991. Structure, and origin by injection of lava under surface crust, of tumuli, “lava rises”, “lava-rise pits”, and “lava-inflation clefts” in Hawaii. Bull. Volcanol. 53 (7), 546–558.

Wilmoth, R.A., Walker, G.P., 1993. P-type and S-type pahoehoe: a study of vesicle distribution patterns in Hawaiian lava flows. J. Volcanol. Geotherm. Res. 55 (1–2), 129–142.

5.2 Artigo 2

TÍTULO: Vesicle-rich segregation structures and recognition of primary and secondary porosities in pahoehoe and rubbly lava flows of the Paraná igneous province, Southern Brazil.

AUTORES: Carla Joana Santos Barreto

Evandro Fernandes de Lima

Karin Goldberg

SUBMETIDO: Em janeiro de 2015 e resubmetido em novembro de 2015 para atender as sugestões dos revisores

PERIÓDICO: Bulletin of Volcanology

Esse artigo cientifico consistiu na caracterização e discussão dos processos responsáveis pela formação das estruturas de segregação ricas em vesículas que ocorrem dentro dos derrames básicos *pahoehoe* e *rubbly* em um perfil de estrada no Sul do Brasil. Além disso, versou sobre os tipos de porosidade que podem ser reconhecidas nesses derrames com o intuito de fornecer dados quantitativos da contribuição das mesmas para o sistema vulcânico estudado, e dessa forma, avaliar a possibilidade de um reservatório vulcânico não convencional na ombreira sul da calha de Torres.

Este estudo confirmou que existe uma relação entre a espessura dos derrames e os tipos de estruturas de segregação formadas. Vesículas do tipo V1 (esféricas e milimétricas) são encontradas em qualquer porção tanto nos derrames *pahoehoe* (de 1 a 6 m espessura) quanto nos derrames *rubbly* (até 50 m). *Pipe* vesículas (tipo V2 – na forma de tubos alongados verticais) estão posicionadas na base de derrames *pahoehoe* e lobos tipo P, enquanto proto-cilindros podem ser observados apenas na base dos derrames *pahoehoe* simples. Vesículas gigantes (tipo V3), zonas vesiculadas denominadas *pods* (tipo V4), cilindros de vesículas e camadas de vesículas do tipo S2 foram observadas apenas nas porções de núcleo dos derrames *paheohoe* simples (~10 m). Por outro lado, camadas de vesículas do tipo S1 foram identificadas apenas no topo de derrames *pahoehoe* simples.

A identificação de porosidades primárias (vesicular, intracristalina e móldica) e secundárias (*drusy*, *spongy*, *cavernous*, *lacy*, intracristalina secundária, intra-

fragmento, intra-matrix, fratura tectônica, fratura de resfriamento) indica grau elevado de porosidade para armazenamento de fluidos, o qual poderia ter implicações para um possível reservatório vulcânico de hidrocarbonetos na ombreira sul da calha de Torres. A conexão das cavidades e vesículas por fraturamentos tardios aliados a presença de diques e camadas de areia poderiam facilitar a migração desses possíveis fluidos. Contudo, a precipitação de minerais secundários nas vesículas e cavidades reduz drasticamente a porosidade total dos derrames, bem como sela a permeabilidade desenvolvida pelo fraturamento.

Vesicle-rich segregation structures and recognition of primary and secondary porosities in pahoehoe and rubbly lava flows of the Paraná igneous province, Southern Brazil

Carla Joana S. Barreto[1,*], Evandro F. de Lima[1], Karin Goldberg[1]

[1] Universidade Federal do Rio Grande do Sul (UFRGS)
Av. Bento Gonçalves 9500, 91501-970 Porto Alegre, Rio Grande do Sul, Brazil.
*Corresponding author. E-mail: carlabarreto.geo@hotmail.com; Tel.: +55-51-3308-7380

Abstract This study focuses on a single road profile in southernmost Brazil where a volcanic succession from pahoehoe to rubbly lavas of the Paraná–Etendeka Province is exposed. This work provides an integrated approach for examining vesicle-rich segregation structures in the mesoscopic scale and quantitatively analyzing the pores and characterizing the porosity types in thin section. This paper establishes a correlation between lava thickness and the type of segregation structure. In pahoehoe flows <1 m thick, the cooling occurs so rapidly that only pipe vesicles and V1 vesicles are frozen. In flows 2-6 m thick, a large amount of vesicle-rich segregation structures occur such as proto-cylinders and cylinders; S1 and S2 sheets and cylinder sheets; and pipe, giant, and V1 vesicles. In rubbly flows thicker than 30 m, V1 and giant vesicles are common. Gas release and deuteric crystal dissolution processes lead to primary porosities. A large amount of secondary porosities in the basic flows are generated by alteration and tectonic fracturing. Precipitation of secondary minerals within the cavities and the filling of fractures, dykes, and layers by sandstone tend to decrease the existing porosities. Volcanic rocks are underestimated by the hydrocarbon industry owing to their lack of reservoir quality. However, better understanding and prediction of the reservoir potential of basic volcanic rocks can be achieved through a quantitative analysis of porosity and permeability as well as that of brittle tectonics.

Keywords: Paraná–Etendeka Province; Vesicle-rich segregation structures; Volcanic porosity; Unconventional volcanic reservoir

Introduction

In large igneous provinces (LIPs), huge volumes of lavas and intrusions are generated and accumulated in a relatively short time to represent anomalous events in Earth's history (Bryan and Ernst 2008). Continental flood basalt provinces (CFBP) represent a type of LIP built with volumes of 10^5–10^7 km^3 in short time intervals of ~10^5–10^6 years (Bryan and Ernst 2008).

CFBP lava flows often contain vesicles that represent gas bubbles trapped during lava solidification. Historically, approximately 20%-60% of spherical vesicles are typically distributed at the base and top of pahoehoe lavas (Aubele et al. 1988). In 'a'a lavas, the irregular and sparse vesicles are less abundant at <20% and are common in top breccias. Recent studies have reported that various vesicle patterns, including those containing segregated material, can be generated in different positions within the flows and are not restricted to the base and top (Caroff et al. 2000).

Identification of the petrophysical properties of basaltic lava flows, including the various shapes, sizes, origins, and filling materials of the vesicles, can determine their suitability as possible unconventional volcanic reservoirs. The high heterogeneity of volcanic rocks compared with that of clastic and carbonatic sedimentary rocks demonstrates their possibility as secondary reservoir targets for the hydrocarbon industry. However, significant volcanic hydrocarbon reservoirs have been reported worldwide (Jinglan et al. 1999; Wu et al. 2006; Lenhardt and Gotz 2011; Gudmundsson and Lotveit 2014).

The Paraná Province in southern Brazil is composed of a thick volcano–sedimentary succession formed by aeolian sandstones of the Botucatu Formation (BF) at the base overlapped by the volcanic pile of the Serra Geral Formation (SGF). The BF is the dominant unit of the Guarani Aquifer, which forms one of the world's largest freshwater reservoirs (Gilboa et al. 1976). However, few studies have been conducted on the role of these volcanic rocks as potential reservoirs for hydrocarbon or groundwater. As a result, many of the existing porosities in basaltic lava flows are largely misidentified or even unnoticed.

The primary objective of this paper is to characterize the vesicle-rich segregation structures that occur in a single road profile in southern Brazil and elucidate the formation of these structures. The secondary aim is to identify the porosity types of the studied lava flows and to provide their porosity degree through a modal analysis in thin sections. Finally, we present the porosity contribution of each portion of the lava flow of the studied volcanic system in the south hinge of the Torres Syncline (TS) to suggest its suitability as an unconventional volcanic reservoir.

Geological background

The Paraná Basin (PB), in central–eastern South America, has an elliptical shape with a N-S direction and includes a thick Upper Ordovician/Upper Cretaceous volcano–sedimentary succession covering an area of 1,300.000 km^2 in Brazil, Paraguay, Uruguay, and Argentina (Fig. 1a). This volcano–sedimentary succession is also present in the Huab basin in northwest Namibia (Jerram et al. 2000).

The BF and its Etendeka-equivalent Twyfelfontein Formation (TF) consist of sets and cosets of cross-strata (Mountney et al. 1998; Scherer 1998) interpreted as dry aeolian (Scherer 2002). The BF deposits reach 400 m thick but are absent in some regions due to non-deposition.

The SGF is mostly composed of tholeiitic basalts and basaltic andesites with minor rhyolites and rhyodacites at the top. The early pahoehoe lavas advanced over the unconsolidated sediments of the BF to generate peperites and lava prints (Petry et al. 2007; Waichel et al. 2008). The confinement of these flows by the topography of the dunes enabled the formation of ponded pahoehoe flows (Waichel et al. 2012).

The basaltic rocks of the SGF are divided into high-Ti, with TiO_2> 2%, occurring in the north and center of the PB and low-Ti, with TiO_2< 2% that predominate in the south (Bellieni et al. 1984). Peate et al. (1992) defined six magma types on the basis of their major and trace elements: Gramado and Esmeralda were classified as low-Ti, and Urubici, Pitanga, Paranapema, and Ribeira were categorized as high-Ti.

The TS a large structure that lies NW–SE (Fig. 1b), has been divided into the main valley, intermediate zone and south hinge (Waichel et al. 2012). In the south hinge, the lava flows of the Gramado-type are divided into early compound pahoehoe, early simple pahoehoe, and late simple rubbly lava (Barreto et al. 2014).

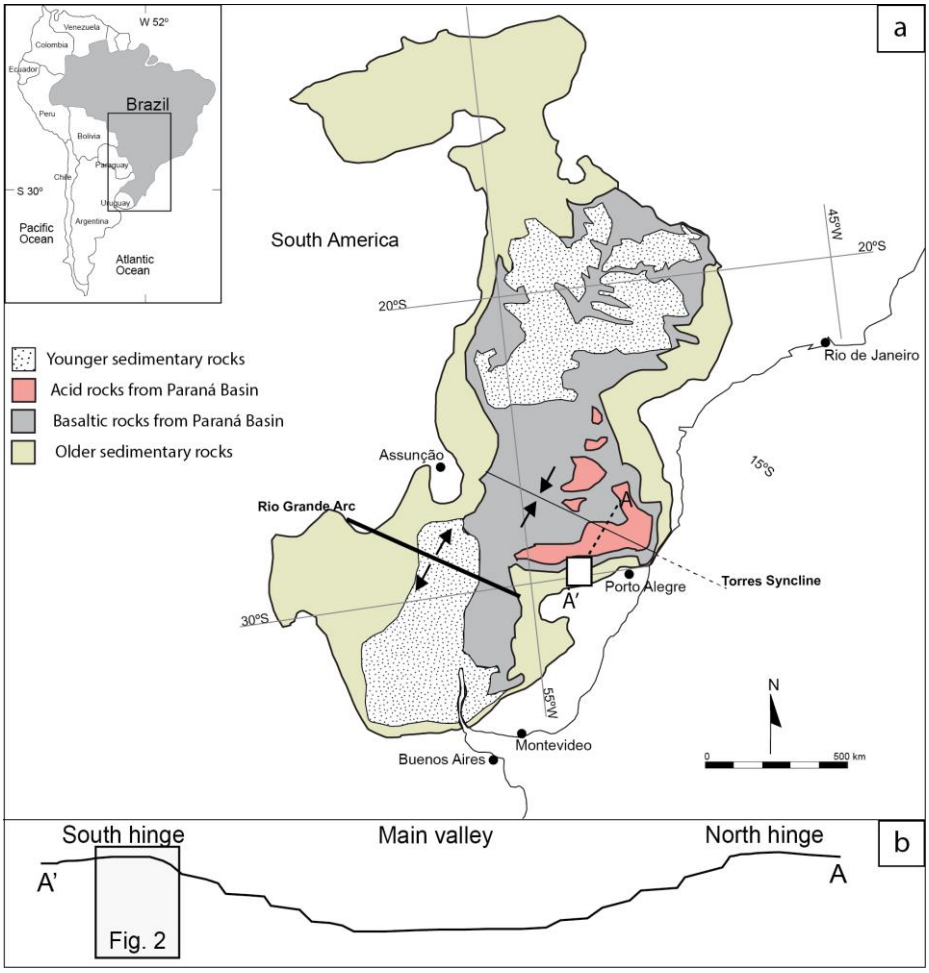

Fig. 1 a Simplified geological map of the PB, highlighting the TS (Waichel et al. 2012). **b** Location of the studied area.

Sampling sites and methods

This study was performed on pahoehoe and rubbly lava flows exhibiting a large variety of vesicle-rich segregation structures. These flows form a single road profile between the localities of Santa Cruz do Sul and Herveiras (SCSH; Fig. 2a), Rio Grande do Sul State, southern Brazil. A complete vertical section of the lava flows and the stratigraphic positions of the samples are shown in Fig. 2b.

The segregation structure documentation includes detailed descriptions at the field scale and photographs of each structure. The modal analysis was conducted by counting 300 points per thin section to examine the textures, fabrics, distribution of primary and secondary mineralogy, habit, amount, and pore types (e.g.,Goldberg et al. 2011). The description and quantification of thin sections impregnated with blue epoxy resin was performed by using Hardledge® software based on the Petroledge® system and adapted to igneous rocks (De Ros et al. 2007). The pore type was characterized relative to the location, morphology, and relationship with secondary minerals. The porosity terminology used in this paper follows that

of Sruoga and Rubinstein (2007). In addition, this study proposes new porosity terminology that resembles those used for sandstones (Schmidt and McDonald 1979) to describe rubbly top breccias that do not fit the previously defined types.

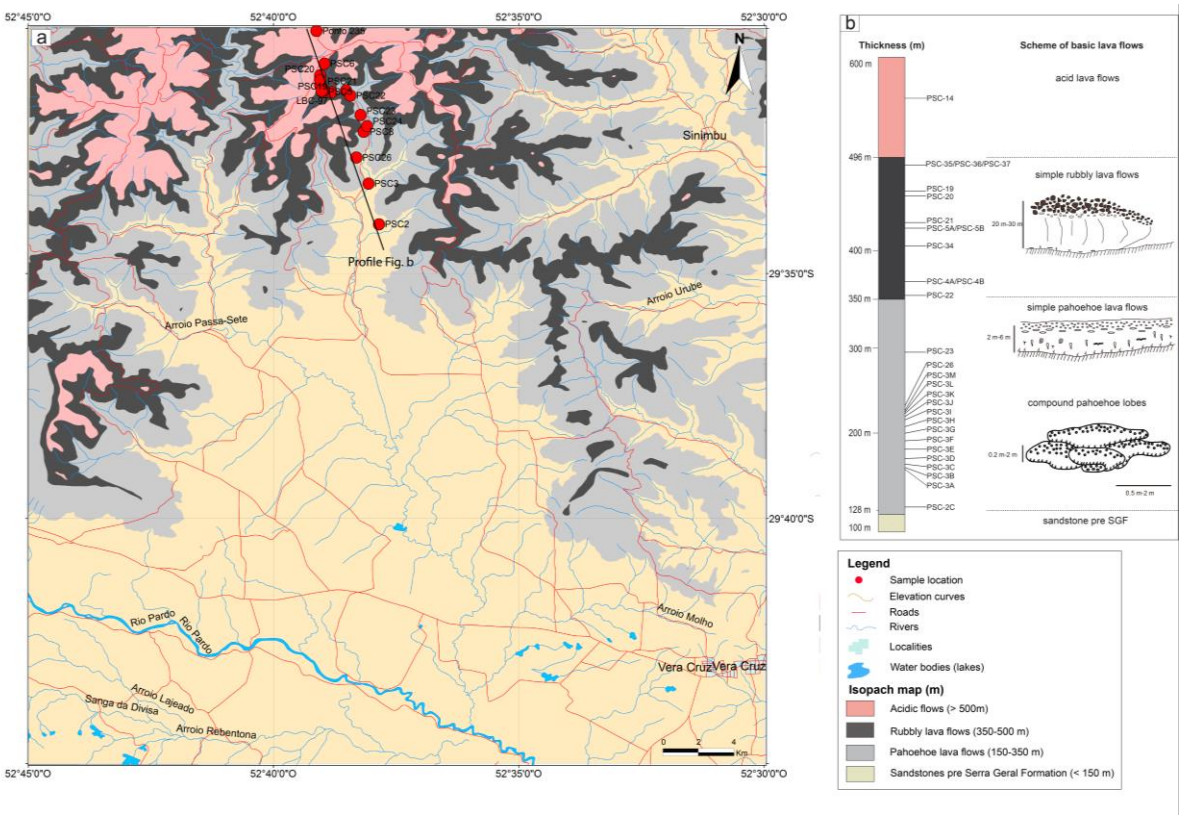

Fig. 2 a Geological map of the SCSH region showing the sampling location. **b** Stratigraphic cross-section based on log correlations.

Stratigraphical framework of volcanic sequence

The SCSH section is approximately 472 m thick and includes compound pahoehoe, simple pahoehoe, and rubbly lava flows (Fig. 2b).

Spongy (S-type) lobes (Walker 1989) with large amounts of millimetric vesicles and pipe vesicle-bearing (P-type) lobes (Wilmoth and Walker 1993) at the base and vesiculated top characterize the compound pahoehoe lavas. Both lobes have a limited aerial extent of 50 cm–1 m in thickness and form the lowermost portion of the SCSH volcanic sequence.

The compound pahoehoe lavas are overlapped by simple pahoehoe 2–6 m thick that consist of laterally extensive sheet flows forming a flat topography. The basal zone of these pahoehoe lavas, 10–50 cm thick, constitutes less than 10% of the total flow thickness. The core is coarse-grained and massive, although microvesiculated domains occur locally. Although the vesicle sizes within the upper crust decrease toward the top, their amounts increase upward. The pahoehoe lavas exhibit cooling fractures perpendicular to the external crust with smooth and ropy surfaces.

The rubbly lavas have thicker tabular geometry of about 50 m and overlap in smooth contact with the pahoehoe lavas. These flows show a slightly vesiculated base, whereas the massive core displays horizontal and vertical cooling fractures with conchoidal and curvilinear patterns. The rubbly top breccias are composed of oxidized and vesiculated sub-rounded to sub-angular fragments encompassed by a very fine basalt matrix and subordinately by sandstone. Felsic lavas overlap the rubbly flows at the top of the volcanic succession.

Description of vesicle-rich segregation structures

The main characteristics of the vesicle-rich segregation structures and their location within the lava flows in the SCSH profile are shown in Table 1 and in Fig. 3.

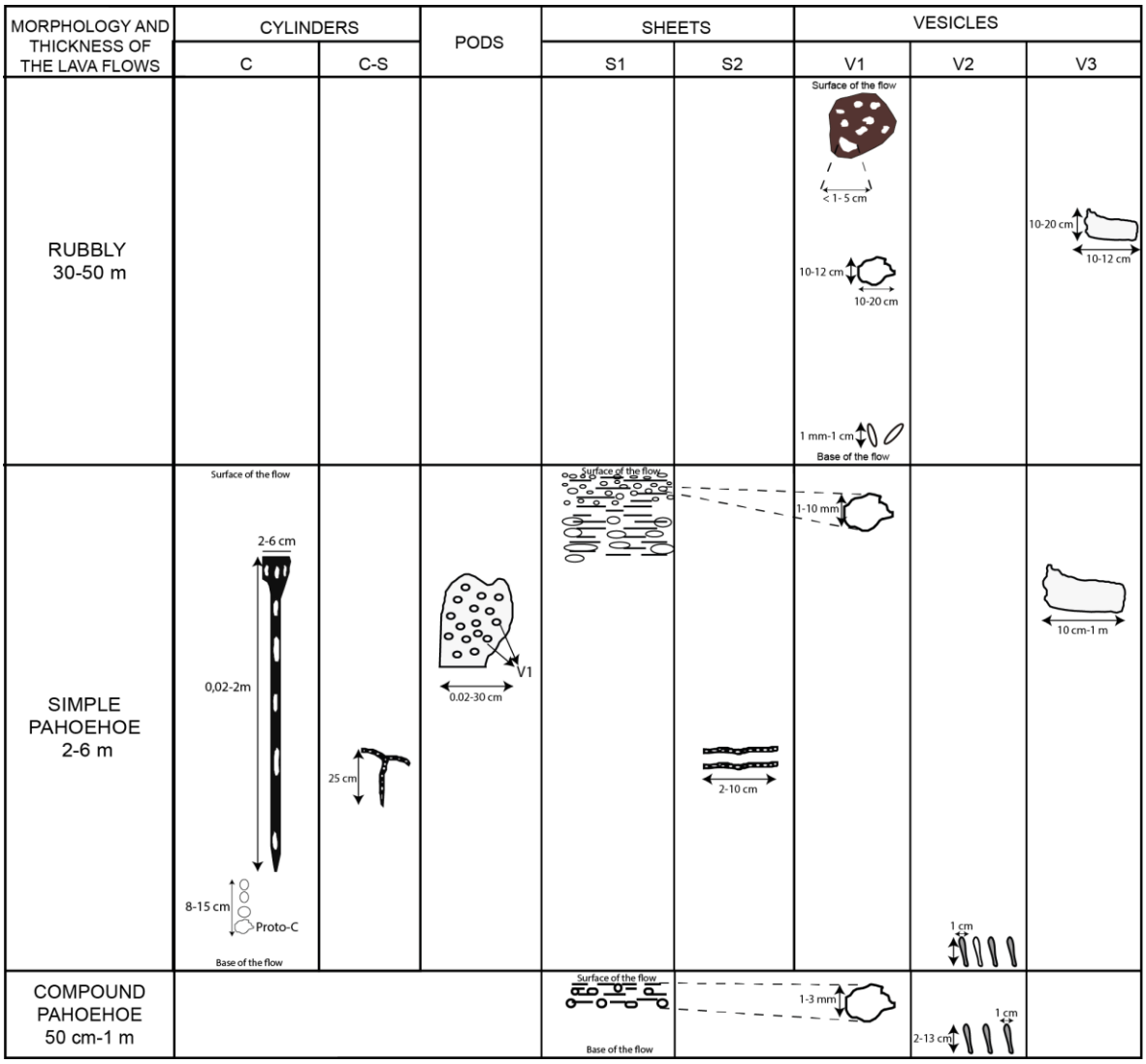

Fig. 3 Location of segregation structures in the lava flows from the SCSH region, based on Caroff et al. (2000). Abbreviations are explained in text.

Table 1 Characteristics of segregation structures in pahoehoe and rubbly lava flows.

Segregation structure type	Definition	Structure size	Flow thickness	Position within the lava flow	Lava flow type	Structure-bearing samples	Interpretation
Cylinders							
Proto-C	Vertical trail of vesicles generated through the same process of vesicle cylinders	8 - 28 cm long	2m - 6 m	Base - lower half of the core interface	Simple pahoehoe	PSC3C	Accumulation of vapor and differentiated melt at an early stage
C	Elongated bodies with orthogonal circular sections filled with vesicular segregation material	2 cm – 2 m long; 2 - 6 cm wide	2m - 6 m	Lower half of the core	Simple pahoehoe	PSC3A, PSC3D, PSC3J	Residual liquids generated within the lower solidification zone move into vesicle-rich low-density areas, through of gas filter-pressing mechanisms
C-S	Cylinder sheets	10 - 25 cm	2m - 6 m	Lower half of the core	Simple pahoehoe	PSC3J	Vesicle cylinders (C) end within of top horizontal vesicle sheets (S2). Solidification fronts advance more slowly in a later stage
Pods	Spherical zone that encompass V1-type vesicles	spherical zone = 15 - 30 cm V1= around 20 mm	2m - 6 m	Upper half of the core	Simple pahoehoe	PSC3J	Accumulation zone of segregation vesicles frozen-in upward-rising gas bubbles
Sheets							
S1	Alternating sheets filled by segregation material and vesicles (V1)	2 mm - 5 cm	2m - 6 m	Upper crust	Simple pahoehoe	PSC3B, PSC3H, PSC3K, PSC22	Cooling front progressing downward into the lava accompanying inflation. Fluctuations of pressure and/or flux during active inflation
S2	Narrow sheets filled by segregation material and vesicles (V1)	2 - 10 cm	2m - 6 m	Lower half of the core	Simple pahoehoe	PSC2B, PSC3G	Last body of differentiated liquid to form in flow when the solidification fronts advance more slowly. Form only after the flow has stagnated and is no longer inflating
Vesicles							
V1	Vesicles partly to completely filled by segregation material and secondary minerals	2 mm – 5 cm	50 cm - 6 m	Everywhere in host lava flow	Simple and compound pahoehoe	Almost all samples	Increase of confining pressure applied to the fluid and shrinkage of gas during cooling
		< 1 – 5 cm	30m - 50 m	Within the flow-top breccias	Rubbly	PSC34,PSC35, PSC36, PSC37	
		1 mm – 1 cm	30m - 50 m	Base	Rubbly	PSC4A, PSC5A	
V2	Vertical elongated bubbles (pipes) slightly tilted	2 – 13 cm long; 1 cm wide	50 cm - 6 m	Base	Simple and compound pahoehoe	PSC3C, PSC3F, PSC3I	Frozen-in upward rising gas bubbles formed perpendicular to the solidification front
V3	Domed giant vesicles	10 cm- 1 m long	2m - 6 m	Interface between upper crust and upper half of the core	Simple pahoehoe	PSC3J, PSC23	Coalescence of bubbles of different sizes by mass transfer above the lower solidification front
		10-12 cm long; 10-20 cm wide	30m - 50 m	Upper half of the core	Rubbly	PSC4B, PSC5B	

Vesicle cylinders, cylinder sheets, and pods

Proto-cylinders (proto-C; Fig. 4a) are recognizable as vertical trails of vesicles with indistinct limits and irregular shapes that are smaller than the cylinders. These structures occur only at base of simple pahoehoe flows. Vesicle cylinders (C) are primarily vertical (Fig. 4b) and are also curved and extend from approximately 25 cm of the flow base or in the lower half of the core of the simple pahoehoe flows. The horizontal sections of the cylinders are also observed (Fig. 4c). Cylinders are almost always rootless and are filled by segregation material, although connections with pipe vesicles in the basal portion are not observed. Occasionally, cylinders may splay into single horizontal sill-like vesicle sheets at the core of simple pahoehoe flows to form cylinder sheets (C-S; Fig. 4d).

Pods 30 cm in diameter are common at the upper half of the massive core of the simple pahoehoe lavas. Pods exhibit large concentrations (>10%) of vesicles, some of which are filled by segregated material or zeolite (Fig. 4e).

S1 and S2 vesicle sheets

Occurring only in the upper crust of the simple pahoeohe lavas, the S1 vesicle sheets exhibit a striking alternating band appearance (Fig. 4f), in which each band is relatively continuous and symmetrical. They are constituted by aligned V1 vesicles filled partly to completely by glass and secondary minerals.

The S2 sheets are horizontal and contain glass and V1 vesicles of 5 mm–1 cm in diameter (Fig. 4g). The S2 are different from the S1 sheets because they occur only in the lower half of core of the simple pahoehoe lavas, and their boundaries with the host basalts are always sharp (Fig. 4g–i). At certain points, these sheets change laterally to giant vesicles about 40 cm in width (Fig. 4h). Locally, the S2 occur as alternating bands at the core (Fig. 4i).

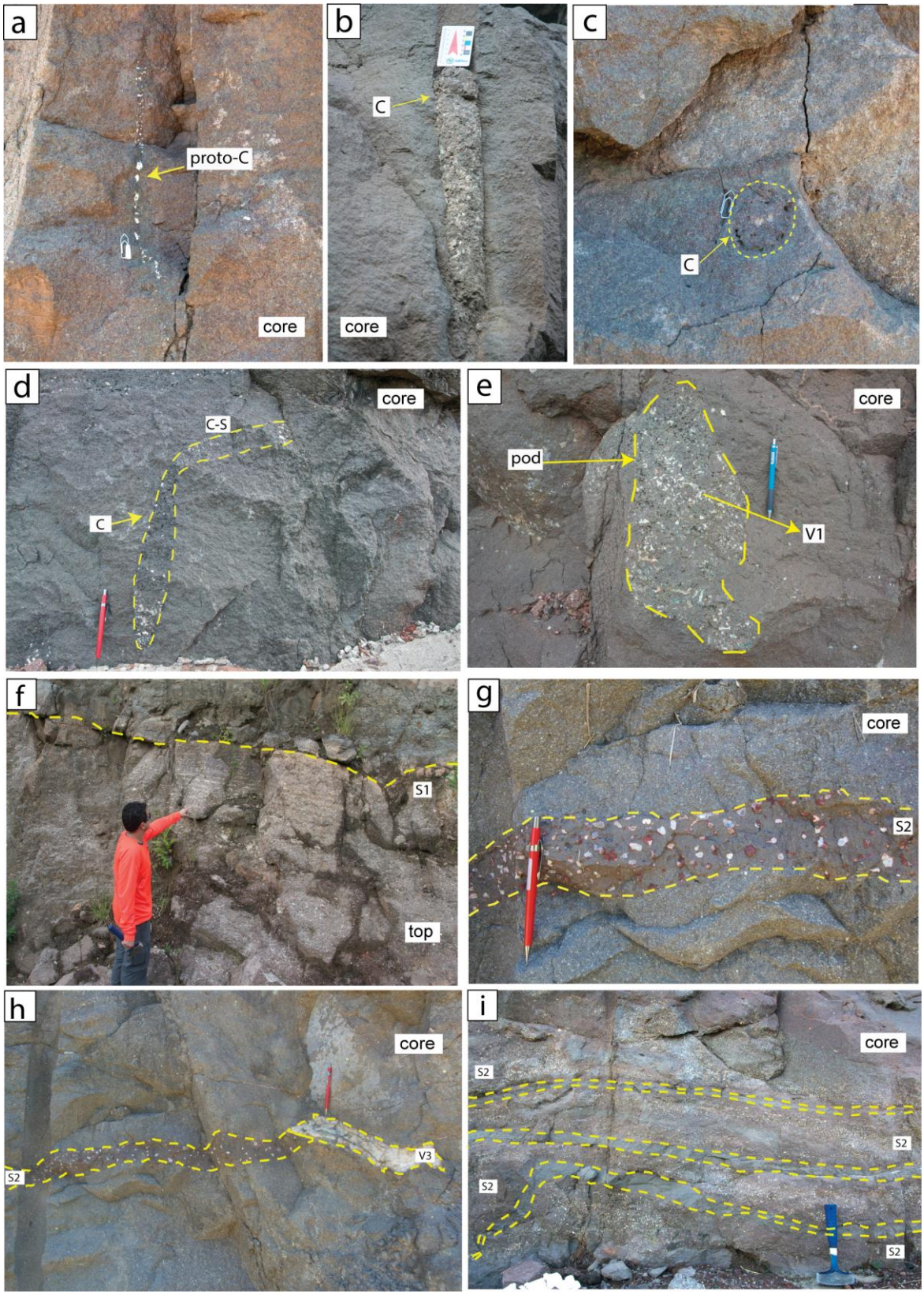

Fig. 4 Field photographs of cylinders, pods, and sheets. **a** Proto-cylinder (sample PSC-3C). **b** Vesicle cylinder (sample PSC-3D). **c** Cylinder in a horizontal section (sample PSC-3D). **d** C-S sheet (sample PSC-3J). **e** Pod (sample PSC-3J). **f** S1 with an alternating banded appearance (sample PSC-22). **g** S2 composed of glass and V1 (sample PSC-3G). **h** S2 showing lateral change to V3. **i** S2 occurring as alternating bands.

V1, V2, and V3 vesicles

Of the three types of vesicles observed in the SCSH region, the most common, V1 are <1 cm in diameter. Most of the spherical and elongated vesicles are filled partly to completely by glass and secondary minerals and occur throughout the pahoehoe lavas (Fig. 5a). Unfilled flattened and irregular vesicles typically occur at the top and base (Fig. 5b) of the rubbly lavas. The smallest spherical vesicles, at 2–5 mm, change downward to larger elongated vesicles of 1–5 cm, characterizing a typical normal gradation in the upper crust of simple pahoehoe lavas (Fig. 5c). S1 sheets occur in this gradation zone (Fig. 4f). In addition, elongated and flattened vesicles aligned in different directions are typical of the thin, glassy surface of pahoehoe lava (Fig. 5d).

At the base of compound and simple pahoehoe lavas, elongated and slightly tilted vertical bubbles characterize the pipe vesicles (V2); bubbles longer in length appear in the simple flows. The pipes are filled by glass, zeolite, and quartz (Fig. 5e). Locally, the V2 are distributed in overlapping clusters (Fig. 5f).

Domed giant vesicles (V3) occur in the interface between the top and upper half of the core of the simple pahoehoe lavas and in the upper half of core of the rubbly lavas. Most of these V3 are filled partly to completely by glass and secondary minerals such as zeolite and quartz (Fig. 5g–h).

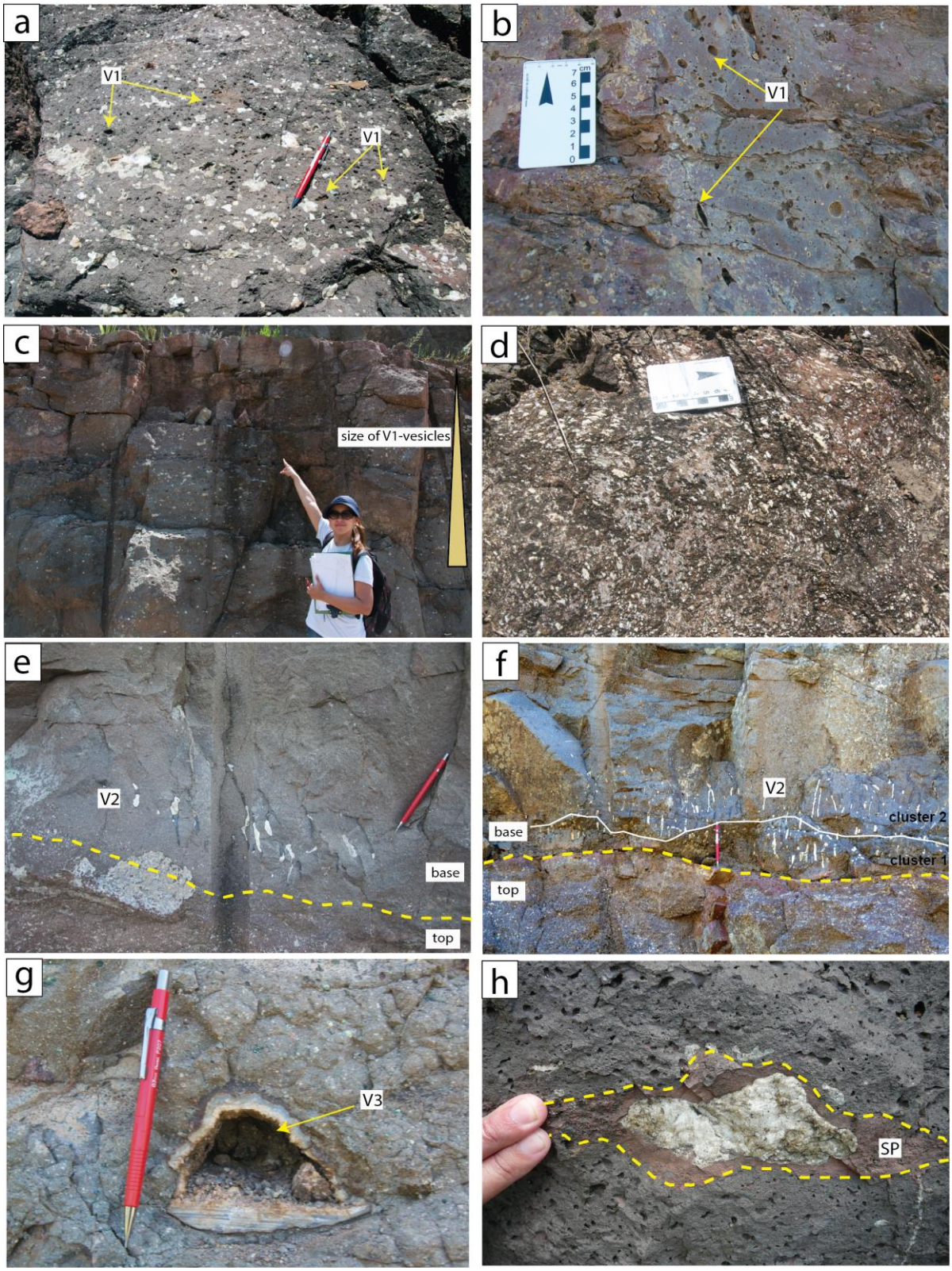

Fig. 5 Field photographs of vesicles. **a** Elongated and spherical V1 partly and completely filled by zeolite (sample PSC-3B). **b** Irregular and spherical V1 with no filling (sample PSC-5A). **c** Normal gradation in size distribution of V1 (sample PSC-3H). **d** Elongated and flattened V1 aligned in different directions (sample PSC-3M). **e** Slightly tilted V2 (sample PSC-3C). **f** V2 distributed in overlapping clusters (sample PSC-3I). **g-h** V3 filled by secondary minerals (sample PSC-3J) and segregation product (SP).

Mineralogy and textures

Pahoehoe lavas

The pahoehoe lavas are dominated by augite and plagioclase; titanomagnetite and apatite occur as minor phases. Olivine is present only in the pahoehoe lavas at base of the volcanic succession.

The base of pahoehoe lavas is aphanitic and hypocrystalline with porphyritic, intersertal, vesicular, and amygdaloidal textures (Fig. 6a–b). The intersertal texture consists of plagioclase (31%–44%; average - av. 36%); augite (18%–23%, av. 21%); and olivine (5%–10%, av. 8%), embedded in a mesostasis (15%–24%, av. 19.55%), replaced by iron oxide (av. 4%) and smectite. Some vesicles are filled completely by zeolite (Fig. 6b), carbonate, chalcedony, and quartz.

The core of pahoehoe lavas displays holocrystalline, aphyric, and intergranular textures (Fig. 6c). Plagioclase crystals (30%–45%, av. 38%), display no alignment, whereas augite (21%–27%, av. 23%) occurs between plagioclase crystals. The diktytaxitic texture is characterized by micro cavities that are filled by smectite and celadonite (Fig. 6d). The mesostasis (12%–27%, av. 16%), is altered to iron oxides (1%–7%, av. 5%) and smectite, whereas the olivine (0.7%–8%, av.6%) is replaced by iddingsite and bowlingite.

The pahoehoe lava tops display the same textures as those in the base, although higher amounts of vesicles and amygdales occur (Fig. 6e). Some vesicles are filled by zeolites with prismatic, botryoidal, and fibro-radiated habits. The mesostasis (15%–20%, av. 17%) is altered to iron oxides and smectite. The plagioclase crystals (19%–31%, av. 26%) range from unaltered to those replaced by albite and zeolite. Augite (13%–25%, av. 20%) show that some crystals are partly altered to iron oxide. The olivine crystals (1%–6%, av. 3%) are altered to iddingsite in the core and to bowlingite in the rims (Fig. 6f).

Rubbly lavas

The rubbly lavas show the same mineralogy those of pahoehoe lavas, although the olivine phenocrysts are lacking. The modal analysis of the rubbly lava cores is not provided herein owing to their very fine-grained texture. Hypocrystalline and intersertal textures are common in the core of these flows (Fig. 6g). Diktytaxitic voids are filled by smectite. Anhedral opaque minerals are scattered throughout the mesostasis.

Hypocrystalline basalt fragments (23%–76%, av. 45%) constitute the top breccias (Fig. 6h). These fragments contain plagioclase microphenocrysts and microlites (9%–16%, av. 12%), as well spherical and irregular vesicles filled by zeolite and carbonate (Fig. 6h). The

matrix of breccias is formed by mesostasis altered to zeolite and quartz (19%–25%, av. 21%; Fig. 6i), whereas two rubbly lavas, PSC4A and PSC4B, show a sandstone matrix (av. 29%; Fig. 9h).

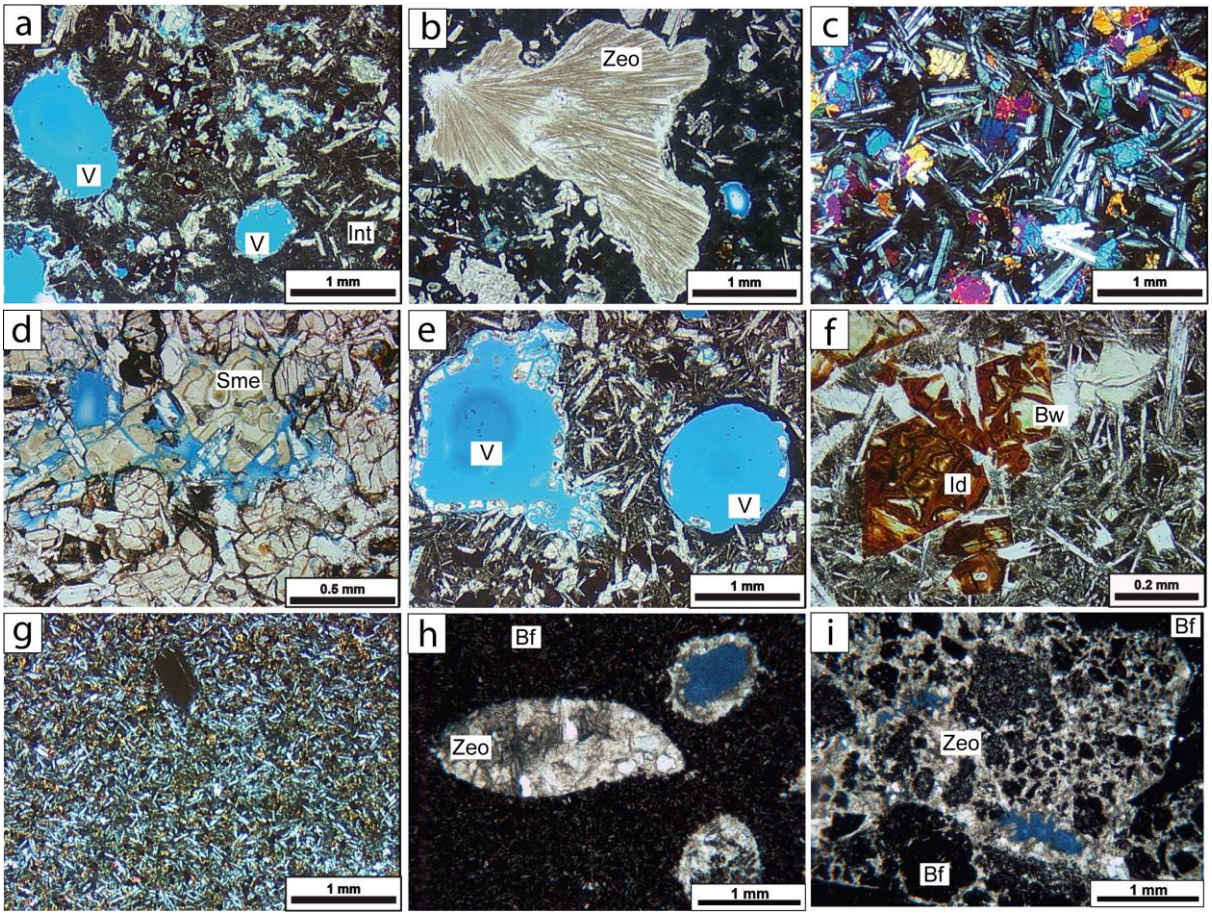

Fig. 6 Photomicrographs of mineralogy and texture. **a** Vesicular and intersertal textures. **b** Amygdale filled by zeolite with fibro-radiated habit. **c** Intergranular and subophitic textures. **d** Cavities filled by smectite. **e** Vesicular texture. **f** Olivine replaced by iddingsite and bowlingite. **G** Hypocrystalline and aphyric textures. **h** Basalt fragment containing vesicles filled by zeolite. **i** Matrix replaced by zeolite. V: vesicular; Int: intersertal; Zeo: zeolite; Sme: smectite; Id: iddingsite; Bw: bowlingite; Bf: basaltic fragment.

Porosity

In the pahoehoe and rubbly lavas, primary and secondary porosities can be distinguished on the basis of origin process and morphological relationships (Table 2).

Table 2 Primary and secondary processes and the resulting porosity types.

Origin	Process		Porosity type	Occurrence inside the lava flow
Primary	Gas release		vesicular	Base and top of pahoehoe Top of rubbly
	Deuteric crystal dissolution		Intracrystalline sieve to moldic	Base, core and top of pahoehoe
Secondary	Alteration Diagenetic hydrothermal	Initial dissolution of the primary mineralogy and precipitation of secondary minerals in the open spaces	Spongy to cavernous	Core of rubbly Base, core and top of pahoehoe
		Dissolution of mafic phenocrysts and precipitation of secondary minerals	lacy	Base of pahoehoe Top of rubbly
		Precipitation of secondary minerals inside the vesicles and cavities	drusy	Base and top of pahoehoe Top of rubbly
		Mechanical removal of secondary minerals from phenocrysts	Intracrystalline sieve	Base, core and top of pahoehoe
		Dissolution of glassy basalt fragments	Intra-fragment	Top of rubbly
		Dissolution and precipitation of secondary minerals in the basaltic matrix	Intra-matrix	Top of rubbly
		Dissolution of carbonate cement between quartz crystals in the sandstone matrix	Intra-cement	Top of rubbly
	Tectonic		Tectonic fracture	Top of pahoehoe Core of rubbly
	Quenching		Quench fracture	Top of pahoehoe

Primary porosity

The vesicular porosity corresponds to former bubbles and gas pockets created by exsolution of volatile magma contents during the cooling of the lava flows. This type of porosity is common in the pahoehoe lavas at the base (3.6%–4%, av. 4%); core (av. 3%) and top (5%–8%, av. 6%) (Fig. 7a), and inside the top fragments of the rubbly lavas (Fig. 7b). Vapor-phase quartz crystals usually rim the vesicles in both rubbly (Fig. 7b) and pahoehoe lavas (Fig. 7c).

The intracrystalline sieve porosity occurs in the initial dissolution stage of the plagioclase followed by precipitation of new feldspar phases, which generated minute cavities distributed in the center of the crystal (Fig. 7d) and large cavities randomly distributed (Fig. 7e). This porosity is distributed in the pahoehoe lava flows at the base (0.3%–6%, av. 6%);

core (1%–9%, av. 6%); and top (2%–9%, av. 8%). The associated moldic porosity is developed when the plagioclase phenocrysts were almost completely dissolved, which generated large relict crystals (Fig. 7f). This porosity is observed only at the top of the pahoehoe lavas (av. 1%).

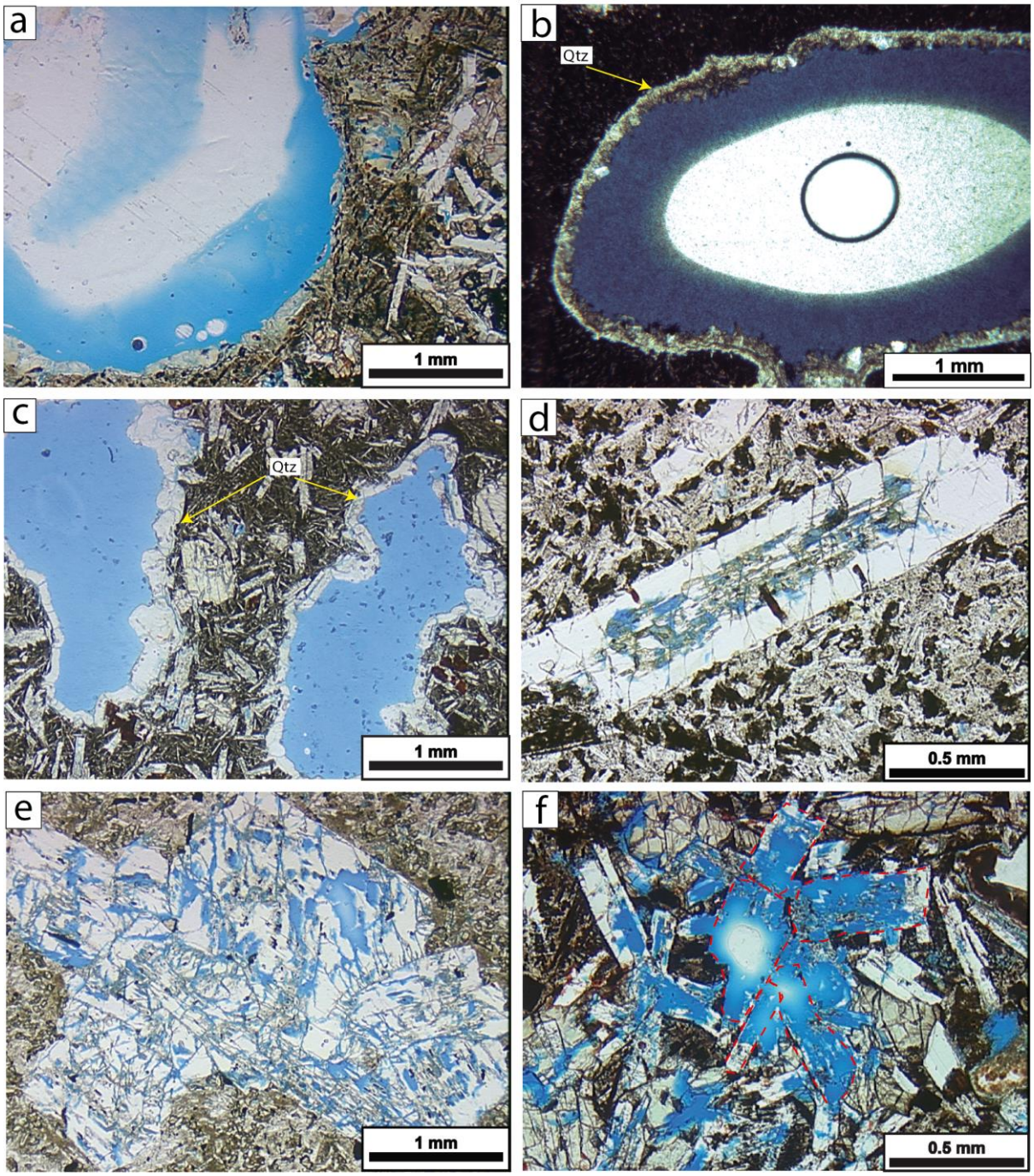

Fig. 7 Photomicrographs of primary porosities. **a** Vesicular porosity in pahoehoe lavas. **b-c** Quartz vapor-phase crystals rimming the vesicles in the rubbly and pahoehoe lavas, respectively. **d-e** Intracrystalline porosity in plagioclase with minute cavities distributed in center of crystal and large cavities randomly distributed. **f** Moldic porosity in plagioclase. Dashed lines indicate the original crystal shape.

Secondary porosity

Secondary minerals often partly to completely fill the vesicles and cavities, leading to drusy porosity. This porosity is distributed in the pahoehoe lavas at the base (av. 0.7%); core (av. 0.3%); and top (1%–2%, av. 1.5%) (Fig. 8a–c) and also occurs in the fragments in the top breccias of the rubbly lavas (6%–22%, av. 12%), where secondary mineral precipitate in spherical (Fig. 8d) and irregular vesicles (Fig. 8e).

The spongy porosity occurs through initial dissolution of the primary mineralogy and precipitation of secondary minerals in the open spaces originating from small to medium pores. This porosity is observed in the pahoehoe lavas at the base (1.7%–2%, av. 1.8%); core (0.7%–3%, av. 1.3%); and top (1.3%–2.3%, av. 1.8%) (Fig. 8f), as well as in the core of the rubbly lavas (Fig. 8g). Cavernous porosity occurs where the pores are significantly larger in diameter than the spongy (Fig. 8h). This porosity is common in the pahoehoe lavas at the core (0.7%–6%, av. 3%) and top (av. 0.7%).

Lacy porosity represents the initial dissolution of mafic phenocrysts and precipitation of secondary minerals (Fig. 9a). This porosity is common in augite phenocrysts in pahoehoe flows at the base (av. 0.33%) and top (av. 2%). The secondary intracrystalline sieve porosity occurred when the secondary minerals were mechanically or chemically removed from the olivine (Fig. 9b). This porosity of the pahoehoe lavas is at the base (0.33%–0.67%, av. 0.56%) and core (av. 1.33%).

Planes of parting in the rock that cut through crystals, mesostasis, and cavities generated the tectonic fracture porosity observed at the top of both pahoehoe (av. 0.33%; Fig. 9c) and rubbly lavas (av. 1.33%; Fig. 9d). The quench fracture porosity occurs in polyhedric cuviplanar fractures connected in a network (Fig. 9e) only at the top of pahoehoe flows (av. 1.33%).

Intra-fragment porosity, formed through the dissolution of glassy basalt fragments (Fig. 9f), occurs in the top breccias of rubbly flows (0.33%–6.67%, av. 3.5%). Most of these fragments are immersed in a basaltic matrix, which its dissolution and precipitation of secondary minerals generated the intra-matrix porosity (Fig. 9g). The intra-cement porosity is created when the incomplete internal dissolution of carbonate cements occur between the quartz crystals in a sandstone matrix of one rubbly flow (Fig. 9h).

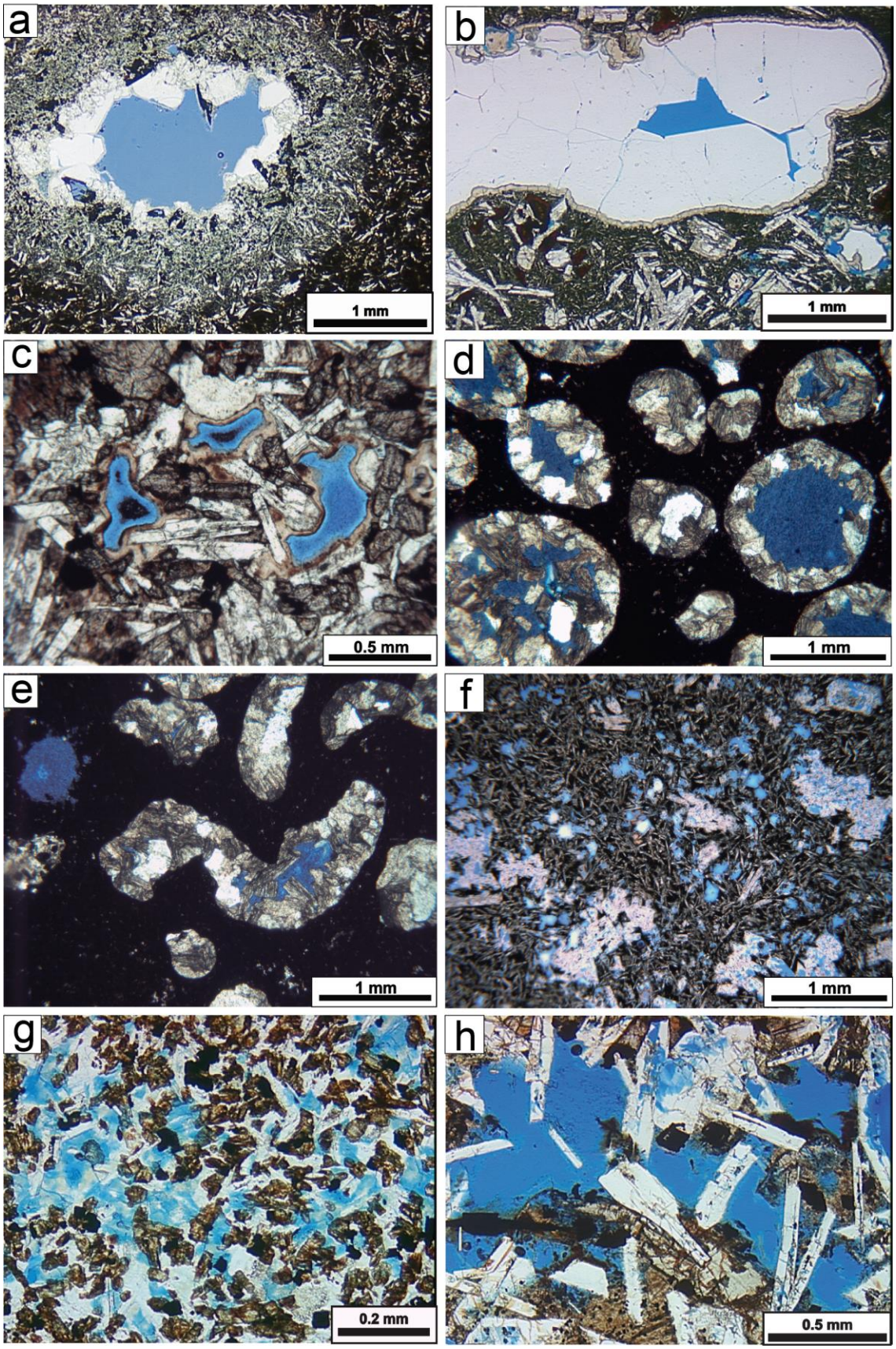

Fig. 8 Photomicrographs of secondary porosities. **a-c** Drusy porosity in pahoehoe lavas. **d-e** Drusy porosity in spherical and irregular vesicles in rubbly top breccias. **f-g** Spongy porosity in pahoehoe and rubbly lavas, respectively. **h** Cavernous porosity.

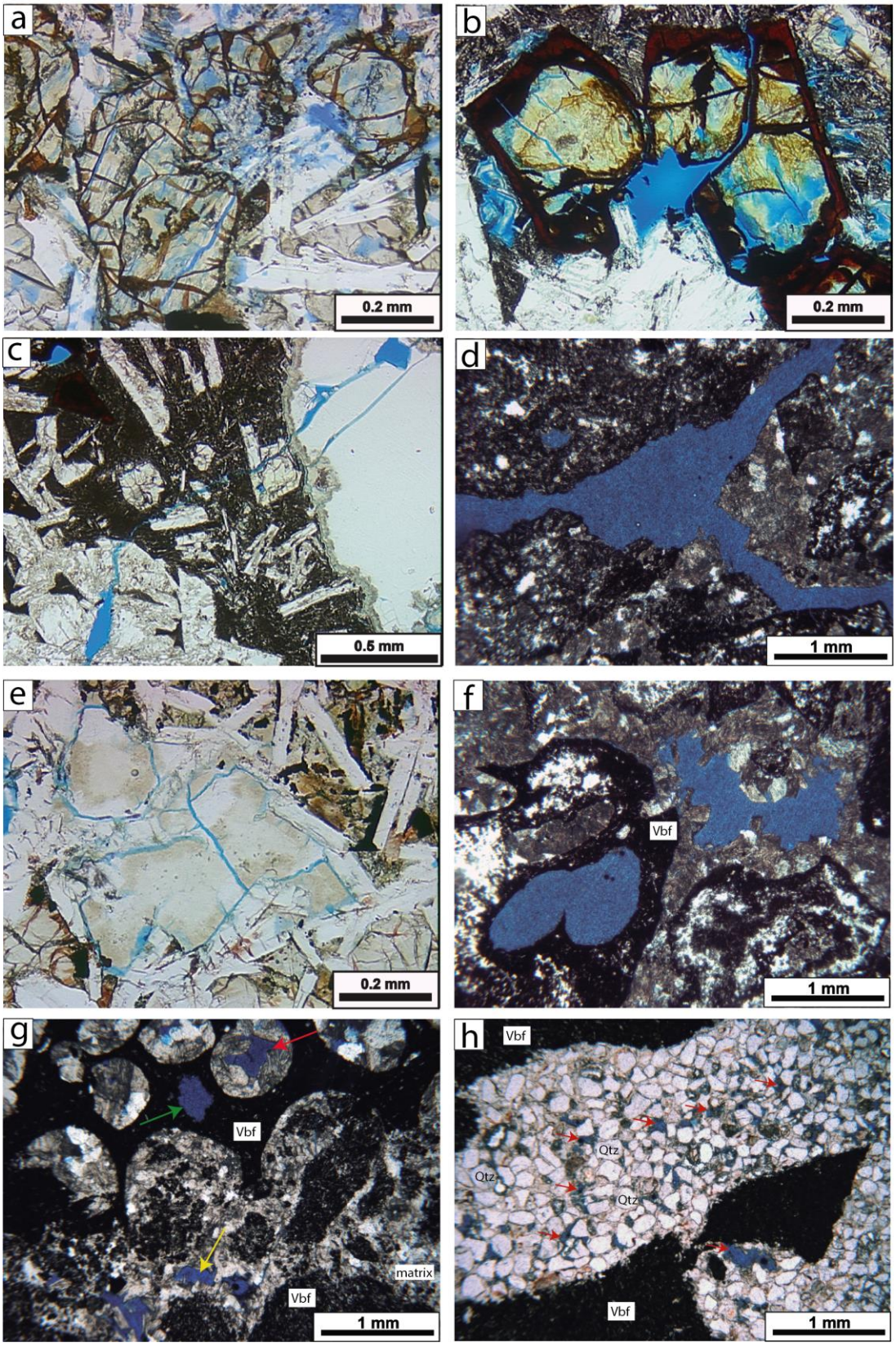

Fig. 9 Photomicrographs of secondary porosities. **a** Lacy porosity. **b** Intracrystalline sieve porosity in olivine. **c-d** Tectonic fracture porosity in pahoehoe and rubbly lavas, respectively. **e** Quench fracture porosity. **f** Intra-fragment porosity. **g** Rubbly breccias with intra-matrix (yellow arrow), intra-fragment (green arrow), and drusy porosities (red arrow). **h** Intra-cement porosity. Red arrows indicate the pores. Vbf: vesiculated basalt fragment; Qtz: quartz.

Discussion

Relationship of the vesicle-rich segregation structures with the morphology and thickness of the lava flows

Mapping of segregation structures at the field scale can be used to define the lava flow morphology and thickness because the structures occur in specific positions within the lavas (Fig. 3). A representation of vertical zonation of the segregation structures within lava flows and the transition among the different types is shown in Fig. 10a.

The segregation structures progressively increase in abundance in the SCSH region as the flow thickness increases from compound pahoehoe at about 1 m in thickness toward 6-m simple pahoehoe flows. However, most of the segregation structures disappear in the rubbly flows thicker than 30 m.

The cooling of the compound pahoehoe flows is so rapid that only the V1 and V2 vesicles froze inside the flows (Fig. 10b). The V1 result from an increase in confining pressure applied to the fluid within the vesicles coupled with shrinkage of gas during cooling (Smith 1967). V2 occur in the base of the P-type compound pahoehoe lavas that formed on low slopes (Walker 1987; Wilmoth and Walker 1993).

The inflation process (Hon et al. 1994) may have been important in the formation of the abundant segregation structures in the simple pahoehoe lavas. The cooling was sufficiently rapid at the beginning of the emplacement of these lavas that froze only the earliest structure of S1 located in the lava tops (Fig. 10c). The S1 formed when the sustained influx of lava under low effusion rates during a long-lived eruption allowed the slow advance of the flow front by continued outbreaks. In these cases, the uplift of thicker brittle crust through the inflation process produced the alternation of bands that bound the sheet-flow margins.

Proto-cylinders marking the base of simple pahoehoe lavas occurred through the accumulation of vapor and differentiated melt formed by the same process as those in the cylinder formation (Fig. 10d). When the proto-cylinders increased in diameter as they rose through the flow, their contact with the host lava became sharp and generated the cylinders themselves. The preservation of cylinders in the lower half of the core of simple pahoehoe flows (Fig. 10e) is explained by migration of residual liquids during the cooling of magmas to vesicle-rich, low-density areas generated only above the lower solidification front by a gas filter-pressing mechanism (Goff 1996). Other hypotheses of the cylinder origin have been reported (Manga and Stone 1994; Caroff et al. 2000; Fowler et al. 2015).

The gas filter-pressing process is described as the migration of residual liquid through a porous and permeable network including rigid interlocking crystals. In this process, the gas pressure builds up due to the second boiling process (Bowen 1928) that occurs when the magma cools and anhydrous minerals begin to crystallize out, which allows the residual liquid to become increasingly enriched in gas and migrate into previously formed vesicles (Anderson et al. 1984). To generate the segregation structures, the degree of crystallization should be at least 35% to form the required crystal framework (Anderson et al. 1984; Caroff et al. 2000).

The pods are segregation structures that occur only in the upper half of core of simple pahoehoe lavas. These structures formed when residual liquids penetrate the accumulation zone of vesicles in response to the pressure gradient generated by vapor-saturated crystallization during the freezing of upward-rising gas bubbles (Anderson et al. 1984). Although these pods could be cylinders viewed in a cross-section, their diameters, at about 30 cm, are larger than the 6-cm cylinders.

V1 vesicles occur throughout the pahoehoe flows and contain segregated material or secondary mineral fill. The top of simple pahoehoe lavas are highly vesiculated, at >50%, with a range of vesicle shapes and sizes characterizing normal gradation. The overall decrease in vesicle size upward is attributed to progressive bubble loss with transport (Wilmoth and Walker 1993). Flattened vesicles in the thin, glassy surface of the pahoehoe lavas are important because they indicate flow direction.

V2 vesicles concentrated in the base of the simple pahoehoe lavas (Fig. 10d, 10e) are attributed to continued exsolution of gas bubbles rising through lava at the point at which acquired sufficient yield strength for preventing closure behind them (Walker 1987). Thordarson and Self (1998) reported that V2 often converge to form cylinders; thus, these structures should be genetically linked. However, such a relationship was not found in the study area. V2 should not be confused with cylinders and proto-cylinders because these two segregation structure types invariably occur above the basal zone of these flows and extend upward toward the upper half of core (Fig. 10d, 10e).

V3 vesicles mark the interface between the upper half of the core and the top of the simple pahoehoe lava flows. These vesicles originated above the lower solidification front by bubble coalescence of different sizes and growth by mass transfer (McMillan et al. 1987).

In the last stage of emplacement of the simple pahoehoe lava flows, the solidification fronts advanced more slowly, stagnated, and stopped inflating, which enabled the formation of the C-S and S2 sheets, in the lower half of the core of these lavas.

Pahoehoe flows thicker than 6 m were not found in the SCSH. Moreover, rubbly flows with thickness up to 50 m occur. These flows emplaced under high effusion rates on shallow slopes, which enabled the thickening caused by the inflation process (Barreto et al. 2014). Pulses in the effusion rates and subsequent increases in viscosity led to tensile stress in the upper crusts, resulting in degassing, rupturing, and top brecciation. For this reason, most of the segregation structures are not preserved, except for V1 in the base and top (Fig. 10f–g) and V3 in the upper half of the core.

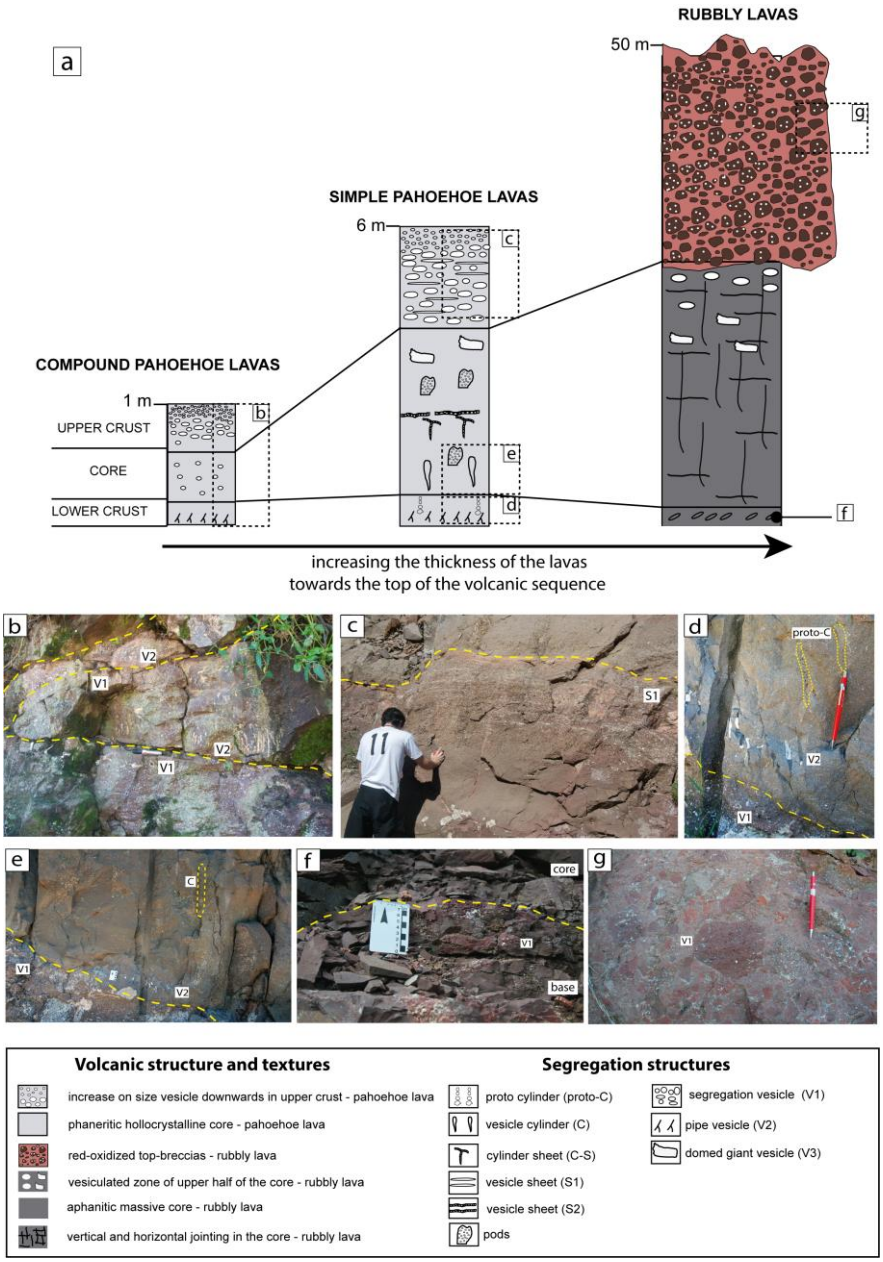

Fig. 10 a Location of segregation structures within basic lava flows. **b** Compound pahoehoe lavas with V1 at the top and V2 at the base. **c** S1 at the top of simple pahoehoe lavas. **d-e** V1 at the top of the underlying simple pahoehoe flow; overlying flows show V2 and proto-cylinders at the base and cylinders in at lower half of the core. **f** Irregular V1 mark the base of the rubbly lavas. **g** Spherical and irregular V1 constituting the fragments of rubbly breccias.

Processes responsible for formation of primary and secondary porosities

Primary process

The exsolution of volatile magma content during cooling is recorded in the formation of vesicles through the primary process of gas release. Because the gas is less dense and has a tendency to rise, greater amounts of vesicles are concentrated in the top of the lavas. The vesiculated nature of lavas creates a pore space suitable for releasing the dispersed gas, the basic mechanism of which is bubble coalescence. The vesicles represents most of the pahoehoe porosity, although the rare connection of pores results in low permeability.

The primary process of deuteric crystal dissolution is formed by the initial dissolution of earlier-formed minerals by deuteric fluids in late stages of igneous activity followed by precipitation of new feldspar phases (Sruoga and Rubinstein 2007), which generated the intracrystalline porosity. Although these pores can contribute to enhancement of the total lava porosity, the permeability is always low because the pores are rarely connected. Although the porosity degree was larger when the moldic pores originated, the permeability is low.

Secondary process

The alteration and fracturing processes of ancient volcanic rocks are important in the development of secondary porosity or the enlargement of existing cavities in basaltic lava flows.

The alteration process includes all mineralogical and textural modifications produced by chemical and physical factors such as diagenesis, weathering, and hydrothermal alteration. Three types of processes occur through alteration: dissolution and precipitation of secondary minerals, precipitation of secondary minerals in open spaces, and mechanical removal of secondary minerals.

The spongy, lacy, and intra-matrix porosities result from the initial dissolution and precipitation of secondary minerals in open spaces. This process originates unconnected small- and medium-sized pores with irregular shapes, which provide a minor contribution to the total porosity of lavas owing to the low connection of the pores. The cavernous pores exhibit large sizes and frequently occur together with packing inhomogeneity forming channels. This porosity is generated by the same process as spongy type and can increase the permeability of these lavas owing to the formation of channels interconnecting the available pores.

The process of mechanical removal of secondary minerals from olivine phenocrysts characterizes the intracrystalline sieve porosity. This process generates disconnected small

pores that have a low effect on porosity increase.

The dissolution of constituents such as basalt fragments inside the rubbly breccias generated the intra-fragment porosity in which the pores are too restricted to provide a minor contribution to the effective porosity. The selective dissolution of carbonate cement between quartz crystals in a sandstone matrix generated the intra-cement porosity, which should have a strong contribution to effective porosity of the rubbly flows. However, this matrix is restricted to the one rubbly lava.

Although several mechanisms are responsible for the formation of porosity in the basaltic lava flows from the SCSH, the precipitation of secondary minerals inside the vesicles and cavities created the drusy porosity. Such precipitation may partially occlude or seal open spaces, which dramatically decreases the available primary and secondary porosity and frequently obscures the evidence of pore origin.

Mechanisms such as tectonic and quenching formed fractures can increase the permeability of the flows. Tectonic fractures provide a minor contribution for the total porosity of these lavas, although their main importance is the permeability they impart to some lava flows. Although thermal stresses associated with abrupt cooling of magmas generated a network of polyhedric fractures that generated the quench fracture porosity, this process provided a negligible contribution to the lava flow porosity.

Contribution of primary and secondary porosities and implications for a volcanic reservoir

Previous studies reported that the basic lava flows of the SGF should constitute a volcanic reservoir in which the main porosity is associated with a large amount of fracturing (Reis et al. 2014). However, the data obtained in this paper show that several porosities could influence the petrophysical characteristics of these lavas. In this case, the alteration and fracturing processes that affected the lava flows of the south hinge of the TS influenced the storage quality for hydrocarbons or groundwater in this region. However, the reservoir quality enhancement through the generation of secondary porosity was partially counteracted by the precipitation of secondary minerals.

The modal counting of pores in thin section indicates that the porosity is relatively low in the studied lava flows in comparison with sedimentary rocks. However, the variations in porosity degree can be correlated with specific positions inside the flows. The pahoehoe lavas exhibit higher porosity in the top (20.66%), whereas the base (12%) and the core (13%) show similar and slightly lower porosity. The main contribution is the primary vesicular type,

which is common at the base and top of these flows, where the segregation structures such as V2, S1, and V1 with different shapes and sizes can store hydrocarbons.

The core of the pahoehoe lavas exhibits little vesicular porosity and several secondary porosities such as spongy, cavernous, lacy and quench fracture. The presence of segregation structures such as cylinders, proto-cylinders, S2, V3, and pods should enhance the total porosity of pahoehoe lavas. However, these structures show sharp contact with the host basalt, reducing any connectivity between the pore-rich structures and the host basalt.

The alteration of rubbly top breccias produces several secondary porosities that provide a significant contribution of 19% to the total porosity of the SCSH section. However, the core of rubbly flows tends to cool faster than that of pahoehoe lavas, which allows only the formation of small amount of spongy pores, which provide a negligible contribution to the total porosity.

The observed fractures within the studied lava flows are associated with tectonic process with many of them forming when the lavas cooled after the emplacement. The fractures are particularly important for hydrocarbons storage because they create efficient channel networks for possible hydrocarbon migration and entrapment owing to their ability to connect isolated cavities (Gudmundsson and Lotveit 2014; Spence et al. 2014).

The core of pahoehoe lavas of the SCSH section exhibits irregular jointing where the lava breaks into hackly fragments owing to late-stage fracturing (Fig. 11a). Locally, a massive and oxidized zone known as an entablature was created by the very rapid cooling between two columnar joints in the core of pahoehoe lavas (Fig. 11b). The entablature zone can contribute only to effective porosity if later fractures occur. Simple pahoehoe lavas display cooling fractures perpendicular to external crust as a result of the inflation process, which can connect the existing vesicles inside the flows (Fig. 11c). Dykes and layers filled by sandstone from BF (Fig. 11d, 11e) in addition to intertrap successions (Fig. 11f) developed by interactions between lavas and sediment can create a porous network in flows that could be favorable for hydrocarbon migration. Although previous studies show that the SGF can act as a fractured volcanic reservoir (Reis et al. 2014), the observed fractures in the SCSH region are often sealed by sandstone and secondary minerals, which contributes to reduced permeability.

In summary, this study argues that the development of pores and the high fracturing alone is not a sufficient condition for creating hydrocarbon reservoirs in the studied basaltic lava flows because the connectivity of the pores is low. Future studies should obtain quantitative data of permeability and porosity at the field scale coupled with brittle tectonic studies. Such data are important for quantifying the transmissivity of these lavas and for

building predictive models of volcanic reservoir suitability for hydrocarbon or groundwater storage in the south hinge of the TS.

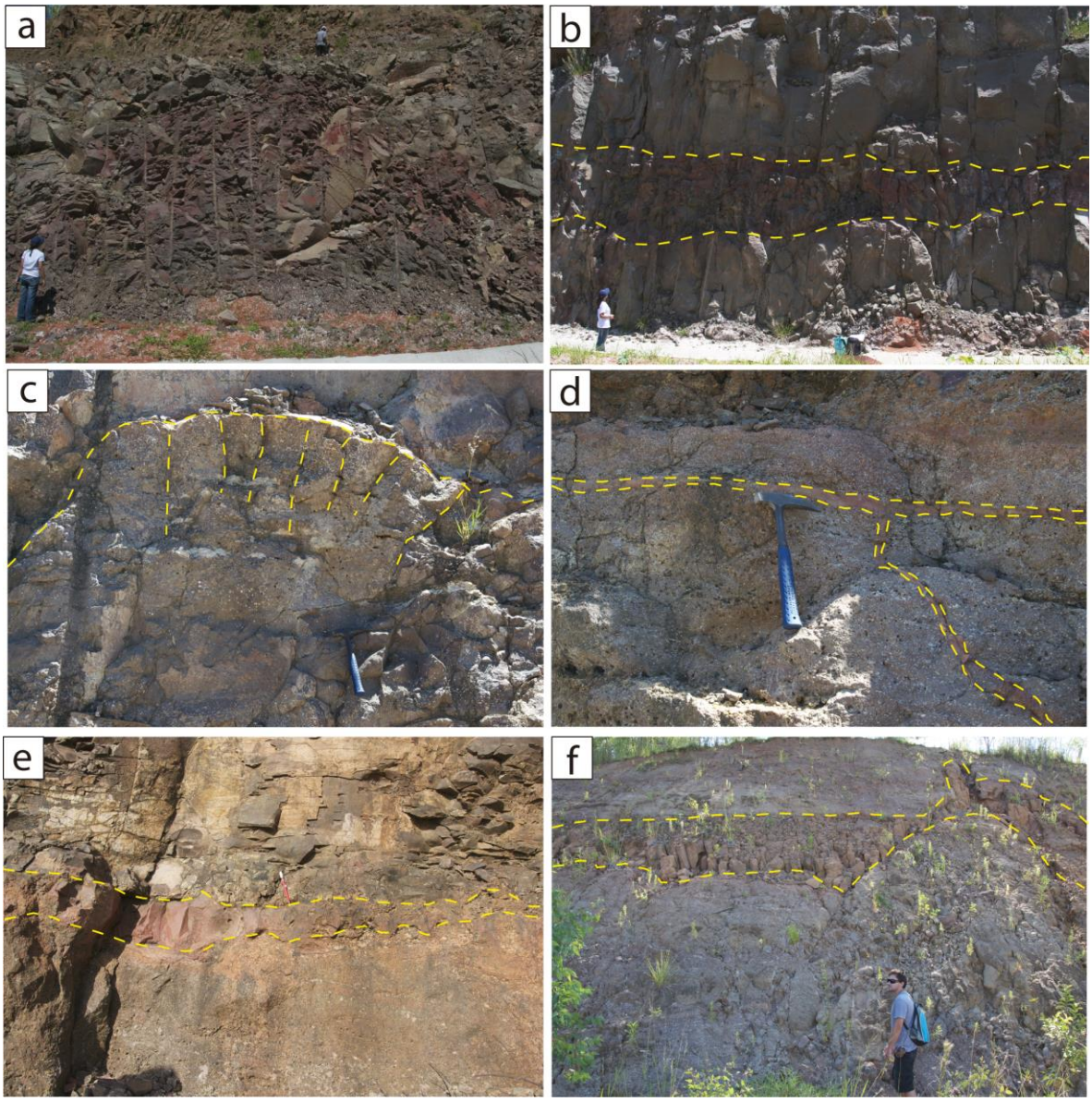

Fig. 11 a Irregular late-stage fracturing. **b** Oxidized massive entablature zone. **c** Cooling fractures perpendicular to external crust of pahoehoe lavas. **d** Sandstone dyke. **e** Layer filled by sandstone. **f** Intertrap features.

Concluding remarks

This study shows a link between the lava flow thickness and vesicle-rich segregation structures in the SCSH region. In the compound pahoehoe flows, V1 appear throughout the flows, and V2 at the base are formed. Simple pahoehoe lava flows exhibit proto-cylinders and V2 at the base. Cylinders, C-S and S2 sheets, and V3 occur only at core of these lavas; S1 and V1 occur at top. In the rubbly lava flows only the V1 occur in the base and top; V3 appear in upper half of the core.

Numerous primary and secondary porosities are observed in the studied lava flows. Gas release and the dissolution of deuteric crystals formed the vesicular, intracrystalline sieve and moldic pores that represent primary porosities. Processes such as alteration and fracturing generated the secondary porosities including spongy, cavernous, lacy, intra-fragment, intra-matrix, intra-cement, quench and tectonic fractures.

The precipitation of secondary minerals in vesicles and cavities created the drusy porosity that strongly decreases the existing primary and secondary porosities. Although, the existence of fractures, dykes, and layers in the SCSH region could represent an efficient channel network for hydrocarbon migration, these structures are also sealed by sandstone and secondary minerals, which reduces the available space for hydrocarbon storage.

This study emphasizes the importance of recognizing the available porosities to better understand the petrophysical characteristics of basaltic flows. However, we argue that the existence of pores alone is insufficient for creating reservoirs in igneous rocks; high permeability is also necessary. Therefore, the integrated approach of quantitative analysis of porosity and permeability coupled with brittle tectonic studies is needed to define the effective porosity degree of rocks of the south hinge of TS, which could help to build predictive models of reservoir quality in lava flows for hydrocarbon storage.

Acknowledgements

The authors acknowledge the financial support of the PRH PB-215, FAPERGS 2311-2551/14, CAPES FCT-13991/13-2, FAPESP 2012/06082-6, and CNPq 479784/20124; 404774 and 3038/20098 projects.

References

Anderson AT, Swihart GH, Artioli G, Geiger CA (1984) Segregation vesicles, gas filter-pressing, and igneous differentiation. J Geol 92:55-72.

Aubele JC, Crumpler LS, Elston WE (1988) Vesicle zonation and vertical structure of basalt flows. J Volcanol Geotherm Res 35:349-374.

Barreto CJS, Lima EF, Scherer CM, Rossetti LMM (2014) Lithofacies analysis of basic lava flows of the Paraná igneous province in the south hinge of Torres Syncline, Southern Brazil. J Volcanol Geotherm Res 285:81-99.

Bellieni G, Comin-Chiarmonti P, Marques LS, Melfi AJ, Piccirillo EM, Nardy AJR, Roisenberg A (1984) High- and Low-Ti flood basalts from the Paraná plateau (Brazil): Petrogenetic and geochemical aspects bearing on their mantle origin. Neues Fahrbuch Min Abh 150:272-306.

Bowen NL (1928) The evolution of the Igneous Rocks, 334 p. Dover, Mineola N.Y.

Bryan SE, Ernst RE (2008) Revised definition of Large Igneous Provinces (LIPs). Earth Sci Rev 86:175-202.

Caroff M, Maury RC, Cotton J, Clément JP (2000) Segregation structures in vapor-differentiated basaltic flows. Bull Volcanol 62:171-187.

DeRos LF, Goldberg K, Abel M, Victorinetti F, Mastella L, Castro E (2007) Advanced acquisition and management of petrographic information from reservoir rocks using the Petroledge® System. AAPG Annual Conference and Exhibition, Long Beach, CA, USA, Extended Abstracts, 6.

Fowler AC, Rust AC, Vynnycky M (2015) The formation of vesicular cylinders in pahoehoe lava flows. Geophys Astrophys Fluid Dynamics 109: 38-61.

Gilboa Y, Meri F, Mariano IB (1976) The Botucatu aquifer of South America, model of an untapped continental aquifer. J Hydrology 29:165-179.

Goff F (1996) Vesicles cylinders in vapor-differentiated basalt flows. J Volcanol Geotherm Res 71:167-185.

Goldberg K, Morad D, Al-Aasm IS, DeRos LF (2011) Diagenesis of Paleozoic playa-lake and ephemeral-stream deposits from the Pimenta Bueno Formation, Siluro-Devonian (?) of the Parecis Basin, central Brazil. J S Am Earth Sci 32:58-74.

Gudmundsson A, Lotveit IF (2014) Sills as fracturated hydrocarbon reservoirs: examples and models. Geol Soc London Spec Pub 374:251-271.

Hon K, Kauahikaua J, Denlinger R, Mackay K (1994) Emplacement and inflation of pahoehoe sheet flows: observations and measurements of active lava flows on Kilauea volcano, Hawaii. Geol Soc Am Bull 106:351-370.

Jerram DA, Mountney NP, Howell JA, Long D, Stollhofen H (2000) Death of a sand sea: an active aeolian erg systematically buried by the Etendeka flood basalts of NW Namibia. J Geol Soc London 157:513-516.

Jinglan L, Chengli Z, Zhihao Q (1999) Volcanic reservoir rocks: a case study of the cretaceous Fenghuadian Suite, Huanghua Basin, Eastern China. J Petrol Geol 22:397-415.

Lenhardt N, Gotz AE (2011) Volcanic settings and their reservoir potential: An outcrop analog study on the Miocene Tepoztlan Formation, Central Mexico. J Volcanol Geotherm Res 204:66-75.

Manga M, Stone HA (1994) Interactions between bubbles in magmas and lavas: effects of bubble deformation. J Volcanol Geotherm Res 63:267-279.

McMillan K, Cross RW, Long PE (1987) Two-stage vesiculation in the Cohassett flow of the Grande Ronde Basalt, south–central Washington. Geology 15:809-812

Peate DW, Hawkeswort CJ, Mantovani MSM (1992) Chemical stratigraphy of the Paraná lavas (South America): classification of magma types and their spatial distribution. Bull Volcanol 55:119-139.

Petry K, Jerram DA, Almeida DPM, Zerfass H (2007) Volcanic sedimentary features in the Serra Geral Fm., Paraná Basin, southern Brazil: Example of dynamic lava–sediment interactions in an arid setting. J Volcanol Geotherm Res 159:313–325.

Reis GS, Mizusaki AM, Roisenberg A, Rubert RR (2014) Formação Serra Geral (Cretáceo da Bacia do Paraná): um análogo para os reservatórios ígneo-básicos da margem continental brasileira. Pesquisas Geoc 41:155-168.

Scherer CMS (1998) Análise Estratigráfica e Litofaciológica da Formação Botucatu (Cretáceo Inferior da Bacia do Paraná) no Rio Grande do Sul. Ph.D. Thesis, Universidade Federal do Rio Grande do Sul.

Scherer CMS (2002) Preservation of aeolian genetic units by lava flows in the Lower Cretaceous of the Paraná Basin, southern Brazil. Sed 49:97-116.

Schmidt V, McDonald DA (1979) Texture and recognition of secondary porosity in sandstones. SEPM Special Publication 26:209-225.

Smith RE (1967) Segregation vesicles in basaltic lavas. Am J Sci 265:696–713.

Spence GH, Couples GD, Bevan TG, Aguilera R, Cosgrove GW, Daniel JM, Redfern J (2014) Advances in the study of naturally fractured hydrocarbon reservoir: a broad integrated interdisciplinary applied topic. Geol Soc London, Spec Pub 374:1-22.

Sruoga P, Rubinstein N (2007) Processes controlling porosity and permeability in volcanic reservoirs from the Austral and Neuquén basins, Argentina. AAPG Bull 91:115-129.

Thordarson T, Self S (1998) The Roza Member; Columbia River Basalt Group: a gigantic pahoehoe lava flow field formed by endogenous processes? J Geophys Res 103:27411-27445.

Waichel BL, Lima EF, Viana AR, Scherer CM, Bueno GV, Dutra G (2012) Stratigraphy and volcanic facies architecture of the Torres Syncline, Southern Brazil, and its role in understanding the Paraná–Etendeka Continental Flood Basalt Province. J Volcanol Geotherm Res 215–216:74–82.

Waichel BL, Scherer CMS, Frank HT (2008) Basaltic lava flows covering active aeolian dunes in the Paraná Basin in southern Brazil: Features and emplacement aspects. J Volcanol Geotherm Res 171:59-72.

Walker GPL (1987) Pipe vesicles in Hawaiian basaltic lavas: their origin and potential as paleo-slope indicators. Geology 15:84-87

Walker GPL (1989) Spongy pahoehoe in Hawaii: A study of vesicle distribution patterns in basalt and their significance. Bull Volcanol 51:199-209.

Wilmoth RA, Walker GP (1993) P-type and S-type pahoehoe: a study of vesicle distribution patterns in Hawaiian lava flows. J Volcanol Geotherm Res 55:129–142.

Wu C, Gu L, Zhang Z, Ren Z, Chen Z, Li W (2006) Formation mechanisms of hydrocarbon reservoirs associated with volcanic and subvolcanic intrusive rocks: examples in Mesozoic–Cenozoic basins of eastern China. AAPG Bull 90:137–147.

5.3 Artigo 3

TÍTULO: Geochemical and Sr-Nd-Pb isotopic insights of the Low-Ti basalts from southern Paraná Igneous Province, Brazil: the role of crustal contamination.

AUTORES: Carla Joana Santos Barreto

Jean Michel Lafon

Evandro Fernandes de Lima

Carlos Augusto Sommer

ACEITO PARA PUBLICAÇÃO: Em janeiro de 2016.

PERIÓDICO: International Geology Review

Esse artigo cientifico consistiu na primeira tentativa de registrar as variações geoquímicas e isotópicas de derrames básicos pertencentes ao magma BTi Gramado usando como guia uma estratigrafia em escala local. Essas variações são importantes para a discussão da petrogênese desses derrames dentro de um único tipo de magma, além de possibilitar uma avaliação qualitativa e quantitativa do papel da contaminação crustal bem como dos potenciais contaminantes envolvidos.

Geoquimicamente, as composições variam de basaltos a andesito basálticos de afinidade toleítica nos perfis Santa Cruz e Lajeado, enquanto na área do Morro da Cruz, os derrames do tipo *ponded pahoehoe* exibem composições de andesitos.

Diversas características geoquímicas, tais como valores muito baixos de Mg#, Ni, MgO, Ti/Y suportam a hipótese de contaminação crustal nesses magmas BTi. Essas características combinadas com baixas razões Rb/Ba e altas de Ba/Nb, anomalias negativas de Nb, enriquecimento em Th e U em relação a Ta e Hf, bem como aumento das razões de $^{87}Sr/^{86}Sr_i$ com uma razão constante de Ba/Yb reforçam o papel da contaminação por crosta continental superior. Além disso, a diminuição da razão P_2O_5/K_2O com o aumento da razão $^{87}Sr/^{86}Sr_i$ também sugere que magmas basálticos assimilaram material da crosta.

A assimilação crustal sugerida para estas sequências vulcânicas permite explicar as altas razões isotópicas iniciais de Sr (0,707798–0,715751), e os valores baixos de ε_{Nd} (-8,36 a -5,41), com associadas variações isotópicas de Pb (18,42 $<^{206}Pb/^{204}Pb<$ 18,86; 15,65 $<^{207}Pb/^{204}Pb<$ 15,71; 38,62 $<^{208}Pb/^{204}Pb<$ 39,37). O comportamento aleatório dos elementos traços e as variações isotópicas de Sr-Nd-Pb na sucessão vulcânica poderiam ser explicados por graus variados de assimilação de contaminantes Paleoproterozoicos e Neoproterozoicos concomitantes a recargas periódicas de magma basáltico.

Geochemical and Sr–Nd–Pb isotopic insights of the low-Ti basalts from southern Paraná Igneous Province, Brazil: the role of crustal contamination

Carla Joana Santos Barreto[1, *a], Jean Michel Lafon [2, b], Evandro Fernandes de Lima [3, c], Carlos Augusto Sommer[3, d]

[1]*Programa de Pós-Graduação em Geociências, Universidade Federal do Rio Grande do Sul, Porto Alegre, Brazil;* [2] *Laboratório de Geologia Isotópica, Universidade Federal do Pará, Belém, Brazil;* [3] *Instituto de Geociências, Universidade Federal do Rio Grande do Sul, Porto Alegre, Brazil*

[*] Corresponding author. [a] Av. Bento Gonçalves, 9500, CEP 91501-970, Porto Alegre-RS, Brazil. Tel.: +55 51 33087380. E-mail address: carlabarreto.geo@hotmail.com

[b] Rua Augusto Corrêa 1, CEP 66075-110, Belém-PA, Brazil. Tel.: +55 91 32017483. Email address: lafonjm@ufpa.br

[c] Av. Bento Gonçalves, 9500, CEP 91501-970, Porto Alegre-RS, Brazil. Tel.: +55 51 33087380. E-mail address: evandro.lima@ufrgs.br

[d] Av. Bento Gonçalves, 9500, CEP 91501-970, Porto Alegre-RS, Brazil. Tel.: +55 51 33087398. E-mail address: casommer@sinos.net

Abstract

The south hinge of the Torres Syncline in southernmost Brazil hosts a volcanic succession of pahoehoe and rubbly Gramado-type lavas belonging to the ~132 Ma Paraná–Etendeka igneous Province. We evaluate the geochemical and Sr-Nd-Pb isotopic variations using local-scale stratigraphy in order to discuss the petrogenesis of lava flows in a single magma type and to estimate the role of crustal contamination and the potential contaminants involved. The geochemical and isotopic variations along the lava pile are not systematic, implying that the magma chamber could have undergone successive replenishments of basaltic magma. The process of crustal assimilation explains the high and widespread initial Sr isotopic ratios at 0.707798–0.715751 and the very low ε_{Nd} at −8.36 to −5.41, with associated Pb isotopic variations (18.42 < $^{206}Pb/^{204}Pb$ < 18.86; 15.65 < $^{207}Pb/^{204}Pb$ <15.71; 38.62 < $^{208}Pb/^{204}Pb$ < 39.37). The magmatic evolution of the SCSH and LJ lava flows begins with the storage of mafic liquids during a short period at shallow-level magma chamber allowed the magma ascent with composition of olivine basalts. The continuous fractional crystallization within the magma chamber coupled with variable assimilation degrees of distinct contaminants with Paleoproterozoic and Neoproterozoic ages, in addition to significant contribution of magma recharge led to magma ascent with basaltic andesite composition that display at surface the simple pahoehoe morphology. The continuous magma recharge in the magma chamber coupled with higher assimilation degree allowed the

formation of basaltic andesite lavas with more contaminated isotopic signatures that exhibit rubbly morphology at the surface. Differentiation process of liquids coupled with the highest assimilation degrees of distinct contaminants during longer time in a shallow-level magma chamber, which is distinct from that where SCSH and LJ magmas have been stored, led to formation of andesites of the Morro da Cruz section that exhibit the most contaminated isotopic signatures.

Key words: Paraná Igneous Province; Low-Ti basalts; Sr-Nd-Pb isotopes; whole-rock geochemistry; crustal contamination; lava stratigraphy

1. Introduction

Large igneous provinces (LIP) represent anomalous events in the Earth's history. Continental flood basalts (CFB) constitute a type of LIP developed in a relatively short time span of 10^6 years in which huge volumes of lavas on the order of 10^5 to 10^7 km^3 were generated and accumulated along with intrusions (Coffin and Eldholm 1994; Storey *et al.* 2007; Bryan and Ernst 2008).

The extensive lava flow sequences of CFB that give the provinces 'layer-cake' or, when eroded, step-like appearances were previously considered as thick, homogeneous volcanic piles. For this reason, the chemical compositions of several CFB have been used as the most effective means of subdiving lava sequences in order to build the internal stratigraphy of the entire province. The CFB have been usually divided into high-Ti (HTi) and low-Ti (LTi) provinces (Bellieni *et al.* 1984) and have been grouped according to magma type (Peate *et al.* 1992). The basalts from Paraná igneous Province (PIP) have been mapped with stratigraphic control only at a regional scale, in which the sequences of lava flows belonging to a particular magma type behave as a relatively coherent stratigraphic unit (Fodor *et al.* 1985; Bellieni *et al.* 1986; Hawkesworth *et al.* 1986; Petrini *et al.* 1987; Piccirillo *et al.* 1989; Peate *et al.* 1992).

Remaining fundamental question about CFB concerns the degree to which these lava flows are crustally contaminated or whether their geochemical signatures are derived from enriched mantle, affected by generic metasomatic processes (Wilson 1989; Anderson 2005). The crustal contamination process has been particularly well documented for the LTi Gramado basalts from Paraná–Etendeka Province (Mantovani *et al.* 1985; Petrini *et al.* 1987; Hawkesworth *et al.* 1988; Piccirillo *et al.* 1989; Peate and Hawkesworth 1996; Ewart *et al.*

1998). On the other side, it has been argued that some isotopic compositions primarily reflect contributions from incompatible-element-enriched source regions in the sub-continental mantle lithosphere (Hawkesworth *et al.* 1988), though is difficult identify a simultaneous crustal contamination process. Then, the contaminant types involved in the petrogenesis of these basalts remain poorly understood, mainly in the southern part of the PIP.

Mesozoic magmatism in southern Brazil, particularly the Serra Geral Formation, has received increasing attention in the last decade through geological mapping and dating in addition to research on its lava flow stratigraphy, petrographical patterns, and geochemical signature (Waichel *et al.* 2006a, 2006b, 2012; Janasi *et al.* 2011; Lima *et al.* 2012; Barreto *et al.* 2014; Polo and Janasi 2014; Rossetti *et al.* 2014). However, the isotopic data are still scarce for this magmatism, and integrated approaches of geochemistry, modelling, and isotopic studies accompanied by stratigraphy at the local scale are rare in this region.

The flow-by-flow mapping performed in southern Brazil allowed us to achieve a finer resolution of the lava stratigraphy within a restricted region in the south hinge of Torres Syncline (TS), which constitutes a large structure oriented NW–SE located in the south Brazilian margin. This successful approach on a local scale provided information about the progressive emplacement of the lava pile, the role of pre-existing topography, and effusion rates. These factors contributed to the control of the present-day configuration of lavas along the studied area.

This study is the first attempt to record the geochemical and Sr–Pb–Nd isotopic variations of the basaltic lava flows belonging to LTi Gramado magmatism using the local-scale stratigraphy as guidelines. In addition, our work also aims (1) to discuss the petrogenesis of these lava flows within a single magma type; and (2) to qualitatively and quantitatively evaluate the role of crustal contamination in the lava flows and the potential contaminants involved.

2. Geological background

The Paraná intracratonic basin has an elliptical shape with a N–S direction covering an area of 917,000 km^2 in central–eastern South America (Frank *et al.* 2009; Figure 1). The basin includes a thick Upper Ordovician/Upper Cretaceous volcano–sedimentary succession divided into six supersequences separated by regional unconformities (Milani 1997).

The Gondwana III Supersequence covers an area of more than 1,500,000 km^2 in Brazil, Paraguay, Uruguay, and Argentina (Frank *et al.* 2009). This supersequence is

composed of Botucatu Formation (BF) aeolian sandstones at the base overlapped by the Serra Geral Formation (SGF) volcanic pile. Similar sections of aeolian sandstones and volcanic rocks are exposed in the Huab basin in NW Namibia (Jerram *et al.* 2000).

The BF and its Etendeka equivalent, Twyfelfontein Formation, consist of sets and cosets of cross-strata (Mountney *et al.* 1998; Scherer 1998) interpreted as a dry aeolian system owing to the absence of wet interdune facies (Scherer 2000, 2002). The deposits of BF reach up to 400 m thickness but are missing in some regions owing to non-deposition.

The SGF is a succession of volcanic rocks with a maximum thickness around 1700 m in the center of the basin (São Paulo state–Brazil; Almeida 1986). This unit is composed mostly of tholeiitic basalts and basaltic andesites with minor rhyolites and rhyodacites in the upper portion (Melfi *et al.* 1988). The confinement of early flows by the topography of dunes favored the formation of the ponded pahoehoe flow units (Jerram *et al.* 2009; Waichel *et al.* 2012). The pahoehoe lavas advanced over the unconsolidated sediments of the BF and generated features of interaction such as peperites and lava prints (Scherer 2002; Petry *et al.* 2007; Waichel *et al.* 2008).

The basaltic rocks of the SGF were divided into two groups based on TiO_2 content: HTi basalts (TiO_2 >2%) occurring in the north and central parts of the Paraná basin and LTi basalts (TiO_2 <2%) occurring dominantly in the southern part (Bellieni *et al*. 1984; Mantovani *et al.* 1985).

In order to examine the internal lava flow succession of the PIP as a whole and to simplify the petrogenetic modeling, Peate *et al.* (1992) defined six magma types according to their major and trace element abundances and ratios. The magma types are grouped in Gramado and Esmeralda as LTi, and in Urubici, Pitanga, Paranapanema, and Ribeira as HTi varieties. The two principal magmatic centres of the PIP can be divided into: (1) an older one in the south, comprising the Gramado, Esmeralda and Urubici magma types, and (2) a younger one, developed to the north, which is formed by the Pitanga, Paranapanema and Ribeira magma types. This paper focuses only on the lava flows of Gramado magma type, located in southern Brazil.

The TS (Figure 1) has been divided into main valley, north hinge, and south hinge, with each zone displaying distinct thickness, stratigraphy, and structural evolution (Waichel *et al.* 2012). In the south hinge, the basic lava flows from the Santa Cruz do Sul–Herveiras volcanic succession were grouped into three lithofacies associations: early compound pahoehoe, early simple pahoehoe, and late simple rubbly, which enabled the stratigraphic

reconstruction of this region (Barreto *et al.* 2014). In addition, the large amount of segregation structures and vesiculation patterns in these road profiles allowed detailed studies about petrophysical parameters such as porosity degree of these lavas (Barreto *et al.* submitted).

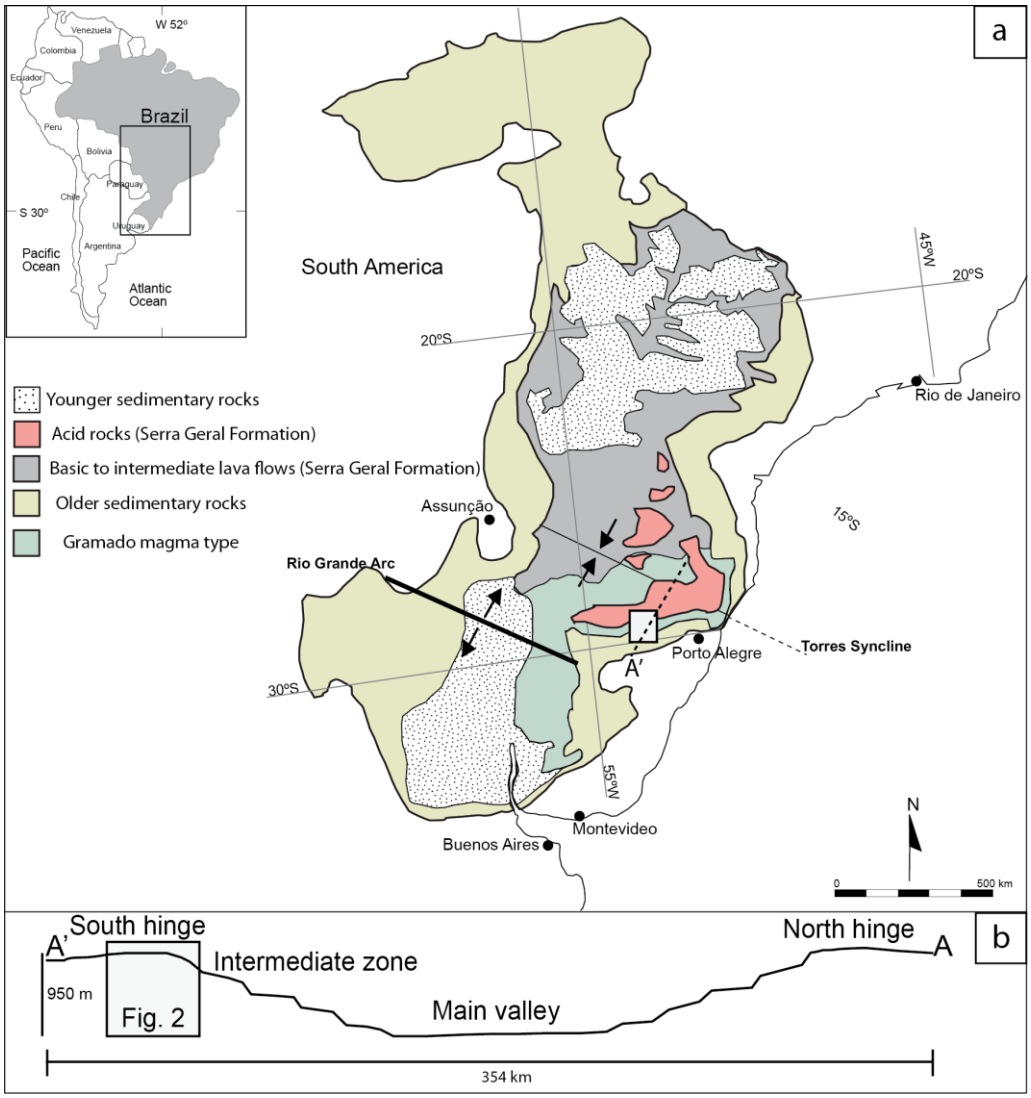

Figure 1. a) Simplified geological map of Paraná Basin, including the Torres Syncline (based on Waichel *et al.* 2012) and the location of the Gramado magma type (based on Polo & Janasi 2014); b) Sketch view of zones of the Torres Syncline with the location of the study area into the south hinge.

3. Study area and sampling

Geochemical and isotope analyses were conducted on samples collected at regular intervals of the three profiles, each of which represents a complete vertical section of the south hinge of the TS (Figure 2). The main profile is located along RSC-153 road between Santa Cruz do Sul and Herveiras (SCSH section; UTM coordinates: 342022/6728123 and 340138/6734162). Twenty-two rock samples from the base, core, and top were collected for geochemistry, nine of which were selected for Sr-Nd-Pb isotope analyses.

The second profile is located in Morro da Cruz natural park (MC section; UTM coordinates: 363241/6710664), around 50 km southeast of the main section. From this section, three samples were selected for geochemical analysis, and isotope analyses were performed in two of them.

The third profile is located near Lajeado, along BR-386 and RS-227 roads (UTM coordinates: 399230/ 6731618 and 386610/6763520), around 100 km E-NE from the SCSH section. Five samples of this profile were collected for geochemical comparisons, of which two were used for isotope determination.

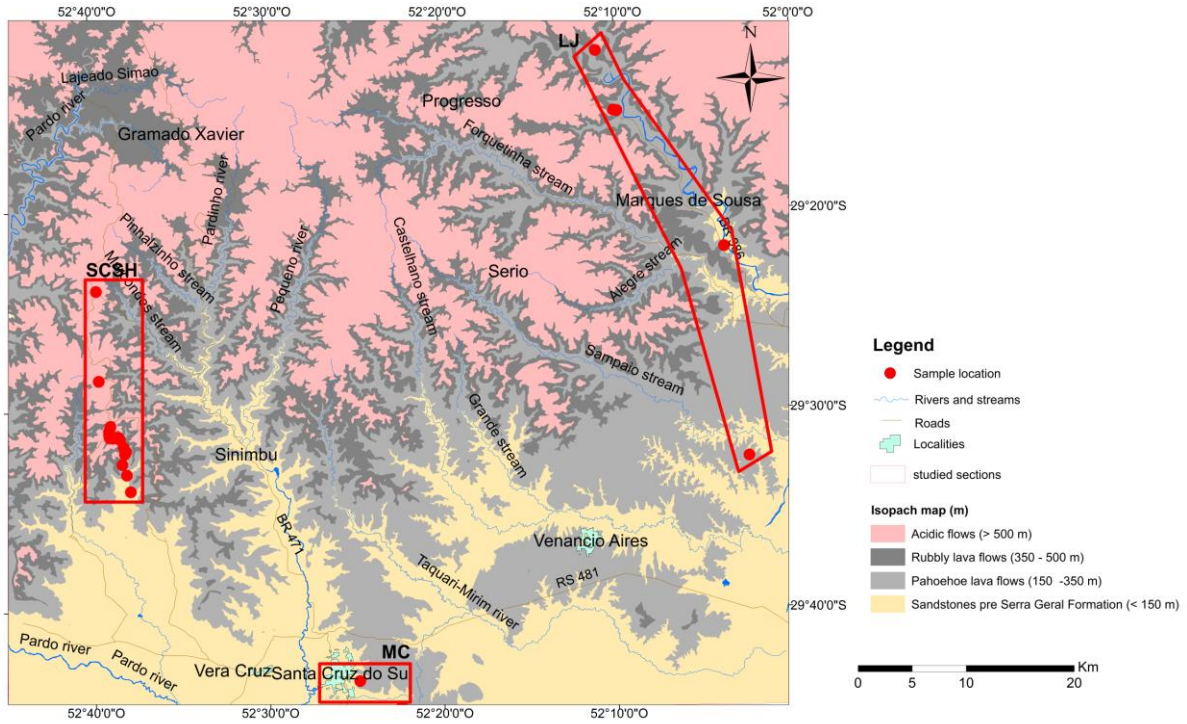

Figure 2. Geological map of south hinge of Torres Syncline with indication of the Santa Cruz do Sul-Herveiras (SCSH), Morro da Cruz (MC) and Lajeado (LJ) sections. The red dots correspond to the location of the samples investigated in the present study.

4. Analytical techniques

4.1. Geochemistry

Whole-rock chemical analyses were performed at ACME Laboratories Ltd. (Vancouver, Canada) in which the 4A+4B package was used to analyze major oxides by inductively Coupled Plasma Atomic Emission Spectrometry (ICP–AES). Trace elements and rare earth elements (REE) were analysed by inductively Coupled Plasma Atomic Mass Spectrometry (ICP–MS). The analytical protocol at ACME laboratory included the analysis of reference material STD SO-18 in addition to five sample duplicates including PSC-3D, PSC-

3L, PSC-3M, PSC-4A, and PSC-4B. The geochemical results were processed through the GeoChemical Data toolkit software version 2.3 available at http://www.gcdkit.org/download.

4.2. Sr, Nd, and Pb isotopes

The Sr, Nd, Sm, and Pb isotope analyses were conducted in the Isotope Geology Laboratory at Universidade Federal do Pará (Pará–Iso–UFPA), Belém–Brazil.

For the sample digestion procedure, ~100 mg of the rock sample was first mixed with a ^{149}Sm–^{150}Nd spike and was then dissolved with HNO_3, HCl, and HF in Teflon Savillex® bombs in a microwave oven. A two-step ion-exchange chromatography procedure was used for Pb, Sr Nd, and Sm purification. The first step consisted of loading the sample solution in Teflon columns filled with cationic resin (Biorad Dowex AG 50W-X8) using 2N HCl and 3N HNO_3 to separately collect Pb, Sr, and REEs.

In the following stage, the Nd and Sm were separated from each other and from other REEs in Teflon columns filled with Eichron® Ln resin using 0.2N and 0.3N HCl. For multi-collector ICP–MS (MC–ICP–MS) isotopic analysis of Sr, a second stage of separation with Eichron® Sr resin and 3.5N HNO_3 was applied to obtain a high-purity Sr fraction and to avoid isobaric interference of heavy REEs (HREEs; Yang *et al.* 2012). For the purification of Pb, a second step of chromatographic separation with Eichron® Sr resin and HCl (2N and 6N) was also required. The Pb was collected after elution with 3 mL of 6N HCl.

The isotopic analyses were conducted in a Thermo-Finnigan Neptune MC–ICP–MS equipped with nine Faraday collectors. Sr, Sm, and Nd fractions were previously dissolved in 2 ml of 3 HNO_3 3 wt.%. The uncertainty calculations for the Sm/Nd and $^{143}Nd/^{144}Nd$ ratios are based on repeated analyses of BCR-1 and La Jolla reference materials, respectively (Oliveira *et al.* 2008). The Sr isotopic ratios were normalized to $^{86}Sr/^{88}Sr = 0.1194$. The Nd isotopic compositions were normalized to $^{146}Nd/^{144}Nd = 0.7219$, and the decay constant used was that revised by Lugmair and Marti (1978), 6.54×10^{-12} y^{-1}. The Pb fraction was dissolved in HNO_3 3 wt.% and mixed with a solution of 50 ppb Tl for the correction of mass discrimination. More details on the experimental procedures are available in Krymsky *et al.* (2007), Oliveira *et al.* (2008), and Romero *et al.* (2013).

5. Stratigraphical framework of basaltic sequence in the south hinge of the Torres Syncline

The stratigraphic framework of the three study sections is depicted in detail in Figure 3, in which the lava flow morphologies and their stratigraphic positions are highlighted.

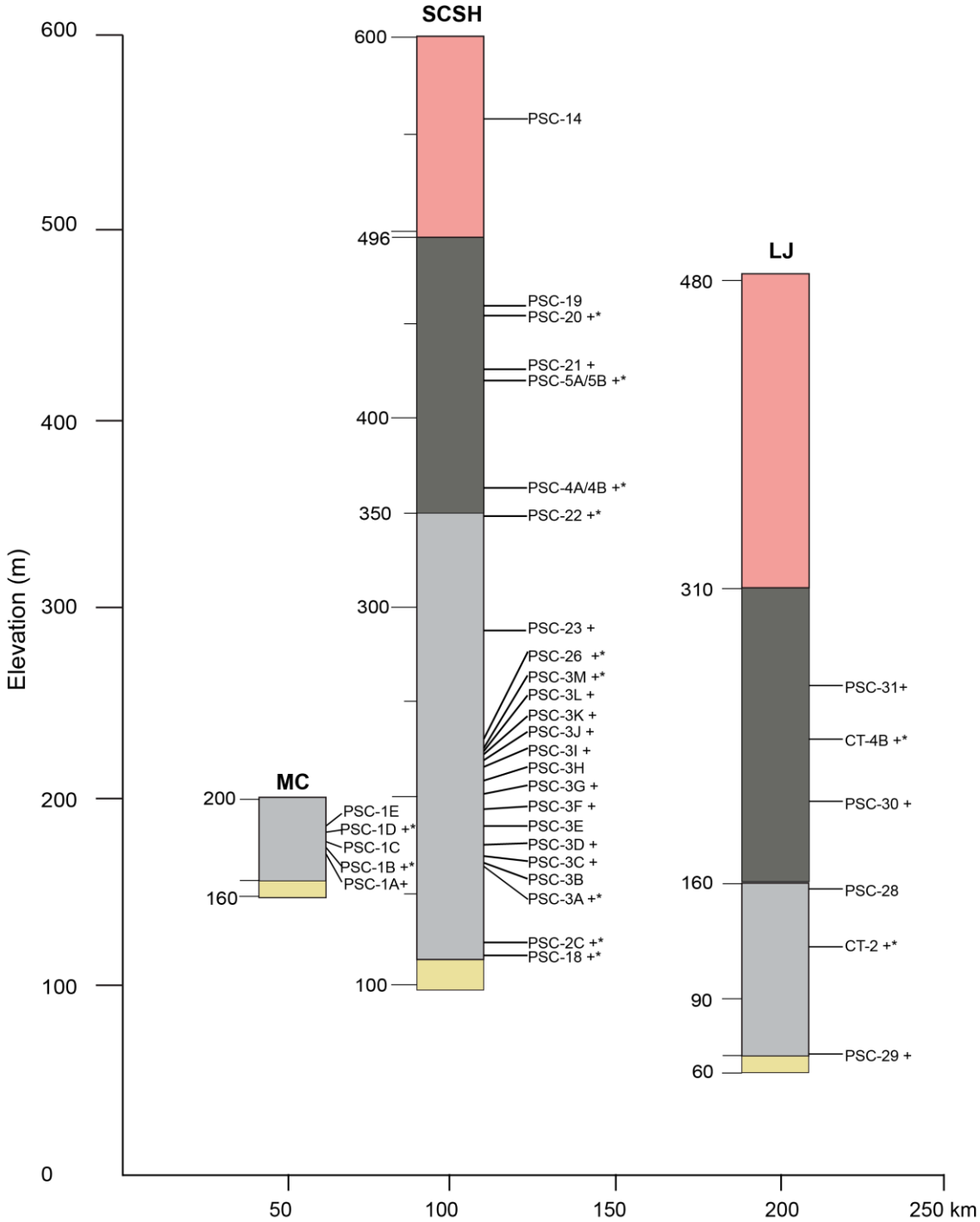

Figure 3. Stratigraphic sections projected from rectangles in Figure 2 with the approximate elevations of samples. Crosses (+) indicate samples with geochemical data and asterisks (*) indicate samples analyzed for Sr-Nd-Pb isotopes. Yellow means the sandstones pre Serra Geral Formation; light gray corresponds to the pahoehoe lava flows; dark grey means rubbly lava flows; pink corresponds to the acid lava flows.

In the SCSH section, pahoehoe and rubbly lava flows are divided by distinct lava flow morphologies based on vesiculation patterns, textures, and surface characteristics (Barreto *et al.* 2014). This ~472 m thick sequence represents a succession of basic volcanic rocks with felsic lavas in the top. The lowermost portion of the section is essentially formed by spongy (S-type) and pipe vesicle-bearing (P-type) pahoehoe lobes, representing compound lava flows (Figure 4 (a)). The S-type lobes (Walker 1989) include a large amount of millimetric vesicles. The P-type lobes (Wilmoth and Walker 1993) exhibit pipe vesicles at the base, microvesiculated massive cores, and vesiculated tops.

The compound pahoehoe lavas are overlapped in the stratigraphy by simple pahoehoe lavas that consist of laterally extensive sheet flows forming a flat topography (Figure 4 (b)). Pipe vesicles and proto-cylinders mark the basal zone. Vesicle cylinders, cylinder sheets, and horizontal vesicle sheets occur in the coarse-grained massive core. Giant vesicles and vesiculated spherical zones (pods) mark the upper crust–core interface. The upper crust of the lavas shows fining upward with a large number of millimetric vesicles at the uppermost portion and a minor number of centimetric vesicles at the lower portion. Spheroidal weathering, cooling fractures perpendicular to external crust, and smooth and ropy surfaces are common in the compound and simple lava flows.

The rubbly flows are characterized by an increase in individual flow thickness forming tabular geometries that overlap the simple pahoehoe lavas in a smooth contact (Figure 4 (c)). Spherical and irregular vesicles occur in the basal zone. The massive core displays a horizontal and vertical jointing pattern with conchoidal and curvilinear cooling fractures. Contorted and stretched giant vesicles are sparsely distributed in the upper half of the core. The rubbly top consists of highly oxidized breccias and sub-rounded to sub-angular vesiculated fragments encompassed by a red/brown very fine matrix. The vesicles within the fragments range from spherical to elongated with different orientations.

Paleosols are not present in the SCSH section, although discontinuous thin sheets of sandstone between pahoehoe and rubbly lava flows and dykes are common. At the top of the volcanic succession, rubbly flows are superimposed by thick (>50 m) felsic sequences that exhibit horizontal and vertical jointing.

SCSH and LJ sections show several similarities. The latter section is represented by a 410 m thick volcanic rock sequence, where S- and P-type pahoehoe lobes are surrounded by a thin, glassy surface with ropy features (Figure 4 (d)). The simple pahoehoe lava flows show pipe vesicles in the base and vesicle cylinders and vesicle sheets in the core. These pahoehoe

lavas are overlapped in the stratigraphy by rubbly lava flows that exhibit blocky and oxidized portions as well as conchoidal fracturing patterns (Figure 4 (e)).

The sequence of the MC is represented by 20 m thick pahoehoe lava flows with ponded morphology in contact with the BF sandstones. The ponded pahoehoe basalts are confined by paleotopography and fill the interdune areas. The features of this interaction without erosion include wave marks in the paleodune surfaces, peperitic breccias, and intertraps (Figure 4 (f)). Vesiculated pahoehoe lobes characterize the base of the MC volcanic succession. These lobes are superimposed by thicker ponded pahoehoe lava flows up to 8 m thick that display massive aspect and irregular columnar disjunctions (Figure 4 (g)).

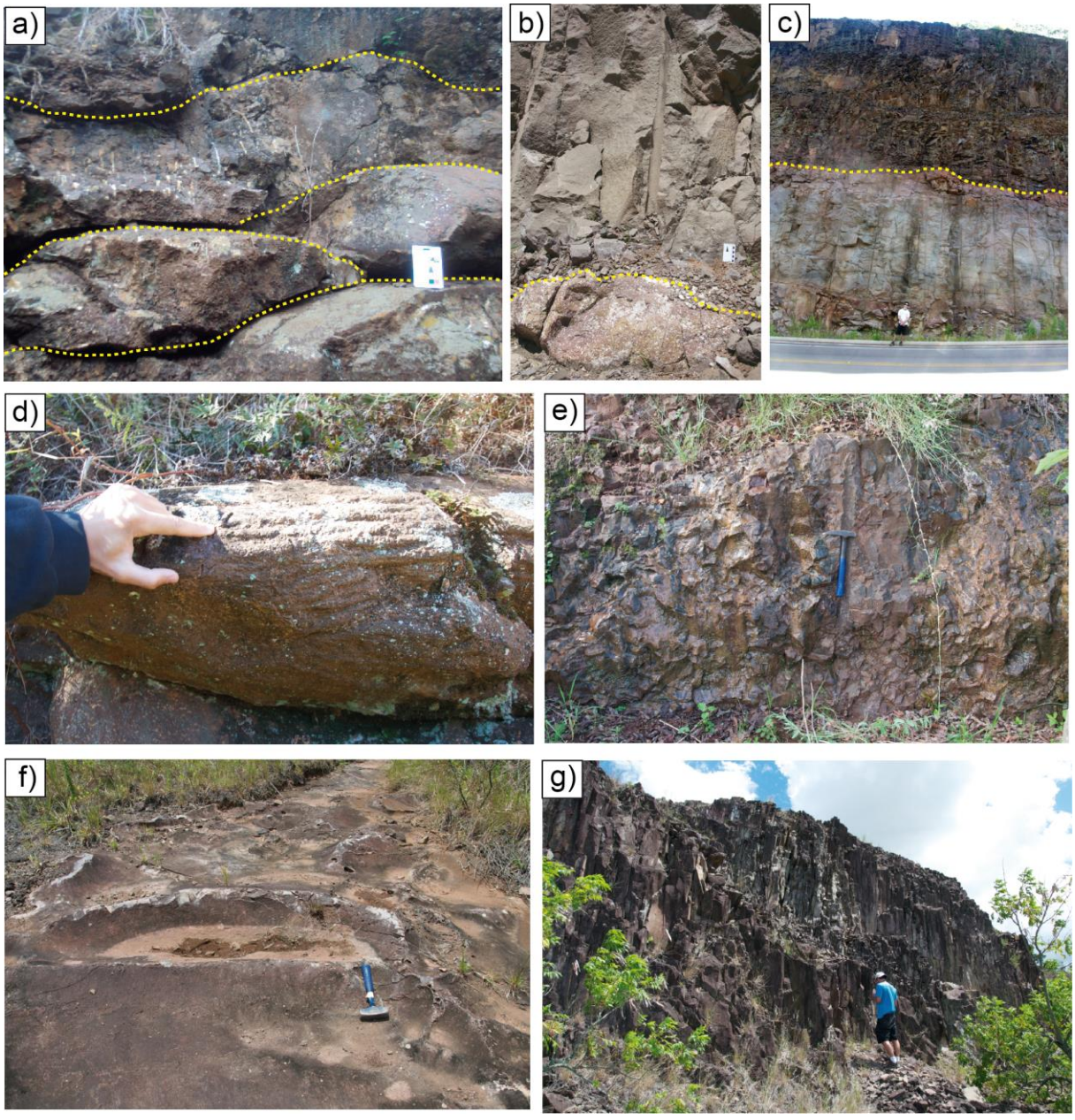

Figure 4. Field photographs of the SCSH, MC and LJ sections. a) S- and P-type pahoehoe lobes in the SCSH section; b) Compound pahoehoe lava flows overlapped by simple pahoehoe lava flows in the SCSH section; c) Simple pahoehoe lava flows overlapped by thicker rubbly lava flows in the SCSH section; d) Pahoehoe lava flows of LJ section with ropy surfaces; e) Oxidized and blocky portions of rubbly lava flows in the LJ section; f) Wave marks in the 'paleodunes' surface in the MC section; g) Ponded pahoehoe lava flows with massive aspect and irregular columnar disjunctions in the MC section.

6. Petrography

Plagioclase, augite, opaque minerals, and apatite constitute the primary mineralogy of the pahoehoe and rubbly lava flows. Olivine crystals highly altered to bowlingite and iddingsite are restricted to early pahoehoe lobes at the bases of the three sections.

The ponded pahoehoe lava flows in the MC section exhibit porphyritic, glomeroporphyritic, intersertal, vesicular, and corona textures. However, the aphanitic, hypocrystalline, aphyric, intersertal, vesicular, and amygdaloidal textures are predominant at the base and top of compound and simple pahoehoe lavas in the SCSH and LJ sections. The vesicles are rounded by celadonite and are filled by zeolite, carbonate, chalcedony, and quartz aggregates. Most of the plagioclase crystals are replaced by albite and zeolite. The cores of the pahoehoe flows show holocrystalline, aphyric, subophitic, intergranular, and diktytaxitic textures.

The cores of the rubbly lavas in the SCSH section are aphanitic, hypocrystalline and aphyric with intersertal and diktytaxitic textures. Anhedral grains of opaque phases are scattered throughout the groundmass. Vesicular fragments of hypocrystalline basalt with plagioclase microlites constitute the rubbly flow-top breccias. The spherical and irregular vesicles that occur within the fragments are partly filled by zeolite. The inter-fragment spaces are mainly cemented by zeolite and quartz, whereas the matrix is an admixture of fine-grained rock flour and altered glass.

7. Whole-rock geochemistry of the lavas

The chemical compositions of 22 samples of the SCSH section, in addition to 5 samples from the LJ section and 3 from the MC section are listed in Supplementary Table 1 and illustrated in Figures 5–9. The figures also include fields of the previously analyzed Gramado magma for comparison.

According to the observed morphology, mineralogy, and texture of the SCSH section, the sample set was divided into pahoehoe and rubbly lava flows. This divison emphasizes some of the general stratigraphic variations and simplifies the subsequent discussions.

The pahoehoe lava group from SCSH is characterized by SiO_2 contents of 47–56 wt.%, which is the same range as that of the rubbly lavas at 50–56 wt.%. Rubbly lava flow samples exhibit lower MgO content at 3.06–3.11 wt.% than the contents of MgO in the pahoehoe lava samples at 3.31–7.30 wt.%. The K_2O and Ba contents of the rubbly lava flow samples, at 0.79–2.19 wt.% and 278–404 ppm, respectively, are in the same range than those of the pahoehoe lava samples, at 0.45–2.76 wt.% and 213–621 ppm, respectively.

The samples of LJ section show major and trace element values within the range of SCSH section rocks such as SiO_2 at 47–53 wt.%, MgO at 4.00–6.62 wt.%, Ba at 260–442 ppm, and K_2O at 0.5–1.35 wt.%. However, the samples from the MC section exhibit higher values of SiO_2 at 55–58 wt.%, Ba at 521–662 ppm, and K_2O at 2.62–3.34 wt.%; the MgO values are lower at 2.39–2.83 wt.%. The entire set of analyzed rocks from the three sections exhibit TiO_2 contents from 1.05 to 2.11 wt.% and Ti/Y ratios from 208 to 382. These results confirm that all the samples belong to the LTi basalt series of Gramado magma type (Piccirillo and Melfi 1988; Peate *et al.* 1992).

Most basaltic lava flows of the three sections exhibit CIPW normative quartz from 1.46 to 15.72 wt.% and hypersthene from 5.50 to 21.08 wt.%. These basalts are classified as quartz tholeiites, in which the MC section samples exhibit the highest values of normative quartz. Three samples of SCSH, including PSC-3C, PSC-3F, and PSC-3L, and one sample of the LJ section, PSC-29, display normative hypersthene from 5.50 to 17.36 and olivine from 2.32 to 9.69 wt.% and are classified as olivine tholeiites. The Mg-numbers [Mg# = 100 × MgO/(MgO + FeO)] range from 23 to 49, where FeO = Fe_2O_3 x 0.89981.

In the total alkali–silica (TAS) classification diagram (LeBas and Streckeisen 1986; Figure 5 (a)), the pahoehoe lavas of the SCSH section plot in the basalt and basaltic andesite fields. Four of five rubbly lavas of the SCSH plot in the basaltic andesite field, with the exception of PSC-21, located in the basaltic field. The lavas from LJ section also plot in the basaltic andesite field, except PSC-29 sample located in the basaltic field. The ponded pahoehoe lavas of the MC section plot in the andesitic field. In the AFM diagram (Irvine and Baragar 1971), most of the samples exhibit a trend with tholeiitic affinity, except for PSC-3F, PSC-18, and PSC-26 pahoehoe lavas of the SCSH section and CT-2 of the LJ section, which plot into calc–alkaline field (Figure 5 (b)).

Table 1. Major and trace element data for selected basic lavas from Santa Cruz do Sul-Herveiras, Morro da Cruz and Lajeado sections.

Section	Santa Cruz do Sul-Herveiras																					Morro da Cruz						Lajeado			
Lava flow type	pahoehoe																				rubbly	ponded pahoehoe						pahoehoe			rubbly
Sample	PSC2C	PSC3A	PSC3C	PSC3D	PSC3F	PSC3G	PSC3I	PSC3J	PSC3K	PSC3L	PSC3M	PSC18	PSC22	PSC23	PSC26	PSC27	PSC28	PSC4A	PSC4B	PSC5B	PSC20	PSC21	PSC1A	PSC1B	PSC1D	PSC29	PSC30	PSC31	CT2	CT4B
Major elements																														
SiO_2	49.45	50.4	46.7	48.83	49.05	50.39	52.34	49.51	50.02	48.19	49.48	52.95	51.21	47.97	53.2	50.3	56.41	55.96	55.46	53.83	52.22	50.16	55.01	58.35	57.83	46.97	52.76	51.6	51.65	52.61
TiO_2	1.07	1.19	1.11	2.11	1.13	1.77	1.2	1.44	1.39	1.13	1.34	1.38	1.17	1.05	1.14	1.44	1.41	1.55	1.56	1.41	1.47	1.4	1.47	1.31	1.36	0.98	1.4	1.04	0.95	1.03
Al_2O_3	15.39	14.91	15.22	12.72	14.01	13.4	14.00	15.4	14.42	14.36	15.63	16.17	16.35	15.65	14.88	15.34	14.82	12.9	12.97	13.54	14.24	14.39	14.84	13.68	14.05	15.5	13.31	14.19	13.33	14.09
$Fe_2O_{3(t)}$	11.72	11.07	10.89	13.34	10.51	12.83	10.83	12.51	12.08	10.97	12.37	10.35	10.27	10.97	10.68	11.67	10.85	13.66	13.69	13.03	13.09	13.03	10.81	10.51	10.23	10.56	13.1	12.2	10.08	11.88
MnO	0.16	0.17	0.17	0.21	0.15	0.18	0.14	0.17	0.14	0.14	0.17	0.15	0.15	0.2	0.17	0.18	0.16	0.18	0.19	0.17	0.2	0.18	0.09	0.13	0.14	0.17	0.18	0.18	0.14	0.19
MgO	5.96	6.37	7.3	6.28	6.4	5.14	3.94	4.79	4.38	6.87	5.58	4.58	5.12	6.6	5.45	4.04	3.31	3.06	3.11	4.37	4.77	5.48	2.39	2.92	2.83	6.62	4.00	5.66	4.88	5.73
CaO	10.42	10.48	10.74	8.17	7.81	8.63	7.12	8.63	7.46	9.3	9.29	8.46	9.55	10.63	8.91	8.39	7.09	6.57	6.57	8.04	8.63	9.34	2.74	6.2	5.8	10.08	8.04	8.98	7.46	9.32
Na2O	2.09	2.07	1.9	2.1	3.92	2.25	2.41	2.2	2.81	2.51	2.07	2.4	2.27	1.76	2.21	1.82	2.24	2.64	2.57	2.59	2.53	2.33	2.55	2.43	2.24	2.16	2.00	2.31	3.15	2.24
K2O	0.85	1.12	0.93	1.77	1.01	1.00	1.42	1.95	1.97	1.16	1.6	1.84	1.28	0.45	1.92	0.82	2.76	2.11	2.19	1.79	1.17	0.79	3.34	2.67	2.62	1.25	0.82	1.35	0.5	0.79
P_2O_5	0.15	0.21	0.2	0.37	0.21	0.33	0.18	0.19	0.18	0.2	0.18	0.19	0.21	0.15	0.17	0.22	0.21	0.21	0.2	0.19	0.2	0.18	0.21	0.2	0.17	0.11	0.17	0.12	0.15	0.12
LOI	2.5	1.7	4.6	3.8	5.5	3.8	6.2	3.0	4.9	4.9	2.1	1.3	2.2	4.4	1.1	5.5	0.5	0.9	1.3	0.8	1.2	2.5	6.3	1.3	2.5	5.4	3.9	2.2	7.4	1.7
Total	99.79	99.75	99.8	99.68	99.76	99.74	99.77	99.78	99.79	99.79	99.8	99.78	99.78	99.82	99.80	99.78	99.77	99.74	99.76	99.76	99.77	99.78	99.76	99.75	99.77	99.83	99.74	99.8	99.75	99.76
Fe_2O_3/MgO	1.77	1.56	1.34	1.91	1.48	2.24	2.47	2.35	2.48	1.44	1.99	2.03	1.80	1.49	1.76	2.60	2.95	4.01	3.96	2.68	2.47	2.14	4.07	3.24	3.25	1.43	2.94	1.94	1.86	1.86
Minor elements																														
Ba	350	420	301	621	524	380	341	320	326	279	282	406	396	213	358	319	512	381	404	315	330	278	662	521	533	285	326	260	442	263
Co	40.9	43.5	39	39.7	36.4	32.9	38.9	43.3	40.3	37.2	40.7	31.5	33	41.9	38.1	29.6	25.8	40.1	39.1	36.6	36.7	36.3	25.7	28.5	29.4	42.6	39	43.8	32.3	49.3
Ni	44.5	55.4	63.8	47.5	70.9	23.5	34.3	28.3	24.7	54.7	21.9	26.7	9	46.4	23.4	4.4	8.3	10.2	7.2	19.4	8.8	12.2	15.0	12.5	11.2	105.2	2.8	19.6	48.3	-
Sc	35	36	35	36	34	36	33	36	36	37	37	31	31	34	32	31	30	33	33	34	34	36	31	30	30	34	34	37	31	39
Rb	49.3	32.1	38.9	45.5	19.4	18.4	38.5	63.8	71.8	48.1	35.2	49.8	28.6	15.2	73.2	17.3	75.5	75.7	81.3	68	41.5	13.8	93.3	89.7	85.7	23.2	21.6	32.3	14.7	32.1
Sr	258.2	355.8	304.6	336.3	528.3	390.1	465.5	221.3	235.6	337.4	206.6	239	294.3	246	211	273.4	204.4	207.7	214.6	207.9	225.7	230.2	155.0	204.1	180.1	159.3	420.3	219.2	598.9	255.4
Ta	0.5	0.7	0.7	1.1	0.6	1.2	0.5	0.9	0.4	0.7	0.5	0.7	0.6	0.4	0.6	0.9	0.8	0.8	0.8	0.6	0.5	0.5	0.9	0.8	0.9	0.5	1.2	0.4	1.4	0.5
Nb	6.6	13.4	10	22.6	10.8	17.2	9	8.8	7.6	10.6	7.4	11.7	7.4	6.3	8.7	13.7	12.1	12.3	12.9	10.5	9.4	8.9	15.0	16.2	17.1	5.6	12.1	7.7	7.1	6.6
Th	3.6	2.9	2.3	5.2	2.2	4.5	4.1	5.1	4.2	2.7	4.5	7.2	4.5	3.4	5.9	11.2	11.1	7.4	7.1	5.8	5.7	4.6	11.5	10.8	10.4	3.8	7.2	3.6	3.7	4
U	0.6	0.7	0.3	0.8	0.5	0.7	1.2	1.2	0.9	0.4	1	0.4	1.3	0.7	1.1	1.2	1.1	1.8	1.4	1.6	1.5	1	1.5	1.1	1.2	0.5	1.5	0.7	0.3	0.7
Zr	115	131.5	107.5	221.2	112.3	188.8	116.6	140.5	133.7	119.3	124.2	174.4	139.1	114.3	144.3	226.3	218.3	170.9	168.5	136.6	147.7	128.7	234.6	217.0	218.3	94.4	162.5	98.8	103.4	112.9
Y	30.8	23.1	18.4	33.1	18.3	28.2	21.3	26.7	23.8	21	23.6	28.1	23.8	21.3	24.3	35.6	32.1	31.7	31.1	27.5	29	27.3	34.5	34.4	32.9	19.4	33.4	20.1	18.5	23.5
Pb	2.6	1.8	3.4	4.2	3.4	4.9	3.2	2.8	2.4	5.2	3.2	2.8	5.5	5	1.9	14	3.7	2.6	2.9	3.2	3.1	3.7	5.4	4.2	4.7	2.9	7.8	2	6.6	3.4
Hf	3.8	3.2	2.6	5.4	3.1	4.8	3.1	3.3	3.2	3.3	3.2	4.4	3.4	2.9	4.1	6	5.5	4.7	4.8	3.9	4.1	3	6.6	6.2	5.4	2.6	4	2.6	3.1	2.7
Ga	18	22	17.3	23.4	12.4	17.1	20	19.3	17.7	16.6	17.6	18	17.6	16.7	16.8	21.5	17.5	22.8	23.2	21.8	20	18.6	19.6	24.1	24.0	13.8	21.1	18.5	12.9	19.3
Cs	2.5	0.8	1.8	1.4	2.5	0.3	1	1.1	1.6	2.9	0.8	0.3	0.7	0.4	2.2	0.4	0.8	2.4	2.7	2.6	1.9	1.1	0.6	0.9	1.0	0.5	2.1	0.7	0.7	1.7
La	24.7	22.3	18.6	34.5	19.5	28.8	17.9	21	19.6	20.2	18.9	30.2	22.9	17.6	22	39.4	37.9	26.4	26.7	21.6	23.1	19.7	41.9	34.3	35.0	15	27.1	14.9	14.7	16.7
Ce	41.4	46.7	36.2	73.1	36.9	58.2	36.2	43.8	39.8	37.6	38.5	56.8	45.7	35.3	46.2	79.7	76.7	56.1	54.7	41.9	46	40.8	80.3	73.8	74.9	29.4	56.9	32.3	31.3	34.8
Pr	6.24	5.44	4.6	8.7	4.56	7.23	4.67	5.37	4.97	4.94	4.99	6.95	5.67	4.36	5.84	9.33	9.0	6.82	6.8	5.42	5.69	5.03	10.15	8.89	8.82	3.72	6.73	3.83	4.1	4.27
Nd	27.8	21.5	18	34.8	20.3	29.4	18.7	23.7	21.3	19.2	18.9	29.6	25.6	17.1	25.4	37.9	35.7	28.8	27.9	22.4	22	19.8	39.8	34.1	32.8	14.8	25.3	13.9	17.8	16
Sm	5.53	4.65	3.84	6.9	4.08	6.06	4.28	4.64	4.7	3.91	4.35	5.77	5	3.93	4.82	7.31	6.79	6.01	5.88	4.83	4.96	4.79	7.94	6.94	6.46	3.17	5.89	3.64	3.78	4.06
Eu	1.61	1.37	1.21	1.81	1.16	1.58	1.16	1.29	1.3	1.28	1.2	1.56	1.37	1.16	1.33	1.71	1.68	1.57	1.53	1.28	1.49	1.35	1.74	1.65	1.59	1	1.39	1.09	1.06	1.19
Gd	6.32	4.53	3.76	6.72	3.96	5.99	4.06	4.94	5.15	4.34	4.76	5.79	5.21	4.45	5.41	7.57	7.12	6.1	6.05	5.14	5.61	4.88	8.03	6.42	6.49	4.05	6.41	4.2	3.85	4.54
Tb	0.91	0.7	0.55	1.05	0.57	0.86	0.66	0.75	0.76	0.62	0.68	0.88	0.69	0.61	0.77	1.06	1.03	0.97	1	0.85	0.84	0.76	1.06	1.01	0.99	0.59	1.04	0.65	0.61	0.75
Dy	5.94	4.13	3.77	5.98	3.51	5.79	4.02	4.24	4.39	3.68	4.54	5.51	4.37	4.06	4.45	6.9	6.36	5.51	5.34	5.56	5.68	4.66	6.26	5.98	5.69	3.42	5.76	3.8	3.96	3.86
Ho	1.13	0.81	0.77	1.24	0.62	1.12	0.83	0.96	0.87	0.71	0.84	1.25	0.87	0.77	0.92	1.34	1.27	0.95	1.22	1.08	1.07	0.93	1.45	1.15	1.25	0.67	1.23	0.83	0.77	0.84
Er	3.17	2.23	1.99	3.18	1.68	3.05	2.07	2.4	2.69	2.21	2.36	3.17	2.37	2.23	2.55	3.64	3.5	3.14	3.19	3.34	2.73	2.88	3.77	3.27	3.17	2.25	3.35	2.1	2.18	2.53
Tm	0.44	0.35	0.28	0.53	0.32	0.45	0.32	0.33	0.36	0.3	0.36	0.45	0.33	0.31	0.38	0.49	0.48	0.47	0.44	0.41	0.43	0.38	0.55	0.52	0.48	0.32	0.51	0.34	0.31	0.35
Yb	2.78	2.12	1.68	3.07	1.82	2.63	2.28	2.37	2.56	2.04	2.43	2.81	2.56	2.03	2.45	3.57	3.64	3.38	2.75	2.92	2.92	2.55	3.31	3.26	3.36	2.06	3.34	2.32	1.99	2.28
Lu	0.43	0.34	0.27	0.47	0.31	0.44	0.31	0.41	0.37	0.3	0.31	0.42	0.38	0.28	0.39	0.53	0.49	0.47	0.44	0.42	0.41	0.37	0.5	0.49	0.44	0.29	0.45	0.33	0.3	0.31
*Q	2.11	2.73	-	3.16	-	7.14	10.9	1.96	2.35	-	1.46	6.33	4.7	2.9	5.43	11.05	11.4	11.23	10.74	6.6	5.72	3.98	15.72	15.21	13.05	-	12.8	3.82	8.25	6.77
*Hy	19.42	18.17	15.97	19.97	5.5	17.77	16.09	18.45	16.88	17.36	20.23	15.4	16.5	21.08	17.06	17.73	13.35	15.9	16.13	16.91	18.35	19.87	15.43	12.33	16.68	12.63	18.1	20.09	16.63	19.79
*Ol	-	-	3.73	-	9.69	-	-	-	-	2.32	-	-	-	-	-	-	-	-	-	-	-	-	-	-	-	5.26	-	-	-	-

* CIPW normative quartz (Q), olivine (Ol), hypersthene (Hy) and atomic Mg/Mg+Fe^{2+} (mg). All Fe expressed as Fe_2O_3

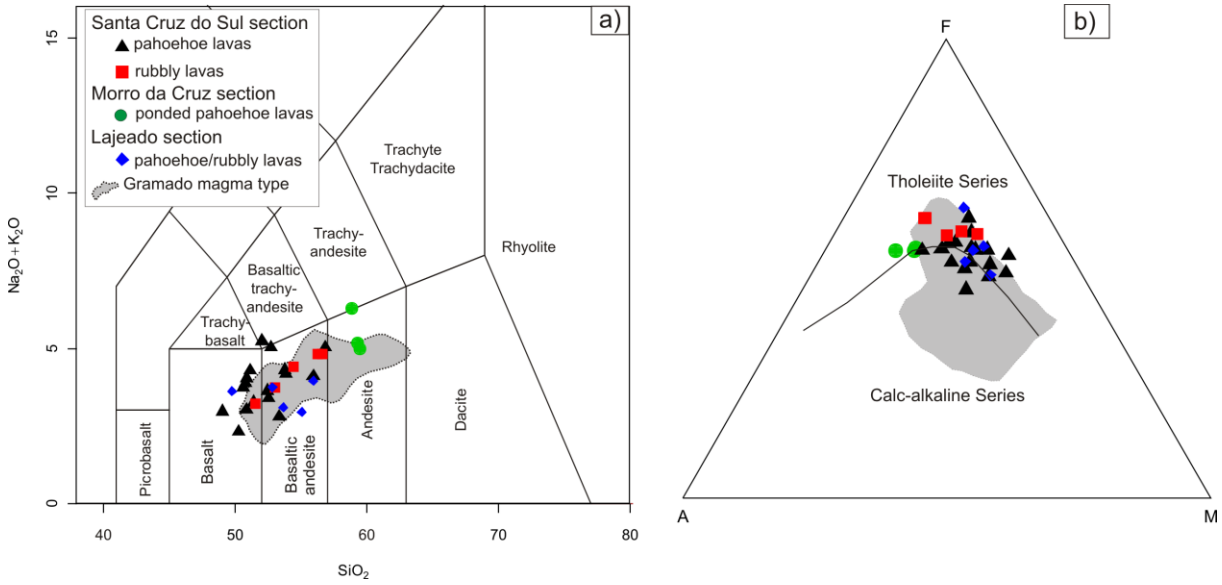

Figure 5. a) Total alkalis versus silica classification diagram of Le Bas *et al.* (1986) showing the lava flows of the three sections from this study, including the field ascribed for the previously analyzed Gramado magma (Mantovani *et al.* 1985; Peate and Hawkesworth 1996); b) AFM diagram (Irvine and Baragar 1971) showing the tholeiitic affinity of this magmatism.

In the bivariate diagrams for major elements, the CaO exhibit a positive correlation trend with an increase of MgO index, while the Al_2O_3 show more scaterred concentrations with this same differentiation index (Figures 6 (a-b)). Although with some scatter SiO_2, TiO_2, and K_2O display good correlation trends that increase with decreasing MgO (Figures 6 (c-f)). On the other side, Na_2O, Fe_2O_{3t} and P_2O_5 values remain nearly constant during decreasing MgO. The MC samples generally plot at the end of the trends defined by the rocks of other sections in the bivariate diagrams because of their lowest MgO associated to the highest SiO_2 and K_2O and lowest CaO.

The lava flows of the three sections show roughly positive correlations of Ni and Co against MgO (Figures 7 (a-b)). Most samples display scattered Sr behavior except for some pahoehoe samples that show decrease with increasing MgO (Figure 7 (c)). The more immobile high field strength elements (HFSE) such as Zr, Y, and Nb (Figures 7 (d-f)) and the much more mobile large ion lithophile elements (LILE) such as Ba, Rb, Th, and U (Figures 7 (g-j)) roughly increase with decreasing MgO. The various petrographic groups from the three sampling localities cannot be distinguished on the basis of the trace element contents. However, the samples of the MC section exhibit higher values of Zr, Ba, Rb and Th when compared with the rocks of other sections.

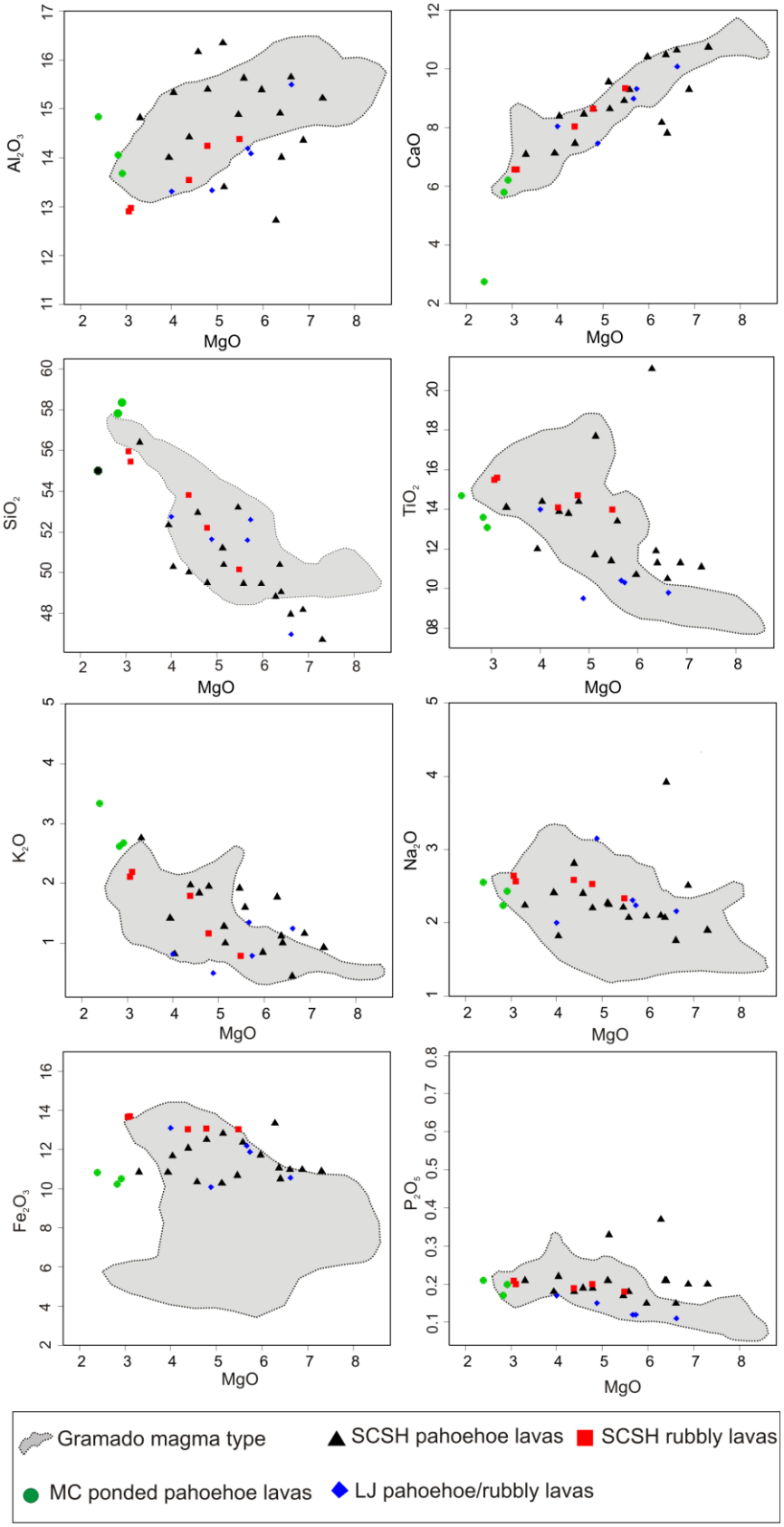

Figure 6. Major element variation diagrams for studied lava flows that include the fields attributed for the previously analyzed Gramado magma (Peate *et al.* 1992). SCSH – Santa Cruz do Sul-Herveiras section; MC – Morro da Cruz section; LJ – Lajeado section.

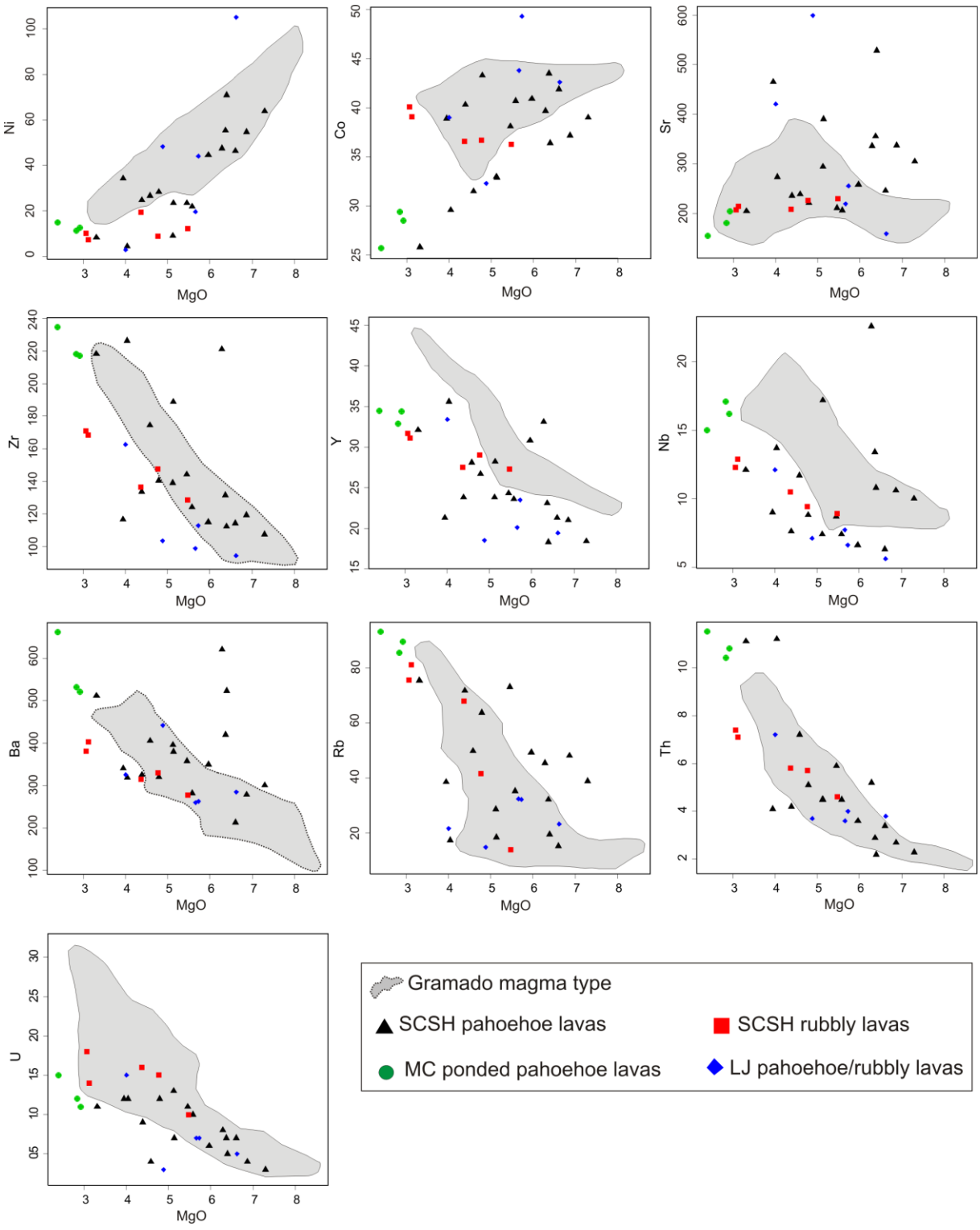

Figure 7. Trace element variation diagrams including the fields for the previously analyzed Gramado magma (Peate *et al.* 1992).

The chondrite-normalized incompatible element patterns (Thompson 1982) are reported in Figure 8. The analyzed samples show enrichment in Rb, Ba, Th, and K elements and depletion in Nb, Ta and P, in addition to variable Sr anomalies that range from negative to positive depending on plagioclase removal or accumulation. The pattern of the analyzed samples is broadly similar to those previously analyzed lavas of the Gramado type fit the field of Gramado magma, though some samples of SCSH and LJ sections exhibit Nb and Ta values below of the Gramado type field. All incompatible element patterns of the SCSH samples show a parallel behavior regarding the fractionation degree of the lavas towards the basaltic andesites, while the LJ samples exhibit the lowest values for most of the elements and the MC samples display the highest ones. All the studied samples exhibit depleted patterns for most of the incompatible elements when compared to Urubici magma, except for Rb, Th and K.

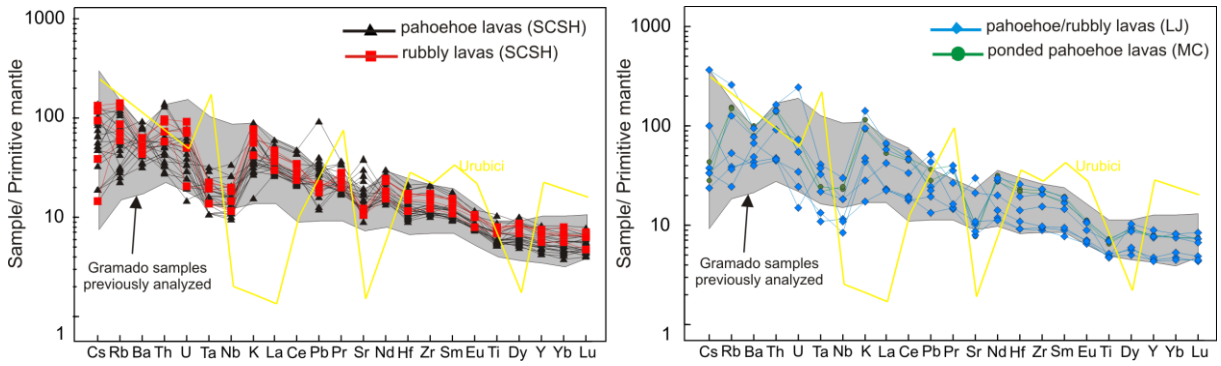

Figure 8. Primitive mantle-normalized incompatible element diagram (McDonough and Sun 1995) comparing the samples of SCSH, LJ and MC sections with the field attributed to Gramado magma (Peate *et al.* 1992). An average value of Urubici magma was inserted for comparison.

Chondrite CI-normalized REE patterns (Boynton 1984) of the three sections are parallel to each other (Figure 9), which reflect an increasing of differentiation degree of the LJ samples with the lowest values, SCSH samples with intermediate values towards the MC samples with higher contents of REE. All samples are enriched in light REE [$(La/Sm)_N$ = 2.45–3.51] relative to heavy REE [$(Gd/Yb)_N$ = 1.42–1.96], with low REE fractionation [$(La/Yb)_N$ = 4.33–8.53] and weak to more pronounced negative Eu anomalies (Eu/Eu* = 0.66–0.96). The studied basalts show depleted REE values in comparison with previously analyzed Urubici magma, except for the LREE La and Ce; and the HREE Tm, Yb and Lu.

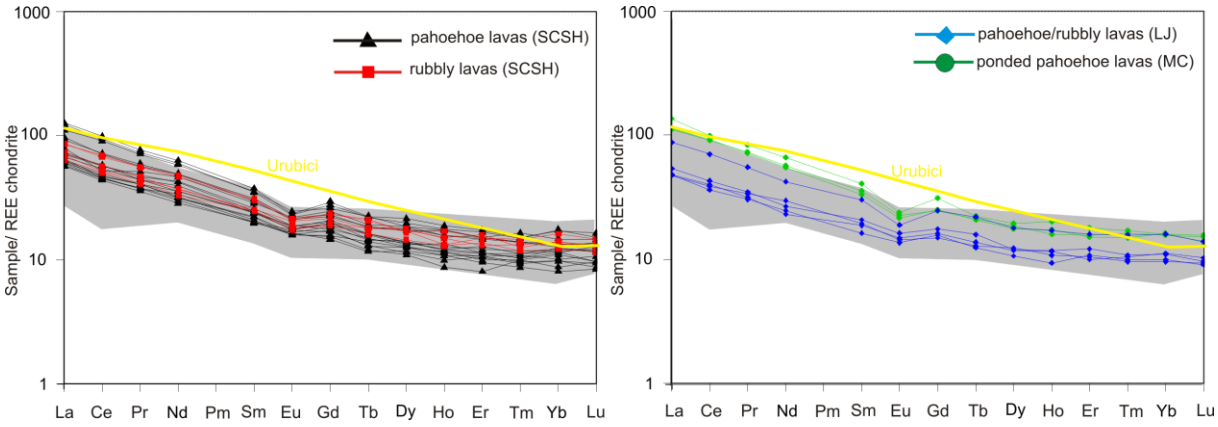

Figure 9. Chondrite-normalized rare earth element patterns (Boynton 1984) for lava flows of the SCSH, LJ and MC sections compared to field ascribed to Gramado magma. An average REE pattern of Urubici magma was inserted for comparison.

8. Isotope geochemistry

The Sr, Nd, and Pb isotope analyses are shown in Supplementary Table 2 and Figures 10 and 11. These figures also include the fields of regional HTi (Pitanga, Paranapanema, Urubici) and LTi (Gramado and Esmeralda) magmas of the PIP (Mantovani *et al.* 1985; Hawkesworth *et al.* 1986; Petrini *et al*. 1987; Piccirillo *et al.* 1989; Peate *et al.* 1992, 1999; Peate and Hawkesworth 1996; Rocha-Júnior *et al.* 2013). Based on published Ar–Ar ages for Paraná basalts (e.g., Renne *et al.* 1992; Thiede and Vasconcelos 2010) and U–Pb ages for Paraná felsic rocks (Janasi *et al.* 2011), the initial $^{87}Sr/^{86}Sr$ and $^{143}Nd/^{144}Nd$ ratios were re-calculated to an average age of 132 Ma.

The pahoehoe and rubbly basalts of the SCSH show initial $^{87}Sr/^{86}Sr$ ratios ranging from 0.707798 to 0.712962 and $\varepsilon_{Nd(132)}$ values ranging from −8.36 to −5.41 ($^{143}Nd/^{144}Nd_i$ = 0.512045–0.512194). The LJ samples display nearly uniform initial $^{87}Sr/^{86}Sr$ ratios of 0.710396 and 0.710575 with corresponding $\varepsilon_{Nd(132)}$ values ranging from −8.36 to −6.75 ($^{143}Nd/^{144}Nd_i$ = 0.512042 and 0.512125). Conversely, the ponded pahoehoe lavas from the MC section exhibit higher initial $^{87}Sr/^{86}Sr_i$ ratios at 0.715629–0.715751 than those in other sections as well as $\varepsilon_{Nd(132)}$ values ranging of −8.20 and −8.08 ($^{143}Nd/^{144}Nd_i$ = 0.512051-0.512057).

The investigated rocks from the SCSH section show present-day Pb isotope compositions of 18.42–18.87 for $^{206}Pb/^{204}Pb$, 15.65–15.70 for $^{207}Pb/^{204}Pb$, and 38.62 and 39.29 for $^{208}Pb/^{204}Pb$. The lava flows of the LJ section display Pb isotope data whithin the range of those of the SCSH section. The ratios are 18.47–18.61 for $^{206}Pb/^{204}Pb$, 15.65–15.66

for $^{207}Pb/^{204}Pb$, and 38.83 and 38.85 for $^{208}Pb/^{204}Pb$. The ponded pahoehoe lavas of the MC section exhibit values of 18.55 and 18.56 for $^{206}Pb/^{204}Pb$ and 15.70 and 15.71 for $^{207}Pb/^{204}Pb$ ratios within the intervals of the other sections, although the $^{208}Pb/^{204}Pb$ ratios are higher at 39.34 and 39.37.

Table 2. Isotopic compositions of Sr, Nd, and Pb in basalt samples of the Serra Geral Formation in the south hinge of Torres Syncline.

Sample No.	Basalt type	$(^{87}Sr/^{86}Sr)$	2σ	$(^{87}Sr/^{86}Sr)i$	$(^{147}Sm/^{144}Nd)$	σ	$(^{143}Nd/^{144}Nd)$	σ	$(^{143}Nd/^{144}Nd)i$	$\varepsilon_{Nd(0)}$	$\varepsilon_{Nd(132)}$	T_{DM} (Ma)	$(^{206}Pb/^{204}Pb)$	2σ	$(^{207}Pb/^{204}Pb)$	2σ	$(^{208}Pb/^{204}Pb)$	2σ
Santa Cruz do Sul-Herveiras section																		
PSC-20	rubbly	0.711125	0.000022	0.710127	0.1334	0.0005	0.512295	0.000008	0.512180	-6.69	-5.68	1.42	18.781	0.003	15.669	0.002	38.847	0.006
PSC-5B	rubbly	0.711899	0.000018	0.710123	0.1374	0.0003	0.512294	0.000011	0.512175	-6.71	-5.77	1.49	18.771	0.004	15.669	0.003	38.847	0.008
PSC-4B	rubbly	0.715020	0.000035	0.712962	0.1323	0.0002	0.512232	0.000012	0.512118	-7.92	-6.89	1.52	18.795	0.006	15.669	0.005	38.913	0.014
PSC-22	pahoehoe	0.710103	0.000009	0.709575	0.1264	0.0003	0.512186	0.000012	0.512077	-8.82	-7.69	1.49	18.578	0.004	15.658	0.004	38.618	0.011
PSC-26	pahoehoe	0.714303	0.000015	0.712419	0.1300	0.0001	0.512220	0.000004	0.512108	-8.15	-7.09	1.50	18.742	0.002	15.698	0.002	39.082	0.006
PSC-3M	pahoehoe	0.712784	0.000012	0.711859	0.1377	0.0005	0.512308	0.000006	0.512189	-6.44	-5.50	1.47	18.865	0.006	15.703	0.006	38.947	0.014
PSC-3A	pahoehoe	0.708288	0.000027	0.707798	0.1217	0.0017	0.512299	0.000009	0.512194	-6.61	-5.41	1.23	18.424	0.019	15.649	0.017	38.716	0.040
PSC-2C	pahoehoe	0.711284	0.000117	0.710247	0.1320	0.0011	0.512159	0.000012	0.512045	-9.34	-8.31	1.65	18.499	0.016	15.678	0.014	38.909	0.036
PSC18	pahoehoe	0.713003	0.000019	0.711871	0.1182	0.0006	0.512228	0.000014	0.512126	-8.00	-6.73	1.30	18.494	0.006	15.694	0.005	39.290	0.014
Morro da Cruz section																		
PSC-1D	pahoehoe	0.718214	0.000024	0.715629	0.1265	0.0006	0.512160	0.000023	0.512051	-9.32	-8.20	1.54	18.558	0.007	15.710	0.006	39.369	0.017
PSC-1B	pahoehoe	0.718139	0.000017	0.715751	0.1148	0.0006	0.512156	0.000009	0.512057	-9.40	-8.08	1.37	18.552	0.001	15.700	0.001	39.340	0.003
Lajeado section																		
CT-4B	rubbly	0.711257	0.000012	0.710575	0.1369	0.0021	0.512243	0.000009	0.512125	-7.71	-6.75	1.58	18.609	0.023	15.654	0.021	38.825	0.050
CT-2	pahoehoe	0.710529	0.000009	0.710396	0.1327	0.0003	0.512157	0.000013	0.512042	-9.38	-8.36	1.66	18.466	0.006	15.663	0.005	38.848	0.013

Initial ratios for Sr and Nd and epsilon values corrected to 132 Ma.

Pb ratios are measured

In the $^{143}Nd/^{144}Nd_i$ versus $^{87}Sr/^{86}Sr_i$ diagram (Figure 10), the lavas of the SCSH and LJ sections exhibit low $^{143}Nd/^{144}Nd_i$ and high $^{87}Sr/^{86}Sr_i$ ratios pointing towards ancient continental crust fields. Moreover, the isotopic data of the MC section exhibits values of $^{87}Sr/^{86}Sr_i$ that extends towards more radiogenic Sr isotope ratios, at similar $^{143}Nd/^{144}Nd$ of the other sections. Most of the studied samples nearly plot within the field ascribed for Gramado magma, though four samples plot outside this field, at boundary of the Low-Ti Etendeka CFB field.

The lava flows of the three sections show slight variations in Pb isotope compositions; two pahoehoe samples, PSC-3M and PSC-26, display higher $^{208}Pb/^{204}Pb$ and $^{207}Pb/^{204}Pb$ isotope ratios. The isotope compositions displayed in $^{207}Pb/^{204}Pb$ versus $^{206}Pb/^{204}Pb$ and $^{208}Pb/^{204}Pb$ versus $^{206}Pb/^{204}Pb$ diagrams (Figure 11) define essentially subparallel arrays, lying close to the Gramado magma field, though some samples are more radiogenic towards higher $^{207}Pb/^{204}Pb$ and $^{208}Pb/^{204}Pb$ ratios.

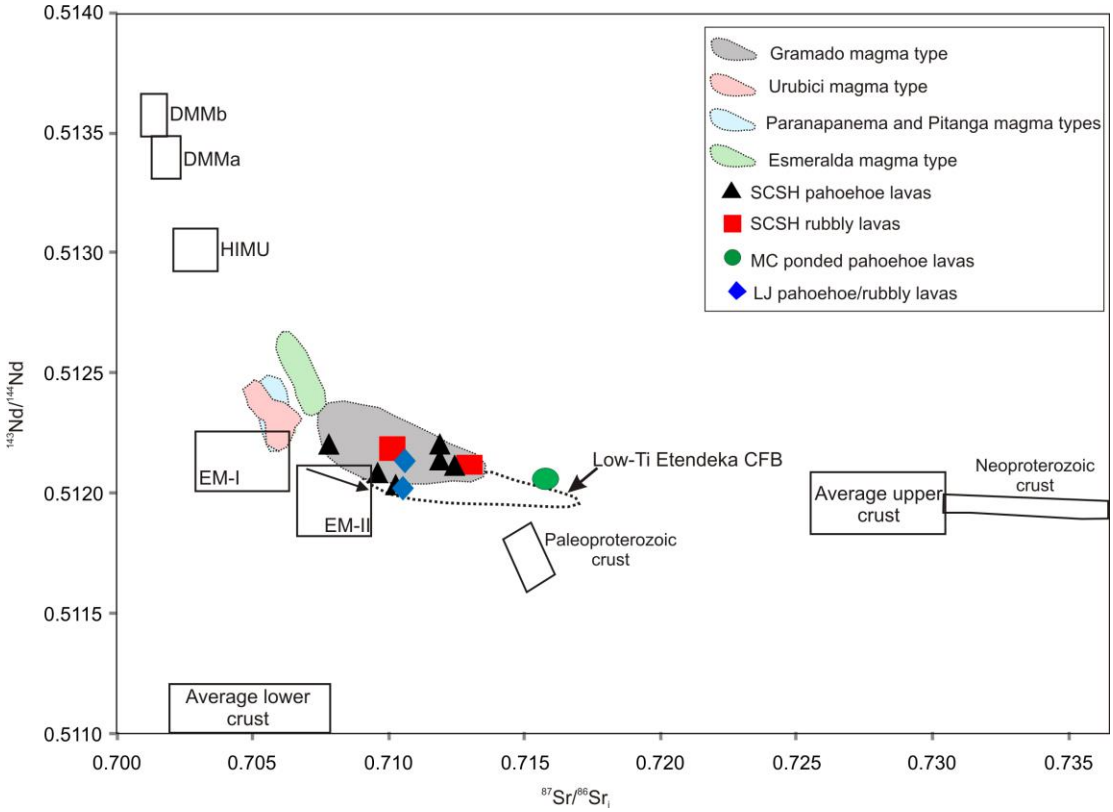

Figure 10. $^{143}Nd/^{144}Nd_i$ versus $^{87}Sr/^{86}Sr_i$ variation diagram for the studied lava flows. Dotted fields ascribed for magma types of the Paraná-Etendeka CFB (Mantovani *et al.* 1985; Petrini *et al.* 1987; Piccirillo *et al.* 1989; Peate *et al.* 1992, 1999; Peate and Hawkesworth 1996; Ewart *et al.* 1998; Rocha-Júnior *et al.* 2013) were inserted for comparison. The mantle components DMMa, DMMb, HIMU, EM-I, and EM-II are from Zindler and Hart (1986). The boxes for average upper and lower crusts are from Taylor and McLennan (1985). The Paleoproterozoic (Gregory 2014) and Neoproterozoic crusts (Florisbal *et al.* 2009) of the PIP basement are also represented.

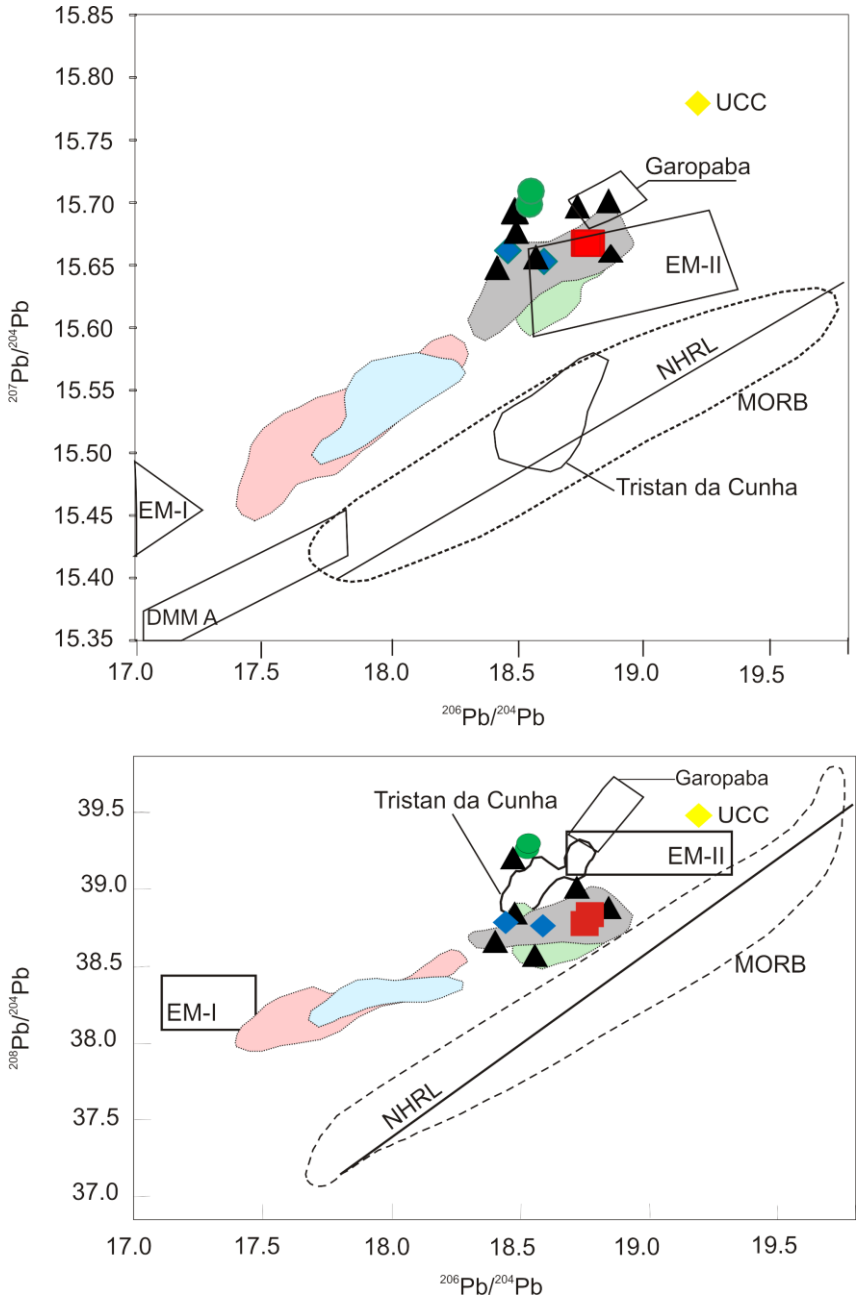

Figure 11. Lead isotope compositions for the lava flows of the SCSH, LJ and MC sections in comparison to the fields for Tristan da Cunha volcanics (Rohde *et al.* 2013), and the mantle components EM-I, EM-II and DMMA (Zindler and Hart 1986). Neoproterozoic crust (Florisbal *et al.* 2009) of the PIP basement is also represented. NHRL = Northern Hemisphere Reference Line (Hart 1984). Symbols and fields of magma types as in Figure 10 caption.

9. Discussion

9.1. Petrogenesis of the magmas

Fractional crystallization

Petrographic observations and major element behavior of the lava flows of the SCSH section suggest fractional crystallization of an essentially basaltic mineral assemblage including plagioclase, clinopyroxene, olivine, and subordinate titanomagnetite. Some major and trace element variations reinforce this assumption. The linear trend of increasing concentrations of incompatible elements such as Nb, Y, and Zr with decreasing MgO are consistent with the hypothesis of olivine and clinopyroxene fractionation (e.g., Hanson 1989). Despite the scattered behavior of Sr contents in the samples, most of them exhibit weak negative Eu anomalies and decreases in CaO and Al_2O_3 with decreasing MgO, which is consistent with plagioclase fractionation (± pyroxene and olivine).

We tested this fractional crystallization hypothesis using the mass balance (Stormer and Nicholls, 1978; Supplementary Table 3) to calculate the percentage of fractionated minerals and the fractionated magma total. These calculations are based on the literature mineral chemistry data of phenocrysts and microphenocrysts of Gramado magma (Bellieni *et al.* 1984; Renner 2010).

The mass balance calculations were conducted only for the samples of the SCSH section using two of the least differentiated samples, PSC-3M and PSC-23, as our starting composition. An insufficient number of samples from the other sections prevented confident mass balance calculations.

The results show the evolution from basalts to basaltic andesites (initial liquid: PSC-3M to final liquid: PSC-4B) can be modelled by 49% fractionation in the proportions of 58 wt.% plagioclase–21 wt.% clinopyroxene–13 wt.% olivine–7.18 wt.% titanomagnetite with a low sum of squares of the differences between observed and calculated compositions (Σres^2 = 0.2301). An additional mass balance calculation using sample PSC-23 as the initial liquid shows that the transition of basalt to basaltic andesite was modelled by 64% fractionation in the proportions of 55 wt.% plagioclase– 30 wt.% clinopyroxene–11 wt.% olivine–3 wt.% titanomagnetite, which also exhibits a low sum of squares (Σres^2 = 0.3053). This fractional crystallization model provides a good fit to the major elements considering the reasonable required proportions of the fractionated phases and the low sum of square of residuals.

Table 3. Mass balance calculations of lava flows of the SCSH section.

Test 1	Lo (PSC-3M)	Lf (PSC-4B)	Plag	Ti-mag	Cpx	Ol	XL-frac	Δ_0	Δf	residual (Δ0-Δf)
SiO_2	51.13	57.09	49.94	-	50.11	39.94	45,083	5,961	5,850	0.11
TiO_2	1.38	1.61	-	16.58	1.25	0.05	1,463	0.221	0.069	0.152
Al_2O_3	16.15	13.35	32.04	1.00	1.93	0.14	19,207	-2.8	-2.855	0.055
FeO_{tot}	11.82	12.69	-	81.91	13.91	16.67	11,028	0.871	0.811	0.06
MnO	0.18	0.20	-	0.29	0.31	0.20	0.114	0.02	0.04	-0.02
MgO	5.77	3.20	-	0.21	13.90	42.64	8,563	-2.564	-2.613	0.049
CaO	9.60	6.76	14.79	0.02	18.33	0.36	12,600	-2.836	2,845	0.008
Na_2O	2.14	2.65	2.94	-	0.26	-	1,772	0.507	0.426	0.081
K_2O	1.65	2.25	0.29	-	-	-	0.169	0.601	1,016	-0.415
P_2O_5	0.19	0.21	-	-	-	-	-	0.02	0.100	-0.08
χres^2										0.2301
subtracted phases (100%)			58.39	7.18	21.35	13.09				
fractionated total (%)										48.74
Test 2	**Lo (PSC-23)**	**Lf (PSC-4B)**	**Plag**	**Ti-mag**	**Cpx**	**Ol**	**XL-frac**	**Δ_0**	**Δf**	**residual (Δ0-Δf)**
SiO_2	50.85	57.09	49.94	0	50.11	39.94	47.115	6,239	6,404	-0.165
TiO_2	1.11	1.61	0	16.58	1.25	0.05	0.970	0.493	0.408	0.085
Al_2O_3	16.59	13.35	32.04	1	1.93	0.14	18.201	-3,238	-3,115	-0.123
FeO_{tot}	10.47	12.69	0	81.91	13.91	16.67	8.985	2,219	2.38	-0.161
MnO	0.21	0.20	0	0.29	0.31	0.2	0.128	-0.016	0.043	-0.06
MgO	7.00	3.20	0	0.21	13.9	42.64	9.014	-3,795	-3,732	-0.062
CaO	11.27	6.76	14.79	0.02	18.33	0.36	13.737	-4,505	-4,478	-0.027
Na_2O	1.87	2.65	2.94	0	0.26	0	1.691	0.78	0.613	0.167
K_2O	0.48	2.25	0.29	0	0	0	0.159	1,777	1,346	0.432
P_2O_5	0.16	0.21	0	0	0	0	0	0.047	0.132	-0.085
χres^2										0.3053
subtracted phases (100%)			54.82	3.52	30.47	11.19				
fractionated total (%)										64.21

Ol= olivine; Plag= plagioclase; cpx= clinopyroxene; Ti-mag= titano magnetite
Lo= initial liquid; Lf= final liquid; F= crystallized fraction in the parental magma;
Δ0= observed difference between the magmas ; Δ0= calculated difference between the magmas
χres2= sum of the squares of residuals.

Crustal contamination

Despite the major elements can be reproduced by fractional crystallization modeling, the relatively large variations in isotope signatures associated to enrichment of incompatible trace elements such as K, Rb, and Ba suggest additional contributions by contamination from lower and/or upper crusts in the formation of basic lava flows from the south hinge of the TS. The high $^{87}Sr/^{86}Sr_i$ ratios combined with geochemical variations presented in this study imply that assimilation and fractional crystallization (AFC; De Paolo 1981) were simultaneous processes in the magma residence within the magma chamber or during ascent of the magmas through the crust.

In order to test the crustal contamination effect on the behavior of the trace elements, AFC trends were calculated for the starting magma compositions of the more mafic lavas of the SCSH section (samples PSC-3M and PSC-23). Quantitative analysis of the crustal

contaminant is dificult to constrain for these lavas because the geological basement of the southern part of the PIP is poorly known, and thus the possible crustal contaminants with known composition are limited.

The contaminants were selected from Neoproterozoic and Paleoproterozoic rocks of basement units from southern part of the PIP with geographic proximity to the study area and for which detailed geochemical and Sr-Nd data are available in the literature. The preferred contaminants used in the construction of the AFC curves are the Neoproterozoic Ponta Grossa granite (sample 630 of Philipp *et al.* 2007), a Paleoproterozoic tonalite of the Arroio dos Ratos Complex (sample TG-02O of Gregory 2014) and a Paleoproterozoic gneiss of the Encantadas Complex (sample RSM-59A – May 1990). Other Neoproterozoic and Paleoproterozoic contaminants of Paraná basement were also tested, but the curves that are generated did not reach the lava flows with final compositions (basaltic andesites with rubbly morphology) of the SCSH section.

The AFC modeling was performed by using Petrograph software (version 2.0 beta), which AFC curves with variable r-values were superimposed on the Ba–Zr, Rb-Zr, Y-Zr, Nb-Y diagrams (Figure 12). These immobile versus immobile trace elements were selected because they act as sensitive indicators of both fractionated crystallization and crustal contamination processes. The resultant AFC curves in the Ba–Zr and Y-Zr plots (Figure 12 (a-b)) suggest that it is possible to obtain basaltic andesite magmas (final liquid) after crystallization from 20% to 33% and assimilation from 6% to 10% of Paleoproterozoic crust (sample TG-02O – Tonalite of the Arroio dos Ratos Complex). In the Rb-Zr and Nb-Y diagrams (Figure 12 (c-d)), the basaltic andesite magmas of rubbly lava flows are obtained after crystallization of 8% to 20% with assimilation from 6% to 10% of Neoproterozoic crust (sample 630 - Ponta Grossa Granite). An attempt of AFC modeling with other Paleoproterozoic contaminant (sample RSM-59A) is also plotted using the same trace element pairs. In the Ba-Zr and Nb-Y plots (Figure 12 (e-f)), the basaltic andesites are achieved after 12-40% of crystallization and 3-14% of assimilation. On the other side, in the Rb-Zr and Y-Zr plots, either the AFC curves do not achieve all the basaltic andesites using a single starting magma (Figure 12 (g)) or even do not achieves the samples regardless of use of the low (0.1) and high (0.8) r-values (Figure 12 (h)).

The above results show that most of the random variations of trace elements cannot be explained by simple AFC modeling calculations, in part due to processes that affect these lava flows are complex and also because the selected contaminants are partly unsatisfactory. This

inconstant behavior of the trace elements not allowed to identify a single crustal contaminant to account for the AFC trends. In this case, both Paleoproterozoic and Neoproterozoic crustal materials associated to distinct degrees of assimilation are needed.

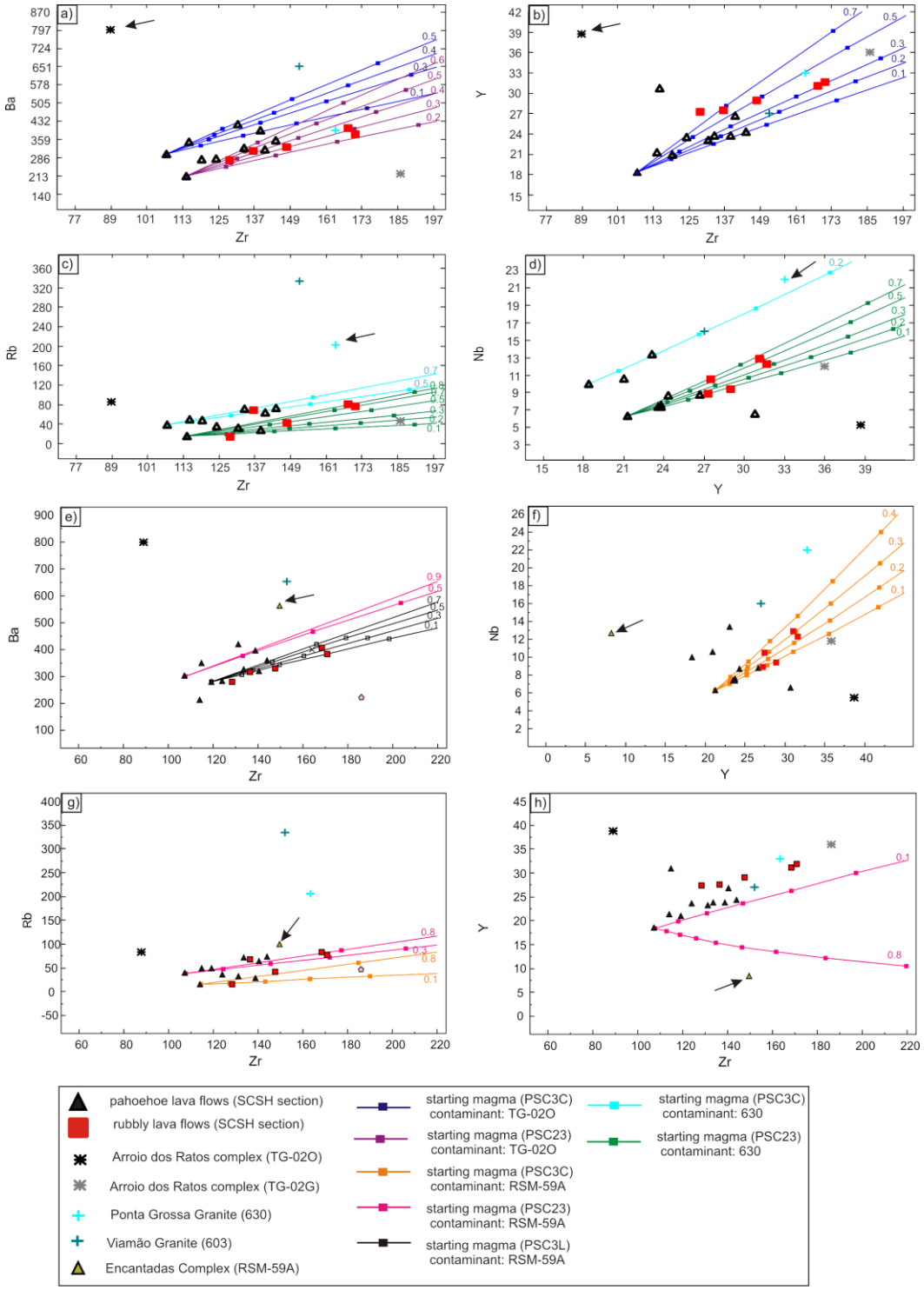

Figure 12. Variation diagrams of selected trace elements, illustrating the results of modeling of assimilation-fractional crystallization (AFC) of the studied lava flows of SCSH section. Variations in *r* (degree of assimilation/ degree of crystallization), depending on the magma starting composition are placed on the evolution curves of AFC process. The squares represent increases of 10% in the crystallization degree.

9.2. The effects of the crustal contamination on the primary isotopic and geochemical signatures of the LTi basalts

The huge areal extent of most CFB makes them potential sources of information on the nature of the subcontinental upper mantle. Unfortunately, characterization of the mantle source regions for CFB is hampered by uncertainities such as a lack of detailed knowledge about the chemical and isotopic heterogeneity of the subcontinental mantle as well as the degree of interaction of magmas with the continental crust. This has led to considerable controversy in CFB studies, in which some authors favor trace element-enriched mantle sources (Hawkesworth *et al.* 1983; Jourdan *et al.* 2007), whereas others authors prefer crustal contamination models (Mahoney *et al.* 1982; Mantovani *et al.* 1985; Peate and Hawkesworth 1996).

Characteristics such as strong Nb and Ta negative anomalies relative to La; enrichment in LREE relative to HREE together with enrichment in LILE, as well as negative ε_{Nd} signatures support models of generation of the CFB that involve contributions from incompatible element-enriched (EM-II) sources in the sub-continental lithospheric mantle (SCLM; Hergt *et al.* 1991; Lightfoot *et al.* 1993; Peate and Hawkesworth 1996; Marques *et al.* 1999; Jourdan *et al.* 2007; Rocha-Júnior *et al.* 2013). The SCLM source is located in a region isolated from the main vigorous convection mantle affected by metasomatic components that may be related to previous supra-subduction environments (e.g., Hawkesworth *et al.* 1988). This hypothesis, in general, explains the geochemical and isotopic characteristics of HTi lavas of Paraná–Etendeka Province (Rocha-Júnior *et al.* 2013).

The basalts of the SCSH and LJ sections exhibit radiogenic isotope signatures with initial $^{87}Sr/^{86}Sr$ ratios plotting toward radiogenic values reaching 0.7130. The samples of the MC section were displaced toward significantly more radiogenic Sr, reaching values of 0.7157. These signatures overlap those of the fields for Gramado magma and LTi Etendeka lavas, plotting towards to the fields ascribed to Paleoproterozoic and Neoproterozoic crusts (Figure 10). The Pb isotope signatures obtained for basalts of the three sections are also relatively high and overlap the regional Gramado basalt field; some samples plot in the fields attributed for Neoproterozoic crust and mantle reservoir EMII (Figure 11).

Similarly, the studied basalts plot within or in close proximity to the field ascribed for Gramado magma on bivariate diagrams, except for the samples of the MC section that plot outside of those fields (Figure 6, Figure 7). Although this behavior confirms the clear compositional affinity between the studied lava flows and the data of literature, the

geochemical and isotopic data reported in the present study show a wider variation, suggesting that the Gramado field could be expanded.

Given the chemical and isotopic characteristics of the studied lava flows with high initial $^{87}Sr/^{86}Sr$ ratios and low $^{143}Nd/^{144}Nd$ ratios, it is difficult to constrain any prior information on the mantle sources of these magmas. Fractional crystallization and crustal assimilation within the magma chamber obscured many if not all of the original chemical signatures of the parental melt. The initial $^{87}Sr/^{86}Sr$ signatures obtained in this study are substantially higher than those of any previously reported subcontinental lithospheric mantle sources (Duncan *et al.* 1984; Hawkesworth *et al.* 1984; Jourdan *et al.* 2007). Moreover, crustal contamination of these magmas after leaving the source appears to be more plausible, considering that even the more primitive rocks such as the early pahoehoe basalts exhibit high initial Sr ratios.

The pahoehoe and rubbly lavas from all of the studied sections show a very low Mg# between 20 and 43, low Ni at 2.8–105.2 ppm, and MgO at 2.39–7.30 wt.%. These characteristics combined with low Ti/Y and high Rb/Ba and Ba/Nb ratios, high initial Sr isotopic ratios, very low ε_{Nd}, and high $^{207}Pb/^{204}Pb$ ratios support the hypothesis that these magmas must have undergone significant crustal contamination in the magma chamber. The Pb contents in the studied samples are higher than those previously analyzed Gramado magma, which reinforce the role of crustal contamination process due to Pb element be enhanced in the crust. In addition, high Rb/Sr ratios are likely to persist long enough in the upper crust to generate these signatures (Hawkesworth *et al.* 1983; Mantovani *et al.* 1985).

Negative Nb anomalies and enrichment in Th and U with respect to Ta and Hf (Figure 8) as well as increasing $^{87}Sr/^{86}Sr$ with a constant Ba/Yb ratio (Figure 13) reinforce the important role of contamination by upper continental crust. The $^{87}Sr/^{86}Sr$ versus Ba/Yb plot is considered as the trace element analogue of the Nd-Sr isotope diagram and define closely similar trends (Wilson 1989).

Another sensitive indicator of contamination by intermediate to felsic crust is the P_2O_5/K_2O ratio (e.g., Carlson and Hart 1987; Hart *et al.* 1997), since crustal rocks with silicic composition have low P_2O_5/K_2O, generally lower than 0.1, compared to mantle derived magmas which typically have high ratios. Decreasing P_2O_5/K_2O along with increase in $^{87}Sr/^{86}Sr$ ratios are expected for basic magmas mixing with crustal materials. This behaviour was clearly observed in the analyzed basalts (Figure 14 (a)), which probably indicate that these rocks were significantly affected by crustal contamination. In the same way, a positive

correlation between $^{87}Sr/^{86}Sr_i$ and SiO_2 is well defined for lavas with SiO_2 ranging from 52 wt.% to 58 wt.% and at a lesser extent for some early pahoehoe lavas with SiO_2 ranging from 51 wt.% to 54 wt.% (Figure 14 (b)). This correlation reinforces the hypothesis that the crustal assimilation increases with the differentiation.

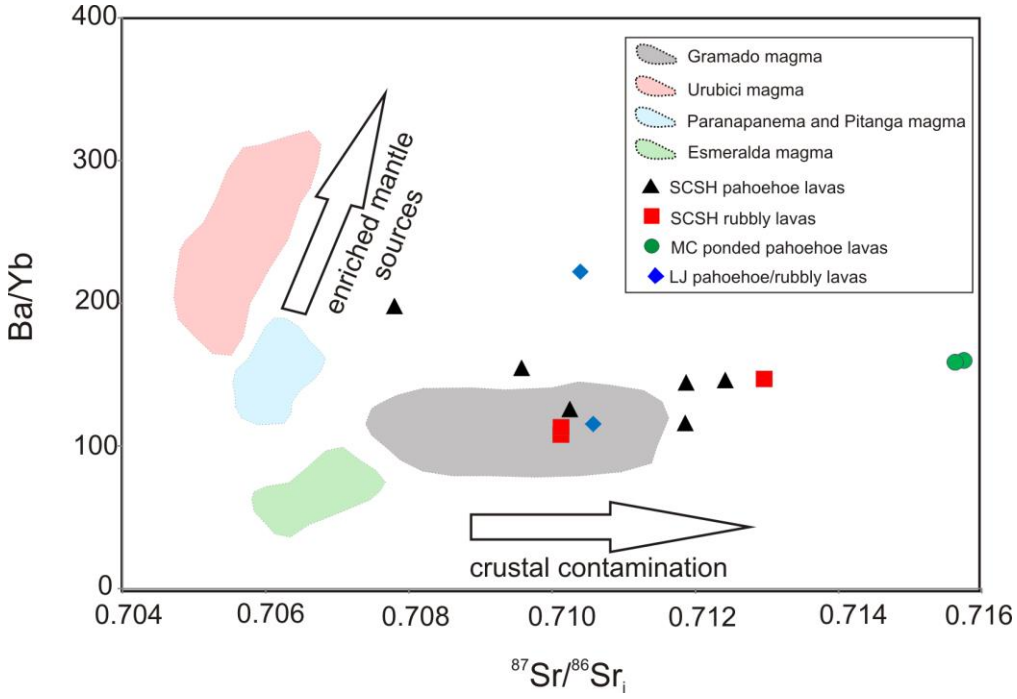

Figure 13. Ba/Yb versus $^{87}Sr/^{86}Sr_i$ diagram that reinforce the role of the upper crustal contamination. The vectors are from Wilson (1989) and refer to open-system fractional crystallization (AFC) and closed-system fractional crystallization (FC).

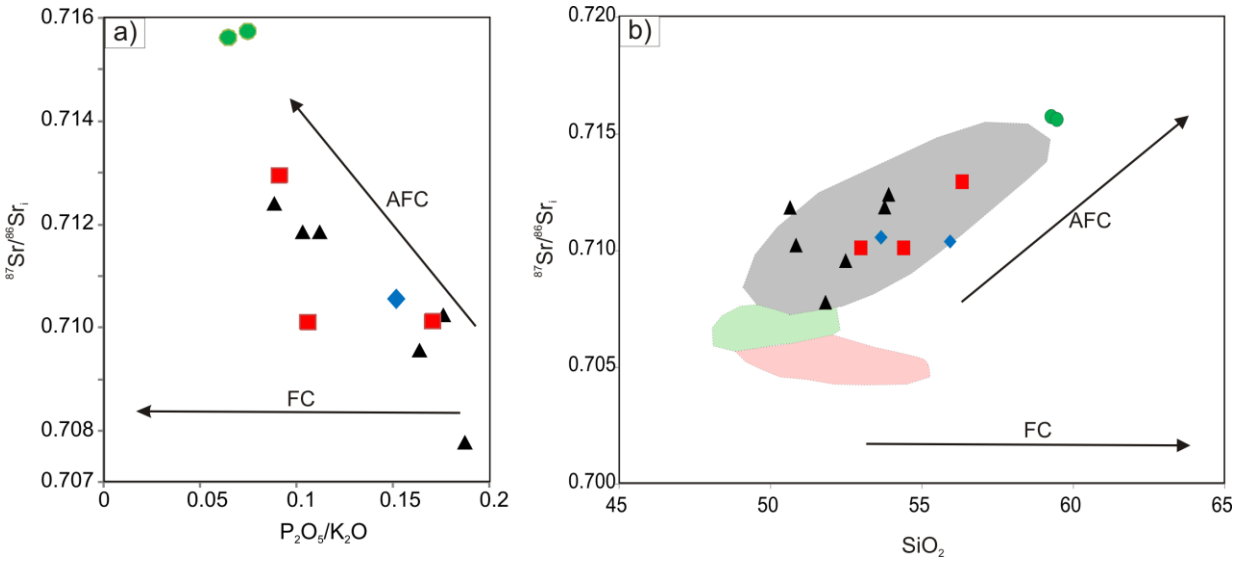

Figure 14. a) $^{87}Sr/^{86}Sr_i$ versus P_2O_5/K_2O plot as indicator of crustal contamination; b) Plot of initial Sr isotope ratios versus SiO_2 (wt.%) for the studied lava flows compared with the magma types of the Paraná Province. Symbols and fields of magma types as in Figure 13 caption. Data sources are in the text.

The relationship between Pb and Sr isotopes in the $^{87}Sr/^{86}Sr$ versus $^{206}Pb/^{204}Pb$ diagram (Figure 15 (a)) and Pb and Nd isotopes in the $^{143}Nd/^{144}Nd$ versus $^{206}Pb/^{204}Pb$ diagram (Figure 15 (b)) shows that to explain these lava flows is needed some contribution of EM-II reservoir or assimilation of Neoproterozoic crust. The lack of Pb isotope data of the Paleoproterozoic basement rocks of Paraná Province not allowed a discussion about the contribution of this crust to account for the Pb isotopic signature of the samples.

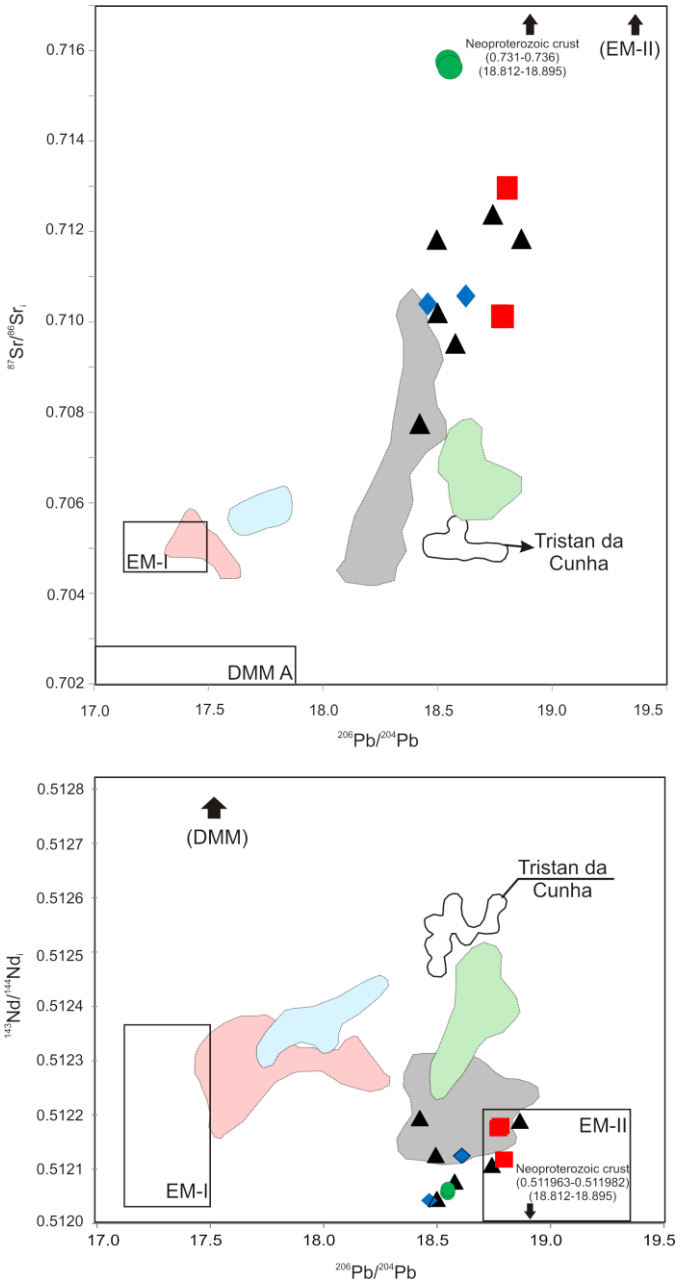

Figure 15. $^{87}Sr/^{86}Sr_i$ and $^{143}Nd/^{144}Nd_i$ against present-day Pb isotope compositions for lava flows of the SCSH, MC and LJ sections compared to the fields for Tristan da Cunha volcanics, and the mantle components EM-I, EM-II and DMM (Zindler and Hart 1986). Neoproterozoic crust of the PIP basement is also represented (Florisbal *et al.* 2009). Symbols and fields of magma types as in Figure 13 caption. Data sources are in the text.

9.3. Geochemical and isotopic variations in a local scale stratigraphy

The extensive lava flow sequences of the CFB were previously considered as thick, homogeneous volcanic piles resulting in a 'layer-cake' appearance. To facilitate the study of this extensive magmatism, the entire stratigraphy of the majority of the CFB has been constructed from province-wide magma-type correlations based on geochemical data from regional sampling and a few deep oil drilling boreholes (Peate *et al.* 1992; Peate 1997).

A disadvantage of this magma type succession is that the regional-scale sampling does not have flow-by-flow control, which lava flows with different morphologies and emplacement histories are grouped under the same magma type. According to Macdonald (1953) and Macdonald *et al.* (1983), pahoehoe and a'a end-member basalts are not the result of systematic differences in the chemistry of rocks. Rather, they are related to surface processes of flow dynamics such as viscosity, shear rate, effusion rate, and changes that accompany degassing.

In a restricted area of the TS area, which constitutes the southern part of the PIP, a stratigraphy was reconstructed on the basis of morphology, surface features, and vesiculation patterns (Barreto *et al.* 2014). The lavas were split into lithofacies and lithofacies associations, which demonstrate that this method may be efficient for studying basaltic lava flows at the local scale.

Compound pahoehoe lavas of base of the SCSH section show basaltic composition and the overlapping simple pahoehoe lavas range from basalt to basaltic andesites. The rubbly lava flows in the top of volcanic sequence exhibit basaltic andesite compositions except for sample PSC-20, the last rubbly flow, which shows basaltic composition (Figure 5 (a)). These geochemical data suggest that there is not a direct relationship between pahoehoe and rubbly lava morphologies and chemical signature, which implies that the chemistry is not a key factor for distinguishing different lava flow morphologies and that the distinction between different chemical compositions cannot be achieved through the morphological aspects. Thus, the geochemistry should be used with caution as tool for reconstructing the stratigraphy of lava flow sequences of CFB.

The most striking feature in the SCSH section is that many of the compositional and isotopic variations are not systematic and continuous upward through the lava pile (Figure 16). The pahoehoe lavas with stratigraphic heights up to 350 m exhibit SiO_2, Mg#, Rb, Ba, Th, and U with random behavior regardless of whether the lavas are in the base or top of the pahoehoe sequence. The rubbly lava flows, which occur above 350 m also show an apparently

random behavior of these elements. The first rubbly lava flow exhibits high values of SiO_2, Rb, Ba, Th, and lower Mg# in comparison with the other overlying rubbly lava flows. SiO_2 and Mg# were selected because they are differentiation index, whereas Rb, Ba, Th, and U are enriched in the upper crust and, thus are more sensitive to crustal contamination.

In relation to isotopic signature variations with the stratigraphic height, the $^{87}Sr/^{86}Sr$ ratio of the pahoehoe lavas decreases from 0.7119 to 0.7078 along the first 160 m. Then an abrupt change occurs at 220 m, with values changing towards higher ratios (0.7124), followed by an abrupt decrease of Sr isotopic ratios (0.7096) in the upper level-of the pahoehoe lavas. The $^{206}Pb/^{204}Pb$, $^{207}Pb/^{204}Pb$, $^{208}Pb/^{204}Pb$ ratios show similar behavior to Sr ratios with an initial decreasing up to 160 m (from 18.49 to 18.42; from 15.69 to 15.65; from 39.29 to 38.72) and an abrupt increase of the ratios at the 200 m elevation (18.86; 15.70; 39.08) and once again a negative shift at 350 m elevation (18.58; 15.66; 38.62). Changings of the neodymium isotopic compositions seem to be disconnected from those of the Pb and Sr isotopes. The initial $^{143}Nd/^{144}Nd$ ratios vary from 0.512045 to 0.512126 in the first 130 m and increase to 0.512194 at 165 m and then decrease again towards the top of pahoehoe lavas (0.512189). The samples, PSC-18 and PSC-22 exhibit an unexpected behavior with the decreasing of neodymium ratios together with decrease of the isotopic composition of Sr-Pb. The sample PSC-3M shows a strong increase of Sr-Pb isotopic composition without the expected decreasing of Nd ratio, which may indicate the existence of several contaminants of different age.

The rubbly lavas exhibit $^{87}Sr/^{86}Sr$ ratios decreasing from 0.7101 to 0.7130 towards the top of the volcanic succession. The $^{206}Pb/^{204}Pb$ and $^{208}Pb/^{204}Pb$ ratios show a similar behavior with slight decrease (from 18.79 to 18.77; from 38.91 to 38.85) and then increase (18.78; 38.85) towards the top, while the $^{207}Pb/^{204}Pb$ ratio remains constant (15.67). The rubbly lavas show a more coherent behavior of $^{143}Nd/^{144}Nd$ ratios that increase towards the top of rubbly lavas (from 0.512118 to 0.512179) together with the decreasing of Sr and Pb isotopes.

The random behavior of the trace elements and the trends observed for the $^{87}Sr/^{86}Sr$ and $^{206}Pb/^{204}Pb$ ratios as well as the decrease and then abrupt increase of the $^{143}Nd/^{144}Nd$ ratios suggest (1) a random crustal contamination with change in the contaminant types (2) a recharge episode with the successive replenishment of basaltic magma in the magma chamber (Figure 16). O'Hara and Matthews (1981) proposed that the life of a magma chamber includes a series of cycles each having four stages: fractional crystallization, magma eruption, wall rock contamination, and replenishment.

The abrupt decreasing in the Sr and Pb and Nd isotopic ratios of the pahoehoe lavas at 220 m elevation and a subsequent increase of these ratios at 350 m suggest variation in the assimilation rate at this stratigraphic height, though the change in the behavior of the Nd ratios at 160 m and 220 m suggest a change of the contaminant type, from Neoproterozoic to Paleoproterozoic. Likewise, these same characteristics could be explained by the influence of a recharge process with re-injection of a fresh pulse of less evolved magma. This assumption is reinforced by SiO_2 (from 53% to 48%) and Mg# (from 41 to 46) contents that show decrease and increase at 220 m, respectively. The isotopic signatures of the rubbly lavas suggest a decreasing of contamination towards the top of the volcanic succession and also reinforce the role of simultaneous recharge process that subsequently affect these isotopic compositions and regularly replenish the open magma chamber.

Overall, the crustal contamination and the magma recharge processes would have disturbed the behavior of the trace elements, which could explain the unsuccessful AFC modeling of these elements in the petrogenesis section.

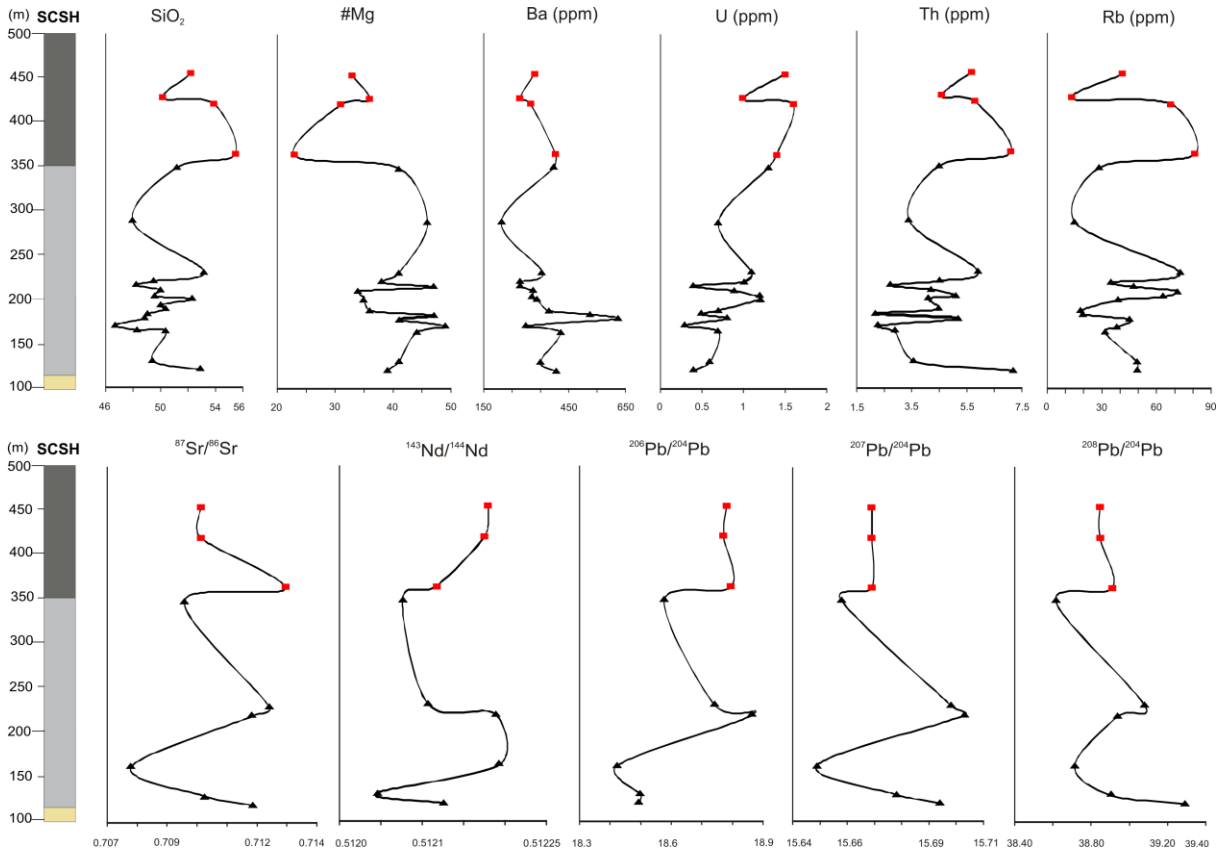

Figure 16. Diagrams showing the variations of SiO_2, Mg#, Ba, U, Th, Rb, $^{87}Sr/^{86}Sr$, $^{143}Nd/^{144}Nd$, $^{206}Pb/^{204}Pb$, $^{207}Pb/^{204}Pb$, $^{208}Pb/^{204}Pb$ of the lava flows in the SCSH section with the stratigraphic height. The symbols of the studied samples as in Figure 13.

9.4. Isotopic AFC calculations and the potential crustal contaminants of LTi basalts

The geochemical and isotopic variations of the studied lava flows as demonstrated in the previous sections suggested pronounced crustal contamination. In order to estimate the role of this contamination and to identify the possible crustal contaminants involved, an isotopic Assimilation-Fractional Crystallization modeling of Nd-Sr has been performed, according to the AFC model of De Paolo (1981).

The main challenge to construct a reliable AFC model is to assign the appropriate compositions of the uncontaminated parental magma and contaminant end-members. None of the studied basalts may be considered as representative of uncontaminated parental magma, because even the least evolved sample already shows high $^{87}Sr/^{86}Sr_i$ and low $^{143}Nd/^{144}Nd_i$, which suggest a pronounced crustal contribution for these lava flows. Thus, in the following discussion, we present two distinct mafic end-members that were selected as parental magmas in order to verify whether the LTi basalts may have derived directly by contamination of the same mantle source than the HTi basalts or whether the LTi basalts were affected by crustal assimilation during ascent of magmas for the surface.

Firstly, an arc-mantle peridotite sample (sample MQ1; Handler *et al.* 2005) was selected as a sub-lithospheric mantle end-member because this composition was successfully used for the petrological modeling of the source of HTi basic magmas of the northern Paraná (Rocha-Júnior *et al.* 2013). The alternative for parental magma is one Urubici magma sample, (sample DUP-37; Peate et al. 1999), which was selected because these magmas are considered contemporaneous and are linked by different degrees of melting to a common mantle source with Gramado magma. Additionally, the Urubici magmas are believed to have experienced minimal crustal interaction (Peate *et al.* 1992, 1999).

The crustal contaminants selected for the isotopic AFC modeling were the same as those used for AFC calculations of trace elements (Neoproterozoic 630 sample; Paleoproterozoic TG020 and RSM-59A samples; Figure 12). The following new samples were also used for the modeling: Neoproterozoic rocks including the Viamão suite (sample 603 of Philipp *et al.* 2007), and Garopaba Granite (sample GS-16B of Florisbal *et al.* 2009); and Paleoproterozoic metadiorite and diorite from the Arroio dos Ratos Complex (samples TG-01O and TG-02G of Gregory 2014).

Figure 17a displays the possible isotopic AFC pathways, which involve the arc-mantle peridotite and the Urubici magma as the parental magmas and the Paleoproterozoic and Neoproterozoic crustal contaminants. In the AFC modeling involving the arc-mantle

peridotite, the most of calculated AFC curves plot far away from any possible Nd-Sr isotopic composition of the studied lava flows, except the AFC modeling involving arc-mantle peridotite and a Paleoproterozoic diorite as contaminant (sample TG-02G) that show curves with good fit for a few samples of SCSH section (Figure 17a). Thus, the arc-mantle peridotite must be discarded as representative of uncontaminated parental magma.

The best mixing curves to account the majority of the pahoehoe and rubbly lava flows were obtained by using the Urubici magmas as uncontaminated parental magma (Figure 17 (a-b)). However, all the attempts involving a single crustal contaminant, which include Neoproterozoic (samples 603, 630 and GS-22A) and Paleoproterozoic crusts (samples TG-01O, TG-02G and RSM-59A) furnished AFC curves that not fit all the samples, even those using high r-values up to 0.8 (Figure 17 (a)). Only one Paleoproterozoic crustal contaminant (sample RSM-59A) is able to produce curves that fit all studied samples (Figure (17b)). Most of the studied samples are achieved after AFC from 45% to 60% of Paleoproterozoic crust (r-values range from 0.25 to 0.7). However, to account for two samples of the SCSH section (PSC-2C and PSC-22) and one sample from the LJ section (CT-2) that exhibit $^{143}Nd/^{144}Nd$ ratios lower than the other studied samples, an r-value of 0.98 is needed. Although the Sr and Nd isotopic compositions of the ponded pahoehoe lava flows of the MC section are achieved by 62% (r=0.40) of assimilation of Paleoproterozoic crust (sample RSM-59A), these rocks are more contaminated and plot away from the other rocks toward more radiogenic $^{87}Sr/^{86}Sr$ ratios (Figure 17 (b)). Therefore, it remains difficult to reconcile the isotopic variations of these ponded pahoehoe lavas with those of the SCSH and LJ sections considering in terms of same magmatic evolution.

Despite of AFC modeling with the contaminant RSM-59A furnish a good fit for most of the samples, the high r-value of 0.98 required for achieve those three samples with lower $^{143}Nd/^{144}Nd$ ratios cannot be sustained from a geochemical perspective, because some effect in the major elements should have been observed in the mass balance, which yet have not been seen (Supplementary Table 3). Alternatively, a Paleoproterozoic lower crust was tested as contaminant (not shown) for the studied lava flows. The Nd elemental and $^{143}Nd/^{144}Nd_i$ isotopic composition of this crust is similar to contaminant RSM-59A, while the strontium elemental and isotopic compositions are 995 ppm and 0.7031, respectively (Taylor and McLennan 1985). However, this crust is discarded due to their low $^{87}Sr/^{86}Sr_i$ ratios, which they are unlikely to generate AFC curves that achieve the studied samples.

In this way, a new attempt of isotopic AFC modeling was performed using a hypothetical Paleoproterozoic crust as contaminant. The Nd elemental and $^{143}Nd/^{144}Nd_i$ isotopic composition of this crust was inferred based on sample RSM-59A, while the strontium elemental and isotopic compositions adopted are hypothetical values of 500 ppm and 0.717, respectively. The resulting AFC curves of this new modeling achieve the three samples with the lower $^{143}Nd/^{144}Nd$ ratios considering an r-value of 0.7 and assimilation from 20% to 25%. On the other side, the samples of MC section are not achieved by the AFC curves using this hypothetical contaminant.

Qualitative observations and quantitative AFC modeling based on trace element and isotope systematic suggest a major role of crustal contamination process in the petrogenesis of these rocks, though both fail to assign a single contaminant for the studied basalts. This suggest that assimilation with variable degrees (r-values) of both Paleoproterozoic and Neoproterozoic crustal components as well as some contribution of recharge process are needed to constrain most of the isotopic variations of the studied lava flows of the south hinge of the TS (Figure 19). However, a major contribution of the Paleoproterozoic crust is considered, which is supported by the T_{DM} model ages of the studied samples ranging from 1.66 to 1.23 Ga (Supplementary Table 2), in addition to the fact that all samples lies within the field ascribed to Paleoproterozoic crustal contaminant, though some samples also plot in the Neoproterozoic contaminant field in Figure 17 (c).

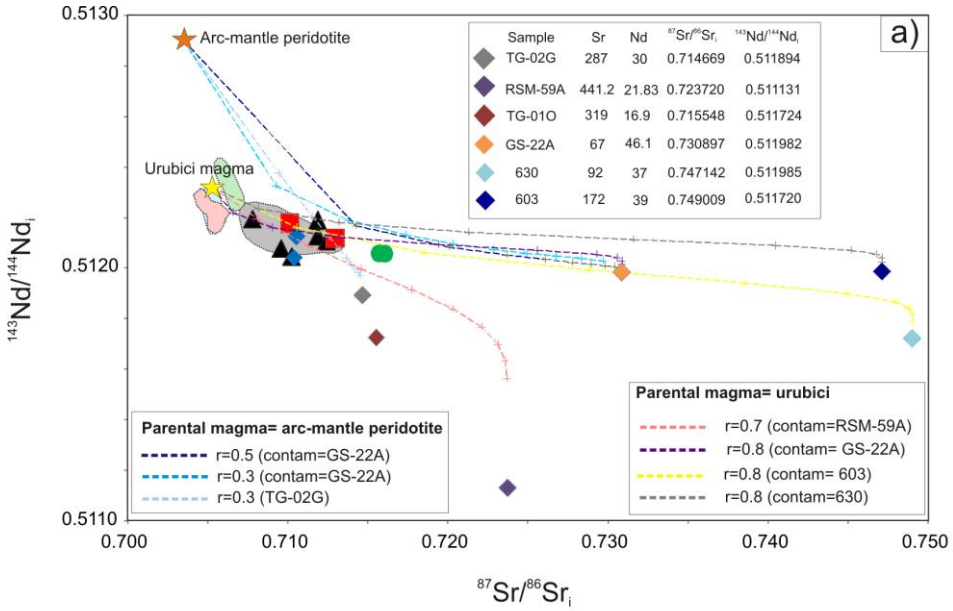
a)
Arc-mantle peridotite
Urubici magma
Sample Sr Nd 87Sr/86Sri 143Nd/144Ndi
TG-02G 287 30 0.714669 0.511894
RSM-59A 441.2 21.83 0.723720 0.511131
TG-01O 319 16.9 0.715548 0.511724
GS-22A 67 46.1 0.730897 0.511982
630 92 37 0.747142 0.511985
603 172 39 0.749009 0.511720
Parental magma= arc-mantle peridotite
r=0.5 (contam=GS-22A)
r=0.3 (contam=GS-22A)
r=0.3 (TG-02G)
Parental magma= urubici
r=0.7 (contam=RSM-59A)
r=0.8 (contam= GS-22A)
r=0.8 (contam= 603)
r=0.8 (contam=630)
143Nd/144Ndi
87Sr/86Sri

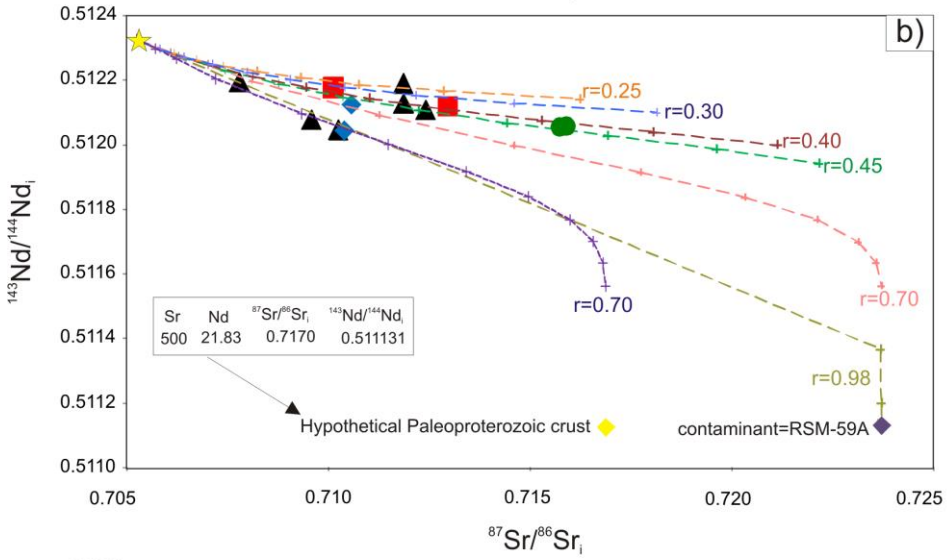
b)
r=0.25
r=0.30
r=0.40
r=0.45
r=0.70
r=0.70
r=0.98
Sr Nd 87Sr/86Sri 143Nd/144Ndi
500 21.83 0.7170 0.511131
Hypothetical Paleoproterozoic crust
contaminant=RSM-59A
143Nd/144Ndi
87Sr/86Sri

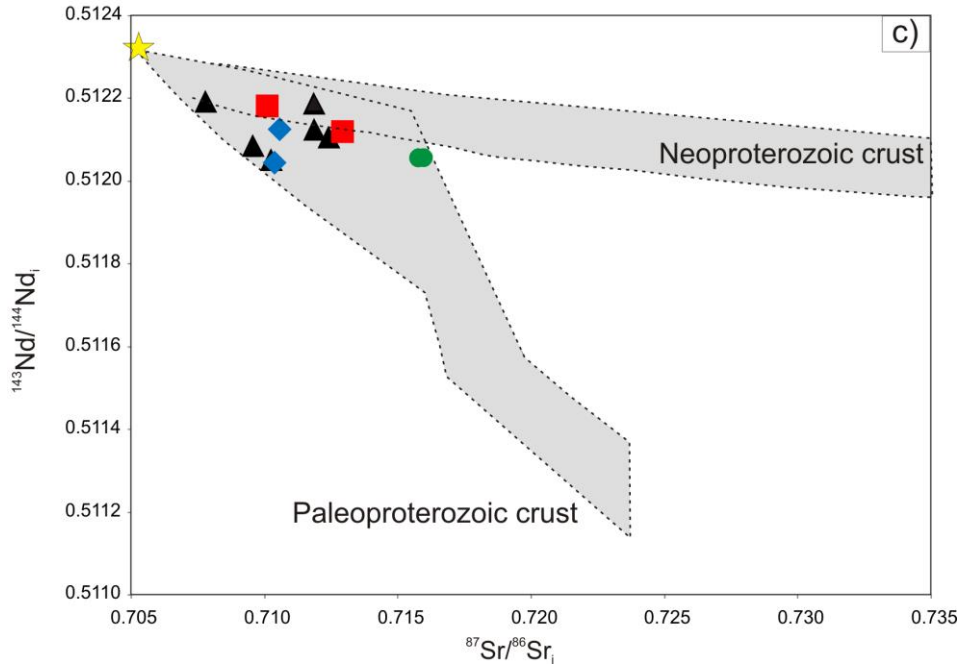
c)
Neoproterozoic crust
Paleoproterozoic crust
143Nd/144Ndi
87Sr/86Sri

Figure 17. $^{87}Sr/^{86}Sr_i$ (at 132 Ma) plotted against $^{143}Nd/^{144}Nd_i$ diagram. a) Isotopic AFC modeling assumes sub-lithospheric mantle (arc-mantle peridotite) and average Urubici magma as the uncontaminated parental magmas and distinct compositions of PIP basement as the contaminants. The r-values are variable, which D_{Sr}= 1.4031 and D_{Nd}= 0.1942 calculated for an assemblage with plagioclase, clinopyroxene, olivine and Fe-Ti oxide in the proportions 56/31/10/2; b) Isotopic AFC modeling using the Urubici as uncontaminated parental magma, and the Encantadas gneiss (Paleoproterozoic crust - sample RSM-59A) and a hypothetical Paleoproterozoic crust (parameters inserted in the text) as contaminants. Crosses on curves indicate percentage of assimilated contaminant at 0.1 intervals; c) Fields ascribed to Paleoproterozoic and Neoproterozoic crusts based on AFC curves of the selected contaminants. Symbols of the studied samples and fields of magma types as in Figure 13 caption.

A summary of the main processes that occur in the magma chamber prior to eruption and the stacking of the lava flow fields of the SCSH, LJ and MC recorded at surface is shown in the Figure 18 and Figure 19, respectively. The storage of mafic liquids during a short period at shallow-level magma chamber allowed the magma ascent with composition of olivine basalts (Figure 18). The crustal contamination process plays an important role in the genesis of these early magmas, considering the high initial $^{87}Sr/^{86}Sr$ ratio (0.7078) and the negative value of ε_{Nd} (-8.31) of the parental basalt samples (Supplementary Table 2). The intermittent lava supply with low effusion rate led to emplacement of lavas with olivine basalt composition that show compound pahoehoe morphology at surface (Figure 19), which represent the early stage of evolution of the SCSH, LJ sections.

The continuous fractional crystallization within the magma chamber coupled with variable assimilation degrees of distinct contaminants with Paleoproterozoic and Neoproterozoic ages, in addition to significant contribution of magma recharge led to magma ascent with basaltic andesite compositions (Figure 18). These basaltic andesite magmas effused under low effusion rate, although with sustained lava supply generating lava flows with simple pahoehoe morphology, which overlap the compound pahoehoe lavas at SCSH and LJ sections (Figure 19).

The continuous magma recharge in the magma chamber coupled with higher assimilation degree allowed the formation of basaltic andesite lavas with more contaminated isotopic signatures than the olivine basalts (Figure 18). The emplacement of these magmas under high effusion rate and sustained lava supply over time generate lava flows with rubbly morphology that are located in top of the volcanic succession of the SCSH and LJ sections and represent the climax of volcanism in the south hinge of TS (Figure 19).

Differentiation process of liquids coupled with the highest assimilation degrees of

distinct contaminants during longer time in a shallow-level magma chamber, that is distinct from that where SCSH and LJ magmas have been stored led to formation of andesites, that exhibit the most contaminated isotopic signatures with initial $^{87}Sr/^{86}Sr$ ratios of 0.7157 (Figure 18). The emplacement of these andesitic magmas occurs under sustained lava supply and low effusion rates originating lava flows with ponded pahoehoe morphology that fills the interdune areas of paleoerg Botucatu in the Morro da Cruz section (Figure 19).

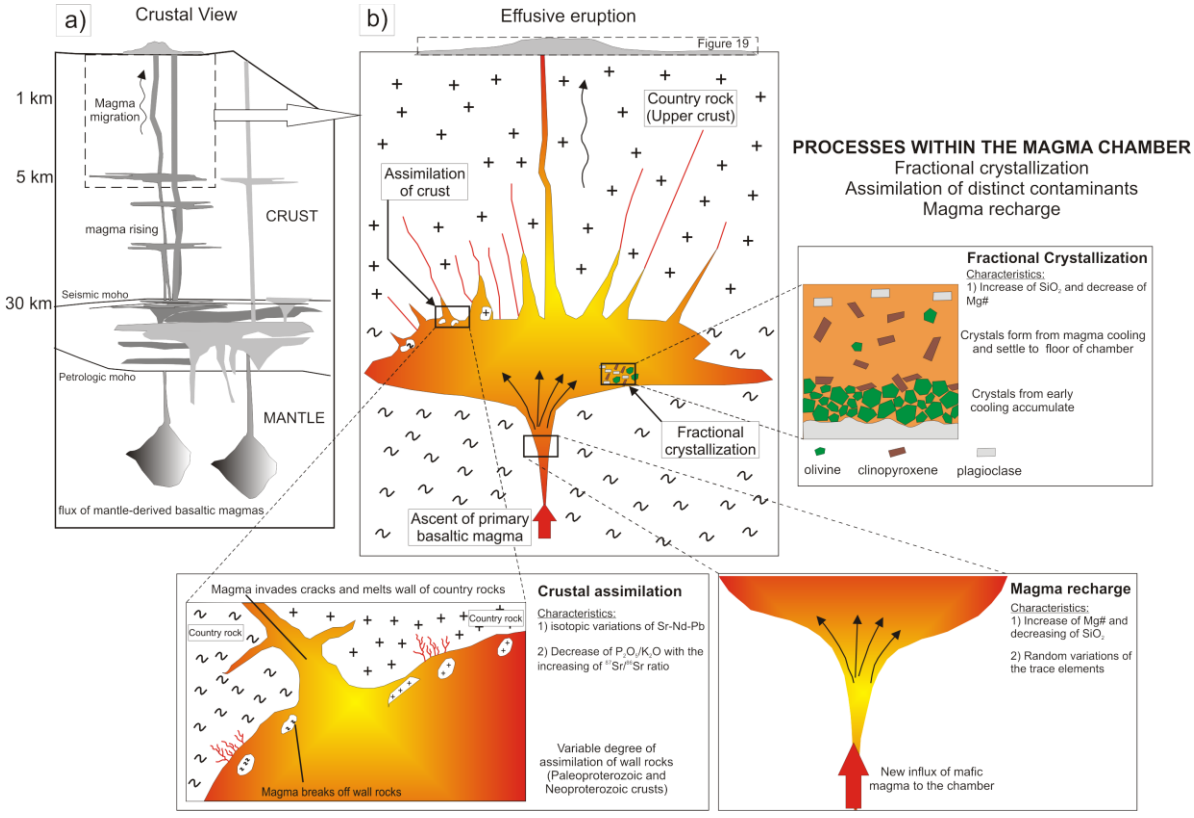

Figure 18. Conceptual crustal view (not to horizontal scale) of the basaltic eruptions in the Paraná Province (modified from Bryan *et al.* 2010). a) Sills of mantle-derived basaltic magma are injected near the crust-mantle boundary. In the following stage, LTi basaltic magmas may be storage in shallow-level magma chambers, which the magmas become subject to fractional crystallization and assimilation of crust with intermediate to silicic composition; b) Detail view of the basaltic magma chamber, where three processes occur concurrently: fractional crystallization, crustal assimilation and magma recharge (not to vertical and horizontal scales).

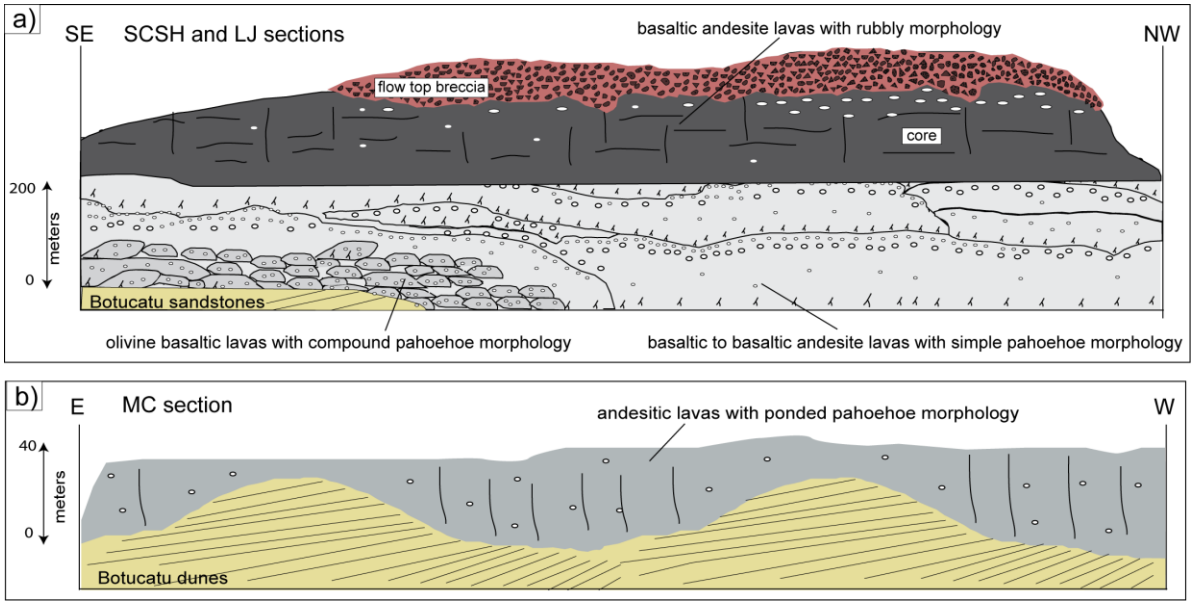

Figure 19. Field sketches of sections across studied lava flows (not to horizontal scale). a) Stacking of the lava flows recorded in the SCSH and LJ sections. The base consists of olivine basaltic lavas with compound pahoehoe morphology that are overlapped by basaltic andesite lavas with simple pahoehoe morphology. Basaltic andesite lavas with rubbly morphology characterize the top of the volcanic succession; b) Andesitic lavas with ponded pahoehoe morphology filling the interdune areas of the Botucatu paleoerg in the MC section.

10. Concluding remarks

Traditionally, the basaltic lava flows of the SGF have been studied through sampling at regional scale. In this study, we performed a first attempt to record the geochemical and isotopic variations of the lava flows within a single Gramado magma type following a local-scale stratigraphy.

The variations in isotope signatures associated to enrichment of incompatible elements such as K, Rb, and Ba suggest that open-system processes operated in the formation of basic lava flows from the south hinge of the TS. The high $^{87}Sr/^{86}Sr_i$ ratios combined with geochemical variations imply that AFC process affects the studied lavas. However, most of the random variations of trace elements cannot be explained by simple AFC modeling calculations, in part due to processes that affect these lava flows are complex and also because the selected contaminants are partly unsatisfactory for account the AFC geochemical modeling. The inconstant behavior of the trace elements evidenced in the AFC curves not allowed to identify a single crustal contaminant for these lavas. In this case, both Paleoproterozoic and Neoproterozoic crustal materials associated to distinct degrees of assimilation are needed.

Several geochemical characteristics combined with increasing $^{87}Sr/^{86}Sr$ with a constant

Ba/Yb ratio, decreasing P_2O_5/K_2O with increase in $^{87}Sr/^{86}Sr$ ratios and positive correlation between $^{87}Sr/^{86}Sr_i$ and SiO_2 reinforce the hypothesis of assimilation of crustal materials by basic magmas.

Many of the compositional and isotopic variations of the lava flows in the SCSH section are not systematic and continuous upward through the lava pile. The random behavior of the trace elements and the trends of the $^{87}Sr/^{86}Sr$ and $^{206}Pb/^{204}Pb$ ratios with the stratigraphic height as well as the decrease and then abrupt increase of the $^{143}Nd/^{144}Nd$ ratios suggest a random crustal contamination with change in the contaminant types from Neoproterozoic to Paleoproterozoic, and a recharge episode with the successive replenishment of the magma chamber. The isotopic signatures of the rubbly lavas suggest a decreasing of contamination towards the top of the volcanic succession and also reinforce the role of magma replenishment that subsequently affects these isotopic compositions.

Qualitative observations and quantitative AFC modeling based on trace element and isotope systematic suggest a major role of crustal contamination process in the petrogenesis of these rocks, though both fail to certify a single contaminant for the studied basalts. This suggest that assimilation of both Paleoproterozoic and Neoproterozoic crustal components as well as some contribution of recharge process are needed to constrain most of the isotopic variations of the studied lava flows of the south hinge of the TS. However, a major contribution of the Paleoproterozoic crust is considered in this study.

The magmatic evolution of the SCSH and LJ lava flows begins with the storage of mafic liquids during a short period at shallow-level magma chamber associated to significant crustal contamination, which allowed the magma ascent with composition of olivine basalts that exhibit compound pahoehoe morphology at surface.

The continuous fractional crystallization within the magma chamber coupled with variable assimilation degrees of distinct contaminants with Paleoproterozoic and Neoproterozoic ages, in addition to significant contribution of magma recharge led to magma ascent with basaltic andesite composition that display at surface the simple pahoehoe morphology. The continuous magma recharge in the magma chamber coupled with higher assimilation degree allowed the formation of basaltic andesite lavas with more contaminated isotopic signatures that exhibit rubbly morphology at the surface.

Differentiation process of liquids coupled with the highest assimilation degrees of distinct contaminants during longer time in a shallow-level magma chamber, which is distinct

from that where SCSH and LJ magmas have been stored, led to formation of andesites of the Morro da Cruz section that exhibit the most contaminated isotopic signatures.

Acknowledgements

This work is a part of the Ph.D. thesis of C.J.S.B. The authors are grateful to technical staff of geochronology laboratory of Federal University of Pará (Pará-Iso/ UFPA) for acquisition of the Sr-Nd-Pb isotopes, with special thanks to the Elma Oliveira, Jeferson Barbosa, and Izanete Melo. Acknowledgement is made to Robert Stern and an anonymous reviewer for valuable input and constructive reviews of this manuscript. We acknowledge the financial support of the PRH PB-215 (Doctoral scholarship) and FAPESP 2012/06082-6 project.

References

Almeida, F.F.M., 1986, Distribuição regional e relações tectônicas do magmatismo pós Paleozóico no Brasil: Revista Brasileira de Geociências, v. 16, p. 325-349.

Anderson, D.L., 2005, Large igneous provinces, delamination, and fertile mantle: Elements, v.1, p. 271-275.

Barreto, C.J.S., Lima, E.F., Scherer, C.M., Rossetti, L.M.M., 2014, Lithofacies analysis of basic lava flows of the Paraná igneous province in the south hinge of Torres Syncline, Southern Brazil: Journal of Volcanology and Geothermal Research, v. 285, p. 81-99.

Barreto, C.J.S., Lima, E.F., Goldberg, K, Vesicle-rich segregation structures and recognition of primary and secondary porosities in pahoehoe and rubbly lava flows of the Paraná Igneous Province, Southern Brazil (submitted).

Bellieni, G., Comin-Chiarmonti, P., Marques, L.S., Melfi, A.J., Piccirillo, E.M., Nardy, A.J.R., Roisenberg, A., 1984, High- and Low-Ti flood basalts from the Paraná plateau (Brazil): Petrogenetic and geochemical aspects bearing on their mantle origin: Neues Jahrbuch für Mineralogie - Abhandlungen, v. 150, p. 273-306.

Bellieni, G., Comin-Chiaramonti, P., Marques, L.S., Melfi, A.J., Nardy, A.J.R., Papatrechas, C., Piccirillo, E.M., Roisenberg, A., Stolfa, D., 1986, Petrogenetic aspects of acid and basaltic lavas from the Paraná Plateau (Brazil): geological, mineralogical and petrochemical relationships: Journal of Petrology, v. 27, p. 915-944.

Boynton, W.V., 1984, Geochemistry of the rare earth elements: Meteorite studies, in Henderson, P., ed., Rare earth element geochemistry: Amsterdam, Elsevier, v. 63, p. 114.

Bryan, S.E., Ernst, R.E., 2008, Revised definition of Large Igneous Provinces (LIPs): Earth-Science Reviews, v. 86, p. 175-202.

Bryan, S.E., Peate, I.U., Peate, D.W., Self, S., Jerram, D.A., Mawby, M.R., Marsh, J.S., Miller, J.A., 2010, The largest volcanic eruptions on Earth: Earth-Science Reviews, v. 102, p. 207-229.

Carlson, R.W., Hart, W.K., 1987. Crustal genesis on the Oregon Plateau. Journal of Geophysical Research 92, 6191-6206.

Coffin, M.F., Eldholm, O., 1994, Large igneous provinces: crustal structure, dimensions, and external consequences: Reviews of Geophysics, v. 32, p. 1-36.

De Paolo, D.J., 1981, Nd isotopic studies: Some new perspectives on Earth Structure and Evolution: EOS, v. 62, p. 137-145.

Duncan, A.R., Erlank, A.J., Marsh, J.S., 1984, Regional geochemistry of the Karoo igneous province. In: Erlank, A.J. (ed.) Petrogenesis of the volcanic rocks of the Karoo Province: Special Publication of the Geological Society of South Africa, v. 13, p. 355-388.

Ewart, A., Milner, S.C., Armstrong, R.A., Duncan, A.R., 1998, Etendeka volcanism of the Goboboseb Mountains and Messum Igneous Complex, Namibia. Part I: geochemical evidence of Early Cretaceous Tristan plume melts and the role of crustal contamination in the Paraná-Etendeka CFB: Journal of Petrology, v. 39 (2), p. 191-225.

Florisbal, L.M., Bitencourt, M.F., Nardi, L.V.S., Conçeição, R.V., 2009, Early post-collisional granitic and coeval mafic magmatism of medium- to high-K tholeiitic affinity within the Neoproterozoic Southern Brazilian Shear Belt: Precambrian Research, v. 175, p. 135-148.

Fodor, R.V., Corwin, C., Roisenberg, A., 1985, Petrology of Serra Geral (Paraná) continental flood basalts, southern Brazil: crustal contamination, source material, and South Atlantic magmatism: Contributions to Mineralogy and Petrology, v. 91, p. 54-65.

Frank, H.T., Gomes, M.E.B., Formoso, M.L.L., 2009, Review of the areal extent and the volume of the Serra Geral Formation, Paraná Basin, South America: Pesquisas em Geociências, v. 36, p. 49-57.

Gregory, T.R., 2014, Evolução Petrológica do magmatismo TTG Paleoproterozóico do Complexo Arroio dos Ratos, distrito de Quitéria, São Jerônimo/RS [Ph.D Thesis]: Porto Alegre, Universidade Federal do Rio Grande do Sul, 100 p.

Handler, M.R., Bennett, V.C., Carlson, R.W., 2005, Nd, Sr and Os isotope systematics in young, fertile spinel peridotite xenoliths from northern Queensland, Australia: a unique view of depleted MORB mantle?: Geochimica et Cosmochimica Acta, v. 69 (24), p. 5747-5763.

Hanson, G.N., 1989, An approach to trace element modelling using a simple igneous system as an example, in Lipin, B.R., McKay, G.A., eds., Geochemistry and mineralogy of rare earth elements: Mineralogical Society of America: Reviews in Mineralogy, v. 21, p. 79-97.

Hart, S.R., 1984, A large-scale isotope anomaly in the southern hemisphere mantle: Nature, v. 309, p. 753.

Hart, W.K., Carlson, R.W., Shirey, S.B., 1997. Radiogenic Os in primitive basalts from the northwestern U.S.A.: implications for petrogenesis. Earth and Planetary Science Letters, v. 150, p. 103-116.

Hawkesworth, C.J., Marsh, J.S., Duncan, A.R., Erlank, A.J., Norry, M.J., 1984, The role of continental lithosphere in the generation of the Karoo volcanic rocks: evidence from combined Nd- and Sr-isotope studies. In: Erlank, A.J. (ed.) Petrogenesis of the volcanic rocks of the Karoo Province. Special Publication of the Geological Society of South Africa, v. 13, p. 341-354.

Hawkesworth, C.J., Erlank, A.J., Marsh, J.S., Menzies, M.A., Van Calsteren, P., 1983, Evolution of the continental lithosphere: evidence from volcanics and xenoliths in Southern Africa, in

Hawkesworth, C.J., Norry, M.J., eds., Continental basalts and mantle xenoliths: Nantwich, Shiva, p. 111-138.

Hawkesworth, C.J., Mantovani, M.S.M., Peate, D., 1988, Lithosphere remobilization during Paraná CFB magmatism: Journal of Petrology-Special Lithosphere Issue, v. 1, p. 205-223.

Hawkesworth, C.J., Mantovani, M.S.M., Taylor, P.N., Palacz, Z., 1986, Evidence from the Paraná of South Brazil for a continental contribution to Dupal basalts: Nature, v. 322, p. 356-359.

Hergt, J., Peate, D.W., Hawkesworth, C.J., 1991, The petrogenesis of Mesozoic Gondwana low-Ti flood basalts: Earth and Planetary Science Letters, v. 105, p. 134-148.

Irvine, T.N., Baragar, W.R.A., 1971, A guide to the chemical classification of the common volcanic rocks: Canadian Journal of Earth Sciences, v. 8, p. 523-548.

Janasi, V.A., Freitas, V.A., Heaman, L.H., 2011, The onset of flood basalt volcanism, Northern Paraná Basin, Brazil: A precise U–Pb baddeleyite/zircon age for a Chapecó-type dacite: Earth and Planetary Science Letters, v. 302, p. 147-153.

Jerram, D.A., Mountney, N.P., Howell, J.A., Long, D., Stollhofen, H., 2000, Death of a sand sea: an active aeolian erg systematically buried by the Etendeka flood basalts of NW Namibia: Journal of the Geological Society of London, v. 157, p. 513-516.

Jerram, D.A., Single, R.T., Hobbs, R.W., Nelson, C.E., 2009, Understanding the offshore flood basalt sequence using onshore volcanic facies analogues: an example from the Faroe–Shetland basin: Geological Magazine, v. 146 (3), p. 353–367.

Jourdan, F,. Bertrand, H., Scharer, U., Blichert-Toft, J., Féraud, G., Kampunzu, B., 2007, Major and trace element and Sr, Nd, Hf, and Pb isotope compositions of the Karoo Large Igneous Province, Botswana-Zimbabwe: Lithosphere vs Mantle plume contrinution: Journal of Petrology, v. 48 (6), p. 1043-1077.

Krymsky, R.S., Macambira, M.J.B., Lafon, J.M., Estumano, G.S., 2007, Uranium-lead dating method at the Pará-Iso Isotope Geology laboratory, UFPA, Belém – Brazil: Academia Brasileira de Ciências, v. 79, p. 115–128.

Le Bas, M.J., LeMaitre, R.W., Streckeisen, A., Zanettin, B., 1986, A chemical classification of volcanic-rocks based on the total alkali silica diagram: Journal of Petrology, v. 27 (3), p. 745-750.

Lightfoot, P.C., Hawkesworth, C.J., Hergt, J., Naldrett, A.J., Gorbachev, N.S., Fedorenko, V.A., Doherty, W., 1993, Remobilisation of the major, trace-element, and from picritic and tholeiitic Siberian Trap, Russia continental lithosphere by a mantle plume: Sr-, Nd-, and Pb-isotope evidence from picritic and tholeiitic lavas of the Noril'sk District: Contributions to Mineralogy and Petrology, v. 114, p. 171–188.

Lima, E.F., Waichel, B.L., Rossetti, L.M.M., Viana, A.R., Scherer, C.M., Bueno, G.V., Dutra, G., 2012, Morphology and petrographic patterns of the pahoehoe and 'a'a flows of the Serra Geral Formation in the Torres Syncline (Rio Grande do Sul state, Brazil): Revista Brasileira de Geociências, v. 42, p. 744-753.

Lugmair, G.W., and Marti, K., 1978, Lunar initial $^{143}Nd/^{144}Nd$: Differential evolution of the lunar crust and mantle: Earth and Planetary Science Letters, v. 39, p. 349-357.

Macdonald, G.A., 1953, Pahoehoe, ´a´ā, and block lava: American Journal of Science, v. 251, p. 169-191.

Macdonald, G.A., Abbot, A.T., Peterson, F.L., 1983, Volcanoes in the Sea the Geology of Hawaii: Honolulu, Univ Hawai'i Press, 517 p.

Mahoney, J., Macdougal, J.D., Lugmair, G.W., Murali, A.V., Sankar, D.M., Gopalan, K., 1982, Origin of the Deccan trap flows at Mahabaleshwar inferred from Nd and Sr isotopic and chemical evidence: Earth and Planetary Science Letters, v. 60, p. 47-60.

Mantovani, M.S.M., Atalla, L., Civetta, L., De Sousa, M.A., Innocenti, F., Marques, L.S., 1985, Trace element and strontium isotope constraints on the origin and evolution of Paraná continental flood basalts of Santa Catarina State, southern Brazil: Journal of Petrology, v. 26, p. 187-209.

Marques, L.S., Dupré, B., Piccirillo, E.M., 1999, Mantle source compositions of the Paraná Magmatic Province: evidence from trace element and Sr-Nd-Pb isotope geochemistry: Journal of Geodynamics, v. 28, p. 439-459.

May, S.E., 1990, Pan-African magmatism and regional tectonics of South Brazil [Ph.D thesis]: Department of Earth Sciences, The Open University, 280 p.

McDonough, W.S., Sun, S., 1995, The composition of the Earth: Chemical Geology, v. 120, p. 223-253.

Melfi, A.J., Nardy, A.J.R., Piccirillo, E.M., 1988, Geological and magmatic aspects of the Paraná Basin: An introduction, *in* Piccirillo, E.M., Melfi, A.J., eds., The Mesozoic flood volcanism of the Paraná Basin: Petrogenetic and geophysical aspects: IAG-USP, p. 1-13.

Milani, E.J., 1997, Evolução tectono-estratigráfica da Bacia do Paraná e seu relacionamento com a geodinâmica fanerozóica do Gondwana sul-ocidental [Ph.D. Thesis]: Porto Alegre, Universidade Federal do Rio Grande do Sul, 199 p.

Mountney, N., Howell, J., Flinth, S., Jerram, D., 1998, Aeolian and alluvial deposition within the Mesozoic Etjo Sandstone Formation, nortwest Namibia: Journal of African Earth Sciences, v. 27, p. 175–192.

O'Hara, M.J., Matthews, R.E., 1981, Geochemical evolution in an advancing, periodically replenished, periodically tapped, continuously fractionated magma chambre: Journal of Geological Society of London, v. 138, p. 237-277.

Oliveira, E.C., Lafon, J.M., Gioia, S.M.C.L., Pimentel, M.M., 2008, Datação Sm-Nd em rocha total e granada do metamorfismo granulítico da região de Tartarugal Grande, Amapá Central: Revista Brasileira Geociências, v. 38, p. 116-129.

Peate, D.W., 1997, The Paraná-Etendeka Province, *in* Mahoney, J.J., Coffin, M.F., ed., Large Igneous Provinces: American Geophysical Union, Washington D.C., p. 217-245.

Peate, P.W., Hawkesworth, C.J., 1996, Lihospheric to astenospheric transition in Low-Ti flood basalts from southern Paraná, Brazil: Chemical Geology, v. 127, p. 1-24.

Peate, D.W., Hawkesworth, C.J., Mantovani, M.S.M., 1992, Chemical stratigraphy of the Paraná lavas (South America): classification of magma types and their spatial distribution: Bulletin of Volcanology, v. 55, p. 119-139.

Peate, D.W., Hawkesworth, C.J., Mantovani, M.S.M., Rogers, N.W., Turner, S.P., 1999, Petrogenesis and stratigraphy of the high-Ti/Y Urubici magma type in the Paraná flood basalt province and implications for the nature of 'Dupal'- type mantle in the South Atlantic region: Journal of Petrology, v. 40, p. 451-473.

Petrini, R., Civetta, L., Piccirillo, E.M., Bellieni, G., Comin-Chiaramonti, P., Marques, L.S., Melfi, A.J., 1987, Mantle heterogeneity and crustal contamination in the genesis of low-Ti continental flood basalts from the Paraná plateau (Brazil): Sr-Nd isotope and geochemical evidence: Journal of Petrology, v. 28, p. 701-726.

Petry, K., Jerram, D.A., Almeida, D.P.M., Zerfass, H., 2007, Volcanic sedimentary features in the Serra Geral Fm., Paraná Basin, southern Brazil: Example of dynamic lava-sediment interactions in a arid setting: Journal of Volcanology and Geothermal Research, v. 159, p. 313–325.

Philipp, R.P., Machado, R., Junior, F.C., 2007, A geração dos granitóides Neoproterozóicos do Batólito Pelotas: Evidências dos isótopos de Sr e Nd e implicações para o crescimento continental da Porção Sul do Brasil, in Iannuzzi, R., Frantz, J.C., eds., 50 anos de Geologia. Instituto de Geociências: Contribuicões, Comunicação e Identidade, 399 p.

Piccirillo, E.M., Civetta, L., Petrini, R., Longinelli, A., Bellieni, G., Comin-Chiaramonti, P., Marques, L.S., Melfi, A.J., 1989, Regional variations within the Paraná flood basalts (southern Brazil): evidence for subcontinental mantle heterogeneity and crustal contamination: Chemical Geology, v. 75, p. 103-122.

Piccirillo, E.M., Melfi, A.J., 1988, The mesozoic Flood volcanism of the Paraná Basin: petrogenetic and geophysical aspects: Instituto Astronômico e Geofísico, University of São Paulo, Brazil.

Polo, L.A., Janasi, V.A., 2014, Volcanic stratigraphy of intermediate to acidic rocks in southern Paraná Magmatic Province, Brazil: Geologia USP (Série Científica), v. 14, p. 83-100.

Renne, P.R., Ernesto, M., Pacca, I.G., Coe, R.S., Glen, J.M., Prévot, M., Perrin, M., 1992, The age of Paraná flood volcanism, rifting of Gondwanaland, and the Jurassic-Cretaceous boundary: Science, v. 258, p. 975-979.

Renner, L.C., 2010, Geoquímica de sills basálticos da Formação Serra Geral, sul do Brasil, com base em rocha total e micro-análise de minerais [Ph.D. thesis]: Porto Alegre, Universidade Federal do Rio Grande do Sul, 226 p.

Rocha-Júnior, E.R.V., Marques, L.S., Babinski, M., Nardy, A.J.R., Figueiredo, A.M.G., Machado, F.B., 2013, Sr-Nd-Pb isotopic constraints on the nature of the mantle sources involved in the genesis of the high-Ti tholeiites from northern Paraná Continental Flood Basalts (Brazil): Journal of South American Earth Sciences, v. 46, p. 9-25.

Rohde, J., Hoernle, K., Hauff, F., Werner, R., O'Connor, J., Class, C., Garbe-Schonberg, D., Jokat, W., 2013, 70 Ma chemical zonation of the Tristan-gough hotspot track: Geology, v. 41, p. 335-338.

Romero, J.A.S., Lafon, J.M., Nogueira, A.C.R., Soares, J.L., 2013, Sr isotope geochemistry and Pb-Pb geochronology of the Neoproterozoic cap carbonates, Tangará da Serra, Brazil: International Geology Review, v. 55, p. 185-203.

Rossetti, L.M.M., Lima, E.F., Waichel, B.L., Scherer, C.M., Barreto, C.J.S., 2014, Stratigraphical framework of basaltic lavas in Torres Syncline main valley, southern Paraná-Etendeka Volcanic Province: Journal of South American Earth Sciences, v. 56, p. 409-421.

Scherer, C.M.S., 1998, Análise Estratigráfica e Litofaciológica da Formação Botucatu (Cretáceo Inferior da Bacia do Paraná) No Rio Grande do Sul [Ph.D. Thesis]: Porto Alegre, Universidade Federal do Rio Grande do Sul, 202 p.

Scherer, C.M.S., 2000, Eolian dunes of the Botucatu Formation (Cretaceous) in Southernmost Brazil: morphology and origin: Sedimentary Geology, v. 137, p. 63-84.

Scherer, C.M.S., 2002, Preservation of aeolian genetic units by lava flows in the Lower Cretaceous of the Paraná Basin, southern Brazil: Sedimentology v. 49, p. 97-116.

Storey, M., Duncan, R.A., Tegner, C., 2007, Timing and duration of volcanism in the North Atlantic Igneous Province: Implications for geodynamics and links to the Iceland hotspot: Chemical Geology, v. 241, p. 264–281.

Stormer, J.C., Nicholls, J., 1978, XLFRAC: a program for the interactive testing of magmatic differentiation models: Computers and Geosciences, v. 4, p. 143-159.

Taylor, S.R., McLennan, S.M., 1985, The Continental Crust: its Composition and Evolution: Cambridge, MA, Blackwell Scientific, 312 p.

Thiede, D.S., Vasconcelos, P.M., 2010, Paraná flood basalts: rapid extrusion hypothesis confirmed by new $^{40}Ar/^{39}Ar$ results: Geology, v. 38, p. 747–750.

Waichel, B.L., Lima, E.F., Lubachesky, R., Sommer, C.A., 2006a, Pahoehoe flows from the central Paraná Continental Flood Basalts: Bulletin of Volcanology, v. 68, p. 599-610.

Waichel, B.L., Lima, E.F., Sommer, C.A., 2006b, Tipos de Derrame e Reconhecimento de Estruturas nos Basaltos da Formação Serra Geral: Terminologia e Aspectos de Campo: Pesquisas em Geociências, v. 33, p. 123-133.

Waichel, B.L., Lima, E.F., Viana, A.R., Scherer, C.M., Bueno, G.V., Dutra, G., 2012, Stratigraphy and volcanic facies architecture of the Torres Syncline, Southern Brazil, and its role in understanding the Paraná–Etendeka Continental Flood Basalt Province: Journal of Volcanology and Geothermal Research, v. 215–216, p. 74–82.

Waichel, B.L., Scherer, C.M.S., Frank, H.T., 2008, Basaltic lava flows covering active aeolian dunes in the Paraná Basin in southern Brazil: Features and emplacement aspects: Journal of Volcanology and Geothermal Research, v. 171, p. 59-72.

Walker, G.P.L., 1989, Spongy pahoehoe in Hawaii: A study of vesicle distribution patterns in basalt and their significance: Bulletin of Volcanology, v. 51, p. 199-209.

Wilmoth, R.A., Walker, G.P., 1993, P-type and S-type pahoehoe: a study of vesicle distribution patterns in Hawaiian lava flows: Journal of Volcanology and Geothermal Research, v. 55, p. 129–142.

Wilson, M., 1989, Igneous Petrogenesis: a global tectonic approach: Ed. Springer, 466 p.

Yang, Y.H., Wu, F.Y., Liu, Z.C., Chu, Z.Y., Xie, L.W., Yang, J.H., 2012, Evaluation of Sr chemical purification technique for natural geological samples using common cation-exchange and Sr-specific extraction chromatographic resin prior to MC-ICP-MS or TIMS measurement: Journal of Analytical Atomic Spectrometry, v. 27, p. 516-522.

Zindler, A., Hart, S., 1986, Chemical geodynamics: Annual Review of Earth and Planetary Sciences, v. 14, p. 493-571.

CAPÍTULO 6

Síntese integradora e considerações finais

A tese foi organizada na forma de artigos conforme exigência do Programa de Pós-Graduação em gociências da Universidade Federal do Rio Grande do Sul.

No primeiro artigo aplicou-se um modelo análogo para o uso de litofácies e associações de litofácies em PBCs, utilizando para isso levantamento de seções geológicas verticais e construção de fotomosaicos. A aplicação desse método foi possivel devido à área selecionada estar inserida em ambientes de platôs continentais onde existe uma grande continuidade lateral das estruturas e texturas vulcânicas.

A partir do método da análise de fácies, os derrames foram subdivididos em 16 litofácies e agrupados em três associações de litofácies: (1) *pahoehoe* composto precoce (2) *pahoehoe* simples precoce (3) *rubbly* simples tardio. Além disso, foi apresentado nesse artigo um mapa geológico com escala de 1:50.000 separando de forma pioneira esses diferentes tipos de derrames básicos e as lavas ácidas da FSG na área estudada. Com os dados de gamaespectrometria também foi possível realizar essa separação, sendo que os derrames *pahoehoe* compostos e simples apresentaram os valores mais baixos de contagem total, seguidos pelo aumento desses valores em direção aos derrames *rubbly* simples. As lavas ácidas apresentaram aumentos significativos nos valores da contagem total em relação aos derrames básicos, como já era esperado, considerando suas composições mais diferenciadas variando de dacitos a riolitos. Os elementos K, U e Th seguem o mesmo comportamento da contagem total, cujos valores aumentam em direção as lavas mais diferenciadas.

A mineralogia dos derrames básicos *pahoehoe* e *rubbly* é similar, formada principalmente por plagioclásio e piroxênio, com quantidades subordinadas de minerais opacos e apatita, sendo que cristais de olivina são restritos aos derrames *pahoehoe* compostos. Os contrastes texturais entre esses derrames refletem diferentes graus de subresfriamento, taxas de efusão e estilos de *emplacement*. Derrames *pahoehoe* simples e compostos exibem, de forma geral no núcleo, uma granulação grossa, cujo mecanismo de transferência endógena (processo de

inflação) dentro de uma crosta visco-elástica em um ambiente termicamente confinado favoreceu a formação das texturas holocristalina e ofítica.

Os derrames *rubbly* exibem padrão textural com granulação fina e abundância de plagioclásio, o que poderia ser explicado pelas altas taxas de efusão com que esses derrames foram colocados. A presença de textura *diktytaxitica* no núcleo afanítico e hipocristalino dos derrames *rubbly* sugere que o aprisionamento de bolhas de gases nessa porção do derrame não ocorre exclusivamente em derrames *pahoehoe*, onde essas texturas são mais comumente encontradas.

Os resultados obtidos nesse artigo sugerem que o início do vulcanismo na região estudada foi marcado por lavas *pahoehoe* compostas (~2 m espessura) com olivina, indicando baixas taxas de efusão com um aporte de lavas colocadas de forma intermitente e sem erosão sobre as areias da FB. Derrames *pahoehoe* simples (~ 6m espessura), mais diferenciados, também extravasaram sob baixas taxas de efusão, embora a alimentação desses magmas tenha se mantido mais constante, permitindo que os derrames se espessassem pelo processo de inflação. Os derrames *pahoehoe* foram sucedidos na estratigrafia pelos basaltos e andesitos basálticos com morfologia do tipo *rubbly*, caracterizados por um *emplacement* sob altas taxas de efusão, originando derrames mais espessos (~50 m), e vertical e lateralmente homogêneos.

A análise de litofácies realizada na região Santa Cruz do Sul-Herveiras, como discutida no primeiro artigo, foi essencial para o reconhecimento e documentação de diferentes tipos de vesiculação e estruturas de segregação presentes nos derrames dessa área. A investigação desses padrões de vesiculação em geral tem um papel coadjuvante no estudo de basaltos, sendo genericamente descritos apenas nos topos de derrames *pahoehoe*. No entanto, o processo de vesiculação em derrames básicos subaéreos pode gerar padrões bastante complexos, incluindo distintas estruturas de segregação, as quais são compatíveis com diferentes tipos morfológicos das lavas.

Dessa forma, a importância do reconhecimento e caracterização das estruturas de segregação ricas em vesículas em basaltos de PBCs direcionou a elaboração do segundo artigo. Este consistiu em relacionar os padrões de vesiculação com os tipos de derrames, suas espessuras e estilos de *emplacement*, com o intuito de recompor a estratigrafia interna dos derrames, bem como tentar

associar esses padrões de vesiculação com os tipos possíveis de porosidade existentes.

Este estudo confirmou que existe uma relação entre a espessura dos derrames e os tipos de estruturas de segregação formadas. Vesículas do tipo V1 (esféricas e milimétricas) são encontradas em qualquer porção tanto nos derrames *pahoehoe* (de 1 a 6 m espessura) quanto nos derrames *rubbly* (até 50 m). *Pipe* vesículas (tipo V2 – na forma de tubos alongados verticais) estão posicionadas na base de derrames *pahoehoe* e lobos tipo P, enquanto proto-cilindros (proto-C) podem ser observados apenas na base dos derrames *pahoehoe* simples. Vesículas gigantes (tipo V3), zonas vesiculadas denominadas *pods* (tipo V4), cilindros de vesículas (C) e camadas de vesículas do tipo S2 foram observadas apenas nas porções de núcleo e topo dos derrames *pahoehoe* simples (~6 m). Camadas de vesículas do tipo S1 foram identificadas apenas no topo de derrames *pahoehoe* simples.

O reconhecimento de porosidades primárias (vesicular, intracristalina e móldica) e vários tipos de porosidades secundárias (*drusy*, *spongy*, *cavernous*, *lacy*, intracristalina secundária, intra-fragmento, intra-matrix, fratura tectônica, fratura de resfriamento) sugere um alto grau de porosidade nessas lavas básicas, o qual poderia ter implicações para um possível reservatório vulcânico nessa região. A conexão das cavidades e vesículas por fraturamente tardios aliados a presença de diques e camadas de areia poderiam facilitar a migração de possíveis fluidos. No entanto, a precipitação de minerais secundários nas vesículas e cavidades reduz drasticamente a porosidade total dos derrames, bem como sela a permeabilidade desenvolvida pelo fraturamento. Desta forma, reconhece-se que o desenvolvimento de poros não é a única condição para as rochas ígneas serem bons reservatórios de hidrocarbonetos. Nesse caso, estudos futuros devem agregar a caracterização dos tipos de porosidade com dados quantitativos de porosidade e permeabilidade para melhor previsão do espaço disponível para armazenamento de óleo/gás ou mesmo para sistemas aquíferos.

Por fim, os dados geoquímicos combinados com isótopos de Sr-Nd-Pb apresentados no terceiro artigo são cruciais para o modelo evolutivo da ombreira sul da ST. Esse artigo reforça que a origem das morfologias *pahoehoe* e *rubbly* não está diretamente relacionada à composicão química dos derrames, devido às variações

composicionais não serem sistemáticas e contínuas ao longo da sequência vulcânica.

Cristalização fracionada e assimilação com graus variáveis de contaminantes Paleoproterozoicos e Neoproterozoicos concomitantes a recargas periódicas de magmas na câmara magmática representariam os processos mais favoráveis para explicar o comportamento geoquímico aleatório dos elementos traços e as variações isotópicas de Sr, Nd e Pb, incluindo as altas razões iniciais de $^{87}Sr/^{86}Sr$, e os valores muito negativos de ε_{Nd}, mesmo daqueles basaltos mais precoces.

A evolução magmática dos derrames básicos de Santa Cruz do Sul-Herveiras e Lajeado iniciou com o armazenamento de líquidos máficos durante um curto período em câmaras magmáticas rasas que permitiu a ascensão de magmas com composição de olivina basaltos. O processo de contaminação crustal exerceu um papel fundamental na gênese desses magmas iniciais, considerando as altas razões de $^{87}Sr/^{86}Sr_i$ (0.7078) e os valores negativos de ε_{Nd} (-8.31), mesmo das amostras de basaltos menos diferenciadas. O *emplacement* desses magmas com composição de olivina basaltos ocorreu sob baixas de efusão e aporte intermitente de lava, favorecendo a formação de derrames que mostram morfologia *pahoehoe* composta em superfície.

A contínua cristalização fracionada dentro da câmara magmática concomitante com assimilação em graus variáveis de distintos contaminantes com idades Paleoproterozoica e Neoproterozoica, somada a uma contribuição significativa de recarga periódica de magma permitiu a ascensão de magma com composição andesito basáltica. O *emplacement* desses magmas ocorreu sob baixas taxas de efusão, embora com aporte de lava contínuo, gerando derrames com morfologia *pahoehoe* simples em superfície.

A contínua recarga de magma na câmara magmática concomitante a graus mais elevados de assimilação levaram a formação de lavas andesito basálticas com assinaturas isotópicas mais contaminadas. O *emplacement* desses magmas sob altas taxas de efusão e aporte de lava contínuo ao longo do tempo permitiu gerar derrames com morfologia *rubbly* que estão localizados no topo da sucessões vulcânicas de SCSH e LJ e representam o clímax do vulcanismo na ombreira sul da calha de Torres.

Processos de diferenciação dos líquidos concomitantes as maiores taxas de assimilação de distintos contaminantes durante um período prolongado em uma câmara magmática rasa, a qual é distinta daquela onde os magmas de Santa Cruz do Sul-Herveiras e Lajeado estavam armazenados, favoreceu a formação de andesitos com as assinaturas isotópicas mais contaminadas (razões iniciais de $^{87}Sr/^{86}Sr$ em torno de 0.7157) da ombreira sul da calha de Torres. O *emplacement* desses magmas andesíticos ocorreu sob baixas taxas de efusão e aporte de lava contínuo, o qual favoreceu o preenchimento dos espaços interdunas do *paleoerg* Botucatu na área do Morro da Cruz, originando derrames com morfologia *ponded pahoehoe*.

CAPÍTULO 7

Referências bibliográficas

Almeida, F.F.M. 1953. Ventifactos do deserto Botucatu no estado de São Paulo. *Boletim da Divisão de Geologia e Mineralogia*, 69: 1-14.

Almeida, F.F.M. 1986. Distribuição regional e relações tectônicas do magmatismo pós Paleozóico no Brasil. *Revista Brasileira de Geociências*, 16: 325-349.

Anderson, D.L. 2005. Large igneous provinces, delamination, and fertile mantle. *Elements*, 1: 271-275.

Arndt, N.T., Bruzak, G., Reischmann, T. 2001. The oldest continental and oceanic plateaus: geochemistry of basalts and komatiites of the Pilbara craton, Australia. In Ernst, R.E. & Buchan, K.E. (Eds.), Mantle Plumes: Their Identification through Time. *GSA Special Publication,* 352: 359–387.

Arndt, N.T., Czamanske, G.K., Wooden, J.L., Fedorenko, V.A. 1993. Mantle and crustal contributions to continental flood volcanism. *Tectonophysics*, 223: 39–52.

Aubele, J.C., Crumpler, L.S., Elston, W.E. 1988. Vesicle zonation and vertical structure of basalt flows. *Journal of Volcanology and Geothermal Research*, 35**:** 349-374.

Avni, Y., Segev, A., Ginat, H. 2012. Oligocene regional denudation of the northern Afar dome: pre- and syn-breakup stages of the Afro-Arabian plate. *Geological Society of America Bulletin*, 124: 1871–1897.

Barreto, C.J.S., Lafon, J.M., Rosa-Costa, L.T., Lima, E.F. 2014a. Palaeoproterozoic (~1.89 Ga) felsic volcanism of the Iricoumé Group, Guyana Shield, South America: geochemical and Sm-Nd isotopic constraints on sources and tectonic environment. *International Geology Review*, 56(11): 1332-1356.

Barreto, C.J.S., Lima, E.F., Scherer, C.M., Rossetti, L.M.M. 2014b. Lithofacies analysis of basic lava flows of the Paraná igneous province in the south hinge of Torres Syncline, Southern Brazil. *Journal of Volcanology and Geothermal Research*, 285: 81-99.

Bellieni, G., Comin-Chiaramonti, P., Marques, L.S., Melfi, A.J., Nardy, A.J.R., Papatrechas, C., Piccirillo, E.M., Roisenberg, A., Stolfa, D. 1986. Petrogenetic aspects of acid and basaltic lavas from the Paraná Plateau (Brazil): geological, mineralogical and petrochemical relationships. *Journal of Petrology*, 27: 915-944.

Bellieni, G., Comin-Chiarmonti, P., Marques, L.S., Melfi, A.J., Piccirillo, E.M., Nardy, A.J.R., Roisenberg, A. 1984. High- and Low-Ti flood basalts from the Paraná plateau (Brazil): Petrogenetic and geochemical aspects bearing on their mantle origin. *Neues Jahrbuch für Mineralogie (Abhandlungen)*, 150: 272-306.

Bonaparte, J.F. 1996. Late Jurassic vertebrate communities of eastern and western Gondwana. *Geores, Forum,* 1**:** 427-432.

Bondre, N.R., Duraiswami, R.A., Dole, G. 2004. Morphology and emplacement of flows from the Deccan Volcanic Province, India. *Bulletin of Volcanology*, 66: 29-45

Bondre, N.R. & Hart, W.K. 2008. Morphological and textural diversity of the Steens Basalt lava flows, Southeastern Oregon, USA: implications for emplacement style and nature of eruptive episodes. *Bulletin of Volcanology*, 70: 999-1019.

Bortoluzzi, C.A. 1974. Contribuição a geologia da região de Santa Maria, Rio Grande do Sul. *Revista Pesquisas*, 4(1): 7-86.

Branney, M.J. & Kokelaar, P. 2002. Pyroclastic Density Currents and the Sedimentation of Ignimbrites. *Geological Society of London, Memoirs*, 143 p.

Brown, R.J., Blake, S., Bondre, N.R., Phadnis, V.M., Self, S. 2011. ´A´ā lava flows in the Deccan Volcanic Province, India, and their significance for the nature of continental flood basalt eruptions. *Bulletin of Volcanology,* 73: 737-752.

Bryan, S.E. 2007. Silicic Large Igneous Provinces. *Episodes*, 30**:** 20-31.

Bryan, S.E. & Ernst, R.E. 2006. Proposed Revision to Large Igneous Province Classification. http://www.mantleplumes.org/LIPClass2.html.

Bryan, S.E. & Ernst, R.E. 2008. Revised definition of Large Igneous Provinces (LIPs). *Earth-Science Reviews*, 86: 175-202.

Bryan, S.E. & Ferrari, L. 2013. Large Igneous Provinces and Silicic Large Igneous Provinces: progress in our understanding over the last 25 years. *Geological Society of America Bulletin*, 125: 1053–1078.

Bryan, S.E., Peate, I.U., Peate, D.W., Self, S., Jerram, D.A., Mawby, M.R., Marsh, J.S., Miller, J.A. 2010. The largest volcanic eruptions on Earth. *Earth-Science Reviews,* 102: 207-229.

Bryan, S.E., Riley, T.R., Jerram, D.A., Leat, P.T., Stephens, C.J. 2002. Silicic volcanism: an under-valued component of large igneous provinces and volcanic rifted margins. In: Menzies, M.A., Klemperer, S.L., Ebinger, C.J., Baker, J. (Eds.). Magmatic Rifted Margins. *Geological Society of America Special Paper*, 362: 99-120.

Camp, V.E., Ross, M.E., Hanson, W.L. 2003. Genesis of flood basalts and Basin and Range volcanic rocks from Steens Mountain to Malheur River Gorge, Oregon. *Geological Society of America Bulletin*, 115: 105-128.

Carlson, R.W. 1991. Physical and chemical evidence on the cause and source characteristics of flood basalt volcanism. *Australian Journal of Earth Sciences*, 38: 525–544.

Caroff, M., Maury, R.C., Cotton, J., Clément, J.P. 2000. Segregation structures in vapor-differentiated basaltic flows. *Bulletin of Volcanology*, 62: 171-187.

Cas, R.A.F. & Wright, J.V. 1987. Volcanic succession, modern and ancient: a geological approach to processes, products and successions. London, 528 p.

Cashman, K.V. & Kauahikaua, J.P. 1997. Reevaluation of vesicle distributions in basaltic lava flows. *Geology*, 25: 419-422.

Cashman, K.V., Thornber, C., Kauahikaua, J.P. 1999. Cooling and crystallization of lava in open channels, and the transition of Pahoehoe lava to 'A'a. *Bulletin of Volcanology*, 61: 306-323.

Chenet, A.L., Courtillot, V., Fluteau, F., Gérard, M., Quidelleur, X., Khadri, S.F.R., Subbarao, K.V., Thordarson, T. 2009. Determination of rapid Deccan eruptions across the Cretaceous–Tertiary boundary using paleomagnetic secular variation: Constraints from analysis of eight new sections and synthesis for a 3500-m-thick composite section. *Journal of Geophysical Research: Solid Earth*, 114, issue B06103. DOI: 10.1029/2008JB005644.

Coffin, M.F. & Eldholm, O. 1992. Volcanism and continental break-up: A global compilation of large igneous provinces. *Geological Society of London Special Publication*, 68: 17-30.

Coffin, M.F. & Eldholm, O. 1994. Large igneous provinces: Crustal structure, dimensions and external consequences. *Reviews of Geophysics*, 32(1): 1-36.

Coffin, M.F. & Eldholm, O. 2005. Large igneous provinces. In: Selley, R.C., Cocks, R., Plimer, I.R. (Eds.). Encyclopedia of Geology. Elsevier, Oxford, 315-323.

Comin-Chiaramonti, P., Bellieni, G., Piccirillo, E.M., Melfi, A.J. 1988. Classification and petrography of continental stratoid volcanic and related intrusive from the Paraná Basin (Brasil). In: Piccirillo, E.M., Melfi A.J. (Eds). The Mesozoic flood volcanism of the Paraná Basin: petrogenetic and geophysical aspects. São Paulo, Instituto Astronômico e Geofísico, 600p.

Cordani, U.G., Civetta, L., Mantovani, M.S.M., Petrini, R., Kawashita, K., Hawkesworth, C.J., Taylor, P., Longinelli, A., Cavazzini, G., Piccirillo, E.M. 1988. Isotope geochemistry of flood volcanics from the Paraná Basin (Brazil). In: Piccirillo, E.M. & Melfi, A.J. (Eds.). The Mesozoic flood volcanism of the Paraná Basin: petrogenetic and geophysical aspects. São Paulo, Instituto Astronômico e Geofísico, p. 157-178.

Cordani, U.G., Sartori, P.L.P., Kawashita, K. 1980. Geoquímica dos isótopos de estrôncio e a evolução da atividade vulcânica na Bacia do Paraná (Sul do Brasil) durante o Cretáceo. *Anais da Academia Brasileira de Ciências*, 52: 811-818.

Cordani, U.G. & Vandoros, F. 1967. Basaltic rocks of the Paraná Basin. In: Bigarella, J.J., Becker, G.D., Pinto, I.D. (Eds.). Problems in Brazilian Gondwana geology. Curitiba, Mac Roesner, pp. 207-231.

Courtillot, V. 1990. Deccan volcanism at the Cretaceous-Tertiary boundary: past climatic crises as a key to the future?. *Palaeogeography, Palaeoclimatology, Palaeoecology*, 189: 291-299.

Courtillot, V. 1995. Mass extinctions in the last 300 million years: One impact and seven flood basalts. *Israel Journal of Geology* (in press).

Courtillot, V. 1999. Evolutionary Catastrophes: The Science of Mass Extinction. Cambridge University Press, Cambridge, 173 p.

Courtillot, V., Besse, J., Vandamme, D., Montigny, R., Jaegar, J.J., Cappetta, H. 1986. Deccan flood basalts at the Cretaceous/Tertiary boundary?. *Earth and Planetary Science Letters*, 80: 361-374.

Courtillot, V.E., Jaupar, C., Manighetti, I., Tapponnier, P., Besse, J. 1999. On causal link between flood basalts and continental break-up. *Earth and Planetary Science Letters,* 166: 77-195.

Courtillot, V.E. & Renne, P.R. 2003. On the ages of flood basalt events. *Comptes Rendus Geoscience*, 335: 113-140.

Cox, K.G. 1980. A model for flood basalt volcanism. *Journal of Petrology*, 21: 629-650.

Cox, K.G. & Hawkesworth, C.J. 1985. Geochemical Stratigraphy of the Deccan Traps at Mahabaleshwar, Western Ghats, India, with implications for open system magmatic processes. *Journal of Petrology,* 26(2): 355-377.

Dalrymple, R.W. 2010. Interpreting Sedimentary successions: Facies, Facies Analysis and Facies Models. In James, N.P. & Dalrymple, R.W. Facies model 4. Geotext 6, 572 p.

Dickson, W.R. 1970. Interpreting detrital modes of greywackes and arkoses. *Journal of Sedimentary Petrology*, 40(2): 695-707.

Dickson, B.L. & Scott, K.M. 1997. Interpretation of aerial gamma-ray surveys adding the geochemical factors. *AGSO Journal of Australian Geology & Geophysics, Austrália*, 17(2): 187-200.

Duraiswami, R.A., Bondre, N.R., Managave, S. 2008. Morphology of rubbly pāhoehoe (simple) flows from the Deccan Volcanic Province: implications for style of emplacement. *Journal of Volcanology and Geothermal Research*, 177: 822-836

Duraiswami, R.A., Dole, G., Bondre, N.R. 2003. Slabby pahoehoe from the western Deccan Volcanic Province: evidence for incipient pahoehoe-aa transitions. *Journal of Volcanology and Geothermal Research*, 121: 195-217.

Duraiswami, R.A., Gadpallu, P., Shaikh, T.N., Cardin, N. 2014. Pahoehoe–a'a transitions in the lava flow fields of the western Deccan Traps, India-implications for emplacement dynamics, flood basalt architecture and volcanic stratigraphy. *Journal of Asian Earth Sciences*, 84: 146-166.

Dutton, C.E. 1884. Hawaiian volcanoes: U.S. Geol. Survey 4th Ann. Rept., pp. 75-219.

Erlank, A.J., Marsh, J.S., Duncan, A.R., Miller, R.McG., Hawkesworth, C.J., Betton, P.J., Rex, D.C. 1984. Geochemistry and petrogenesis of the Etendeka volcanic rocks from SWA/Namibia. In: Erlank, A.J. (Ed.). *Geological Society of South Africa Special Publication*, 13: 195-245.

Ernesto, M., Marques, L.S., Piccirillo, E.M., Molina, E.C., Ussami, N., Comin-Chiaramonti, P., Bellieni, G. 2002. Paraná Magmatic Province-Tristan da Cunha plume system: fixed versus mobile plume, petrogenetic considerations and alternative heat sources. *Journal of Volcanology and Geothermal Research*, 118: 15-36.

Ernst, R.E. 2014. Large Igneous Provinces. Cambridge University Press, united kingdom, 667 p.

Ernst, R.E. & Buchan, K.L. 1997. Layered mafic intrusions: a model for their feeder systems and relationship with giant dyke swarms and mantle plume centers. *South African Journal of Geology*, 100: 319–334.

Ernst, R.E. & Buchan, K.L. 2001. Large mafic magmatic events through time and links to mantle-plume heads. In Ernst, R.E. & Buchan, K.L. (eds.), Mantle Plumes: Their Identification through Time. *Geological Society of America, Special Paper*, 352: 483–575.

Ernst, R.E. & Buchan, K.L. 2003. Recognizing mantle plumes in the geological record. *Annual Reviews Earth and Planetary Science*, 31: 469–523.

Ewart, A., Marsh, J.S., Milner, S.C., Duncan, A.R., Kamber, B.S., Armstrong, R.A. 2004. Petrology and geochemistry of early cretaceous bimodal continental flood volcanism of the NW Etendeka, Namibia: Part 1. Introduction, mafic lavas and re-evaluation of mantle source components. *Journal of Petrology*, 45: 59–105.

Ewart, A., Milner, S.C., Armstrong, R.A., Duncan, A.R. 1998. Etendeka volcanism of the Goboboseb Mountains and Messum Igneous complex Namibia. Part I: Geochemical evidence of Early Cretaceous Tristan plume melts and the role of crustal contamination in the Paraná–Etendeka CFB. *Journal of Petrology*, 39: 191-225.

Ewart, A., Milner, S.C., Duncan, A.R., Bailey, M. 2002. The Cretaceous Messum igneous complex, S.W. Etendeka, Namibia: reinterpretation in terms of a downsag-cauldron subsidence model. *Journal of Volcanology and Geothermal Research*, 114: 251-273.

Farrell, R.E. 2010. Volcanic Facies Architecture of the Chilcotin Group Basalts at Chasm Provincial Park, British Columbia. The University of British Columbia (Vancouver). The Faculty of Graduate Studies (Geological Sciences). Thesis of master of Science, 151 p.

Feng, Z. 2008. Volcanic rocks as profilic gas reservoir: A case study from the Qingshen gas field in the Songliao Basin, NE China. *Marine and Petroleum Geology*, 25: 416-432.

Florisbal, L.M., Heaman, L.M., Janasi, V.A., Bitencourt, M.F. 2014. Tectonic significance of the Florianópolis Dyke Swarm, Paraná–Etendeka Magmatic Province: A reappraisal based on precise U–Pb dating. *Journal of Volcanology and Geothermal Research*, 289: 140-150.

Fodor, R.V., Corwin, C., Roisenberg, A. 1985. Petrology of Serra Geral (Paraná) continental flood basalts, southern Brazil: crustal contamination, source material, and South Atlantic magmatism. *Contributions to Mineralogy and Petrology*, 91: 54-65.

Garfunkel, Z. 2008. Formation of continental flood volcanism – the perspective of setting of melting. *Lithos*, 100: 49–65.

Garland, F., Hawkesworth, C.J., Mantovani, M.S.M. 1995. Description and petrogenesis of the Parana rhyolites, southern Brazil. *Journal of Petrology*, 36: 1193–1227.

Gazzi, P. 1966. Le arenaire del flysch sopra Cretaceo dell Appenino modenese, correlazioni con il flysch de Monghidoro. *Mineral et Petrologica Acta*, 12: 69-97.

Gibson, S.A., Thompson, R.N., Dickin, A.P., Leonardos, O.H. 1995. High-Ti and low-Ti mafic potassic magmas: key to plume-lithosphere interactions and continental flood-basalt genesis. *Earth and Planetary Science Letters*, 136: 149-165.

Glen, W. 1994. The Mass-Extinction Debates: How Science Works in a Crisis. Stanford, Calif.: Stanford University Press, 370 p.

Goff, F. 1996. Vesicles cylinders in vapor-differentiated basalt flows. *Journal of Volcanology and Geothermal Research*, 71: 167-185.

Gordon Jr, M. 1947. Classification of the gondwanic rocks of Paraná, Santa Catarina and Rio Grande do Sul. *Notas preliminares da Divisão de Geologia e Mineralogia*, 38: 1-19.

Gudmundsson, A. & Lotveit, I.F. 2014. Sills as fracturated hydrocarbon reservoirs: examples and models. *Geological Society of London Special Publication*, 374: 251-271.

Hamilton, M.A., Pearson, D.G., Thompson, R.N., Kelley, S.P., Emeleus, C.H. 1998. Rapid eruption of Skye lavas inferred from precise U-Pb and Ar-Ar dating of the Rum and Cuillin plutonic complexes. *Nature*, 394: 260-263.

Hartmann, L.A., Wildner, W., Duarte, L.C., Duarte, S.K., Pertille, J., Arena, K.R., Martins, L.C., Dias, N.L. 2010. Geochemical and scintillometric characterization and correlation of amethyst geode-bearing Paraná lavas from the Quaraí and Los Catalanes districts, Brazil and Uruguay. *Geological Magazine*, 147: 954–970

Hawkesworth, C.J., Mantovani, M.S.M., Peate, D.W. 1988. Lithosphere remobilisation during Parana CFB magmatism, in Oceanic and Continental Lithosphere; Similarities and Differences, edited by Menzies, M.A. & Cox, K. *Journal of Petrology*, special volume(1): 205-223.

Hawkesworth, C.J., Mantovani, M.S.M., Taylor, P.N., Palacz, Z. 1986. Evidence from the Paraná of South Brazil for a continental contribution to Dupal basalts. *Nature*, 322: 356-359.

Henry, C.D. & Wolff, J.A. 1992. Distinguishing strongly rheomorphic tuffs from extensive silicic lavas. *Bulletin of Volcanology*, 54: 171-186.

Hon, K., Gansecki, C., Kauahikaua, J. 2003. The transition from ‘a’ā to pāhoehoe crust on flows emplaced during the Pu’u‘Ō’ō-Kū paianaha eruption. *United States Geological Survey professional paper*, 1676: 89-103.

Hon, K., Kauahikaua, J., Denlinger, R., Mackay, K. 1994. Emplacement and inflation of pahoehoe sheet flows: observations and measurements of active lava flows on Kilauea volcano, Hawaii. *Geological Society of America Bulletin*, 106: 351-370.

Hooper, P.R. 1997. The Columbia River Flood Basalt Province: Current status. In: Mahoney, J.J.; Coffin, M.F. eds. Large igneous provinces: continental, oceanic, and planetary flood volcanism. American Geophysical Union. Geophysical Monograph, 100: 1-27.

Hooper, P.R., Camp, V.E., Reidel, S.P., Ross, M.E. 2007. The Origin of the Columbia River Flood Basalt Province: Plume versus Nonplume Models. *GSA Special Papers*, 430: 635-668.

Hooper, P.R., Widdowson, M., Kelley, S. 2010. Tectonic setting and timing of the final Deccan flood basalt eruptions. *Geology*, 38: 839–842.

Ingle, S. & Coffin, M.F. 2004. Impact origin for the greater Ontong Java Plateau?. *Earth and Planetary Science Letters*, 218: 123–134.

Isley, A.E. & Abbott, D.H. 2002. Implications of the temporal distribution of high- Mg magmas for mantle plume volcanism through time. *Journal of Geology*, 110: 141–158.

Ivanov, A.V., He, H.Y., Yan, L.K., Ryabov, V.V., Shevko, A.Y., Palesskii, S.V., Nikolaeva, I.V. 2013. Siberian Traps large igneous province: evidence for two flood basalt pulses around the Permo-Triassic boundary and in the Middle Triassic, and contemporaneous granitic magmatism. *Earth-Science Reviews*, 122: 58–76.

Janasi, V.A, Freitas, V.A., Heaman, L.H. 2011. The onset of flood basalt volcanism, Northern Paraná Basin, Brazil: A precise U–Pb baddeleyite/zircon age for a Chapecó-type dacite. *Earth and Planetary Science Letters*, 302(1): 147-153.

Janasi, V.A., Montanheiro, T.J., Freitas, V.A., Reis, P.M., Negri, F.A., Dantas, F.A., 2007. Geology, petrography and geochemistry of the acid volcanism of the Paraná Magmatic Province in the Piraju-Ourinhos region, SE Brazil. *Revista Brasileira de Geociências*, 37 (4): 745–759.

Jay, A.E. & Widdowson, M. 2008. Stratigraphy, structure and volcanology of the SE Deccan continental flood basalt province: implications for eruptive extent and volumes. *Journal of the Geological Society of London*, 165: 177-188.

Jerram, D.A. 2002. Volcanology and facies architecture of flood basalts. In: Menzies, M. A., Baker, J., Ebinger, C. J., Klemperer, S. L. (Eds.). Volcanic Rifted Margins. *Geological Society of America Special Paper*, 362: 121-135.

Jerram, D.A., Mountney, N., Holzffrster, F., Stollhofen, H. 1999. Internal stratigraphic relationships in the Etendeka Group in the Huab Basin, NW Namibia: understanding the onset of flood volcanism. *Journal of Geodynamics,* 28: 393-418.

Jerram, D.A., Mountney, N.P., Howell, J.A., Long, D., Stollhofen, H. 2000. Death of a sand sea: an active aeolian erg systematically buried by the Etendeka flood basalts of NW Namibia. *Journal of the Geological Society of London*, 157: 513-516.

Jerram, D.A., Single, R.T., Hobbs, R.W., Nelson, C.E. 2009. Understanding the offshore flood basalt sequence using onshore volcanic facies analogues: an example from the Faroe–Shetland basin. *Geological Magazine,* 146(3): 353–367.

Jerram, D.A. & Widdowson, M. 2005. The anatomy of continental flood basalt provinces: Geological constraints on the processes and products of flood volcanism. *Lithos*, 79: 385-405.

Jinglan, L., Chengli, Z., Zhihao, Q. 1999. Volcanic reservoir rocks: a case study of the cretaceous Fenghuadian Suite, Huanghua Basin, Eastern China. *Journal of Petroleum Geology*, 22: 397-415.

Jourdan, F., Bertrand, H., Scharer, U., Blichert-Toft, J., Féraud, G., Kampunzu, B. 2007. Major and Trace Element and Sr, Nd, Hf, and Pb Isotope Compositions of the Karoo Large Igneous Province, Botswana-Zimbabwe: Lithosphere vs Mantle Plume Contribution. *Journal of Petrology*, 48(6): 1043-1077.

Kelley, S. 2007. The geochronology of large igneous provinces, terrestrial impact craters, and theirrelationship to mass extinctions on Earth. *Journal of the Geological Society of London*, 164: 923-936.

Keszthelyi, L. 1995. Measurements of the cooling at the base of pāhoehoe flows. *Geophysical Research Letters*, 22: 2195–2198.

Keszthelyi, L. & Thordarson, T. 2000. Rubbly pahoehoe: a previously undescribed but widespread lava type transitional between aa and pahoehoe. *Geological Society of America Abstract Programs*, 32: 7.

Keszthelyi, L., Thordarson, T., Self, S. 2001. Rubbly pahoehoe: implications for flood basalt eruptions and their atmospheric effects. *Eos Transactions American Geophysical Union Journal,* 82: F1407.

Kilburn, C. 1990. Surfaces of ´a´ā flows-fields on Mount Etna, Sicily: Morphology, rheology, crystallization and scaling phenomena. In: Fink, J.H. (Ed.). Lava Flows and Domes. Berlin, Springer-Verlag. p. 129-156.

Klein, E.L., Almeida, M.E., Rosa-Costa, L.T. 2012. The 1.89-1.87 Ga Uatuma Silicic Large Igneous Province, northern South America. LIP of the Month, November 2012. See http://www.largeigneousprovinces.org/12nov.

Krymsky, R.S., Macambira, M.J.B., Lafon, J.M., Estumano, G.S. 2007. Uranium-lead dating method at the Pará-Iso Isotope Geology laboratory, UFPA, Belém – Brazil. *Academia Brasileira de Ciências*, 79: 115–128.

Lenhardt, N., Gotz, A.E. 2011. Volcanic settings and their reservoir potential: An outcrop analog study on the Miocene Tepoztlan Formation, Central Mexico. *Journal of Volcanology and Geothermal Research*, 204: 66-75.

Lima, E.F., Philipp, R.P., Rizzon, G.C., Waichel, B.L., Rossetti, L.M.M. 2012a. Sucessões Vulcânicas e Modelo de Alimentação e Geração de Domos de Lava Ácidos da Formação Serra Geral na Região de São Marcos-Antonio Prado (RS). *Revista Geologia da USP, Série Científica*, 12: 49-64.

Lima, E.F., Waichel, B.L, Rossetti, L.M.M., Viana, A.R., Scherer, C.M., Bueno, G.V., Dutra, G. 2012b. Morphology and petrographic patterns of the pahoehoe and 'a'a flows of the Serra Geral Formation in the Torres Syncline (Rio Grande do Sul state, Brazil. *Revista Brasileira de Geociências*, 42: 744-753.

Lockwood, J.P. & Lipman, P.W. 1980. Recovery of datable charcoal from beneath young lava flows-lessons from Hawaii. *Bulletin Volcanologique*, 43(3): 609-615.

Loock, S., Vries, B.V.W., Hénot, J.M. 2010. Clinker formation in basaltic and trachybasaltic lava flows. *Bulletin of Volcanology*, 72: 859-870.

Lorenzatti, A., Santin, C.A., Castro, E.E.S., Goldberg, K., De Ros, L.F., Abel, M., Paesi, O. 2011. Hardledge workstation 1.1.0.1111. Endeeper. Porto Alegre, Brasil.

Luchetti, A.C.F. 2010. Aspectos vulcanológicos dos traquidacitos da região de Piraju – Ourinhos (SP). Dissertação de mestrado, São Paulo: USP. 115 p.

Lugmair, G.W. & Marti, K. 1978. Lunar initial $^{143}Nd/^{144}Nd$: Differential evolution of the lunar crust and mantle. *Earth and Planetary Science Letters*, 39: 349-357.

Macdonald, G.A. 1953. Pahoehoe, ´a´ā, and block lava. *American Journal of Science*, 251: 169-191.

Managave, S. 2000. The geology around Kurundwad. Unpubl. M.Sc. Dissertation, University of Pune, 104 p.

Mantovani, M.S.M., Atalla, L., Civetta, L., De Sousa, M.A., Innocenti, F., Marques, L.S. 1985. Trace element and strontium isotope constraints on the origin and evolution of Paraná continental flood basalts of Santa Catarina State, southern Brazil. *Journal of Petrology*, 26: 187-209.

Mantovani, M.S.M. & Hawkesworth, C.J. 1990. An inversion approach to assimilation and fractional crystallisation processes. *Contributions to Mineralogy and Petrology*, 105: 289-302.

Marques, L.S. 1988. Caracterização geoquímica das rochas vulcânicas da Bacia do Paraná: implicações petrogenéticas. Unpublished MSc thesis, University of São Paulo, Brazil, 175 p.

Marques, L.S., Dupré, B., Piccirillo, E.M. 1999. Mantle source compositions of the Paraná Magmatic Province: evidence from trace element and Sr-Nd-Pb isotope geochemistry. *Journal of Geodynamics*, 28: 439-459.

Marsh, J.S., Ewart, A., Milner, S.C., Duncan, A.R., Miller, R.MCG. 2001. The Etendeka Igneous Province: magma types and their stratigraphic distribution with implications for the evolution of the Paraná–Etendeka Flood Basalt Province. *Bulletin of Volcanology*, 62: 464-486.

McPhie, J. & Allen, R.L. 1992. Facies Architecture of Mineralized Submarine Volcanic Sequences — Cambrian Mount Read Volcanics, Western Tasmania. *Economic Geology and the Bulletin of the Society of Economic Geologists*, 87(3): 587–596.

McPhie, J., Doyle, M., Allen, R. 1993. Volcanic Textures: A guide to the interpretation of textures in volcanic rocks. Tasmania, 191 p.

Melfi, A.J., Nardy, A.J.R., Piccirillo, E.M. 1988. Geological and magmatic aspects of the Paraná Basin: An introduction. In: Piccirillo, E.M. & Melfi, A.J. (eds.). The Mesozoic flood volcanism of the Paraná Basin: Petrogenetic and geophysical aspects. *IAG-USP*, pp. 1-13.

Miall, A.D. 2000. Principles of Sedimentary Basin Analysis, 3rd edition: New York, Springer-Verlag Inc., 616 p.

Milani, E.J., Faccini, U.F., Scherer, C.M.S., Araújo, L.M., Cupertino, L.M. 1998. Sequences and stratigraphic hierarchy of the Paraná Basin (Ordovician to Cretaceous), Southern Brazil. *Boletim IG USP, Série Científica*, 29: 125–173.

Milani, E.J., Fernandes, L.A., França, A.B, Melo, J.H.G., Souza, P.A. 2007. Bacia do Paraná. In: Milani, E.J. (ed.). *Boletim de Geociências da Petrobrás, Cartas estratigráficas*, 15(2): 265-287.

Milani , E.J. & Ramos, V.A. 1998. Orogenias Paleozóicas no Domínio Sul-Ocidental do Gondwana e os ciclos de subsidência da Bacia do Paraná. *Revista Brasileira de Geociências*, 28(4): 473-484.

Milner, S.C., Duncan, A.R., Ewart, A. 1992. Quartz latite rheoignimbrite flows of the Etendeka Formation, north-western Namibia. *Bulletin of Volcanology*, 54: 200-219.

Milner, S.C., Duncan, A.R., Whittingham, A.M., Ewar, A. 1995. Trans-Atlantic correlation of eruptive sequences and individual silic volcanic units within Paraná-Etendeka Igneous Province. *Journal of Volcanology and Geothermal Research*, 69: 137-157.

Milner, S.C. & LeRoex, A.P. 1996. Isotope characteristics of the Okenyenya igneous complex, northwestern Namibia: constraints on the composition of the early Tristan plume and the origin of the EM 1 mantle componente. *Earth and Planetary Science Letters*, 141: 277-291.

Mincato, R.L. 2000. Metalogenia dos elementos do grupo da platina com base na estratigrafia e geoquímica da Província Basáltica Ígnea Continental do Paraná. São Paulo. Tese de Doutorado em Geociências, Instituto de Geociências, Universidade de Campinas, 172 p.

Mitsuhata, Y., Matsuo, K., Minegishi, M. 1999. Magnetotelluric survey for exploration of a volcanic-rock reservoir in the Yurihara oil and gas field, Japan. *Geophysical Prospecting,* 47: 195-218.

Mountney, N., Howell, J., Flinth, S., Jerram, D. 1998. Aeolian and alluvial deposition within the Mesozoic Etjo Sandstone Formation, nortwest Namibia. *Journal of African Earth Sciences*, 27: 175–192.

Nardy, A.J.R. 1995. Geologia e petrologia do vulcanismo mesozóico na região central da Bacia do Paraná. Tese de doutoramento, Instituto de Geociências e Ciências Exatas, Unesp, 316 p.

Nardy, A.J.R., Machado, F.B., Oliveira, M.A.F. 2008. As rochas vulcânicas mesozóicas ácidas da Bacia do Paraná: litoestratigrafia e considerações geoquímico-estratigráficas. *Revista Brasileira de Geociências*, 38(1): 178-195.

Németh, K. & Martin, U. 2007. Practical Volcanology. Lecture Notes for understanding Volcanic Rocks from Field Based Studies. *Occasional Papers of the Geological Institute of Hungary*, v. 207, Budapeste.

Neumann, E.R., Svensen, H., Galerne, C.Y., Planke, S. 2011. Multistage evolution of dolerites in the Karoo Large Igneous Province, Central South Africa. *Journal of Petrology*, 52: 959–984.

Oliveira, E.C., Lafon, J.M., Gioia, S.M.C.L., Pimentel, M.M. 2008. Datação Sm-Nd em rocha total e granada do metamorfismo granulítico da região de Tartarugal Grande, Amapá Central. *Revista Brasileira Geociências*, 38: 116-129.

Oppenhein, V. 1934. Rochas gondwanicas e geologia do petróleo do Brasil Meridional. *Boletim de Divisão de Fomento de Produção Mineral*, 5: 2-50.

Pankhurst, R.J., Leat, P.T., Sruoga, P., Rapela, C.W., Márquez, M., Storey, B.C., Riley, T.R. 1998. The Chon Aike silicic igneous province of Patagonia and related rocks in Antarctica: a silicic large igneous province. *Journal of Volcanology and Geothermal Research*, 81: 113-136.

Pankhurst, R.J., Riley, T.R., Fanning, C.M., Kelley, S.R. 2000. Episodic silicic volcanism along the proto-Pacific margin of Patagonia and the Antarctic Peninsula: plume and subduction influences associated with the break-up of Gondwana. *Journal of Petrology*, 41: 605-625.

Peate, D.W. 1997. The Paraná-Etendeka Province. In: Mahoney, J.J. & Coffin, M.F. (Eds.) Large igneous provinces: continental, oceanic and planetary flood volcanism. *Geophysics Monography*, 100, AGU, pp. 217-245.

Peate, D. & Hawkesworth, C.J. 1996. Lithospheric to astenospheric transition in low-Ti Flood basalts from Southern Paraná, Brazil. *Chemical Geology*, 127: 1-24.

Peate, D.W., Hawkeswort, C.J., Mantovani, M.S.M. 1992. Chemical stratigraphy of the Paraná lavas (South America): Classification of magma types and their spatial distribution. *Bulletin of Volcanology*, 55: 119-139.

Peterson, D.W. & Tilling, R.I. 1980. Transition of basaltic lava from pahoehoe to aa, Kilauea Volcano, Hawaii: field observations and key factors. *Journal of Volcanology and Geothermal Research*, 7: 271-293.

Petrini, R., Civetta, L., Iacumin, P., Longinelli, A., Belliene, G., Comin-Chiaramonti, P., Ernesto, N., Marques, L.S., Melfi, A., Pacca, I., Piccirillo, E.M. 1989. High temperature

flood silicic lavas (?) from the Paraná Basin (Brasil). *New Mexico Bureau of Mines and Mineral Resources Bulletin*, 131: 213.

Petrini, R., Civetta, L., Piccirillo, E.M., Bellieni, G., Comin-Chiaramonti, P., Marques, L.S., Melfi, A.J. 1987. Mantle heterogeneity and crustal contamination in the genesis of low-Ti continental flood basalts from the Paraná plateau (Brazil): Sr-Nd isotope and geochemical evidence. *Journal of Petrology*, 28: 701-726.

Petry, K., Jerram, D.A., Almeida, D.P.M., Zerfass, H. 2007. Volcanic sedimentary features in the Serra Geral Fm., Paraná Basin, southern Brazil: Example of dynamic lava-sediment interactions in an arid setting. *Journal of Volcanology and Geothermal Research*, 159: 313–325.

Piccirillo, E.M., Civetta, L., Petrini, R., Longinelli, A., Bellieni, G., Comin-Chiaramonti, P., Marques, L.S., Melfi, A.J. 1989. Regional variations within the Paraná flood basalts (southern Brazil): evidence for subcontinental mantle heterogeneity and crustal contamination. *Chemical Geology*, 75: 103-122.

Piccirillo, E.M., Raposo, M.I.B., Melfi, A.J., Comin-Chiaramonti, P., Bellieni, G., Cordani, U.G., Kawashita, K. 1987. Bimodal fissural volcanic suites from the Paraná Basin (Brazil): K-Ar age, isotopes and geochemistry. *Geochimica Brasiliensis*, 1(1): 53-69.

Pinkerton, H. & Sparks, R.S.J. 1976. The 1975 sub-terminal lavas, Mount etna: A case history of the formation of a coumpound lava field. *Journal of Volcanology and Geothermal Research*, 1: 176-182.

Pirajno, F. & Hoatson, D.M. 2012. A review of Australia's large igneous provinces and associated mineral systems: implications for mantle dynamics through geological time. *Ore Geology Reviews*, 48: 2–54.

Polo, L.A. & Janasi, V.A. 2014. Volcanic stratigraphy of intermediate to acidic rocks in southern Paraná Magmatic Province, Brazil. *Revista Geologia USP, Série Cientifica*, 14(2): 83-100.

Rampino, M.R. & Haggerty, B.M. 1996. Impact crises and mass extinctions: A working hypothesis. *Geological Society of America Special Papers*, 307: 11-30.

Rampino, M.R. & Stothers, R.B. 1988. Flood basalt volcanism during the past 250 million years. *Science*, 241: 663-668.

Reidel, S.P., Camp, V.E., Ross, M.E., Wolff, J.A., Martin, B.S., Tolan, T.L., Wells, R.E. (Eds.). 2013. The Columbia River Flood Basalt Province. *Geological Society of America, Special Papers*, v. 497.

Reidel, S.P., Tolan, T.L., Hooper, P.R., Beeson, M.H., Fecht, K.R., Bentley, R.D., Anderson, J.L. 1989. The Grande Ronde Basalt, Columbia River Basalt Group; stratigraphic descriptions and correlations in Washington, Oregon and Idaho. In: Reidel, S.P. & Hooper, P.R. (eds.) Volcanism and tectonism in the Columbia River flood-basalt province. *Geological Society of America Special Papers*, 239: 293-306.

Renne, P.R., Ernesto, M., Pacca, I.G., Coe, R.S., Glen, J.M., Prévot, M., Richards, M.A. 1992. The age of the Paraná Flood volcanism, rifting of Gondwanaland, and the Jurassic-Cretaceous boundary. *Science,* 258: 975–979.

Renne, P.R., Glen, J.M., Milner, S.C., Duncan, A.R. 1996. Age of Etendeka Flood volcanism and associated intrusions in southwestern Africa. *Geology*, 24: 659-662.

Renne, P.R., Zichao, Z., Richards, M.A., Black, M.T., Basu, A. 1995. Synchrony and causal relations between Permian-Triassic boundary crises and Siberian Flood volcanism. *Science*, 269: 1413-1415.

Richards, M.A., Duncan, R.A., Courtillot, V.E. 1989. Flood basalts and hot-spot tracks: plume heads and tails. *Science*, 246: 103-107.

Rocha-Júnior, E.R.V., Marques, L.S., Babinski, M., Nardy, A.J.R., Figueiredo, A.M.G., Machado, F.B. 2013. Sr-Nd-Pb isotopic constraints on the nature of the mantle sources involved in the genesis of the high-Ti tholeiites from northern Paraná Continental Flood Basalts (Brazil). *Journal of South American Earth Sciences*, 46: 9-25.

Rocha-Júnior, E.R.V., Puchtel, I.S., Marques, L.S., Walker, R.J., Machado, F.B., Nardy, A.J.R., Babinski, M., Figueiredo, A.M.G. 2012. Re-Os isotope and highly siderophile element systematics of the Paraná Continental Flood Basalts (Brazil). *Earth and Planetary Science Letters*, 337-338: 164-173.

Roisenberg, A. 1989. Petrologia e geoquímica do vulcanismo ácido mesozóico da Província Meridional da Bacia do Paraná. Tese (Doutorado em Geociências-Institutos de Geociências, Curso de Pós-Graduação em Geociências, Universidade Federal do Rio Grande do Sul, Porto Alegre. 285 p.

Roisenberg, A. & Viero, A.P. 2000. O vulcanismo mesozóico da Bacia do Paraná no Rio Grande do Sul. In: Holz, M., De Ros, L.F. (Eds.). Geologia do Rio Grande do Sul. Porto Alegre: Universidade Federal do Rio Grande do Sul. p. 355-374.

Romero, J.A.S., Lafon, J.M., Nogueira, A.C.R., Soares, J.L. 2013. Sr isotope geochemistry and Pb-Pb geochronology of the Neoproterozoic cap carbonates, Tangará da Serra, Brazil. *International Geology Review*, 55: 185-203.

Rossetti, L.M.M., Lima, E.F., Waichel, B.L., Scherer, C.M., Barreto, C.J.S. 2014. Stratigraphical framework of basaltic lavas in Torres Syncline main valley, southern Paraná-Etendeka Volcanic Province. *Journal of South American Earth Sciences*, 56: 409-421.

Rowland, S.K. & Walker, G.P.L. 1987. Toothpaste lava: characteristics and origin of a lava structural type transitional between pahoehoe and aa. *Bulletin of Volcanology*, 52: 631-641.

Rowland, S.K. & Walker, G.P.L. 1990. Pahoehoe and aa in Havaí: volumetric flow rate controls the lava structure. *Bulletin of Volcanology*, 52: 615-628.

Sanford, R.M. & Lange, F.W. 1960. Basin study approach to oil evaluation of Paraná miogeosinclyne of South Brazil. *Bulletin of the American Association of Petroleum Geology*, 44(8): 1316-1370.

Scherer, C.M.S. 1998. Análise Estratigráfica e Litofaciológica da Formação Botucatu (Cretáceo Inferior da Bacia do Paraná) No Rio Grande do Sul. Tese de doutorado em Geociências, Instituto de Geociências, Universidade Federal do Rio Grande do Sul, 202 p.

Scherer, C.M.S. 2000. Eolian dunes of the Botucatu Formation (Cretaceous) in Southernmost Brazil: morphology and origin. *Sedimentary Geology*, 137: 63-84.

Scherer, C.M.S. 2002. Preservation of aeolian genetic units by lava flows in the Lower Cretaceous of the Paraná Basin, southern Brazil. *Sedimentology*, 49: 97-116.

Scherer, C.M.S., Faccini, U.F. and Lavina, E.L. 2000. Arcabouço estratigráfico do Mesozóico da Bacia do Paraná. In: Geologia do Rio Grande do Sul (Eds. Holz , M. & De Ros, L.F.), pp. 335–354. Editora da Universidade/ UFRGS, Porto Alegre.

Schneider, R.L., Muhlmann, H., Tommasi, E., Medeiros, R.A., Daemon, R.F., Nougueira, A. 1974. Revisão estratigráfica da Bacia do Paraná. In: XXIII Congresso Brasileiro de Geologia, Porto Alegre, Anais, Sociedade Brasileira de Geologia, 1: 41-65.

Self, S., Finnemore, S., Hon, K., Keszthelyi, L., Long, P., Murphy, M.T., Thordarson, T., Walker, G.L.P. 1996. A new model for the emplacement of Columbia River basalt as large, inflated pahoehoe lava flows fields. *Geophysical Research Letters*, 23: 2689-92.

Self, S., Jay, A.E., Widdowson, M., Leszthelyi, L.P. 2008. Correlation of the Deccan and Rajahmundry Trap lavas: Are these the longest and largest lava flows on Earth?. *Journal of Volcanology and Geothermal Research*, 172: 3-19.

Self, S., Keszthelyi, L., Thordarson, T. 1998. The importance of pahoehoe. *Annual Review of Earth and Planetary Sciences*, 26: 81-110.

Self, S., Thordarson, T., Keszthelyi, L. 1997. Emplacement of continental flood basalt lava flows. In: Mahoney, J.J.; Coffin, M.L (Eds). Large Igneous Provinces: continental, oceanic, and planetary flood volcanism. *AGU, Geophysics Monography,* 100: 381-410.

Self, S., Thordarson, T., Widdowson, M. 2005. Gas fluxes from flood basalt eruptions. *Elements*, 1: 283–287

Sheth, H.C. 2005. Were the Deccan flood basalts derived impart from ancient oceanic crust within the Indian continental lithosphere?. *Gondwana Research*, 8: 109-127.

Sheth, H.C. 2007. 'Large Igneous Provinces (LIPs)': Definition, recommended terminology, and a hierarchical classification. *Earth-Science Reviews*, 85(3-4): 117-124.

Sheth, H.C. & Vanderkluysen, L. 2014. Flood basalts of Asia. *Journal of Asian Earth Sciences, Special Issue*, 84: 1–200.

Silva, D.R.A., Mizusaki, A.M.P., Anjos, S.M.C., Koester, E., Borba, A.W. 2006. Provenance of fine-grained sedimentary rocks derived from Rb-Sr and Sm-Nd analyses: the example of the Santa Maria Formation (Triassic, Paraná Basin, Southern Brazil). *Latin American Journal of Sedimentology and Basin Analysis*, 13(2): 135-149.

Single, R.T. & Jerram, D.A. 2004. The 3D facies architecture of flood basalt provinces and their internal heterogeneity: examples from the Palaeogene Skye Lava Field. *Journal of the Geological Society of London*, 161: 911-926.

Soares, P.C. 1975. Divisão estratigráfica do Mesozóico no Estado de São Paulo. *Revista Brasileira de Geociências*, 5(4): 229-251.

Sobolev, S.V., Sobolev, A.V., Kuzmin, D.V., Krivolutskaya, N.A., Petrunin, A.G., Arndt, N.T., Radko, V.A., Vasiliev, Y.R. 2011. Linking mantle plumes, large igneous provinces and environmental catastrophes. *Nature*, 477: 312–316.

Soule, S.A. & Cashman, K.V. 2005. Shear rate dependence of the pāhoehoe-to- 'a'ā transition: analog experiments. *Geological Society of America Bulletin,* 33: 361-364

Sruoga, P. & Rubinstein, N. 2007. Processes controlling porosity and permeability in volcanic reservoirs from the Austral and Neuquén basins, Argentina. *AAPG Bulletin*, 91: 115-129.

Sruoga, P., Rubinstein, N., Hinterwimmer, G. 2004. Porosity and permeability in volcanic rocks: a case study on the SerieTobífera, South Patagonia, Argentina. *Journal of Volcanology and Geothermal Research*, 132: 31-43.

Storey, M., Duncan, R.A., Tegner, C. 2007. Timing and duration of volcanism in the North Atlantic Igneous Province: implications for geodynamics and links to the Iceland hotspot. *Chemical Geology*, 241: 264–281.

Storey, B.C., Vaughan, A.P.M., Riley, T.R. 2013. The links between large igneous provinces, continental break-up and environmental change: evidence reviewed from Antarctica. *Transactions of the Royal Society, Edinburgh*, 104: 17–30.

Svensen, H., Corfu, F., Polteau, S., Hammer, Ø., Planke, S. 2012. Rapid magma emplacement in the Karoo Large Igneous Province. *Earth and Planetary Science Letters*, 325–326: 1–9.

Swanson, D.A., Wright, TL., Helz, R.T. 1975. Linear vent systems and estimated rates of magma production and eruption for the Yakima basalt on the Columbia Plateau. *American Journal of Science*, 275: 877-905.

Thiede, D.S. & Vasconcelos, P.M. 2010. Paraná flood basalts: rapid extrusion hypothesis confirmed by new 40Ar/39Ar results. *Geology*, 38: 747–750.

Thordarson, T. 2006. Emplacement of mafic lava flows: role of insulated transport and inflation. *Geophysical Research Abstracts of European Geosciences Union*, 8: 10124.

Thordarson, T., Rampino, M., Keszthelyi, L., Self, S. 2009. Effects of megascale eruptions on Earth and Mars. In: Chapman, M.G., Keszthelyi, L.P. (Eds.). Preservation of random megascale events on Mars and Earth: Influence on geologic history. *Geological Society of America Special Paper*, 453: 37-55

Thordarson, T. & Self, S. 1998. The Roza Member; Columbia River Basalt Group: a gigantic pahoehoe lava flow field formed by endogenous processes?. *Journal of Geophysical Research*, 103: 27411-27445.

Tolan, T.L., Reidel, S.P., Beeson, M.H., Anderson, J.L., Fecht, K.R., Swanson, D. 1989. Revisions to the estimates of the areal extent and volume of the Columbia River Flood Basalt Province: In Reidel, S.P.; Hooper, P.R. (Eds.). Volcanism and tectonism in the

Columbia River flood–basalt province. *Special Paper of the Geological Society of America*, 239: 1-20.

Tomlinson, K.Y. & Condie, K.C. 2001. Archean mantle plumes: evidence from greenstone belt geochemistry. In Ernst, R.E. & Buchan, K.L. (Eds.). Mantle Plumes: Their Identification through Time. *Geological Society of America, Special Paper*, 352: 341–357.

Turner, S., Regelous, M., Kelley, S., Hawkesworth, C.J., Mantovani, M.S.M. 1994. Magmatism and continental break-up in the South Atlantic: high precision $^{40}Ar/^{39}Ar$ geochronology. *Earth and Planetary Science Letters*, 121: 333-348.

Ukstins Peate, I., Baker, J.A., Al-Kadasi, M., Al-Subbary, A., Knight, K.B., Riisager, P., Thirlwall, M.F., Peate, D.W., Renne, P.R., Menzies, M.A. 2005. Volcanic stratigraphy of large-volume silicic pyroclastic eruptions during Oligocene Afro Arabian flood volcanism in Yemen. *Bulletin of Volcanology*, 68: 135-156.

Umann, L.V., Lima, E.F., Sommer, C.A., Liz, J.D. 2001. Vulcanismo ácido da região de Cambará do Sul-RS: litoquímica e discussão sobre a origem dos depósitos. *Revista Brasileira de Geociências*, 31(3): 357-364.

Vail, P.R., Mitchum, R.M.Jr., Thompson, S. 1977. Seismic stratigraphy and global changes of sea level, part four: global cycles of relative changes of sea level. *American Association of Petroleum Geologists Memoir*, 26: 83-98.

Vye-Brown, C., Gannoun, A., Barry, T.L., Self, S., Burton, K.W. 2013a. Osmium isotope variations accompanying the eruption of single lava flow field in the Columbia River Flood Basalt Province. *Earth and Planetary Science Letters*, 368: 183–194.

Vye-Brown, C.L., Self, S., Barry, T.L. 2013b. The architecture and emplacement of flood basalt flow fields: case studies from the Columbia River flood basalts, USA. *Bulletin of Volcanology*, 75(3): 1–21.

Waichel, B.L., Lima, E.F., Lubachesky, R., Sommer, C.A. 2006a. Pahoehoe flows from the central Paraná Continental Flood Basalts. *Bulletin of Volcanology*, 68: 599-610.

Waichel, B.L.; Lima, E.F.; Sommer, C.A. 2006b. Tipos de Derrame e Reconhecimento de Estruturas nos Basaltos da Formação Serra Geral: Terminologia e Aspectos de Campo. *Pesquisas em Geociências*, 33(2): 123-133.

Waichel, B.L., Lima, E.F., Viana, A., Scherer, C.M.S., Bueno, G., Dutra, G.T. 2012. Stratigraphy and volcanic facies architecture of the Torres Syncline, Southern Brazil,

and its role in understanding the Paraná-Etendeka Continental Flood Basalt Province. *Journal of Volcanology and Geothermal Research*, 215: 74-82.

Waichel, B.L., Scherer, C.M.S., Frank, H.T. 2008. Basaltic lava flows covering active aeolian dunes in the Paraná Basin in southern Brazil: Features and emplacement aspects. *Journal of Volcanology and Geothermal Research*, 171: 59-72.

Walker, G.P.L. 1971. Compound and simple lava flows and flood basalts. *Bulletin Volcanologique*, 35: 579-590.

Walker, G.P.L. 1973. Lengths of lava flows. *Philosophical Transactions of the Royal Society of London*, 274: 107-118.

Walker, R.G. 1984. Shelf and shallow marine sands. In: Walker, R.G., (Eds.). Facies models (2nd. Edition). Geological Association of Canada, Geoscience Canada Reprint Series, 1: 141-170.

Walker, G.P.L. 1989. Spongy pahoehoe in Hawaii: A study of vesicle distribution patterns in basalt and their significance. *Bulletin of Volcanology*, 51: 199-209.

Walker, R.G. 1992. Facies, facies models and modern stratigraphic concepts. In: Walker, R.G. & James, N.P. (Eds.). Facies Models: Response to Sea Level Change, GeoText 1. Geological Association of Canada, pp. 1-14.

Wallace, P.J., Frey, F.A., Weis, D., Coffin, M.F. 2002. Origin and evolution of the Kerguelen Plateau, Broken Ridge and Kerguelen Archipelago: editorial. *Journal of Petrology*, 43: 1105–1108.

Wang, P., Chen, S., Liu, W., Shan, X., Cheng, R., Zhang, Y., Wu, H., Qi, J. 2003. Relationship between volcanic facies and volcanic reservoirs in Songliao basin. *Oil Gas Geology*, 24:18–23 (in Chinese with English abstract).

White, I.C. 1908. Relatório Final da Comissão de Estudos das Minas de Carvão de Pedra do Brasil. Rio de Janeiro: DNPM, 1988. Parte I; Parte II, p. 301-617. (ed. Fac-similar).

White, R. & McKenzie, D. 1989. Magmatism at rift zones: The generation of volcanic continental margins and flood basalts. *Journal of Geophysical Research*, 94: 7685-7729.

White, R.S. & McKenzie, D. 1995. Mantle plumes and flood basalts. *Journal of Geophysical Research*, 100(B9): 17543–17585.

Whittingham, A.M. 1989. Geological features and geochemistry of the acid units of the Serra Geral Formation, south Brazil. *IAVCEI abstracts:* Santa Fé, New México, 293 p.

Wignall, P.B. 2001. Large igneous provinces and mass extinctions. *Earth-Science Reviews*, 53: 1-33.

Wignall, P.B. 2005. The link between Large Igneous Province eruptions and mass extinctions. *Elements*, 1: 293–297.

Wilmoth, R.A. & Walker, G.P.L. 1993. P-type and S-type pahoehoe: A study of vesicle distribution patterns in Hawaiian lava flows. *Journal of Volcanology and Geothermal Research*, 55: 129-142.

Wu, C., Gu, L., Zhang, Z., Ren, Z., Chen, Z., Li, W. 2006. Formation mechanisms of hydrocarbon reservoirs associated with volcanic and subvolcanic intrusive rocks: examples in Mesozoic–Cenozoic basins of eastern China. *AAPG Bulletin*, 90: 137–147.

Xu, Y.G., He, B., Chung, S.L., Menzies, M.A., Frey, F.A. 2004. Geologic, geochemical, and geophysical consequences of plume involvement in the Emeishan flood-basalt province. *Geology*, 32: 917–920.

Zalán, P.V., Wolff, S., Conceição, J.C.J., Astolfi, M.A.M., Vieira, I.S. 1987. Tectônica e sedimentação da Bacia do Paraná. In: Simpósio Sul- Brasileiro de Geologia, 3., Curitiba. Atas... Porto Alegre: Sociedade Brasileira de Geologia, 1: 441-477.

Zhao, J.X., Malcolm, M.T., Korsch, R.J. 1994. Characterisation of a plume- related c. 800 Ma magmatic event and its implications for basin formation in central-southern Australia. *Earth and Planetary Science Letters*, 121: 349–367.

Zuffa, G.G. 1980. Hybrid Arenites: their composition and classification. *Journal of Sedimentary Petrology*, 50(1): 21-29.

ANEXOS

CARTAS DE SUBMISSÃO E ACEITE DOS ARTIGOS

ANEXO A

Carta de resubmissão do artigo intitulado: “Vesicle-rich segregation structures and recongnition of primary and secondary porosities in pahoehoe and rubbly lava flows of the Paraná igneous province, Southern Brazil” para o periódico Bulletin of Volcanology.

BV Acknowledgement of Submission

Bulletin of Volcanology Adicionar aos contatos 08/11/2015
Para: Carla Barreto

Dear Miss Barreto,

We acknowledge, with thanks, receipt of the proposed Research Article "Vesicle-rich segregation structures and recognition of primary and secondary porosities in pahoehoe and rubbly lava flows of the Paraná igneous province, Southern Brazil".

James White, Executive Editor, will assess the suitability of your manuscript for submission to the journal and if his decision is favourable we will then assign an Associate Editor to handle the paper.

You may check on the progress of your paper by logging onto Editorial Manager as an author:
http://buvo.edmgr.com/.
Your username is: cjbarreto
Your password is: available at this link http://buvo.edmgr.com/Default.aspx?pg=accountFinder.aspx&firstname=Carla&lastname=Barreto&email_address=carlabarreto.geo@hotmail.com

We expect to be able to contact you again shortly.

Sincerely,

Bulletin of Volcanology
bull.volc@otago.ac.nz

ANEXO B

Carta de aceite para publicação do artigo intitulado: “Geochemical and Sr–Nd–Pb isotopic insights of the low-Ti basalts from southern Paraná Igneous Province, Brazil: the role of crustal contamination” no periódico International Geology Review.

International Geology Review - Decision on Manuscript ID TIGR-2015-0277.R1

rjstern@utdallas.edu Adicionar aos contatos 03:23
Para: carlabarreto.geo@hotmail.com

25-Jan-2016

Dear Miss Barreto:

Ref: Geochemical and Sr–Nd–Pb isotopic insights of the low-Ti basalts from southern Paraná Igneous Province, Brazil: the role of crustal contamination

I have now considered your revised manuscript and am pleased to accept your paper in its current form which will now be forwarded to the publisher for copy editing and typesetting. The reviewer comments are included at the bottom of this letter.

You will receive proofs for checking, and instructions for transfer of copyright in due course.

The publisher also requests that proofs are checked through the publisher's tracking system and returned within 48 hours of receipt.

Thank you for your contribution to International Geology Review, we value your research. Please do check that your institution has access to the journal, and if not encourage them to subscribe. We also offer personal subscriptions if you would like to receive your own copy. Visit our subscription page for more information http://www.tandfonline.com/pricing/journal/tigr20

We look forward to receiving further submissions from you.

Sincerely,
Dr Robert J. Stern
Editor-in-Chief, International Geology Review

ARTIGOS CIENTÍFICOS PUBLICADOS

ANEXO C

Rossetti, L.M., Lima, E.F., Waichel, B.L., Scherer, C.M., Barreto, C.J.S. 2014. Stratigraphical framework of basaltic lavas in Torres Syncline main valley, Southern Paraná-Etendeka Volcanic Province. *Journal of South American Earth Sciences*, 56: 409-421.

Journal of South American Earth Sciences 56 (2014) 409–421

Contents lists available at ScienceDirect

Journal of South American Earth Sciences

journal homepage: www.elsevier.com/locate/jsames

Stratigraphical framework of basaltic lavas in Torres Syncline main valley, southern Parana-Etendeka Volcanic Province

Lucas M. Rossetti [a, *], Evandro F. Lima [a], Breno L. Waichel [b], Claiton M. Scherer [a], Carla J. Barreto [a]

[a] Instituto de Geociências, Universidade Federal do Rio Grande do Sul, Av. Bento Gonçalves, 9500, Prédio 43136, Caixa Postal 15001, Agronomia, CEP: 91501-970 Porto Alegre, RS, Brazil
[b] Universidade Federal de Santa Catarina e UFSC, Campus Universitário Trindade, CEP 88.040-900 Florianópolis, Santa Catarina, Brazil

ARTICLE INFO

Article history:
Received 10 January 2014
Accepted 23 September 2014
Available online 15 October 2014

Keywords:
Continental Basaltic Provinces
Lava morphologies
Lava emplacement
SE Brazil

ABSTRACT

The Paraná-Etendeka Volcanic Province records the volcanism of the Early Cretaceous that precedes the fragmentation of the South-Gondwana supercontinent. Traditionally, investigations of these rocks prioritized the acquisition of geochemical and isotopic data, considering the volcanic stack as a monotonous succession of tabular flows. Torres Syncline is a tectonic structure located in southern Brazil and where the Parana-Etendeka basalts are well preserved. This work provides a detailed analysis of lithofacies and facies architecture, integrated to petrographic and geochemical data. We identified seven distinct lithofacies grouped into four facies associations related to different flow morphologies. The basaltic lava flows in the area can be divided into two contrasting units: Unit I - pahoehoe flow fields; and Unit II - simple rubbly flows. The first unit is build up by innumerous pahoehoe lava flows that cover the sandstones of Botucatu Formation. These flows occur as sheet pahoehoe, compound pahoehoe, and ponded lavas morphologies. Compound lavas are olivine-phyric basalts with intergranular pyroxenes. In ponded lavas and cores of sheet flows coarse plagioclase-phyric basalts are common. The first pahoehoe lavas are more primitive with higher contents of MgO. The emplacement of compound pahoehoe flows is related to low volume eruptions, while sheet lavas were emplaced during sustained eruptions. In contrast, Unit II is formed by thick simple rubbly lavas, characterized by a massive core and a brecciated/rubbly top. Petrographically these flows are characterized by plagioclase-phyric to aphyric basalts with high density of plagioclase crystals in the matrix. Chemically they are more differentiated lavas, and the emplacement is related to sustained high effusion rate eruptions. Both units are low TiO_2 and have geochemical characteristics of Gramado magma type. The Torres Syncline main valley has a similar evolution when compared to other Large Igneous Provinces, with compound flows at the base and simple flows in the upper portions. The detailed field work allied with petrography and geochemical data are extremely important to identify heterogeneities inside the volcanic pile and allows the construction of a detailed lithostratigraphical framework.

1. Introduction

Large Igneous Provinces (LIPs) represent major events in the Earth's history. In a relatively short time span, huge volumes of lavas and related intrusions are generated and accumulated over large surfaces (Coffin and Eldholm, 1994; Bryan et al., 2010). Part of the LIPs are Continental Basaltic Provinces (CBPs), which, according to $^{40}Ar/^{39}Ar$ geochronological data (Siberian Plateau, Karoo/Ferrar, Deccan, Columbia River, Paraná-Etendeka, Ethiopian Plateau, CAMP) were characterized by volumes of the 10^5–10^7 km^3 range in short time intervals (~10^5–10^6 years). The formation of these provinces is related to thermal anomalies at the base of the lithosphere and the subsequent rifting of continents (Morgan, 1972; White and McKenzie, 1995).

The Parana-Etendeka is one of the largest magmatic episodes that occurred in Earth history. It preceded the rift of South Gondwana and the opening of the South Atlantic Ocean. The age of magmatism is Early Cretaceous and Ar–Ar ages range from 138 to 125 Ma, with a marked eruption peak at 133–129 Ma. According to

* Corresponding author. Tel.: +55 51 33087380.
E-mail addresses: lucasross@hotmail.com, lucas.rossetti@ufrgs.br (L.M. Rossetti), evandro.lima@ufrgs.br (E.F. Lima).

http://dx.doi.org/10.1016/j.jsames.2014.09.025
0895-9811/

ANAIS DE CONGRESSOS E SIMPÓSIOS

ANEXO D

Barreto, C.J.S. & Lima, E.F. 2012. Padrões morfológicos e de *emplacement* dos vulcanitos da Formação Serra Geral no nordeste do estado do Rio Grande do Sul (RS). In: II Workshop interno PRH PB 15, Porto Alegre.

II WORKSHOP INTERNO PRH PB 15

PADRÕES MORFOLÓGICOS E DE EMPLACEMENT DOS VULCANITOS DA FORMAÇÃO SERRA GERAL NO NORDESTE DO ESTADO DO RIO GRANDE DO SUL (RS)

Carla Joana Santos Barreto

Orientador: Evandro Fernandes de Lima

RESUMO

Estudos sobre as características morfológicas e estruturas dos derrames de Províncias Basálticas Continentais são indispensáveis na interpretação da dinâmica e volume dos fluxos de lava, na identificação dos tipos de depósitos gerados e na determinação das consequências ambientais relacionadas. No Brasil este enfoque tem sido negligenciado sendo priorizada uma abordagem geoquímica e geocronológica no estudo da Província Magmática Paraná-Etendeka. Estes métodos geralmente não consideram a morfologia e a estruturação dos derrames, pouco contribuindo para correlações estratigráficas e para a percepção do impacto e evolução destes mega eventos vulcânicos.

Dessa forma, o principal objetivo dessa tese é investigar os aspectos físicos dos derrames da Formação Serra Geral e consequentemente, compor um novo arcabouço estratigráfico para esta unidade, no nordeste do estado do Rio Grande do Sul, levando-se em consideração a associação e arquitetura de fácies, com o propósito de estimar as condições que atuaram no preenchimento da bacia durante as diversas manifestações vulcânicas. Os objetivos específicos consistem em identificar estruturas e texturas preservadas nos derrames basálticos da Formação Serra Geral com o propósito de caracterizar e individualizar os tipos de derrames; estabelecer a relação e estruturação destes com os arenitos da Formação Botucatu; individualizar a arquitetura de fácies vulcânicas e os parâmetros físicos do vulcanismo, tais como o sentido de fluxo desses derrames e as taxas de efusão; compreender a paleotopografia e a evolução geológica da área durante os episódios vulcânicos. Como objetivo complementar, pretende-se testar a eficácia do método gamaespectrométrico na caracterização e individualização de diferentes fácies dos derrames basálticos continentais, além de auxiliar na correlação desses derrames com fácies subaquosas que podem estar associadas com hidrocarbonetos.

ANEXO E

Barreto, C.J.S. & Lima, E.F. 2013. Caracterização dos padrões de vesiculação dos basaltos *pahoehoe* da Formação Serra Geral na região de Santa Cruz do Sul (RS) e implicações para porosidade e permeabilidade em rochas vulcânicas. In: Reunião Anual de Avaliação PRH's, Aracaju.

CARACTERIZAÇÃO DOS PADRÕES DE VESICULAÇÃO DOS BASALTOS *PAHOEHOE* DA FORMAÇÃO SERRA GERAL NA REGIÃO DE SANTA CRUZ DO SUL (RS) E IMPLICAÇÕES PARA POROSIDADE E PERMEABILIDADE EM ROCHAS VULCÂNICAS

Carla Joana Santos Barreto[1], Evandro Fernandes de Lima[1]

Bolsista PRH-PB 215, carlabarreto.geo@hotmail.com, [1]Universidade Federal do Rio Grande do Sul.

RESUMO

MOTIVAÇÃO: Os padrões de vesiculação são em geral descritos como típicos e restritos ao topo dos derrames. Nos basaltos subaéreos a vesiculação pode gerar padrões muito complexos. Estes estão relacionados aos tipos morfológicos das lavas e a estruturação dos derrames. Em Ã'ã as vesículas (< 20%), são alongadas e irregulares especialmente no topo dos fluxos onde o resfriamento e a desvolatização são bruscos. Em *pahoehoe* as vesículas são abundantes (20 a 60%) e o confinamento do núcleo promove um resfriamento lento favorecendo ascensão e coalescência das bolhas.

OBJETIVO: Identificar e classificar macroscopicamente e microscopicamente os padrões de vesiculação em basaltos pahoehoe da Formação Serra Geral (FSG) na região de Santa Cruz do Sul para estabelecer os parâmetros petrofísicos.

APLICAÇÃO NA INDÚSTRIA DO PETRÓLEO: A vesiculação em fluxos básicos subaéreos pode gerar padrões de porosidade e permeabilidade distintos, muitas vezes associados à microfraturas geradas durante a contração e resfriamento das lavas. As análises das morfologias das vesículas permitem estimar a porosidade e permeabilidade dos derrames. A porosidade pode ser primária ou secundária e permeabilidade, dependendo da litologia, está sujeita a modificações por processos *sin* e pós emplacement das lavas. A identificação dos padrões e processos são úteis para definir as características de um reservatório.

RESULTADOS OBTIDOS: Os basaltos *pahoehoe* da FSG de Santa Cruz do Sul (RSC-153) são compostos (lobos do tipo P e S) e simples. Nestes últimos são identificadas *sheet vesicles* (S1= de 15 a 50 cm) no topo; vesículas de segregação (V1= 1 a 3 mm nas *sheet vesicles* S1); *pipe vesicles* (V2) de 2 a 7 cm comprimento na base. Nos derrames mais espessos (3 e 8 m) observa-se uma variedade de padrões de vesiculação. *Vesicle cylinders* (C) de 50 cm a 3 m distribuem-se desde o núcleo até a metade inferior; proto *cylinder* (proto-C) ocorrem acima dos *pipe vesicles*, e cilindros tipo S-C ocorrem na metade inferior do núcleo dos derrames. *Sheet vesicles* (S1) de 2 a 3 m concentram-se no topo dos derrames; *sheet vesicles* (S2) de 2 a 15 cm são horizontalmente descontínuas e estão posicionadas na metade inferior dos derrames. Vesículas de segregação (V1) de 0,2 a 10 cm ocorrem tanto no núcleo microvesiculado (textura diktytaxítica) como nas S1. *Pipe vesicles*, com até 10 cm de comprimento, ocorrem na base dos derrames; nos *pods*, as vesículas (0,02-30 cm) começam na metade superior do núcleo até o limite com o topo vesiculado dos derrames.

Palavras-chave: Formação Serra Geral; Basaltos *pahoehoe*; padrões de vesiculacão; porosidade e permeabilidade; rochas vulcânicas.

ANEXO F

Barreto, C.J.S. & Lima, E.F. 2013. Os padrões de vesiculação dos basaltos *pahoehoe* da Formação Serra Geral na região de Santa Cruz (RS). In: VIII Simpósio Sul-Brasileiro de Geologia, Porto Alegre.

Os padrões de vesiculação dos basaltos *pahoehoe* da Formação Serra Geral na região de Santa Cruz do Sul (RS)

[1]Carla Joana Santos Barreto, [1]Evandro Fernandes de Lima.
[1]UFRGS.

Palavras-chave: morfologia, padrões de vesiculação, basaltos.

A investigação dos padrões de vesiculação em geral tem um papel coadjuvante no estudo de basaltos sendo genericamente descritos como típicos de topos dos derrames. No entanto, o processo de vesiculação em fluxos básicos subaéreos pode gerar padrões bastante complexos. Estes são compatíveis com os diferentes tipos morfológicos das lavas tornando possível o uso na estruturação e identificação dos tipos de derrames. Nos basaltos *'a'ā* as vesículas são pouco abundantes (< 20%), com morfologias alongadas e irregulares especialmente no topo dos fluxos onde o resfriamento e a desvolatização são bruscos. Em contrapartida, em *pahoehoe* as vesículas são abundantes (20 a 60%) e o confinamento do núcleo do derrame promove um resfriamento mais lento, possibilitado tentativas de ascensão das bolhas e coalescência. No presente trabalho são descritos os padrões de vesiculação dos basaltos da Formação Serra Geral expostos na RSC-153 entre a cidade de Santa Cruz do Sul e Herveiras. O objetivo é de identificar e, posteriormente, investigar a origem de cada padrão de vesiculação e a sua relação com os parâmetros petrofísicos das rochas. Derrames *pahoehoe* da base da sequência estudada estão em contato deposicional com a Formação Botucatu e em contato tectônico com a Formação Santa Maria. Os *pahoehoe* são compostos, tendo os lobos do tipo P espessuras de 50 cm a 8 m e 1 m nos lobos do tipo S. Em ambos são comuns feições de superfície em corda. Identificou-se nos *pahoehoe* padrões de vesiculação do tipo *vesicle cylinder*, corpos alongados com seções ortogonais circulares, preenchidos com material de segregação vesicular; proto *cylinder* gerados pelo mesmo processo, formando uma trilha incompleta de vesículas; cilindros do tipo S-C, um tipo de *vesicle cylinder* que intercepta *sheet vesicles* (tipo S2); *sheet vesicles*, que são estreitas camadas preenchidas com material de segregação vesicular; *pods*, bolsões com concentrações >10% de vesículas; *pipe vesicles* (V2), vesículas em forma de tubos verticais, típicas da base dos fluxos *pahohoe*; vesículas de segregação, cavidades esféricas preenchidas por materiais de segregação. Nos lobos (2 m) observa-se uma variação pequena nos padrões de vesiculação, onde são identificadas *sheet vesicles* (S1) de 15 a 50 cm no topo; vesículas de segregação (V1) de 1 a 3 mm inseridas nas *sheet vesicles* (S1); *pipe vesicles* (V2) de 2 a 7 cm que marcam a base dos derrames. Lobos maiores (3 e 8 m) possuem uma variedade maior de padrões de vesiculação. *Vesicle cylinders* (C) de 50 cm a 3 m ocorrem desde o núcleo até a metade inferior dos mesmos; proto *cylinder* (proto-C) ocorrem acima dos *pipe vesicles*, e cilindros tipo S-C ocorrem na metade inferior do núcleo dos derrames; *sheet vesicles* (S1) de 2 a 3 m concentram-se no topo dos derrames; *sheet vesicles* (S2) de 2 a 15 cm são horizontalmente descontínuas e estão posicionadas na metade inferior dos derrames; vesículas de segregação (V1) de 0,2 a 10 cm estão posicionadas tanto no núcleo microvesiculado com textura diktytaxitica, quanto inseridas nas S1; *pipe vesicles* até 10 cm de altura são encontradas na base dos derrames; nos *pods* as vesículas (0,02-30 cm) começam a aparecer na metade superior do núcleo até o limite com o topo vesiculado dos derrames. A origem desses padrões de vesiculação pode estar associada a ascensão por *filter pressing* de voláteis e líquidos remanescentes. O padrão de vesiculação nos *pahoehoe* está relacionado com as espessuras dos lobos e estilos de *emplacement* e marcam a base, núcleo e topo dos derrames. As análises das morfologias das vesículas (micro e macro), bem como o volume destas permitirão calcular a porosidade e permeabilidade dos derrames *pahoehoe*.

ANEXO G

Barreto, C.J.S., Pasqualon, N. G., Lima, E.F., Rossetti, M.M.M., Rossetti, L.M.M., Simon, L. 2014. Padrões de vesiculação dos basaltos *pahoehoe* da Formação Serra Geral na região de Santa Cruz do Sul (RS): implicações para porosidade e permeabilidade em sistemas vulcânicos. In: 47º Congresso Brasileiro de Geologia, Salvador.

47º CONGRESSO BRASILEIRO DE GEOLOGIA 21 a 26 / setembro / 2014 Salvador ★ Bahia

PADRÕES DE VESICULAÇÃO DOS BASALTOS *PAHOEHOE* DA FORMAÇÃO SERRA GERAL NA REGIÃO DE SANTA CRUZ DO SUL (RS): IMPLICAÇÕES PARA POROSIDADE E PERMEABILIDADE EM SISTEMAS VULCÂNICOS

Carla J. S. Barreto[1]; Natália G. Pasqualon[1]; Evandro Fernandes de Lima[1] Marcos Rossetti[1] Lucas M. Rossetti[1]; Larissa Simon[1],

[1]Universidade Federal do Rio Grande do Sul

RESUMO: A investigação dos padrões de vesiculação em geral tem um papel coadjuvante no estudo de derrames básicos subaéreos sendo genericamente descritos como típicos de topos dos derrames. Os processos de vesiculação nesses derrames são, no entanto, bastante complexos e compatíveis com os diferentes tipos morfológicos das lavas. Logo os padrões de vesiculação podem auxiliar na estruturação e identificação dos tipos de derrames básicos. O objetivo deste resumo é tipificar os padrões de vesiculação dos basaltos da Formação Serra Geral da ombreira sul da Sinclinal de Torres e relacioná-los com a porosidade e permeabilidade destas rochas. Os primeiros derrames *pahoehoe* são compostos, tendo lobos do tipo P (50 cm a 2 m) e do tipo S (~50 cm). Ocorrem associados diques de areia e arenitos intercalados. Nos lobos são identificados topos vesiculados de até 50 cm, cujas vesículas de segregação (V1) possuem diâmetro de 1 a 3 mm*; pipe vesicles* (V2) de 2 a 7 cm marcam a base dos derrames. Derrames *pahoehoe* tabulares e mais espessos possuem uma variedade maior de padrões de vesiculação. *Vesicle cylinders* (C) de 50 cm a 3 m ocorrem desde o núcleo até a metade inferior dos mesmos; *proto cylinder* (proto-C) ocorrem acima dos pipe vesicles; cilindros S-C ocorrem na metade inferior do núcleo dos derrames; *sheet vesicles* (S1) de 7 a 10 cm concentram-se no topo dos derrames; *sheet vesicles* (S2) 2 a 15 cm são horizontalmente descontínuas e estão posicionadas no núcleo dos derrames; vesículas dômicas gigantes (V3) até 1 m estão posicionadas na porção superior do núcleo juntamente com *pods* (V4) de até 30 cm que englobam V1; vesículas de segregação (V1) <1 cm estão distribuídas por todas as partes do derrames; *pipe vesicles* (V2) até 13 cm de altura são encontrados na base. Foram definidos para os basaltos *pahoehoe* porosidades vesicular, intracristalina em plagioclásio e olivina, intercristalina, de dissolução de zeólitas que preenchem amígdalas, dissolução de esmectita que preenche as cavidades *dyktitaxiticas*, porosidade de fratura em cristal de olivina, porosidade vugular e de dilatação. A conexão das vesículas por fraturamentos tardios comuns pode criar espaços efetivos para a migração de fluidos (p.ex hidrocarbonetos). Amígdalas preenchidas por minerais secundários diminuem a porosidade total dos derrames. Processos posteriores como intemperismo, dissolução de fraturas, amígdalas e minerais secundários, podem contribuir no aumento da microporosidade e permeabilidade da rocha, devido ao alargamento desses espaços. A porosidade das lavas estudadas está relacionada à quantidade de vesículas que compõe o topo e base dos derrames e às microfraturas associadas ao resfriamento rápido dos núcleos. Os estudos das morfologias das vesículas (micro e macro) dos basaltos *pahoehoe* da Formação Serra Geral expostos na RSC-153 entre a cidade de Santa Cruz do Sul e Herveiras permitiram caracterizar os tipos de porosidade dos derrames *pahoehoe*. O reconhecimento desses processos é necessário para definir a qualidade de um possível reservatório. Os diques e camadas de arenitos, abundantes na área de estudo, também podem servir como condutos para possíveis reservatórios.

PALAVRAS-CHAVE: FORMAÇÃO SERRA GERAL; BASALTOS *PAHOEHOE*; PADRÕES DE VESICULAÇÃO.

ANEXO H

Rossetti, L.M., Lima, E.F., Waichel, B.L., Scherer, C.M.S., Barreto, C.J.S. 2014. Arcabouço estratigráfico da Formação Serra Geral no vale principal da Sinclinal de Torres. In: 47º Congresso Brasileiro de Geologia, Salvador.

47º CONGRESSO BRASILEIRO DE GEOLOGIA
21 a 26 / setembro / 2014
Salvador ★ Bahia

ARCABOUÇO ESTRATIGRÁFICO DA FORMAÇÃO SERRA GERAL NO VALE PRINCIPAL DA SINCLINAL DE TORRES

Rossetti, L.M.[1]; Lima, E.F.[1]; Waichel, B.L.[2]; Scherer, C.M.S.[1]; Barreto, C.J.[1]

[1]Universidade Federal do Rio Grande do Sul; [2]Universidade Federal de Santa Catarina

RESUMO: A Sinclinal de Torres é uma estrutura tectônica localizada na porção sul do Brasil onde ocorrem preservadas as seqüência vulcânicas do magmatismo Paraná-Etendeka, denominados Formação Serra Geral. A Província Basáltica Continental do Paraná-Etendeka registra o intenso vulcanismo do Cretáceo inferior que precedeu a fragmentação do supercontinente Gondwana. Tradicionalmente investigações sobre estas rochas priorizaram a aquisição de dados geoquímicos e isotópicos, considerando a pilha vulcânica como uma monótona sucessão de derrames tabulares e espessos. O presente trabalho propõe a análise das características físicas deste vulcanismo aplicando conceitos de arquitetura de fácies vulcânicas, integrados a estudos petrográficos e geoquímicos. A área de estudo localiza-se na região nordeste do estado do Rio Grande do Sul, no vale principal da Sinclinal de Torres. Neste estudo foram analisadas as seqüência vulcânicas basálticas da Formação Serra Geral que recobrem os arenitos eólicos da Formação Botucatu e estão abaixo das unidades vulcânicas ácidas, para tal foram desenvolvidos dois perfis ao longo das rodovias BR-116 entre as cidades de Dois Irmãos e Caxias do Sul, e RS-122, entre as cidades de Feliz e Farroupilha. Neste contexto as rochas vulcânicas básicas podem ser divididas em duas unidades: derrames e campos de derrames *pahoehoe* (Unidade I), que ocorre entre cotas de 35 to 290 m, e derrames simples do tipo r*ubbly* (Unidade II), que afloram entre 290 e 530 metros de cota. Geoquimicamente as duas unidades pertencem a serie de baixo- TiO_2 e ao magma tipo Gramado. As primeiras lavas *pahoehoe* são olivina basaltos, mais primitivos e apresentam os maiores teores de MgO. A unidade I é composta por inúmeros derrames *pahoehoe* que ocorrem sobre os arenitos eólicos da Formação Botucatu. Essas lavas ocorrem como *shee*t pahoehoe, *compound* lavas, e lavas do tipo *ponded* nos vales interduna. O *emplacement* dessas lavas esta relacionado a baixas taxas de erupção sustentadas por longos intervalos de tempo em relevo com paleotopografia relativamente plana. A unidade II é formada por espessas lavas simples, com até 50 metros, do tipo *rubbly*, estas são caracterizadas por topo fragmentado (*rubbly tops*), porção superior de topo coerente vesiculada, núcleo maciço, e base vesiculada. Essas lavas são formadas por altas taxas de erupção e durante a fase principal do vulcanismo na área, onde as maiores quantidades de magma atingem a superfície em um curto intervalo de tempo. O vale principal da Sinclinal de Torres tem uma evolução formada por derrames compostos na porção basal e derrames simples nas porções superiores, similar a de outras Províncias Basálticas Continentais como o Deccan e o Columbia River.

PALAVRAS-CHAVE: PROVÍNCIA BASÁLTICA CONTINENTAL; EMPLACEMENTE DE LAVAS; ESTRATIGRAFIA DE VULCÂNICAS;

ANEXO I

Simon, L., Rossetti, M., Rossetti, L.M., Pasqualon, N.G., Lima, E.F., Barreto, C.J.S., Waichel, B.L. 2014. O uso da morfologia de basaltos e dos padrões petrográficos na interpretação do vulcanismo Serra Geral na Sinclinal de Torres – RS. In: 47º Congresso Brasileiro de Geologia, Salvador.

47º CONGRESSO BRASILEIRO DE GEOLOGIA 21 a 26 / setembro / 2014 Salvador ★ Bahia

O USO DA MORFOLOGIA DE BASALTOS E DOS PADRÕES PETROGRÁFICOS NA INTERPRETAÇÃO DO VULCANISMO SERRA GERAL NA SINCLINAL DE TORRES – RS

Larissa Simon[1]; Marcos Rossetti[1] Lucas M. Rossetti[1] Natália G. Pasqualon[1]; Evandro Fernandes de Lima[1], Carla J. Barreto[1]; Breno L. Waichel[2]

1- Universidade Federal do Rio Grande do Sul
2- Universidade Federal de Santa Catarina

RESUMO: A Sinclinal Torres (RS) é uma estrutura NW que expõe a porção leste da Província Magmática Paraná-Etendeka (132-134Ma), onde afloram toleitos baixo TiO_2. Levantamento estratigráfico, fundamentado em associações de fácies da Formação Serra Geral, permitiram identificar: uma calha principal, zona intermediária e ombreira sul. Nestas áreas pode-se correlacionar lateralmente derrames *pahoehoe* compostos e simples, sucedidos por derrames simples do tipo *rubbly* e, finalmente efusivas ácidas. Basaltos com olivina são as primeiras manifestações, organizados em lobos com texturas hipocristalina, glomeroporfirítica, interseretal e diktitaxítica; esta última indicativa da manutenção dos voláteis durante o resfriamento dos derrames. Estes fluxos compostos anastomosados, decimétricos, do tipo S (*spongy*) e P (*pipe*), ocuparam as regiões de dunas do Botucatu onde os relevos eram mais suaves. Contramoldes de cordas foram preservados nas superfícies das dunas. A baixa taxa de efusão combinada com a topografia do terreno favoreceram a preservação e rápido resfriamento da porção externa, com uma lenta dissipação do calor no interior do derrame. Derrames do tipo *ponded* (andesibasaltos), espessos, faneríticos fino a médio e com disjunções colunares, ocuparam também os espaços interdunas. A presença de arenitos i*ntertrapps,* brechas peperíticas e de diques de areia, gerados por infiltrações nas fraturas de resfriamento, indicam que o aporte sedimentar não foi encerrado nesta fase. Estes derrames são recobertos por *pahoehoe* simples (3m), com um topo vesicular, cujas dimensões das vesículas diminuem em direção ao topo vítreo, um núcleo com menor quantidade de vesículas e *pipes vesicles* na região basal. O padrão de vesiculação é marcado por geometrias arredondadas a subarredondadas, sendo raras as vesículas estiradas. Feições de inflação, como *squeeze-ups* e *tumuli*s também são encontrados nestes derrames. Após esta fase foram colocados andesibasaltos do tipo com simples morfologia *rubbly.* São mais espessos (15-25 m) e caracterizados por uma base suave afanítica, um núcleo hipocristalino maciço e um topo brechado. Ao contrário da morfologia *pahoehoe*, as vesículas são alongadas e estiradas com dimensões maiores em direção ao topo. As texturas das zonas centrais da *rubbly*, diferem dos núcleos das *pahoehoe* simples, sendo normalmente afaníticas. Destacam-se as texturas porfirítica e glomeroporfirítica, com domínio de fenocristais de plagioclásio imersos em uma matriz extremamente fina e rica em micrólitos de plagioclásio. Os fenocristais dos agregados estão em geral fortemente zonados, sugerindo uma história complexa no crescimento. A elevada densidade de micrólitos na matriz, deve-se provavelmente ao aumento no grau de *undercooling*, devido a rápida desvolatização promovida pelo rompimento do topo do derrame. A ruptura da crosta superior da *rubbly* gerou brechas angulosas ao final da sequência geral da estruturação do derrame, provavelmente aumento e oscilações nas taxas de efusão durante o *emplacement*. Neste caso, o rompimento da crosta ocorreu numa fase em que a lava abaixo da crosta era ainda altamente fluída e com baixo grau de cristalização. Os episódios vulcânicos finais da sinclinal são dominados por efusivas ácidas de alta temperatura. Os padrões texturais e composicionais da lavas máficas marcam um aumento das taxas de efusão e no grau de diferenciação durante a história vulcânica da Sinclinal de Torres.

PALAVRAS-CHAVE: MORFOLOGIA DE BASALTOS; FORMAÇÃO SERRA GERAL.

ANEXO J

Barreto, C.J.S., Lima, E.F., Scherer, C.M., Rossetti, L.M.M. 2015. Litofácies vulcânicas no perfil de Santa Cruz do Sul-Herveiras (RS), ombreira sul da Sinclinal de Torres, Sul da Província Ígnea Paraná. In: IX Simpósio Sul-Brasileiro de Geologia, Florianópolis.

IX SIMPÓSIO SUL-BRASILEIRO DE GEOLOGIA
II WORKSHOP DE RECURSOS MINERAIS DA REGIÃO SUL
FLORIANÓPOLIS, SANTA CATARINA 2015

LITOFÁCIES VULCÂNICAS NO PERFIL SANTA CRUZ DO SUL-HERVEIRAS (RS), OMBREIRA SUL DA SINCLINAL DE TORRES, SUL DA PROVÍNCIA ÍGNEA PARANÁ

CARLA JOANA S. BARRETO[1], EVANDRO F. LIMA[2], CLAITON MARLON SCHERER[3], LUCAS DE MAGALHÃES MAY ROSSETTI[4]

1- Universidade Federal do Rio Grande do Sul, Instituto de Geociências, Programa de Pós-Graduação em Geociências, Rio Grande do Sul, carlabarreto.geo@hotmail.com
2- Universidade Federal do Rio Grande do Sul, Instituto de Geociências, Rio Grande do Sul, evandro.lima@ufrgs.br
3- Universidade Federal do Rio Grande do Sul, Instituto de Geociências, Rio Grande do Sul, claiton.scherer@ufrgs.br
4- Universidade Federal do Rio Grande do Sul, Instituto de Geociências, Programa de Pós-Graduação em Geociências, Rio Grande do Sul, lucasross@hotmail.com

No sul do Brasil está exposta uma sucessão vulcânica de derrames *pahoehoe* e *rubbly*, pertencentes a Província Ígnea Paraná-Etendeka. Historicamente, a investigação desse tipo de derrame têm priorizado a aquisição de dados isotópicos e geoquímicos, considerando a pilha vulcânica como uma sucessão monótona de derrames tabulares espessos. Por outro lado, o método de análise de fácies em sequências vulcânicas constitui uma importante ferramenta para estabelecer modelos evolutivos de vulcanismo, onde a sequência pode ser dividida em unidades menores e mais simples (litofácies). Este trabalho fornece uma análise das condições de *emplacement* desses derrames básicos, aplicando o método de análise de fácies baseado nos padrões de vesiculação existentes e feições de superfície. Este estudo foi realizado na ombreira sul da Sinclinal de Torres, Sul do Brasil, no perfil Santa Cruz do Sul-Herveiras, onde a sequência de derrames básicos foi subdividida em 16 litofácies e três associações de litofacies: *pahoehoe* composta inicial, *pahoehoe* simples inicial e *rubbly* simples tardia. Os campos de derrames iniciais são representados por olivina basaltos com morfologia de *pahoehoe* compostos, cujo seu *emplacement* está relacionado a taxas de efusão baixas de caráter intermitente sem erosão termal sobre as areias do *paleoerg* da Formação Botucatu. O *emplacement* dos derrames *pahoehoe* simples mais evoluídos, sobrejacentes aos derrames *pahoehoe* compostos, são mais espessos e estão relacionados a taxas de efusão baixas com aporte de lava contínuo, no qual predomina o processo de inflação. Derrames *pahoehoe* são sucedidos na estratigrafia por andesito basaltos espessos com morfologia *rubbly* simples, os quais estão relacionados a aumentos nas taxas de efusão, originadas durante a principal fase do vulcanismo. A ausência de paleossolos entre os derrames básicos sugere que o *emplacement* sucessivo dos derrames ocorreu em um intervalo de tempo relativamente curto, especialmente entre as associações de litofácies *pahoehoe* simples e *rubbly* simples. A partir do levantamento de seções estratigráficas na ombreira sul da Sinclinal de Torres foi possível definir que a sua evolução geológica é similar às outras Províncias Basálticas Continentais com basaltos *pahoehoe* compostos na base e andesito basálticos simples e espessos no topo da sequência.

Palavras-chave: províncias basálticas continentais, morfologias de basaltos, derrames *pahoehoe*, derrames *rubbly*, litofácies vulcânicas.

ANEXO K

Barreto, C.J.S., Lima, E.F., Lafon, J.M., Sommer, C.A. 2015. Geochemistry and Sr-Nd-Pb isotopes of the basic lava flows from the South hinge of Torres Syncline, Paraná-Etendeka Igneous Province. In: VI Simpósio de Vulcanismo e Ambientes Associados, São Paulo.

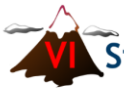

Simpósio de Vulcanismo e Ambientes Associados
2 a 5 de Agosto de 2015 | São Paulo - SP
USP - Cidade Universitária

Geochemistry and Sr-Nd-Pb isotopes of the basic lava flows from the south hinge of Torres Syncline, Paraná-Etendeka Igneous Province

Carla Joana Santos Barreto[1], Evandro Fernandes de Lima[2], Jean Michel Lafon[3], Carlos Augusto Sommer[4]

[1]Universidade Federal do Rio Grande do Sul, e-mail: carlabarreto.geo@hotmail.com;
[2]Universidade Federal do Rio Grande do Sul, e-mail: evandro.lima@ufrgs.br;
[2]Universidade Federal do Pará, e-mail: lafonjm@ufpa.br;
[2]Universidade Federal do Rio Grande do Sul, e-mail: cassomer@sinos.net.

In the southernmost Brazil is exposed a volcanic succession from Low-Ti pahoehoe to rubbly lavas (Gramado type), belonging to Paraná-Etendeka Igneous Province. Geochemical and Sr-Nd-Pb isotope data were obtained on basalts from the south hinge of the Torres Syncline, in order to discuss the petrogenesis of lava flows as well as evaluate the role of crustal contamination and the potential contaminants involved. The lavas exhibit compositions ranging from basalt to andesite and tholeiitic signature. The major and trace element behavior in relation to MgO, suggests an evolutionary trend, involving magmatic differentiation of plagioclase +clinopyroxene+olivine+titanomagnetite. The trace element behavior when normalized to primitive mantle shows strong depletions in Nb, Sr and P elements, while the rare earth element patterns normalized to chondrites exhibit enrichment of LREE relative to HREE with weak negative Eu anomalies. Crustal assimilation is the best process to account for these magmas, considering the high initial Sr isotopic ratios (0.707798 - 0.715751), very low ε_{Nd} (-8.36 to -5.41), high $^{206}Pb/^{204}Pb$ ratios (18.424 - 18.865), and intermediate $^{207}Pb/^{204}Pb$ (15.649 - 15.710) and $^{208}Pb/^{204}Pb$ ratios (38.618 - 39.369). The andesites with ponded pahoehoe morphology erupted at early stages of volcanism, and represent evolved melts that should be strongly susceptible to crustal contamination as they establish pathways to the surface. The basaltic andesites with simple pahoehoe morphology could be explained by longer time residence of liquids in crust with higher degree of crustal assimilation. The basaltic andesites with rubbly morphology are related to late differentiation process in shallow magmatic chambers. This study reinforce that the compositional variations are not systematic and continuous through the lava pile towards up-section, implying that the magma chamber could have suffered periodically replenishments or distinct magma pulses along time or multiple pumbling systems exist. The isotopic ratios of studied lava flows require variable degrees of assimilation of Paleoproterozoic and Neoproterozoic contaminants.

Financial Support: PRH PB-215
Key words: Paraná Igneous Province; whole-rock geochemistry; Sr-Nd-Pb isotopes.

ANEXO L

Barreto, C.J.S., Lima, E.F., Lafon, J.M., Sommer, C.A. 2015. Análise de fácies vulcânicas e assinaturas geoquímicas e isotópicas dos derrames básicos da ombreira sul da Sinclinal de Torres, Sul da Província Ígnea Paraná. In: 1º Semana Acadêmica de Pós-graduandos do Instituto de Geociências da UFRGS – Integrando as Geociências, Porto Alegre.

1ª Semana Acadêmica dos Pós-graduandos do Instituto de Geociências da UFRGS - Integrando as Geociências – De 17 a 20 de agosto de 2015

ANÁLISE DE LITOFÁCIES VULCÂNICAS E ASSINATURAS GEOQUÍMICAS E ISOTÓPICAS DOS DERRAMES BÁSICOS DA OMBREIRA SUL DA SINCLINAL DE TORRES, SUL DA PROVÍNCIA ÍGNEA PARANÁ

Carla Joana S. Barreto[1], Evandro F. de Lima [2], Jean M. Lafon[3], Carlos A. Sommer[4]

[1] UFRGS, carlabarreto.geo@hotmail.com; [2] UFRGS, evandro.lima@ufrgs.br; [3] UFPA, lafonjm@ufpa.br; [4] UFRGS, cassomer@sinos.net

No sul do Brasil está exposta uma sucessão vulcânica de derrames baixo-Ti com morfologias *pahoehoe* e *rubbly*, pertencentes Formação Serra Geral, na Província Ígnea Paraná-Etendeka. Historicamente, a investigação desses derrame básicos tem priorizado a aquisição de dados isotópicos e geoquímicos, considerando a pilha vulcânica como uma sucessão monótona de derrames tabulares espessos. Neste estudo os objetivos consistem em aplicar o método de análise de fácies baseado nos padrões de vesiculação existentes e feições de superfície, bem como discutir a petrogênese dos derrames e avaliar o papel da contaminação crustal e dos potenciais contaminantes através de dados químicos e isótopos de Sr-Nd-Pb. Foram investigados os derrames básicos nos perfis geológicos Santa Cruz do Sul-Herveiras, Morro da Cruz e Lajeado (RS). Na sequência de derrames em Santa Cruz do Sul-Herveiras foram identificadas 16 litofácies e três associações de litofácies: *pahoehoe* composta inicial, *pahoehoe* simples inicial e *rubbly* simples tardia. Em todos os perfis levantados os derrames pertencem geoquimicamente ao tipo Gramado e exibem composições variando de basaltos a andesito basálticos com afinidade toleítica. O comportamento dos elementos maiores e traços sugere um *trend* evolutivo envolvendo diferenciação magmática de plagioclásio+clinopiroxênio+olivina+titanomagnetita. Os elementos traços exibem forte empobrecimento nos elementos Nb, Sr e P, enquanto os padrões de elementos terras raras mostram enriquecimentos de ETRL em relação aos ETRP com fracas anomalias negativas de Eu. Assume-se o processo de assimilação crustal para explicar as altas razões isotópicas iniciais de Sr (0,707798–0,715751), valores muito baixos de ε_{Nd} (-8,36 to-5,41), altas razões de $^{206}Pb/^{204}Pb$ (18,424–18,865), e intermediárias de $^{207}Pb/^{204}Pb$ (15,649-15,710) e $^{208}Pb/^{204}Pb$ (38,618-39,369). Os andesitos (SiO_2 55-58%) com morfologia *pahoehoe ponded* do perfil Morro da Cruz extravasaram nos estágios iniciais do vulcanismo sem erosão termal sobre as areias do *paleoerg* da Formação Botucatu. Esses derrames representam líquidos evoluídos com contaminação crustal. Os derrames iniciais do perfil Santa Cruz do Sul diferentemente são representados por olivina basaltos (SiO_2 47-50%) com morfologia de *pahoehoe* compostas, cujo *emplacement* está relacionado a taxas de efusão baixas de caráter intermitente. O *emplacement* dos andesito basálticos (SiO_2 51-56%) com morfologia *pahoehoe* simples está relacionados a taxas de efusão baixas com aporte de lava contínuo, onde predomina o processo de inflação. A origem destes pode ser explicada por um tempo de residência suficiente para inserir graus maiores de assimilação crustal. Derrames *pahoehoe* são sucedidos por andesitos basálticos (SiO_2 52-56%) espessos com morfologia *rubbly* simples, os quais foram gerados por aumentos nas taxas de efusão que constituem a principal fase do vulcanismo. Estes derrames estão relacionados a processos de diferenciação tardios em câmaras magmáticas rasas. No presente trabalho pode-se identificar que as variações composicionais no vulcanismo não são sistemáticas e contínuas em direção ao topo da sequência, sugerindo que a rede de alimentação magmática pode ter sofrido sucessivos reabastecimentos com distintos pulsos magmáticos ao longo do tempo ou devido a presença de vários sistemas de alimentação comuns em sistemas fissurais. As variações isotópicas observadas nos derrames sugerem graus variados de assimilação de contaminantes paleoproterozoicos e neoproterozoicos.

Palavras-chave: Litofácies vulcânicas; Geoquímica de rocha total; Isótopos Sr-Nd-Pb.

ANEXO M

Barreto, C.J.S, Lafon, J.M., Lima, E.F., Sommer, C.A. 2015. Geochemical and Sr-Nd-Pb isotopic insights of the Low-Ti basalts from Paraná-Etendeka Igneous Province, Southern Brazil: constraints on Petrogenesis and the role of crustal contamination. In: American Geophysical Union, San Francisco.

AGU FALL MEETING

San Francisco | 14 – 18 December 2015

T33F-2995: Geochemical and Sr–Nd–Pb Isotopic Insights of the Low-Ti basalts from Paraná–Etendeka Igneous Province, Southern Brazil: Constraints on Petrogenesis and the Role of Crustal Contamination

ABSTRACT

Wednesday, 16 December 2015 **13:40 - 18:00**

Moscone South - Poster Hall

The south hinge of the Torres Syncline in southernmost Brazil hosts a volcanic succession of pahoehoe and rubbly Gramado-type lavas belonging to the ~132 Ma Paraná–Etendeka Igneous Province. We employ local-scale stratigraphy in three distinct profiles (Santa Cruz do Sul-Herveiras, Morro da Cruz and Lajeado geologic sections) as guidelines for geochemical and Sr-Nd-Pb isotope studies in order to discuss the petrogenesis of lava flows in a single magma type and to quantitatively evaluate the role of crustal contamination and the potential contaminants involved. In all profiles, the lava flows exhibit compositions ranging from basalt to andesite with tholeiitic affinity. The compositional and isotopic variations are not systematic according to stratigraphy, implying that the magma chamber could have undergone periodic replenishments or distinct magma pulses through time or multiple plumbling systems may have existed. The andesites (SiO_2 55–58 wt.%) with ponded pahoehoe morphology represent evolved melts at early stages of volcanism with strong susceptibility to crustal contamination as they established pathways to the surface. The olivine basalts (SiO_2 47–50 wt.%) and basaltic andesites (SiO_2 51–56 wt.%) showing compound morphology and simple pahoehoe morphology, respectively, could be explained by longer time residence of liquids in the crust with higher degrees of crustal assimilation than the ponded pahoehoe lavas. The basaltic andesites (SiO_2 52–56 wt. %) with rubbly morphology are related to late differentiation process in shallow magma chambers. Crustal assimilation process accounts for the high initial $^{87}Sr/^{86}Sr$ ratios at 0.707798–0.715751, very low ε_{Nd} between −8.36 and −5.41, high $^{206}Pb/^{204}Pb$ ratios at 18.424–18.865, with intermediate $^{207}Pb/^{204}Pb$ and $^{208}Pb/^{204}Pb$ ratios at 15.649–15.710 and 38.618–39.369, respectively. The isotopic variations require assimilation of both Paleoproterozoic and Neoproterozoic contaminants at variable degrees.

Authors

Carla Barreto
UFRGS Federal University of Rio Grande do Sul

Evandro Lima
UFRGS Federal University of Rio Grande do Sul

Jean Lafon
UFPA Federal University of Pará, Geociencias, Belém, Brazil

Carlos Sommer
UFRGS Federal University of Rio Grande do Sul

Irene Raposo *
Instituto de Geociências Universidade de Sao Paulo

Breno Waichel
UFSC Federal University of Santa Catarina

ANEXO N

Waichel, B.L., Lima, E.F., Jerram, D., Rossetti, L.M.M., Bueno, G., Viana, A., Barreto, C.J.S. 2015. 3D modelo of the Torres Syncline in the Paraná-Etendeka Province, South Atlantic Margin. In: American Geophysical Union, San Francisco.

AGU FALL MEETING

San Francisco | 14 – 18 December 2015

T33F-2999: 3D MODEL OF THE TORRES SYNCLINE IN THE PARANÁ-ETENDEKA PROVINCE, SOUTH ATLANTIC MARGIN

ABSTRACT

Wednesday, 16 December 2015 **13:40 - 18:00**

Moscone South - Poster Hall

The Paraná-Etendeka Volcanic Province (PEVP) is Early Cretaceous in age and precedes the fragmentation of the south Gondwana. These volcanic rocks cover an area in excess of 1,200,000 km^2 and can reach a maximum thickness of 1,700 m. The PEVP is composed mainly of tholeiitic basalts and subordinately by andesites and rhyolites/quartz-latites. Recently new models considering physical characteristics of the lava flow stratigraphy on both sides, Africa and South America, have been built providing a new vision of the volcanic stratigraphy and flow morphologies inside the province. This work presents a 3D model of the volcanic sequence at theTorres Syncline (Brazil). The 3D model was build using the PETREL E&P Software Platform. Geological sections based on field data and Log data from Paraná Basin (Gama-ray and soniclogs) were used to build the model. The Torres Syncline is a tectonic structure located in southern Brazil with the main orientation NW-SE. In Torres Syncline the basal portion is characterized by pahoehoe lava flows in a compound braided architecture, followed by rubbly lavas in a tabular classic architecture, and in the upper portions silicic units interbedded with basaltic lavas. The central portion of the volcanic pile is characterized by thick tabular lavas with rubbly tops (25-50 m thick). These flows have an internal structure divided in four parts: a smooth vesicular base, aphanitic massive cores with irregular joints, upper vesicular portion and a rubbly top. This unit is thicker along of the Torres Syncline and represents the main phase of the volcanism. Silicic units occur in the upper parts of the PEVP stratigraphy and include lava domes interbedded with rubbly flows and thick tabular flows. The Torres Syncline and Huab constituted one Basin features single active structure in the Early Cretaceous and during the main rifting phase. The onset of the volcanism was characterized by low effusion rate eruptions over the paleoerg, forming pahoehoe flow fields. The main phase of volcanism is build up by thick tabular rubbly pahoehoe flows, formed by larger volume sequences (slightly high effusion rates), that cover the initial pahoehoe flows. At the upper portion of the sequence, the volcanism is more differentiated forming silicic lavas.

Authors

Breno Waichel
UFSC Federal University of Santa Catarina

Evandro Lima
UFRGS Federal University of Rio Grande do Sul

Dougal Jerram *
University of Oslo

Lucas Rossetti
UFRGS Federal University of Rio Grande do Sul

Gilmar Bueno
UFF Federal Fluminese University

Adriano Viana
PETROBRAS

Carla Barreto
UFRGS Federal University of Rio Grande do Sul